Mechanisms involved in the development of androgen independent prostate cancer

Androgen receptor activation leads to a dissociation of E2F1:PHB in prostate cancer

Sarah Koushyar

Cardiff China Medical Research Collaborative

School of Medicine, Cardiff University

July 2017

Thesis submitted to Cardiff University for the degree of Doctor of Philosophy

Acknowledgements

Firstly, I would like to thank my supervisor Dr Alwyn Dart for the constant support, guidance, and always knowing the answer to every one of my questions. This project could not have come together without his endless expertise. Secondly, I would like to thank Professor Wen Jiang for giving me the opportunity to work within CCMRC and being able to support the PhD project.

Further I would like to thank the staff and students of CCMRC who have made my three years at Cardiff a very enjoyable experience through the testing times of a PhD. To my loved ones and friends in Cardiff, thank you for making the last three years the best ones yet.

Finally, I would like to dedicate this thesis to my parents and my brother, who have been the most supportive and proudest family that I could have ever asked for.

Summary

Prostate cancer (PC) is the most common cancer found in men in the Western world. Predominantly, the pathogenesis of PC is driven by aberrant androgen receptor (AR) signalling, resulting in heightened cell proliferation and cell survival. Current treatment options target the AR signalling cascade by androgen ablation therapy, whereby anti-androgens antagonistically bind to the AR. This prevents AR activity, thus inhibiting transcription of genes involved in cell proliferation, survival and metastasis. However, eventually androgen ablation therapy leads to relapse, as the cancer succumbs to a low androgen environment, leading to a poorer prognosis with limited treatment options, otherwise known as 'castration resistant PC' (CRPC). This is where new clinical interventions are urgently required. One mechanism that could allude to androgen independent PC, is the down-regulation of AR co-repressors. One such co-repressor is known as Prohibitin (PHB). PHB is ubiquitously expressed in mammalian cells and displays anti-proliferative functions. Prior to this project, it was identified that AR signalling leads to the down-regulation of PHB at both a transcript and protein level and causes PHB to dissociate from the chromatin. However, over-expression of PHB leads to the down-regulation of androgen responsive genes, and its increased association with the chromatin. Thus within PC, both the AR and PHB are in a dynamic opposition. This project identified that PHB has a repressive role on the cell cycle by holding the cell population within the G1 phase. RNA-sequencing and Q-PCR data identified that PHB had a significant repressive role on gene families involved in DNA replication and cell cycle regulation and progression. Such gene families include cyclins, E2Fs and MCMs. MCMs are gene targets of E2Fs, and therefore it was assessed if PHB had an effect on the promoter activity of two MCM genes; MCM5&6. Interestingly, with PHB over-expression, repression of both MCM5&6 promoter activity was seen. It was then identified that PHB physically interacts with E2F1 in androgen responsive PC cells. However this interaction was reduced upon androgen stimulation of the AR. This led to the preliminary mechanism that PHB can bind to E2F1, potentially preventing E2F from binding to MCM promoter regions, leading to an inhibition of the cell cycle in PC cells. Moreover, it was identified that androgen stimulation led to a likely dephosphorylation event happening to the PHB protein that could explain how PHB dissociates from the chromatin and E2F1. Signalling pathways that could lead to the non-genomic activation of the AR was narrowed down to the Src-pathway highlighted by a Kinexus™ protein array. Interestingly, inhibiting the Src-pathway

stops PHB's likely dephosphorylation event. Accumulating previous data and data collected throughout this thesis, PHB up-regulation leads to cell cycle arrest through a direct interact of a key cell cycle regulator; E2F1. Moreover, PHB was found to have an inhibitory effect on both the migration and adhesion of PC cells, potentially through the down-regulation of *wnt* genes. Thus potentially, PHB up-regulation can inhibit the migratory potential of PC cells, stopping the progression of the disease.

Publications and conferences attended

- S Koushyar, G Economides, S Zaat, W Jiang, C L Bevan and D A Dart. The prohibitin-repressive interaction with E2F1 is rapidly inhibited by androgen signalling in prostate cancer cells. 2017. *Oncogenesis.* 6 (5), e333.
- Koushyar, S. Uysal-Onganer, P. The interaction of Wnt-11 and signaling cascades in prostate cancer. 2016. *Tumour biology.* 37(10):13049-13057.
- Koushyar, S. Jiang WG, Dart DA. Unveiling the potential of prohibitin in cancer. 2015. *Cancer letters* 369(2):316-22.
- Koushyar, S. Economides, G. Dart, DA. Mason, M. 2015. Prohibitin causes the downregulation of E2Fs and MCMs leading to cell arrest in prostate cancer. *Anticancer research* 35:4364.
- Koushyar,S. Uysal-Onganer,P. Grant, G. 2015. Wnt-11 and JNK pathway: The two faces of neuroendocrine-like differentiation in prostate cancer. *Anticancer research* 35(7):4303-4303.
- British Society for Gene and Cell therapy annual conference (2017). Cardiff, UK.
- 14th World Cancer & Anti- Cancer Therapy Convention (2016). Dubai, UAE.
- Chinese-British-American Scholar Forum, Beijing (2015).
- China-UK Cancer conference (2015).

Abbreviations

AAT Androgen ablation therapy

ADT Androgen deprivation therapy

AF-1/2 Activation function 1/2

AIPC Androgen independent prostate cancer

AIS Androgen insensitivity syndrome

APS Ammonium persulphate

AR Androgen receptor

AREs Androgen response elements

ATCC American Type Culture Collection

Bicalutamide-R Bicalutamide-resistant

β-ME Beta-Mercaptoethanol

BSA Bovine serum albumin

CamKII Calcium dependent protein kinase II

CDK Cyclin dependent kinase

CIN Chromosomal instability

CIP Calf intestinal phosphatase

CLL Chronic lymphocytic leukaemia

CREB cAMP responsive element binding protein

CRPC Castration resistant prostate cancer

DAVID Database for annotation, visualisation and integrated discovery

DBD DNA-binding domain

DHFR Dihydrofolate reductase

DHT Dihydrotestosterone

Dox Doxycycline

ECM Extracellular matrix

EGF Epidermal growth factor

EMA European medicines agency

EMT Epithelial to mesenchymal transitioning

ER Estrogen receptor

ER Endoplasmic reticulum

ERG ETS-related gene

FDA The USA Food and Drug Administration

FSH Follicle-stimulating hormone

GADD45a Growth arrest and DNA damage inducible

GIN Genomic instability

GnRH Gonadotropin releasing hormone

GR Glucocorticoid receptor

GSTP1 Glutathione S-transferase pi 1

HAT Histone acetyltransferases

HDACs Histone deacetylases

HPRD Human Protein Reference Database

HRP Horseradish peroxidase

HSP Heat shock proteins

IBS Irritable bowel syndrome

IGF-1 Growth factor-1

Il-6 Interleukin 6

IPA Ingenuity pathway analysis

JNK c-jun kinase

KLF6 Kruppel-like factor 6

KLK Kallikreins

KO Knockout

LBD Ligand binding domain

LH Luteinizing hormone

LHRH Luteinizing hormone-releasing hormone

MCM Minichromosome maintenance

MEF Mouse embryonic fibroblast

MiRNAs micro-RNAs

MR Mineralocorticoid receptor

MTT Thiazolyl blue tetrazolium bromide

NCoR Nuclear receptor co-repressor 1

NR Nuclear receptor

NSCLC Non-small cell lung carcinoma

NTD N terminal domain

OPA1 Optic atrophy 1

PBS Phosphate buffer saline

PC Prostate cancer

PCNA Proliferating-cell nuclear antigen

PHB Prohibitin

PHI Prostate health index

PI3K Phosphoinositide 3-kinase

PIN Prostatic intraepithelial neoplasia

PKC Protein kinase C

PMT Photomultiplier Tube

Poly-Q Poly-glutamine tracts

Poly-G Poly-glycine tracts

PR Progesterone receptor

PSA Prostate specific antigen

PSAV Prostate specific antigen velocity

PTEN Phosphatase and tensin homolog

PTM Post translational modification

PVDF Polyvinylidene fluoride

Rb Retinoblastoma

RNAi RNA interference

RNA-seq RNA sequencing

ROS Reactive oxygen species

RPKM Reads per kilobase million

RTKs Receptor tyrosine kinases

SDS Sodium dodecyl sulfate

SDS-PAGE SDS Polyacrylamide Gel Electrophoresis

SEM Standard error of mean

si-RNA Small inhibitory RNA

SLP-2 Stomatin-like protein

SMRT Silencing mediator for retinoid and thyroid receptors

SNP Single nucleotide polymorphism

SRC-1 Steroid receptor co-activator -1

SSCP Single strand conformation polymorphism

STAT3 Signal transducer and activator of transcription 3

TBS Tris buffered saline

TETO2 Tet operator 2

TETR Tet repressor

TFM Testicular feminised mice

TNM The tumour, node, metastasis system

tPSA Total prostate specific antigen

Tyr Tyrosine

VEGFR-2 Vascular endothelial growth factor receptor-2

Contents

List of figures

List of tables

Chapter I. General introduction.

1 Chapter I: General introduction

1.1 The prostate gland

The prostate gland is known as the largest male accessory gland, positioned inferior to the neck of the bladder and it surrounds the urethra (figure 1.1). Structurally, a fibroelastic tissue layer encapsulates the prostate gland, forming a septum that subdivides the gland into five lobes (1). These lobes are responsible for accommodating saccular glands, excretory ducts, stroma, blood vessels and nerves. Moreover, the prostate gland can be divided into zones, namely; central, peripheral, transitional and the stroma. The central zone is made of 20% glandular tissue that forms the majority of the prostatic base and surrounds the ejaculatory duct apparatus (1). The peripheral zone is made of 70% glandular tissue and is the most common zone for carcinomas to arise. The transition zone is made of two small lobules where benign prostatic hyperplasia (BPH) usually arises (1). The prostate gland is composed of two main cell types; luminal and basal that form the epithelial cell layer that is encapsulated by the stroma (2) (figure 1.1).

Firstly, luminal cells are both polarised and columnar and carry out a secretory role within the lining of the prostate lumen. The basal cells are elongated allowing the separation of the lumen and stroma and are also involved in proliferation (2). Both these cells types are distinguishable by cell markers. For example, the luminal cells express the androgen receptor (AR), cytokeratin 8, 18, and CD57. However, basal cells express a low level of the AR, CD44 and cytokeratin 14 (2). Interestingly, a third cell type can be found with the prostate epithelium known as neuroendocrine cells. This type of cell is very rare, post mitotic, is AR negative and secretes neuropeptides that are vital for the differentiation of the luminal epithelia (1). In terms of stem cells within the prostate, little information is known about their role. It has been thought that within the epidermis of the prostate resides a small population of stem cells that contribute to a growing population of prostate cells, which in turn differentiate into the luminal cells (3).

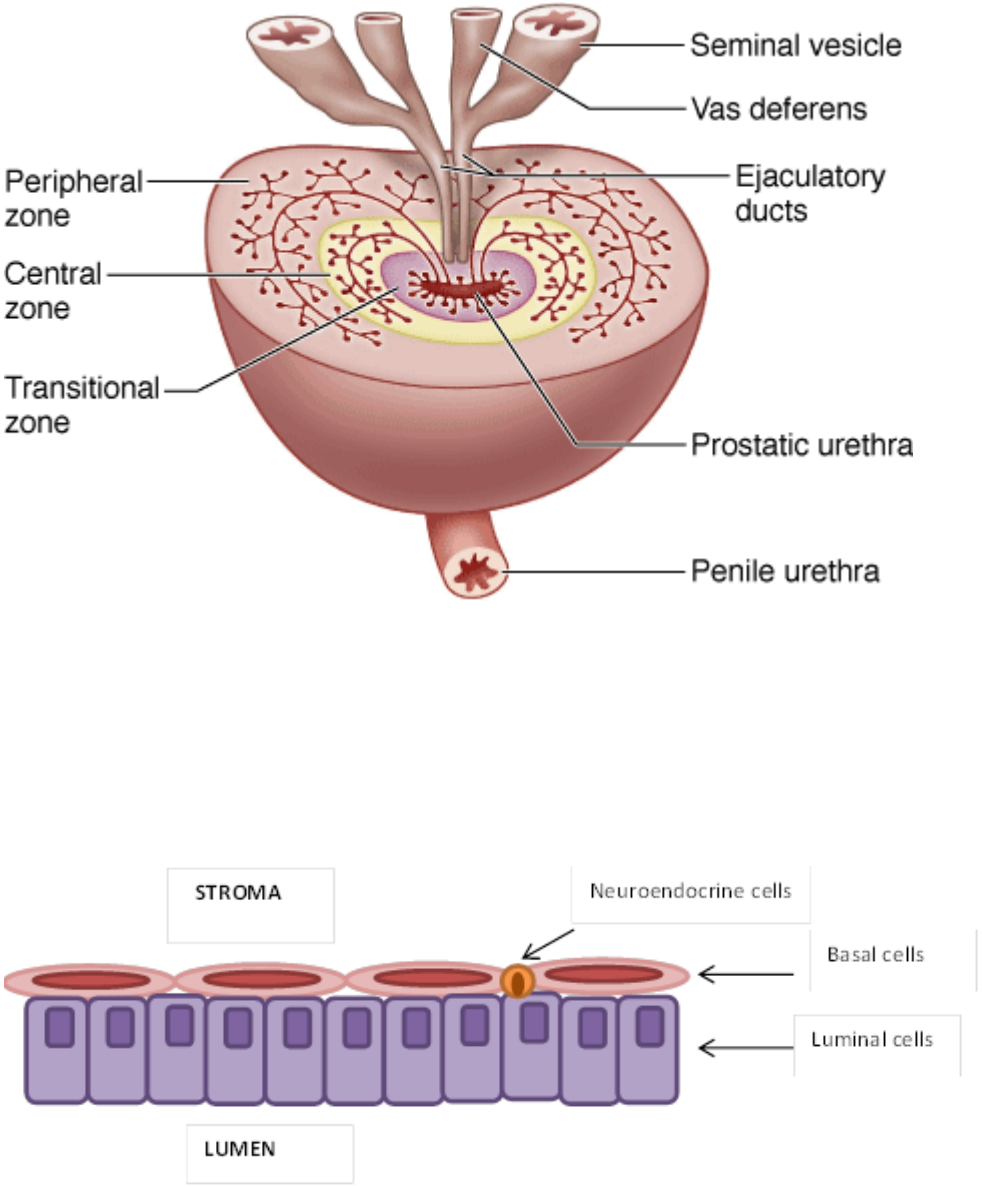

Figure 1.1. Structure of the prostate gland in the male human body (4), alongside the representation of the two major cell types within the prostate epithelium.

1.2 The function of the prostate gland

The prostate gland carries out various functions. Firstly, the mass and musculature of the prostate gland itself, aids the transmission of seminal fluid (5). As it is known as an exocrine gland, it provides an array of molecules and enzymes such as coagulase and fibrinolysin that aid fertility. The prostatic fluid also reduces the acidity of the urethra, protecting sperm viability. The motility of sperm is enhanced by the prostate gland providing albumin and other proteins (5). Finally, as an exocrine gland it participates in the rapid metabolism of the circulating androgen, testosterone to the more potent form; dihydrotestosterone (DHT).

1.3 The development of the prostate gland

In humans, the formation of the prostate gland is seen around week 11 of gestation. The formation begins with multiple outgrowths appearing from the urethral epithelium from both sides of the mesonephric duct. Five epithelial buds mature into five internal prostatic lobes (5). At 22 weeks, the stroma has significantly matured and continues to do so until birth. At birth, the anterior lobule reduces in size and loses its branches, regression of the gland is seen that then enters a quiescent phase at 12-14 years of age until puberty. Maturation of the gland is seen during puberty (5). Figure 1.2 shows the pathway for androgen synthesis in the adult male prostate.

1.4 Prostate Cancer

Prostate cancer (PC) is an extremely complex and heterogeneous disease. PC is the most frequent cancer in the Western male, particularly targeting men over the age of 65 (6). PC, when diagnosed at an early stage, is dependent upon androgen stimulation. If the cancer relapses to anti-androgen therapy, it becomes 'castration resistant' and in some cases, PC can become androgen independent. Androgen dependent PC relies on the androgen receptor (AR) signalling pathway, whereas AIPC is able to adapt to a low androgen environment and thus continue to progress to a more malignant state. The transition from androgen dependence to androgen independence is poorly understood. Mechanisms establishing this transition will identify a more in-depth, understanding, vital for new therapeutic agents. Supplemental figure 1 depicts the stages of PC progression.

1.5 Epidemiology of PC

The diagnosis of PC has greatly improved over the last 50 years, leading to an increase in known cases. Approximately 40,000 cases per annum has been reported in the UK and PC is now the most common non-cutaneous cancer in men in the Western world (7). Epidemiological studies based upon migrating populations uncovered that the environment and lifestyle choices play a vital role in the incidence of PC. This being said, there is no inclusive risk factor that completely determines PC initiation (7). Based on autopsy material, PC prevalence is highest among African American men and lowest in Chinese men (8). Moreover, African American men tend to be diagnosed at a younger age with a more aggressive version of the disease (8). The reasons behind the high incidence rate of PC in African men are still unknown, however a few factors such as socio-economic status, access to healthcare and delayed diagnosis may have some influence on the situation (8). In the United States, the number of diagnosed PC cases varied due to the introduction of the gold standard diagnostic test of the Prostate Specific Antigen (PSA) serum test in the early 1980s. A rise in detection of PC is thought to be due to a rise in the number of biopsy cores taken and lowering of the PSA detection threshold (9). Table 1.1 shows the numbers of recorded PC cases worldwide. With regards to Europe, Tyrol in particular has a higher number of cases recorded for PC than the eastern parts of Austria. This is due to an organised screening PC process being conducted in Tyrol (8). Moreover, epidemiological studies of PC have identified that migrant Asian men adopting a western diet had an increased PC incidence due to dietary vitamin D. Further, American men were identified to be 10 times more likely to be diagnosed with PC than Japanese men, potentially due to Japanese men consuming a diet rich with fatty fish high in vitamin D (10).

Table 1.1. Numbers of recorded PC cases worldwide (9).

Continent	Country	Incidence of PC (per 100,000)
Africa	Congo	29
	Kenya	16.6
	Senegal	7.5
	Uganda	38
	Zimbabwe	27.4
North America	Canada	78.2
	US	124.8
Asia	China	1.7
	Taiwan	3
	Japan	12.6
	Korea	7.6
	Thailand	4.5
Europe	Austria	71.4
	Austria, Tyrol	100.1
	Austria, Vorarlberg	66.4
	France	59.3
	Hungary	34
	Iceland	75.2
	Norway	81.8
	Spain	35.9
	Sweden	90.9
	Switzerland	77.3
	UK	52.2

1.6 Risk factors

Although there is not one specific risk factor that can lead to the onset of PC, there are several which can predispose an individual towards the disease. Similar to breast and ovarian cancer, familial clustering of PC is a known risk factor (7). For example, men who have first-degree relatives with PC incur a two-fold higher chance of developing PC than the rest of the general population (7). A meta-analysis of a Swedish population based cancer database highlighted 5,623 out of 26,651 men were familial cases, underlining that almost 5% of men with a familial case of PC will indeed be predisposed to the disease themselves (11). For example, mutations in the BRCA1 and BRCA2 genes are associated with high risk PC. Men carrying the BRCA1 mutation have a 2-5-fold increased risk of PC. Moreover, men carrying BRCA2 mutations incurred a more aggressive form of the disease. Clinic-pathological analysis of men carrying BRCA1 and BRCA2 mutations displayed higher Gleason scores (> Gleason score 8) and metastasis was found at diagnosis. A hindrance with this screening technique is reports of men with BRCA1 and BRCA2 mutations have been scarce (12).

1.6.1 Ethnicity

Asian men are less prone to developing PC but the aetiology is unknown. On the other hand, African American men have a 60% higher occurrence than the American white population (11). African-American men are also more than twice as likely to die of prostate cancer as white men. Lower cases of PC have been recorded in Asian-American and Hispanic males than in non-Hispanic white males(11). However, when Asian men migrate to the USA, their incidence is the same, thus there could be a dietary influence on PC incidence. The reasons for these racial and ethnic differences are yet to be identified.

1.6.2 Age

Age can greatly influence the onset of PC, for example the probability of developing PC in younger men is 0.005% which rises to 2.2% in men between 40 and 59 years of age (13). Unfortunately this percentage increases to 13.7% in men aged 60-79 years old (13). Worryingly, half of men aged between 70 and 80 years old age show malignancy upon histological analysis (13).

1.6.3 Single nucleotide polymorphisms (SNPs)

Moreover, in terms of genetic predisposition, mutations can be potent and extremely rare or can be quite frequent with an intermediate effect (7). Since 2005, 74 single nucleotide polymorphisms (SNPs) have been identified as a PC risk (7). The first identified SNP at position 8q24 locus, found within the *MYC* gene, can give rise to oncogenic transformation and has had the most amount of independently associated variants (7). Likewise, SNPs have also been identified on chromosome 19, where genes encoding for the Kallikreins (KLK) family are found. This family consists of the well-known serine protease enzyme PSA also known as KLK3. Therefore SNPs within this region has been associated with altered expression levels of PSA (7). Moreover, another identified SNP was located to the DNA mismatch repair (*MMR)* gene. The SNP rs1799977 found in *MLH1* gene was identified with a modest increase in overall PC risk, an increased risk in a more aggressive form of PC and PC recurrence. A similar pattern was seen with this SNP in breast cancer (14). Mutations in the *MLH* genes are damaging to microsatellites causing the failure of DNA repair during DNA replication. Therefore, ideally SNPs can be targeted for prognostic uses (7). In terms of distinguishing between aggressive and indolent disease, there is no known SNP that can do so at present.

1.6.4 Mutations in tumour suppressor genes

Mutations in the tumour suppressor *P53* gene, leading to its inactivation, are the most frequent genetic alteration in human cancers. Whether *P53* mutations are associated with an increased risk in PC still needs to be further elucidated. In around 1000 clinical samples carried out by Rivlin, *et al,* 2011, *P53* mutations were screened. The majority of *P53* alterations identified by immunohistochemistry correlated with a higher Gleason grade. Other studies suggest that nuclear accumulation of *P53* correlates with poor prognosis, following radical prostatectomy, however this was contradicted by another study reviewed by Rivlin, *et al.,* 2011 (15). This could be due to the small study number. It can be said that *p53* mutations are associated with hormone refractory PC as it was confirmed that 94% of hormone refractory specimens had increased mutant P53 protein expression, that has lost its tumour suppressor function and gained oncogenic functions (15). 16 mutant forms of the *P53* gene were identified from an extensive functional analysis of PC. LNCaP cells (wt p53) transfected with four gain-of-function *P53* mutants (*G245S, R248W, R273H*, and *R273C*) were able to grow in the absence of

androgens, which is unique as LNCaP cells are characterized as androgen dependent cells (16). This could potentially link to how androgen dependent PC cells are able to survive and proliferate in an androgen-depleted environment.

Another mutated tumour suppressor gene identified in primary PC is known as Kruppel-like factor 6 (KLF6). Its function still needs to be elucidated. Analysis by (Narla, *et al.,* 2001) (17) revealed that 77% of primary PC tumours had *KLF6* deletions. Functional analysis observed that wt KLF6 significantly reduced proliferation and up-regulated p21 activity, whereas tumour derived KLF6 mutants did not (17). This led to the assumption that KLF6 displays tumour suppressor activity in PC.

Phosphatase and tensin homolog (PTEN) negatively regulates the PI3K/AKT pathway acting as a tumour suppressor gene and is often lost or mutated in cancers (18). A study using a murine *PTEN* cancer model showed that the deletion of *PTEN* gene led to prostatic intraepithelial neoplasia (PIN) that progressed to invasive carcinoma, followed by metastasis (19).

1.6.5 Mutations in oncogenes in PC

Epidermal growth factor receptor (EGFR) is a tyrosine receptor kinase, and is involved in numerous signalling pathways such as Akt, MAPK and STAT. Targeted inhibition of EGFR with microRNA28 resulted in an up-regulated apoptotic response in a PC tumour (20). Immunohistochemical studies showed that with increased PSA serum levels, there was an increased expression of EGFR. Moreover, PC biopsies with a high Gleason grade (>7) were significantly more prone to be co-expressed with EGFR. Already there are EGFR-targeted therapies such as Geftinib that has been approved for the use of non-small cell lung carcinoma (NSCLC) (20) In terms of PC, EGFR has a complicated interaction with the AR. On the one hand, androgen stimulated AR was noted to increase the expression levels of EGFR mRNA. Anti -EGFR antibodies inhibited androgen-stimulated proliferation of PC cells. On the other hand, another study suggested that androgen stimulation caused an increased EGFR degradation (20). Therefore further studies need to confirm the exact role EGFR has in PC.

Another oncogenic signalling pathway that is associated with the progression of PC is the Wnt signalling pathway. The canonical Wnt/βcatenin signalling pathway is associated with malignant PC (21). Inhibition of this pathway by a known Wnt inhibitor, WIF1, significantly reduced the size of PC tumours in a xenograft mouse model. A transducer of the Wnt signalling pathway; CamKII amplified cell motility that could aid future tumour invasion (20). Interestingly, a non-canonical Wnt, known as Wnt-11 increases the invasiveness of both PC-3 and LNCaP cells when over-expressed (21).

The fusion of 5'untranslated region of *TMPRSS2* (21q22) to *ERG* (ETS-related gene) (21q22) has been identified in approximately 50% of PC cases, and this gene fusion has been seen in 90% of PC cases over-expressing *ERG* (22). *ERG* is an oncogene belonging to the ETS family of transcription factors that plays a role in angiogenesis and haematopoiesis (23).

TMPRSS2 is a bona fide androgen-regulated gene, and it was noted that androgen stimulation of PC cells resulted in an upregulation of the *TMPRSS2-ERG* gene fusion. . Transgenic expression of *TMPRSS2-ERG* only resulted in PIN lesions, and additional genetic changes such as *PTEN* loss is needed to initiate carcinogenesis. Over-expression of this gene fusion has been associated with increased cellular proliferation and invasion (22). *TMPRSS2-ERG* gene fusion has had promising results as a PC biomarker in combination with the non-coding RNA *PCA3* (24).

1.7 Current biomarkers for PC

As mentioned, PSA testing is the main diagnostic test used in clinics. Normally PSA is secreted from the prostatic epithelium into the secretary ducts, then onwards into the seminal fluid (18). Upon PC initiation, the basal cell layer may become compromised, allowing PSA to leak into the circulation, causing a rise in its concentration in the blood. Unfortunately, PSA testing can be more sensitive than specific as it can be indicative of benign prostatic hyperplasia, prostatitis or altered due to certain medication. More specifically PSA cannot distinguish between PC stages, or the metastatic state of the disease (18). This causes implications regarding accurate therapeutic decisions, especially as PSA testing can give rise to false positives (18). A concentration above a 4ng/ml threshold is used as an indicator for a prostate biopsy to be taken. 40-50% of diagnosed cases, are classified as indolent cases (clinically insignificant PC), causing

unnecessary treatment. On the opposing hand, false negatives miss 20-30% of cancer cases (18).

There have been developments to incorporate the PSA serum test with different molecular versions of the protein and the rate by which it increases, to try and enable a more refined test. For instance, the rate of total PSA (tPSA) increases PSA velocity (tPSAV), that could hold some potential diagnostic value (18). This holds importance in patients with a history of raised PSA blood concentrations, indicating prostate disorder. Again, this is not completely reliable as false negatives are mis-diagnosed. The prostate health index (PHI) was approved for use in the United States, Europe and Australia (25). This combines tPSA, free PSA and truncated PSA to aid in clinical decision-making (18). Recently, it has come to light that small non-coding RNAs such as micro RNAs (miRNAs) can have diagnostic and prognostic values. miRNAs can either be oncogenic or tumour suppressive, dependent upon the stimuli and type of cancer. For example, members of the oncogenic microRNA family such as miR-21, miR-125b, miR-221 and miR-222 have been noted to be up-regulated in advanced PC (18). As microRNAs are found in tissues and serum, they are stable against the degradation by RNases and freeze thawing, therefore they qualify as non-invasive biomarkers (26).

1.8 Treatment options

The AR is implicated in PC progression, thus therapies rely on targeting the AR signalling pathway. Therapy that targets the AR signalling cascades is known as androgen ablation therapy (AAT). Firstly anti-androgens such as Flutamide and Bicalutamide, both androgen receptor antagonists can be administrated (27). Anti-androgens bind to the AR through competitive antagonism preventing interaction between androgens and the AR. Anti-androgens hold the AR in an inactive state and recruit co-repressors of the AR such as nuclear receptor co-repressor 1(NCoR) and silencing mediator for retinoid and thyroid receptors (SMRT). These closely related co-repressors work in synergy with histone deacetylases leading to condensing of the chromatin structure (27). Co-repressors mediate binding by extending LXXLL-like motifs located at the C terminal of both NCoR and SMRT, these are named co-repressor nuclear receptor boxes (27).

Moreover, another anti-androgen therapy, Enzalutamide can inhibit the translocation of the AR towards the nucleus, inhibiting DNA binding and stops the recruitment of co-activators. This drug has proved to be successful in establishing anti-tumour activities irrespective of previous chemotherapy treatment (28).

Though a highly used treatment option, anti-androgens do not eliminate the main circulating androgen, testosterone, thus Luteinizing hormone-releasing hormone (LHRH) agonists/antagonists are used in combination with anti-androgens to produce higher treatment efficacy. They act as an agonist for the pituitary LHRH receptors initiating a rise in the luteinizing hormone (LH), follicle-stimulating hormone (FSH) and testosterone. Constant activation of these receptors results in a castration level of testosterone. With regards to LHRH antagonists, this signaling cascade is completely inactivated resulting in a faster inhibition of testosterone production (29).

Often in some cases, use of anti-androgen therapy can promoter AR gene mutations, that can result in Flutamide stimulating the AR signalling pathway, causing a relapse in combination therapy, which is the case for a third of patients (30). Needless to say, these treatment options are simply targeted for the androgen dependent disease. 80% of patients undergoing androgen ablation therapy have a positive outcome, however if metastasis is present, after 12 months of AAT the disease progresses causing relapse and is resistant to further AAT therapy (30).

In terms of castration resistant PC (CRPC) there are a limited number of treatment options. One breakthrough in CRPC treatment was the rediscovery of Abiraterone Acetate by the Institute of Cancer Research (31) Abiraterone is an effective oral irreversible inhibitor of the CYP17 enzyme (32). This enzyme can be found in the endoplasmic reticulum (ER) of the testes, adrenal glands and ovaries and is responsible for the synthesis of cortisol and androgens (32). The first use of Abiraterone in humans showed that a daily dose of 800mg was successful enough to reduce the levels of testosterone to undetectable amounts (32). The regulation of CYP17 is determined by cytochrome B5. Usually a high ratio of CYPB5/CYP17 is found within the testes where production of androgens is high and low in the region of the adrenal glands (32).

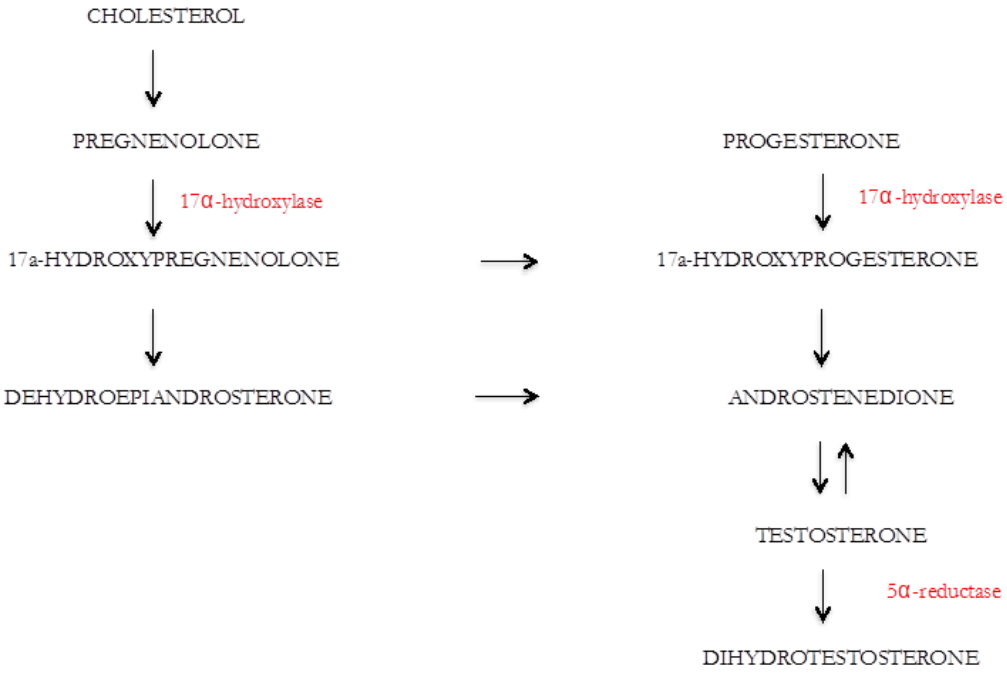

Figure 1.2. Androgen biosynthesis. Enzymes represented in red. Image adapted from (33).

Patients that have relapsed with resistance to anti-androgen therapy are termed castration-resistant. These patients are then treated with taxane-based chemotherapies. However, if patients then become resistant to taxane-based chemotherapies such as Docetaxel, an alternative is available, namely Cabazitaxel. Phase I clinical trials demonstrated that not only did Cabazitaxel overcome cases of CRPC which had not been exposed to chemotherapy before but also Docetaxel pre-treated cases of CRPC. After Phase II and III of clinical trials, the US Food and Drug Administration (FDA) approved Cabazitaxel for advanced cases of PC (32).

Recent advances propose that augmenting the immune response of the patient may be beneficial in terms of a valid therapeutic agent. An array of immunotherapeutic methods is under investigation by clinical trials. Either as a single vaccine, or in conjunction with chemotherapy and radiotherapy, agents aims to modulate the activity of T cells (34). Sipuleucel-T was the first cancer vaccine to receive the FDA administration approval (34). This was based on the evidence that Sipuleucel-T prolonged overall survival of men with CRPC. Stages of Sipuleucel-T treatment begin with the removal of autologous cells via leukapheresis, these are then processed and are coupled with the vaccine target. Following this, the product is intravenously administrated into the patient (34). Prostvac-VF is a viral vaccine made of two recombinant viral vectors that each encode for PSA, B7-1, intracellular adhesion molecule 1, and lymphocyte function-associated antigen 3. Currently, Prostvac-VF is being assessed for CRPC in clinical trials (35). Immunotherapy remains to be further explored in PC, as the number of prostate tumour specific antigens are limited.

1.9 Stage and Grade of PC

Accurate staging of PC is essential for correct prognosis and treatment. The tumour, node, metastasis (TNM) system is the most widely used clinical staging system for PC in deciphering the spread of cancer. In terms of how well differentiated the PC tissue is, the Gleason grading system is the most widely used for pathological staging. Donald Gleason formulated the PC grading system in 1966 (36). PC was unique in the way it was graded as it was solely based on the glandular epithelial architecture rather than cytology. The five tier grading system ranges from 1 meaning well differentiated to 5, the most poorly differentiated pattern. As different areas of the PC often have varying grades, a grade is allocated to the two areas that make up most of the cancer (36). The

grade of these two areas is added together to formulate a Gleason score. The lowest Gleason score a PC biopsy can have means it is well differentiated and less likely to be aggressive. A high Gleason score, confers to a more aggressive and less differentiated cancer.

1.10 Bone metastases from PC

PC has a strong tendency to metastasise to the bones, evidenced by the majority of patients with advanced PC possessing skeletal metastases. The tumour cells infiltrate the trabecular bone of the axial skeleton as well as the proximal ends of the femur. One theory to why PC cells settle within the bone environment is based around the network of veins that receive blood from the prostate, the Batson plexus (37). Between the Batson plexus and the vertebral column a large amount of metastatic PC cells are found in PC patients. These cells form sinusoids, reducing the blood flow rate, facilitating entry of these cells into the bones. PC cells in particular have a strong affinity to attach to the bone epithelium through the recognition of certain protein receptors such as integrins. Tumour cells first bind to the bone-marrow endothelium-specific lectin with low affinity and then firmly adhere onto a bone marrow endothelium-specific integrin. Finally the tumour cells produce proteolytic enzymes to break down the basement membrane of the bone marrow microvessels, where they are able to colonize in the bone environment (37). PC metastases almost always form osteoblastic lesions (with some osteolytic lesions) in the bone, producing a bone-forming phenotype that can be detected via radiographical and histological analyses (38).

1.11 The androgen receptor (AR)

1.11.1 The AR

The AR, a steroid hormone activated transcriptional factor belongs to the nuclear receptor superfamily. The AR gene locus maps to chromosome Xq12 and encodes for a protein with three main functional domains; the N terminal domain (NTD), DNA-binding domain (DBD) and the ligand binding domain (LBD) (39) (figure 1.3). Exon 1 transcribes for activation function 1, exon 2 and 3 encode for the DBD and exon 4-8 encodes for the LBD (40). During embryogenesis, production of androgens by the male foetus causes an AR signalling cascade which is responsible for the male phenotype and is critical for prostate gland biology (39).

1.11.2 The N-terminal domain (NTD)

Exon 1, in the AR gene encodes for the NTD, which is the least conserved out of the four domains (41). The NTD contains two polymorphic trinucleotides that encodes for poly-glutamine (Poly-Q) and poly-glycine (Poly-G) tracts. Variations within these polymorphic regions are associated with altered AR transcriptional activity *in vitro* (42). Variations in the Poly-Q regions are responsible for degenerative neuromuscular diseases such as Kennedy Syndrome. The variation can be between 11-31 repeats and ≤18 repeats has been associated with the onset of PC (42). The NTD allows the AR to recruit co-regulators stimulating androgen dependent transactivation of the AR. The NTD possesses the activation function 1 (AF-1) element that differentiates it from other steroidal receptors that use the activation function 2 element (AF-2) found in the LBD (43).

1.11.3 Mutations in the NTD

Mutations found within the NTD accounts for a third of all mutations in the AR. Many of them are a result of androgen ablation therapy. Located with the ligand dependent TAU-1 region, two mutations at amino acid positions 142 and 221 were discovered in CRPC patients (41). At position 142, valine is substituted for glycine whereas at position 221, aspartic acid is substituted for histidine. Shorter CAG repeats have a positive correlation with a higher PC incidence. Thus these mutations may contribute towards the initiation of the disease and its progression (41). Mutations within the NTD can lead to heightened AR transcriptional activity.

1.11.4 The DNA-binding domain (DBD)

Exons 2 and 3 encode for the two zinc fingers found within the DBD (41). The DBD carries out the responsibility of binding the AR to AR-specific DNA sequences situated within androgen responsive genes. Sequencing analysis of the AR DBD illustrated that it is comparable to the Glucocorticoid (GR), Mineralocorticoid (MR) and Progesterone receptor (PR), all members of the steroid receptor family (42). Three α helices form two zinc fingers along with a C-terminal extension that creates the basic DBD structure. Situated within the first zinc finger is a P-box which is a conserved motif, allowing interaction between specific nucleotides and the DNA within the major groove. The second zinc finger consists of a D-box where receptors are able to bind to and homodimerise (41).

1.11.5 The ligand binding domain (LBD)

The AR LBD found at the C-terminus binds specific ligands (androgens) such as testosterone and dihydrotestosterone (DHT) to the AR. Therefore, this interaction holds immense importance in the androgen signalling cascade, as ligand bound AR increases AR stability and initiates its translocation towards the nucleus. Without ligand, the AR is found in the cytoplasm of cells bound to heat shock proteins (HSP) and chaperones which hold the AR in an inactive state by association of cytoskeletal proteins (41).

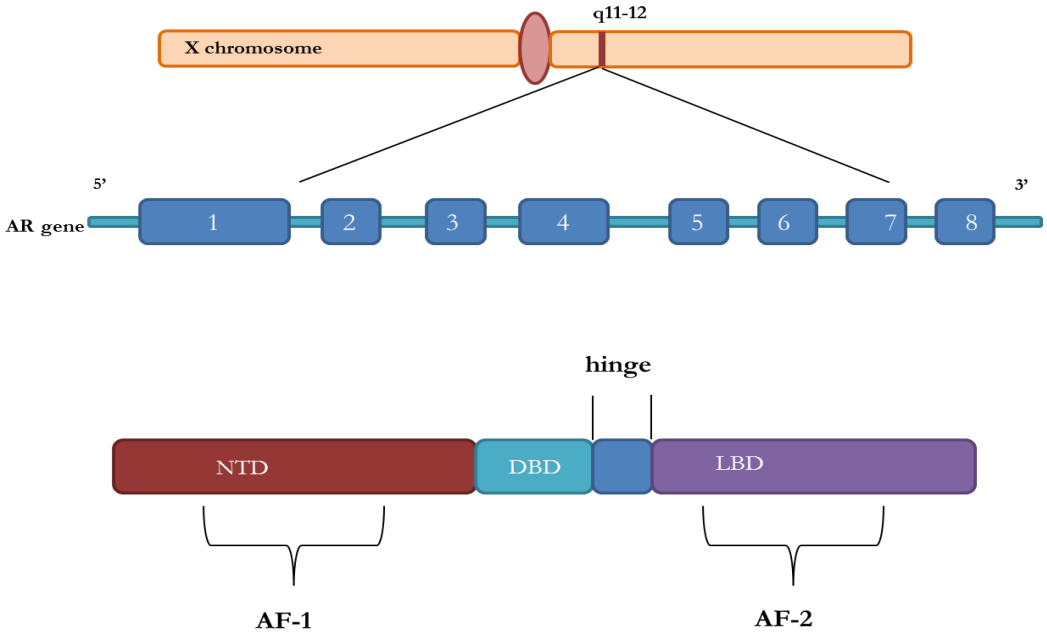

Figure 1.3. The chromosomal location of the AR on the X chromosome. The gene representation of the AR and how this gene transcribes into the AR protein. NTD = N-terminal domain, DBD = DNA binding domain, LBD = Ligand binding domain. AF= activation function. Figure adapted from (44).

1.11.6 Transactivation of the AR

The LBD of steroid hormone receptors fold into 12 helices that form the ligand binding pocket. The folding over of helix 12 in the AR leads to the disclosure of a groove that binds a region of the NTD. Ligand activation of the AR induces its conformational change allowing the formation of AR dimers on androgen response elements (AREs). To increase the rate of target gene transcription, co-activators are recruited, along with chromatin remodelling complexes. Co-activators potentiate the interaction of the AR with basal transcriptonal machinery and also covalently modify histones. Chromatin remodelling proteins ensure the accessibility of nucleosomal DNA to transcriptional factors (45).

1.11.7 Co-activators of the AR

The regulation of the AR transcriptional activity is highly regulated by both co-activators and co-repressors. The AR binding to chromatin occurs in competition with nucleosome histone proteins. AR co-activators aid AR binding to the chromatin by recruitment of chromatin modifying enzymes (39). Such co-activators of the AR include SRC/p160 family members, which bind to the DBD and NTD via TIF2 and carboxyl terminal domains of the AR. Characterisation of the SRC family of co-activators includes an N-terminal tandem basic helix-loop-helix, a C-terminal glutamine rich region and three LXXLL motifs within the central portion of the protein (39). Two major functions are carried out that modulate AR activity. Firstly, p300 a class I co-activator causes the recruitment of transcriptional machinery to nuclear receptors and secondly class II co-activators such as p160 proteins which recruit histone acetyltransferases (HAT), resulting in a more open chromatin structure (39).

1.11.7.1 p300 co-activator

p300 is known to be an adaptable co-activator among steroid receptors such as the oestrogen and androgen receptor. Originally p300 was acknowledged to be bound to the adenovirus E1A and cAMP responsive element binding protein (CREB) (46).This transcriptional co-activator can regulate gene transcription through a manner of mechanisms. Firstly, it can act as a scaffold between DNA bound transcriptional factors and the basal transcriptional machinery (47). Secondly, p300 carries out histone acetyl transferase activity by transferring an acetyl group to the ε-amino group of a lysine residue on histones (48), easing the chromatin structure allowing more accessibility for the transcriptional machinery (47). Not only can p300 acetylate histones, it can acetylate proteins such as transcription factors. This can change protein-protein interactions, protein-DNA interactions or even the half-life of specific proteins (47). In terms of activating the AR, p300 can do so under the influence of hormone induction, causing full ligand induced transcriptional activity of the AR and also influencing the growth of prostate cancer cells (47). The exact acetylation of the AR by p300 occurs at a phylogenetic conserved motif found within the hinge region (46). p300 over-expression instigated heightened cell proliferation and a change in nuclear morphology causing the development of aggressive disease features in PC cells (49). Moreover, it was also found that over-expression of p300 was found in other tumours such as colorectal and breast, indicating its more general role (49). Interestingly, it was shown that p300 was vital for the induction of AR activity by IL-6 in the absence of androgen (49). This was identified through IL-6 induced activation of the *PSA* gene promoter in PC cells (49). Moreover, through the suppression of p300, IL-6 activation of the AR was disrupted. Indeed, silencing p300 with siRNA reduced the proliferation of IL-6 induced PC cells. This highlights the significance of p300 working in synergy with IL-6 aiding the survival of cells in androgen independent PC (46).

1.11.7.2 P160-SRC co-activators

The first cloned nuclear receptor (NR) co-activator was steroid receptor co-activator -1 (SRC-1) (50). SRC-1 interacts with an array of NRs in a hormone dependent manner, increasing their transcriptional activity. Two other members of the SRC-1 family are identified as SRC-2 and SRC-3 and together they form the p160 SRC family, all possessing three structural domains. Firstly the most conserved domain is the N-terminal basic helix-loop-helix-Per/ARNT/Sim that partakes in protein-protein interactions. The central domain contains three LXXLL motifs accountable for the interaction with NRs. Lastly, the bHLH-PAS domain is responsible for the interaction with transcriptional factors such as myogenin ,MEF-2C and AR (50). The C-terminus domain comprises of two transcriptional activation domains (AD1 and AD2). AD1 binds to the p300 histone acetyltransferase that is essential for SRC mediated transcriptional activation. Further, SRC-2 interacts with histone methyltransferases. SRCs can also be co-activators for transcriptional factors such as E2F1, SMADs and STATs. SRCs therefore regulate diverse physiological functions through both NRs and non-NR transcriptional factors.

1.11.8 Co-repressors of the AR

By definition, co-repressors of the AR are molecules that bind to the AR and cause the enlistment of chromatin modifying enzymes and repress its transactivation potential. However this is not the only mechanism by which these molecules repress the AR, as alternative mechanisms include inhibition of the AR N/C terminal interactions, inhibition of co-activator recruitment or disruption of nuclear translocation of the AR (51). An overview of the mechanism involved in AR co-repression is given in (figure 1.4).

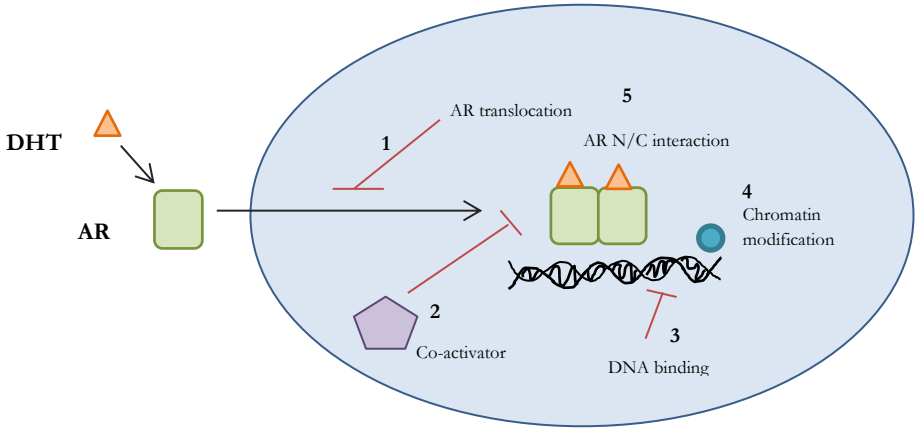

Figure 1.4. Representation of the diverse co-repressor mechanisms (51). Mechanisms include (1) inhibition of the AR translocation, (2) inhibition of co-activator recruitment, (3) inhibition of AR binding to DNA, (4) inhibition of chromatin modification and the (5) inhibition of the AR N/C interaction.

Chromatin modifying co-repressors cause the recruitment of histone deacetylases (HDACs) to the DNA-bound AR complex. HDACs can prevent co-activators acetylating lysine residues on histone tails, causing DNA condensation, causing promoter inaccessibility (27). However HDACs cannot bind to DNA directly and need secondary molecules to activate their enzymatic activity. For instance, HDAC3 needs either NCoR or SMRT to aid in its function. Furthermore, HDACs may promote alternative routes to administrate AR function. One mechanism involves HDACs' ability to counterbalance the AR hinge region acetylation by p300. Thus, although HDACs can condense chromatin with the aid of NCoR and SMRT, they can also elicit their function by modifying the AR itself or by interfering with AR co-activators (27). AR promoter or UTR mutations are rare in CRPC patients (52).

1.11.8.1 Cyclin D1 as a co-repressor of the AR

Cyclin D1 has a crucial role in the cell cycle as a vital component of the CDK4 kinase complex. It binds CDK4 directly, causing the CDK4 mediated phosphorylation of retinoblastoma (Rb) (53). In terms of steroid receptor activation, cyclin D1 has been shown to bind to the oestrogen receptor (ER) causing the activation of its transactivation domain in the absence of ligand. For cyclin D1 to carry this out this function, a leucine rich LXXLL-like motif is needed, that aids the link between steroid receptor and co-activators (53). Mutations within this LXXLL-like motif lead to the production of a protein that can bind to the ER but fails to recruit co-activators (53).

However in PC, cyclin D1 has an opposing role whereby its interaction with the AR causes the repression of its transactivation. The repression occurs by cyclin D1 binding to the N-terminal domain with high affinity, inhibiting AF-1 (53). Interestingly, ectopic expression of cyclin D1 in the LNCaP cell line reduced their proliferation capacity (53).

The AR and cyclin D1 migrate between the cytoplasm and the nucleus in response to cellular signals. In particular, cyclin D1 is exported to the nucleus in response to anti-mitogenic signals through GSK-3β-mediated phosphorylation (53). As the AR translocates to the nucleus in response to ligand binding, it is thought that cyclin D1 inhibits AR activity through cytoplasmic sequestering (53). A nuclear cyclin D1 mutant protein, cyclin D1-T286A was found to be unable to be phosphorylated by GSK-3β, therefore was unable to be transported from the nucleus (53). Interestingly, this mutant form of cyclin D1 was still able to repress AR activity.

To identify the site at which cyclin D1 is active, mapping studies were carried out by Petre *at al.,* (53). This determined the NTD of the AR as the main region where cyclin D1 binds, specifically between amino acids 1-502 (53). On the other hand, according to Reuens *et al,.* (54) it was observed that cyclin D1 was able to bind to amino acids 633-668 within the hinge region of the AR. However, this interaction was only observed as a two-fold higher expression than that of the background level. Therefore, this suggests that cyclin D1 can bind to the NTD of the AR that is highly relevant as this is the most common binding site for co-activators of the AR (24).

1.11.8.2 SMRT and NCoR as co-repressors

The silencing mediator for retinoid and thyroid hormone receptor (SMRT) and its close relative nuclear receptor co-repressor (NCoR) are homologous to one another, and both proteins are 270kDa in size (27). The C-terminal of NCoR possesses three nuclear receptor interaction domains, whereas SMRT contains just two. These nuclear receptor interaction domains aid with the interaction of SMRT and N-CoR with the LBD of nuclear receptors (27). The functional motifs of these interaction domains contain 'coRNR boxes' with the consensus sequence L-X-X-I/H-I-X-X-X-L/I (L: leucine, I: isoleucine, X: any amino acids) (27). The regulation of the binding affinity is affected by any conformational change of the nuclear receptor in response to ligand. Specifically binding of ligand to nuclear receptors induces the movement of helix 12 which is essential for the binding of SMRT/N-CoR to nuclear receptors (27).

1.11.8.3 SMRT and NCoR, mechanism of action

Both SMRT and NCoR have previously been identified to inhibit the transcriptional activity of antagonist bound progesterone receptor (PR) and ER (55). In addition to steroidal nuclear receptors, SMRT/N-CoR can carry out a repressive function with other nuclear receptors such as RevErB and the orphan receptor DAX1. The unrestrained activity of SMRT and N-CoR is also seen in an array of transcriptional factors involved in many cellular functions, such as Bcl-6 which plays a role in the suppression of inflammation (56). Despite there being accumulating evidence to suggest SMRT and N-CoR's ability to repress nuclear receptors activity, less is known about their function involving the AR. Moreover, the ability of SMRT and N-CoR to bind to steroid receptors is weaker than that of non-steroidal receptors (57). However, it is interesting to note that Tamoxifen, the well-known ER antagonist enhances the

interaction between NCoR and the ER which is a contributing factor in aiding Tamoxifen's ability to suppress the ER's targeted gene expression (57).

1.11.8.4 SMRT and NCoR interaction with the AR

Previous studies evidence that a reduction of SMRT/NCoR may link to the ligand-independent activation of the AR, leading to PC progression (27). However, the idea that these co-repressors are able to repress the activity of the AR is more complicated than thought. This is due to studies over-expressing both SMRT/NCoR, failed to suppress the androgen responsive gene transcription in PC cell lines. This refers to the fact that simply over-expressing these co-repressors does not represent what occurs under physiological conditions. However, rather than effecting protein production of these co-repressors, post-translational modification of SMRT/NCoR was found to enhance ligand bound repression of the AR. Specifically, protein kinase A (PKA) is capable of binding directly to the RD1 domain within NCoR, phosphorylating ser-70 (27). This causes an increased nuclear localisation of NCoR where it can carry out its repressive function of the AR (27).

1.11.8.5 Prohibitin (PHB) as a co-repressor of the AR

PHB, a highly conserved 32kDa protein across all species, yeasts and plants displays tumour suppressor characteristics (58). It resides within the inner membrane of the mitochondria, where it co-interacts with a similarly structured protein, BaP37 (PHB2). It has also been identified to reside within the nucleus of ovarian granulosa, breast epithelial and prostate epithelial cells. Within the nucleus, it co-interacts with NCoR, HDAC1 and Rb (59). This interaction inhibits transcription of genes regulated by members of the E2F family. Breast cancer cells treated with Tamoxifen, displayed inhibition of E2F activity through the recruitment of PHB. PHB's participation within a repressive complex of proteins, is thought to hinder growth within hormone sensitive cancer cells. This is relevant to PC, as it was previously shown that androgen stimulation caused a repression of PHB mRNA and protein expression in the LNCaP cell line. This allowed progression of the cell cycle (58). This implies that PHB plays a role in androgen-regulated cell cycle of PC cells which shall be discussed further on.

1.12 AR in the normal prostate gland

Testosterone is the main circulating androgen produced by the testes, with less than 5% of androgen production being made by the adrenal glands. Other androgens include DHT that is a metabolite of testosterone and has a five-fold greater affinity for the AR than testosterone and is produced at target organs. Androgenic precursors such as androstenedione, are produced by the adrenal glands can either be converted to testosterone in the testes by dehydrogenation or converted to estrone (an estrogen) by aromatization (60). DHT is essential for the prenatal development of the prostate gland. The enzyme responsible for the production of DHT is known as 5α-reductase (isotype 2 is the main enzyme found in the prostate gland). In the absence of 5α -reductase the prostate gland can be undetectable during foetal development, suggesting 5α -reductase's crucial role in its development. Heinlein *et al,*. (61) showed the absence of 5α -reductase can cause a partial formation of the prostate gland in response to low levels of DHT, this emphasises that a certain threshold level of DHT must be reached for complete prostate morphogenesis. Models such as AR knockout (KO) mice, testicular feminised mice (TFM) and individuals who have succumbed to AR mutations rendering them androgen insensitive, validate that the AR is vital for the development of the prostate gland and other androgen regulated tissues (61).

Prostatic bud formation is reliant upon a functional AR within the urogenital mesenchyme that allows interactions between the epithelium and stroma to commence. This highlights that is it the mesenchyme that secretes growth factors responsive to DHT that then act on the developing epithelium. Androgens continue to regulate the prostatic epithelium throughout adulthood, and it is the epithelium that is transformed in prostate adenocarcinoma (61).

1.13 AR in the bone, muscle and immune system

During the growth of a male adolescent, the production of androgens influences the skeletal size and shape. This is depicted by the misuse of androgen treatment, as often men self-administrate high doses of androgen for bodybuilding purposes (62). During adulthood, production of androgens maintains bone homeostasis, as AR expression is seen in bone and bone marrow cells (63). Depleting androgen levels leads to bone remodelling and in some cases, bone loss. Germline deletions of the AR in male mouse models displayed low bone mass with a high bone turnover as well as decreased trabecular and cortical bone volume. This emulates androgen deficiency in humans (63).

Androgens within muscle tissue increase both muscle mass and strength. This is in accordance with the withdrawal of testosterone causing muscle mass and strength to lessen. During adulthood, androgens are essential for men to reach peak muscle mass, by influencing myogenic commitment. Androgens also play a role in maintaining muscle mass through suppression of atrophy pathways. Men undergoing androgen deprivation therapy (ADT) displayed reduced upper limb strength as opposed to lower limb strength, indicating androgens influence different anatomical regions. However, there was no effect seen on muscle endurance with ADT, suggesting that slow twitch fibres are less responsive to androgen withdrawal (64).

The AR-signalling pathway has also been identified to function within the immune system. For example, the AR is consistently expressed in the neutrophil lineage from the proliferative precursors to the mature neutrophils. Women suffering from polycystic ovary syndrome with hyper-androgenism have a higher neutrophil count, suggesting that androgens can promote neutrophil production. Supporting this concept, AR knockout mice models demonstrated a 90% reduction in neutrophil count when compared to the wt mice. In human cases, patients undergoing ADT, tend to have a mild reduction in neutrophil count, suggesting the AR has a more intense effect on neutrophils than androgens. Moreover, restoring the AR in AR knockout mouse model resulted in macrophage progenitor cells salvaging neutrophil production, indicating the role the AR has in neutrophil differentiation (65).

1.14 AR in females

The AR is primarily seen to play a role in the development of male-specific phenotypes. However the signalling cascade has also been identified in the development of female reproductive organs and their functions. Specifically, the AR is expressed in the mammary gland, ovaries, uterus and the fallopian tubes of various mammalian species. Within the ovaries, testosterone is produced by theca cells in response to luteinizing hormone. During early follicular development, androgens directly influence the function of the ovaries, however during late pre-ovulatory development androgens then serve as precursors for the production of oestrogens.

In mammalian species, the AR is expressed in different cell types of the ovaries such as stroma, oocytes and granulosa. Exposure of high serum androgen in women leads to the production of larger ovaries with increased numbers of antral follicles. In mice, both testosterone and DHT promote follicular growth, and the ovulation rate in pigs was also enhanced with DHT treatment (66). There is little evidence to understand how the AR influences the development and function of the uterus. However, in a porcine study, it was observed that the AR and ERα interact allowing the regulation of the uterine growth and endometrial gene expression (66).

Interestingly, the secretion of testosterone seems to play a role in breast tissue development. Activation of the AR by DHT is thought to suppress the growth of breast tissue. The majority of breast cancer patients expressing the oestrogen receptor are also positive for the AR and progesterone receptor (PR), and have a longer disease free interval than patients negative for the PR, HER2, ER receptors (67). However, whether the AR signalling pathway is beneficial or detrimental in breast cancer is yet to be discovered and will likely depend on the subtype of the cancer and the menopausal status of the patient (67).

Premature ovarian failure syndrome is depicted by the decline of ovarian function. Knockout of AR (-/-) in 8 week old mice demonstrated a decrease in follicle numbers and a weakened mammary development. Also the number of pups per litter was halved when compared to control mice. At 40 weeks old, the AR (-/-) mice display complete loss of follicles and therefore are infertile (68).

1.15 AR in PC

Androgens are mediators in PC pathogenesis, evidenced by a positive correlation observed between AR expression, a high Gleason Grade and the vascularity of the tumour (41). Even upon AAT, the AR is expressed heterogenously and no change is seen in the pattern of heterogeneity. Interestingly, mutations within the AR have been documented and could elude to how the AR signalling is still active in the absence of androgens. For example, AR mutations can consist of loss of function and gain of function mutations, both of which are associated with androgen insensitivity syndrome (AIS) and PC respectively (41). Specifically within the AR gene, four main types of mutations have been established. These consist of single point mutations, nucleotide insertions or deletions, complete or partial gene deletions and intronic mutations. It is extremely infrequent for AR mutations to evolve in the earlier stages of PC with only 10-30% of patients with CRPC carrying AR mutations (41). There have been over 150 mutations found within the AR in PC tissue, rather than germline mutations, somatic mutations have been noted consisting of single base substitutions. 45% of these somatic mutations arise in the LBD of the AR, whereas 30% arise in exon 1. It is these gain of function mutations which may allow non-specific ligands found in the body such as oestrogen and adrenal androgens to activate the AR signalling pathway causing prostatic epithelial cells to grow in an castration resistant manner (41). Resistance to current therapies is a worrying dilemma, for example mutations in the LBD can cause resistance to Enzalutamide, allowing the AR to become active even in the presence of anti-androgens (41).

1.16 Pathogenesis of androgen independence

It has been suggested that PC pathogenesis is predominantly AR regulated, thus termed 'androgen dependent'. Upon androgen ablation therapy, the AR is no longer able to continue its signalling cascade, thus growth and progression of cancerous cells and androgen regulated cells is halted. Unfortunately, in some cases the cancer initiates adaptation to the new environment in the absence of androgens and begins its own mechanisms of survival. Thus 'androgen independence' occurs. There have been numerous models to support how and why androgen independence arises (figure 1.5).

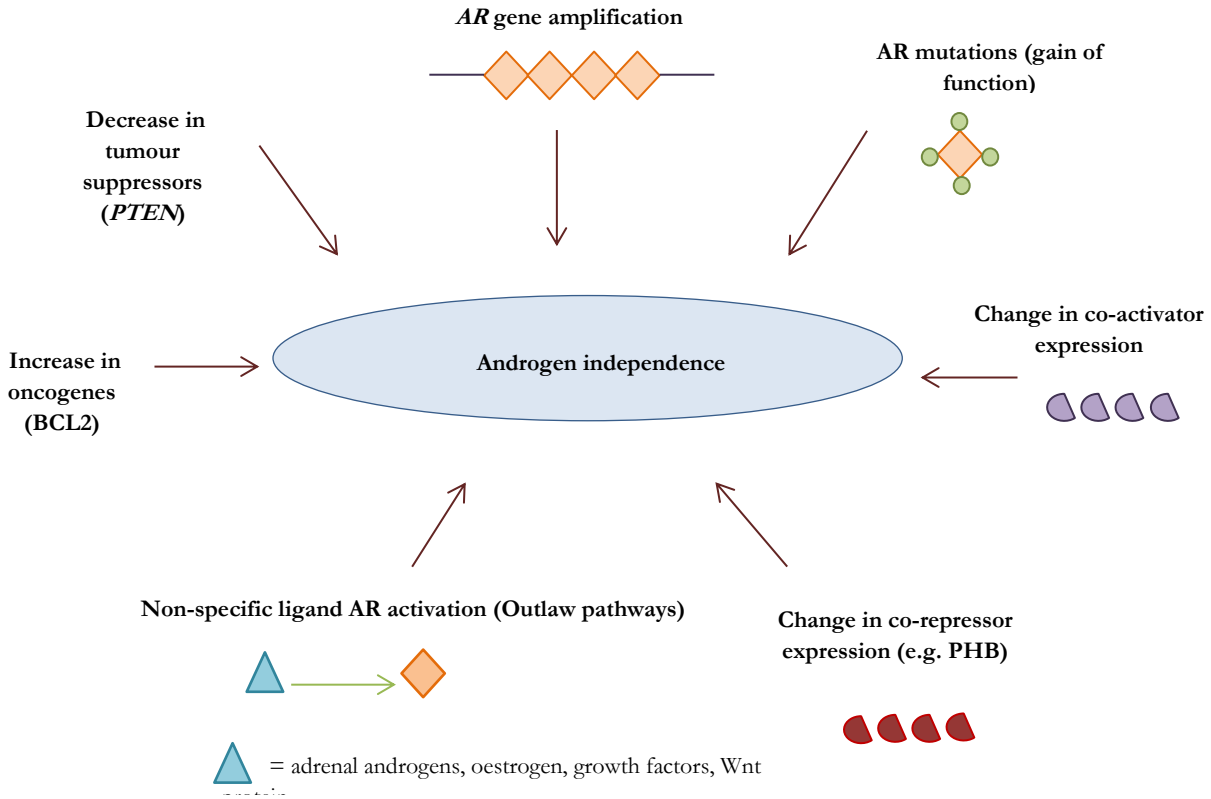

Figure 1.5. Image adapted from Saraon *et al.,* (69). The various mechanisms of AR adaptive activation that have been theorised to date.

1.16.1 AR amplification

25-30% of androgen independent PC (AIPC) cases have AR augmentation both at mRNA and protein level (69). Worryingly, *AR* gene amplification has not been noted in untreated PC cases, leading to the assumption that androgen ablation may lead to the onset of this phenomenon. This AR over-expression initiates cancerous cells to become sensitized to a low androgen environment, promoting more proliferation and survival, ideal for cancerous cells to overcome hormonal therapies used in clinics. In the absence of *AR* gene amplification, over-expression of the AR can still occur, indicating that elements such as epigenetics and miRNAs can regulate this event, independent of gene amplifications (69).

1.16.2 AR mutations

Further, it is particularly rare to find *AR* gene mutations in early onset PC cases (0-4%), however this percentage increases as the grade of the tumour also increases, especially in androgen independent cases. Originally, the first described gene mutation was a mis-sense mutation at codon 877 of the *AR* mRNA causing a substitution of threonine to alanine in the LNCaP cell line. This mutation causes the ligand-binding domain to reduce its specificity and allow non-specific ligands such as anti-androgens and other steroidal hormones to activate the AR. Further ligand binding mutations include H874Y, V715M, L701H, T877A, and Y741C (69).

1.16.3 AR splice variants

A more novel insight to AIPC is splice variants that have been seen to be over-expressed in AIPC cases. It was discovered that three splice variants, namely AR3, AR4 and AR5 are all ligand-binding domain deficient (70). Without a ligand binding domain, the AR is no longer dependent on androgen binding to cause its translocation towards the nucleus and can do so independently. Interestingly, neither androgens nor anti-androgens can activate the transcriptional activity of AR3. AR3 was identified as the most abundantly and ubiquitously expressed splice variant to be seen across a panel of human PC tissues (70). However in normal prostate tissues, AR3 expression is seen in basal and stromal cells and is absent in luminal epithelial cells. Guo *et al,.* (70) suggests that AF3 may play a role in androgen-insensitive regulation of the homeostasis found in the normal prostate gland. Although studies on these variants are still in their

preliminary stages, they could hold huge importance in unveiling how cancerous cells evade androgen ablation.

1.16.4 Non-ligated AR activation

Besides ligand activation, the AR can be activated by signalling pathways and can be induced by growth factors, cytokines and kinases in the absence of androgens.

Firstly in terms of growth factor mediated AR activation, insulin like growth factor-1 (IGF-1) is the most widely studied. IGF-1 can influence the up-regulation of co-activators such as TIF2, enhancing AR activity. Moreover, epidermal growth factor (EGF) can also potentiate AR signalling in the absence of androgens. Over-expression of the EGF regulated SPINK1 protein was seen in aggressive PC cases negative for the ETS chromosomal rearrangements (69). Both IGF-1 and EGF are ligands for receptor tyrosine kinases (RTKs) which are heavily influenced in the progression of PC. The most notorious RTK is known as HER-2/neu, that when overexpressed in PC cells cause the activation of androgen responsive genes in the absence of androgens. However, unlike IGF-1, upon androgen ablation HER-2/neu is still able to carry out its signalling pathway suggesting its independence from the AR (69).

1.16.5 Cytokines

Cytokines have also been shown to activate the AR in AIPC cases, in particular the NF-κB signalling pathway can regulate IL-6 and IL-8, which both can stimulate the AR and activate AR response genes in LNCaP cells (69). Moreover, the canonical Wnt signalling pathway causes the activation and stabilisation of a β-catenin pool that can independently interact with the AR, modifying its function. As well as activation of AR response genes, Wnt response genes can also be activated. *In vivo* studies demonstrate that the AR and β-catenin co-localise and interact with one another in xenografts in castration resistant mice (69).

1.16.6 Bypassing the androgen receptor pathway

All the mentioned mechanisms involve the AR one way or another. However in terms of the outlaw mechanism, signalling pathways can become activated independent of the AR, thus completely bypassing this system. This is known as 'true androgen independence'. For example, an important pathway known as the PI3K/AKT/mTOR pathway plays a crucial role in cancers, especially in PC. The pathway is associated with cell growth and survival during cellular stress. AKT can activate the AR via an outlaw mechanism, nevertheless it plays a vital role in the proliferation and apoptosis status of PC cells. The key tumour suppressor within this signalling pathway *PTEN,* as mentioned before is often lost, causing unregulated cell proliferation, highlighting the importance of this pathway in AIPC (71). Further, throughout androgen ablation, apoptotic signalling pathways are activated, thus anti-apoptotic factors must be released to circumvent cell death in AIPC. For example Bcl-2 is a key anti-apoptotic protein which when expressed, aids PC cells to avoid apoptosis. According to Lui *et al,.* (72) Bcl-2 detection was found in xenografts of castrated mice, upon targeting Bcl-2 with si-RNA, a deferred onset of AIPC in these mice was observed.

Both outlaw and bypass mechanisms can interact with one another to initiate the transition of androgen dependence to androgen independence. Further investigation is needed to verify the exact molecular mechanisms of this transition to depict the main mode of action to how this occurs.

1.16.7 Epigenetic alterations

Normal cellular development is regulated via epigenetic alterations. Hyper-methylation of the AR promoter is an example of an alteration that has been highly implicated in AIPC cases. It has been noted that 20-30% of AIPC cases do not express the AR, which is due to the promoter of the AR being hyper-methylated and is more prominent in severe cases than primary tumours (73). Genes that are often silenced in PC are involved in the cell cycle, cell invasion and DNA damage repair. Such genes include cyclin-dependent kinase inhibitor 2A, CD44 and methylguanine-DNA methyltransferase (MGMT) tumours (73). This could lead to further research involved in aberrantly expressed genes in PC that can translate into prognostic or diagnostic value in clinics as biomarkers.

1.17 Introduction to Prohibitin

An insight into unveiling mechanisms involved in AIPC could be due to the down-regulation of the AR co-repressors. This thesis will study the role of PHB1 (will be referred to as PHB throughout the thesis) as a co-repressor of the AR.

Ubiquitously expressed, PHB also known as B-cell-receptor-associated protein 32 (BAP 32) and its homologue PHB2 (BAP 37) are evolutionally conserved proteins expressed in an array of eukaryotic organisms (74). Remarkably, the sequence of PHB is extremely conserved across species spanning from yeast up to the rat species. The mouse and rat's PHB protein-coding sequence is virtually identical with the human sequence with a differing of one amino acid (75). The *PHB* gene was first identified in the 1980s by McClung's research group, through a screening of potential tumour suppressor genes. It was here that PHB was seen to carry out anti-proliferative functions and thus acknowledged as possessing tumour suppressor characteristics (76). Although the cellular functions of PHB have been recognised in aging, inflammation and obesity, the molecular functions of PHB in carcinogenesis is still to be fully clarified (77). Figure 1.6 shows a schematic representation of the *PHB* gene.

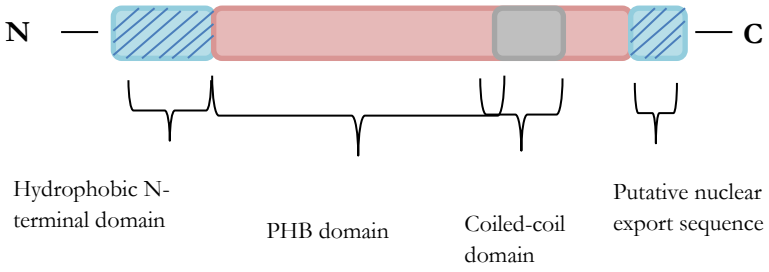

Figure 1.6. Image displaying schematic representation of the human PHB protein. N = N terminal, C = C terminal, adapted from: (78).

The *PHB* gene is located on chromosome 17q21 and consists of two alleles. One allele expresses an exon 6 associated single strand conformation polymorphism (SSCP) identified by cleavage at a polymorphic intronic EcoRI site. The second allele is not similarly cleaved (76). The PHB protein has molecular weight of 32kDa and comprises of 272 amino acid residues. PHB belongs to a family of proteins which have an evolutionary conserved prohibitin-like domain, otherwise known as band-7 family of proteins along with a transmembrane domain at the N-terminus and a coiled coil-domain at the C terminus (76). The structure of the PHB protein lacks motifs characteristic for signal transduction, nuclear localisation, ATP binding sites or transcriptional factors (76).

1.18 Cellular location of prohibitin

1.18.1 Mitochondrial prohibitin

The role of PHB was first seen in the mitochondria in a *C. elegans* model, whereby loss of PHB resulted in fragmentation and disorganisation of the mitochondria when compared to control mitochondria, which appeared to be elongated and well structured. Indeed in mammalian cells the staining for PHB is predominantly mitochondrial, therefore is it often classified as a mitochondrial marker. Correspondingly, PHB can also partake within the dynamics of the mitochondria. For example, stomatin-like protein (SLP-2) can associate with PHB within the inner mitochondrial membrane to form specialised membrane micro-domains that are associated with optimal mitochondrial respiration (79, 80). Upon depletion of SLP-2 in HeLa cells, proteolysis of PHB1 and PHB2 ensued, suggesting PHB stability is dependent upon SLP-2 during mitochondrial stress [41] that is of particular relevance as SLP-2 holds importance in the biogenesis and activity of the mitochondria (81).

The PHB protein complex found within the mitochondria embodies two subunits that physically associated with one another, namely PHB1 and PHB2 (74). Both subunits share more than 50% identical amino acids (77). Upon deletion of PHB2 gene, PHB1 is also reduced suggesting that they are mutually dependent on one another for stability. The loss of PHB1 causes disruption of the mitochondrial structure, which is evidenced by the loss of PHB2 resulting in the deterioration of OPA1 (optic atrophy 1) (82). OPA1 has a specific function in governing the formation of mitochondrial cristae and resides with the inner mitochondrial membrane. The interaction between PHB and

OPA1 was proved by PHB depleted MEF (mouse embryonic fibroblast) cells showing a highly similar fragmentation pattern which was also seen in OPA1 down-regulated MEF cells (82). The C-terminal coiled coil-domain is responsible for the interaction of the two subunits, PHB1 and PHB2, which together form heterodimers (83). These heterodimers organise into ring like structures that establishes the integrity of the mitochondrial structure and regulates mitochondrial function (76). PHB1 and PHB2 affix into the inner membrane of the mitochondria via hydrophobic stretches at the N-terminal (77). In the yeast model, PHB1 transports into the mitochondria, combines with Tim8/13 complexes (translocase of the inner membrane proteins) allowing the biogenesis of transmembrane proteins in the intermembrane space of the mitochondria (78). Moreover, PHB functions as a chaperone for newly made proteins, which form parts of the mitochondrial complex 1 (84). PHB can also act as a scaffold, enlisting membrane proteins into a lipid environment, essential for mitochondrial morphogenesis (82). The localisation of PHB within the mitochondrial membrane may hold importance in preventing apoptosis in yeast and mammalian cells, against metabolic stress (58).

Accumulating evidence suggests that PHB1 also plays a role in preventing oxidative stress in an array of cell lines. For example, oxidative stress occurring in the intestinal epithelial cells causes a drop in PHB1 levels and also in *ex vivo* lung tissue undergoing hypoxia (85). Further, knockdown of *PHB1* in endothelial cells produced reactive oxidative species (ROS) in the mitochondria, as a result of blockade of the electron transport chain (86). Conversely, over-expression of PHB1 in cardiomyocytes served a protection against hydrogen peroxide induced injury and maintained the structure mitochondrial membrane (75).

1.18.2 Nuclear localisation of PHB

Although the roles and location of PHB have been extensively defined in the mitochondria, PHB is also located in the nucleus, depending on cell types (75).

A study showed that PHB was localised to the nucleus and cytoplasm of LNCaP cells (81). In the same study, PHB was consistently expressed in the nucleus of cultured human cells, interacting with E2Fs - suppressing their function and causing the recruitment of HDAC-1 and N-CoR (81). Further, data from this study suggested that PHB translocates from the nucleus towards the mitochondria in response to apoptotic signalling occurring in transformed cells as opposed to untransformed cells (81). The export of PHB out of the nucleus is slightly more complex, as it is usually bound to other proteins such as Rb therefore it is unable to undergo passive diffusion out of the nuclear membrane. Instead it exports via short amino acid stretches known as nuclear export signals. PHB has a well-defined nuclear export signal, similar to the most common type of export sequence seen in the HIV virus and type 1 rev protein (87). This sequence classically has a core of large hydrophobic amino acids that are recognised by the CRM-1 export receptor (88). This receptor aids the nuclear transport of PHB, as the removal of nuclear export signals stopped the transport of PHB out of the nucleus. PHB was shown to localise in the nucleus in breast cancer cells, and localise to the cytoplasm in camptothecin-treated cells (89). This may indicate that PHB undergoes transport out of the nucleus upon receiving apoptotic or stress signalling. This transportation of PHB out of the nucleus in response to camptothecin seems to eliminate its interaction with E2F1 in the nucleus (89). The ability of PHB to translocate to various subcellular locations in response to different signals, along with regulating E2Fs and P53 raises the idea that depending on the environment it is placed in, it can either initiate apoptosis or enhance cell proliferation, which is rather unique.

Likewise, PHB studies in rat ovaries revealed that PHB translocates from the cytoplasm into the nucleus in atretic follicles, germinal vesicle-stage oocytes, zygotes and blastocytes. (Thompson *et al.,* 2004) (90) suggests that PHB has a regulatory role in the nucleus of theca-interstitial cells in the ovum throughout follicular maturation. This could be linked to PHB interacting with steroid receptors such as the AR and ER.

Interestingly, the PHB gene is differentially expressed in the ovaries. Within the ovary, PHB is localised to the granulosa cells and oocyte cells. PHB expression that was seen within these cell types was higher than when compared to proliferating-cell nuclear antigen (PCNA) expression during follicular maturation, suggesting the positive correlation with anti-proliferating cells and PHB expression (91). Similarly, within rat testes, expression of PHB was not noted in the mitochondria of actively dividing spermocytes (91).

1.19 PHB and the AR

PHB is known to interact with proteins that regulate the cell cycle progression and can hinder DNA replication in numerous cell types. The role PHB has in PC via interaction with the AR is further discussed.

Gamble *et al,*. (58), noted that 50% of PHB protein was diminished in LNCaP lysates (weakly metastatic), following androgen stimulation for 16 hours. This was also seen, when the metastatic and androgen independent cell line PC-3 was stably transfected with the AR. Consequently after androgen stimulation, a 30% decrease was seen in PHB protein levels (58). Moreover, to further demonstrate the interaction of the AR signalling pathway and PHB, a study carried out by (Fletcher, 2007) (92) highlighted that a decrease in PHB levels either via androgen stimulation or siRNA mediated knock down, triggered enhanced growth of xenografts in mice, due to increased AR activity. Further, it has to be noted that the down-regulation of PHB by androgens is only partly at the transcriptional level, and it is still not understood how this mechanism occurs. An alternative study (Ummani *et al.,* 2008) (93) used proteomic analysis to identify significant changes in protein expression in needle biopsies of 23 patients diagnosed with high probability of PC. Indeed this confirmed that PHB was recognised as a protein with altered expression in PC. According to (Gamble *et al,*.) (58) stimulation of LNCaP cells transfected with a PHB expression vector with DHT failed to enter the cell cycle, with 97% of the cell population remaining in the G1 state, compared to 80% of cells entering the cell cycle that were not transfected (58). Further, the importance of PHB down-regulation was also assessed. Small inhibitory RNA (si-RNA) oligos complementary to either exon 1 of PHB or to the 3'UTR of PHB were designed and stably transfected into LNCaP cells. FACs analysis of cell cycle entry highlighted that cells with the PHB si-RNA had an increase in cell population entering the S/G_2 M

phase. Specifically 2% of these cells were seen in this phase when compared to control cells, which increased to 10% after DHT stimulation.

There are no specific DNA binding-motifs of PHB, however chromatin bound PHB has been seen. This chromatin bound fraction, can be displaced upon androgen treatment in LNCaP cells, highlighting the dynamic opposing interaction between AR activation and PHB bound-chromatin (94). The dissociation of PHB from chromatin could either be due to androgen stimulation of the AR, or serum derived growth factors allowing the progression of the cell cycle. PHB closely associates with HDACs and HP-1 proteins which are known chromatin modifying proteins. Knockdown of PHB led to more AR-bound chromatin in LNCaP cells in response to DHT treatment. Over-expression PHB had the opposite effect, whereby less AR bound chromatin was seen (94). As the down-regulation of PHB is implicated in the progression of the cell cycle, it could have a role in the onset and progression of PC, especially in cases where the cancer has sensitised to a low androgen environment. However, how the tumour acquires a decrease in PHB levels via androgen stimulation still needs to be understood (figure 1.7). Moreover, there may also be other mechanisms that completely bypass the AR signalling pathway, causing a down-regulation of PHB such as oncomiRs, which also needs to be elucidated.

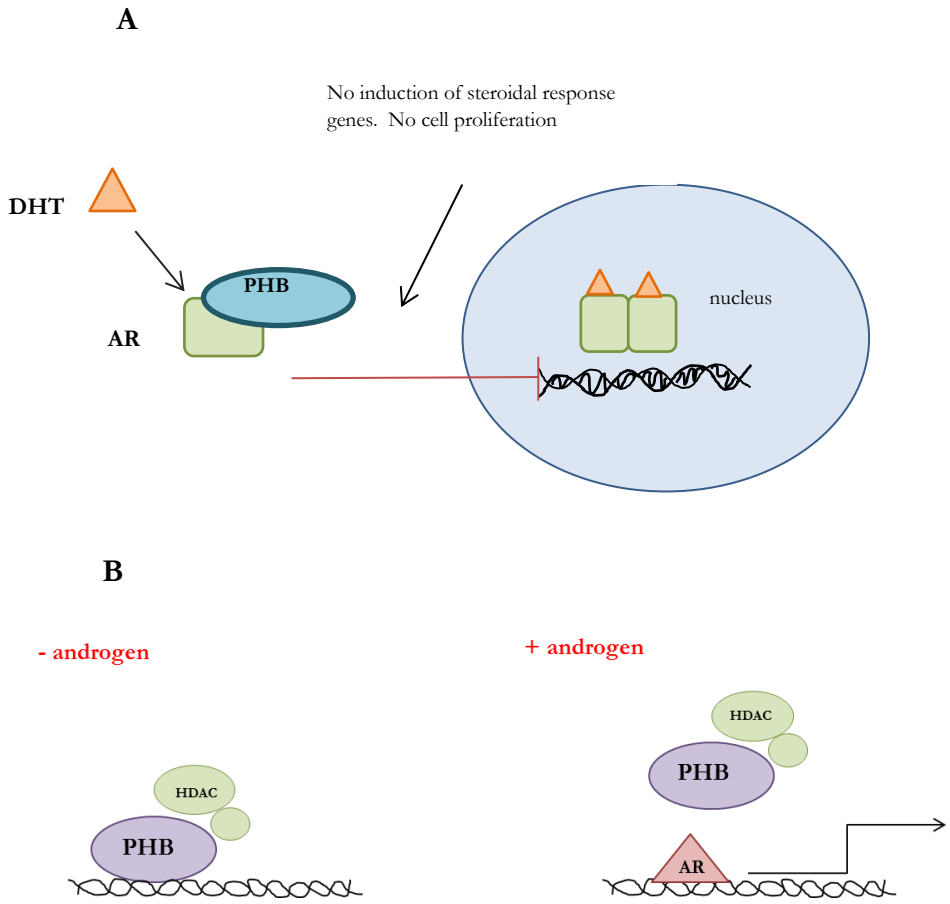

Figure 1.7. Mechanism of action of PHB. **A**, schematic representation of PHB repressing the translocation of the AR-DHT complex towards the nucleus, thus transcription of androgen responsive genes is halted. **B**, chromatin bound PHB that usually associates with HDACs is dissociated from the chromatin in the presence of androgen.

1.20 Mouse PC models

Further, a study entailing the knockout (KO) of *PTEN* in a mouse prostate specific model showed less *PHB* transcripts (figure 1.8A). This was envisaged through data produced by RNA-seq. Data was available through personal communications. (D.Dart).

This could unveil mechanisms involved in early PIN as *PTEN* knockout is the main characteristic of this phenomenon. Figure 1.8B illustrates the quantitative analysis of the decrease seen in *PHB* gene expression in the KO *PTEN* mouse when compared to the wild type.

Although the role PHB has within PC remains the main focus, it is essential to discuss the role PHB has within further cancers. Thus allowing one to assess any similarities or differences PHB has within different cancers, in order to decipher its main mechanism of action, particularly in PC pathogenesis.

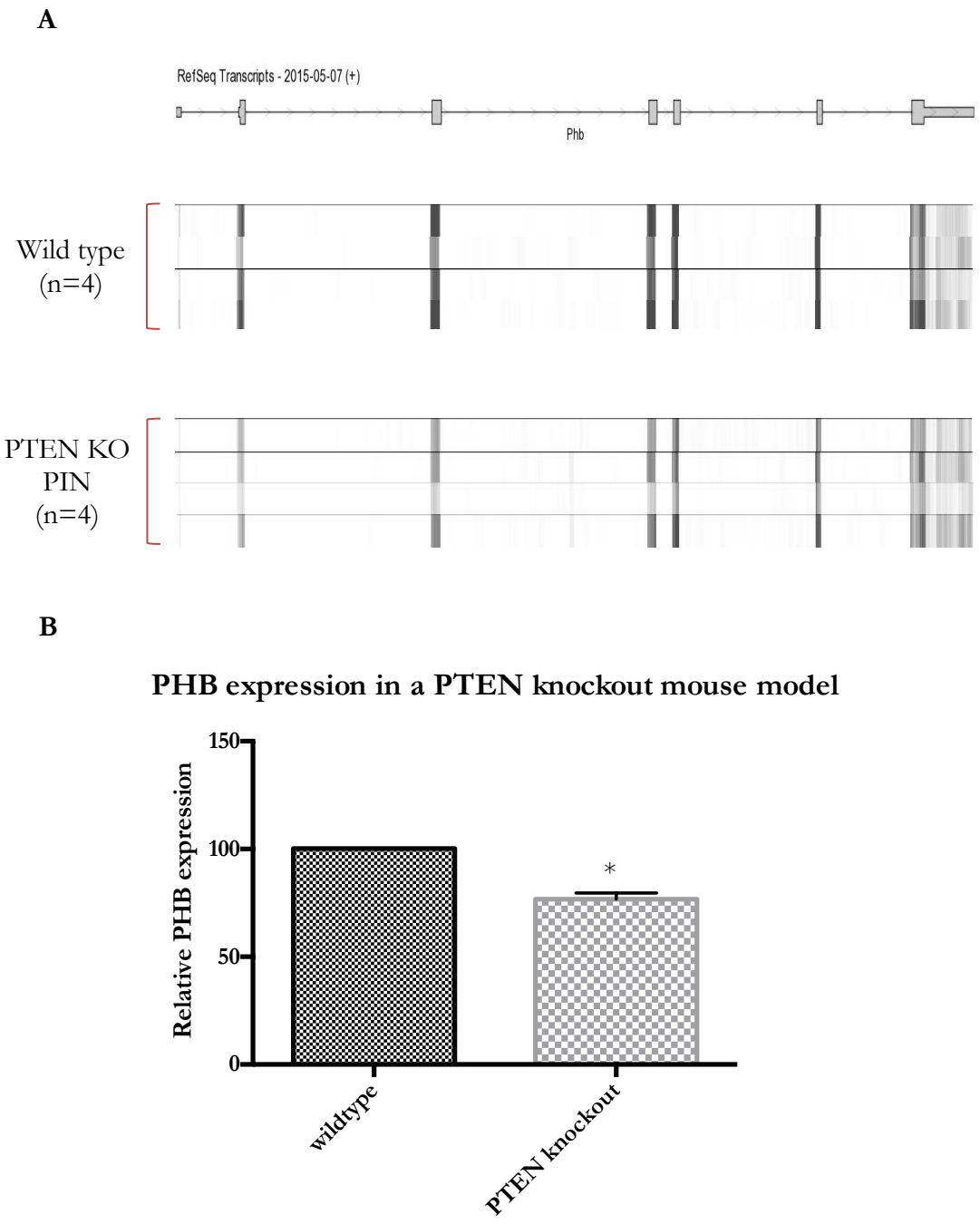

Figure 1.8. Knockout (KO) of *PTEN* in a mouse prostate specific model. **A**, PHB transcript for wild type and PTEN KO mouse. At each exon the expression of PHB is less in the PTEN KO mouse when compared to the wild type n=4. **B**, Relative PHB expression in wt and PTEN KO mice. Data provided by Dr.D.Dart. n=4, $p < 0.05$*.

1.21 PHB, breast cancer and the estrogen receptor

Breast cancer now holds the statistic for being the most common cancer in women worldwide (95), with world regions that previously had low breast cancer incidence showing increases. The ER signalling cascade is implicated in more than 70% of primary breast cancer. The activation of the ERα by oestrogen intensely increases the proliferation and the metastatic potential of breast cancer cells (96).

Firstly, the homologue of PHB, PHB2, can bind to ERα repressing its transactivation to the nucleus, also enhancing the effectiveness of Tamoxifen bound ERα (97). Tamoxifen inhibits the interaction between oestrogen and ERα, therefore PHB can enhance the function of the standard treatment for ERα positive patients. Within the same study, PHB was also identified as an ERα co-repressor in several cell lines such as CV1, MCF-7 and T47D suggesting PHB's role is not cell line specific (97). However, a regulator of the oestrogen/ ERα signalling pathway known as BIG3 was thought to co-localise with PHB2 in the cytoplasm rendering PHB2 unable to repress ERα transcriptional ability (98). However to overcome BIG3 repressing PHB2, a dominant negative peptide named ERAP was shown to competitively bind to PHB2, preventing its interaction with BIG3 thus allowing PHB2 to suppress ERα activity, leading to complete suppression of ERα positive breast cancer cell proliferation both *in vivo* and *in vitro* (98).

Additionally, both PHB and PHB2 were shown to repress SRC-3 activation of ERα. This is extremely important, as SRC-3 is a known co-activator of ERα and is frequently amplified in breast cancer (50). To further confirm this, anti-sense PHB2 RNA causes a heightened fold increase in ERα transactivation, highlighting that endogenous PHB2 dulls the stimulatory effect oestrogen has on ERα. Although the mechanism to how PHB2 counteracts SRC-3's function still needs to be defined, it is clear that PHB and PHB2 compete with SRC-3 for the ERα receptor, causing the recruitment of HDACs, suppressing ERα activation (98). To further highlight PHB's role in oestrogen signalling co-repression, knock out of PHB displayed a hypoplastic uterus and impaired U2-induced uterus proliferation (99). Moreover, during early pregnancy, mRNA levels of PHB found in the uterus of mice were heightened by 2-fold 2 days post coitum. As blastocyst implantation occurred 4.5 days post coitum, this high expression of PHB prior to the implantation suggests its role in maintaining the implantation status of the blastocyst (99). Further, in the same study, treatment of ovariectomized mice with

oestrogen resulted in an increase in PHB mRNA transcripts in 6 hours (99). This suggests that PHB is a probable target of oestrogen in the uterus. Overall, there are clear results indicating that PHB is an oestrogen regulated gene both *in vivo* and *in vitro*.

1.22 PHB, irritable bowel syndrome and Stat3

PHB has also been seen to exhibit its function in inflammatory diseases that often lead to cancer development (100), especially as it is associated with oxidative stress. A known transcriptional factor Stat3 (Signal transducer and activator of transcription 3) is activated via various ligands in an array of tissues. Interestingly, data collected from Han, *et al.,* (101) suggests that there is a link between mitochondrial Stat3 and PHB in the intestinal epithelium. It is thought that this interaction prevents mitochondrial dysfunction and it is this process that is disrupted in the pathogenesis of Irritable bowel syndrome (IBS). Phosphorylation of Stat3 occurs at serine 727 (S727) that is necessary for the mitochondrial function of Stat3 (102). To ensure phosphorylation of Stat3 is needed for PHB interaction, a co-immunoprecipitation assay was carried out (101). This assay determined that PHB interacts with pS727-Stat3 in the mitochondria of cultured intestinal epithelial cell lines and *in vivo* in mouse colonic epithelium (101). This PHB-pS727-Stat3 interaction is lowered throughout mitochondrial stress in response to TNF-α by the means of lowered PHB expression. However, upon PHB overexpression, PHB-pS727-Stat3 interaction is preserved during TNF-α induced stress (103). It has been recognised that PHB expression levels are lower in inflamed epithelia of IBS patients when compared to healthy controls, signifying that down-regulation of PHB may be an event in the early onset of pathogenesis rather than a downstream effect of the disease (101). A transgenic model over-expressing PHB in intestinal epithelial cells demonstrated an up-regulation of protection against experimental colitis and there was notably less oxidative stress present in the colon (101). As previously mentioned, mitochondrial dysfunction is a familiar feature seen in cancers due to ROS (104) and loss of mitochondrial chaperones such as PHB (figure 1.9). A recent report showed that loss of PHB led to the onset of dysplasia during ulcerative colitis (101). Moreover, PHB protein expression found in colonic mucosa was decreased after mice were induced with experimental colitis-associated cancer and vis versa (101). Thus it is theorised that PHB could potentially prevent the onset of tumours by aiding mitochondrial stability. By targeting Stat3, PHB's function could be enhanced to

regulate mitochondria function that could theoretically aid intestinal epithelial cells homeostasis during colitis where PHB is lost.

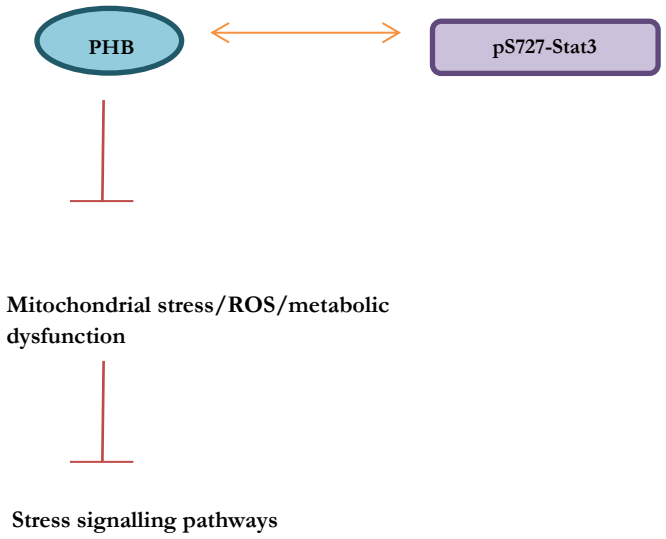

Figure 1.9. Schematic representation of the interaction between PHB and pS727-Stat3, stopping stress signalling pathway activation.

1.23 PHB and cell cycle machinery components in multiple cancers

There is a complex combination of factors / proteins which regulate the progression of the mammalian cell cycle. Members of the Rb family and their downstream targets such as members of the E2F family are examples of proteins which are heavily involved in the progression of the cell cycle (105). Mis-regulation of these proteins have been influenced in the onset of multiple types of cancer (106). Rb and its family members; p107 and p130 repress the G1/S phase transition, however cyclin D phosphorylates Rb preventing Rb from binding to E2F, allowing the transition to the S phase to take place (105). Studies showed that PHB can bind to all three family members of the Rb family; Rb, p107 and p130 with robust efficiency (107). Even though PHB lacks the canonical LXCXE motif which most Rb binding proteins have. However, unlike other Rb binding proteins such as cyclin D, PHB does not have a negative effect on Rb's function, instead it heightens its function much like Brg1 protein. The study also found that PHB can bind to the E2F family members 1,2,3,4 and 5 unlike Rb which can only bind to E2F1,2,3 (107). This suggests that PHB binds to a domain that is alike amongst all the family members of the E2Fs. It was also shown that PHB could suppress the transcriptional activity of E2F1 in T47D cells (107). Furthermore, this suggests that PHB binding to Rb is only one mechanism of action, and there is potential for mechanisms independent of Rb that allows the suppression of E2Fs by PHB. Interestingly, the suppression of E2Fs via PHB cannot be reversed when the adenovirus E1A protein is added, however, this is the case with regards to Rb's suppression of E2Fs (107). With regards to Rb, E1A can disrupt the interaction of Rb and E2Fs in the activation domain, allowing E2F to be uninhibited. It is likely that PHB prevents E1A from carrying out this function, thus suppression of E2Fs is enabled even in the presence of E1A. Overall, there is an established relationship between PHB, Rb, E2Fs and cell proliferation (107). This is supported by evidence showing that PHB lacking an Rb binding domain cannot suppress E2Fs nor cellular proliferation. Specifically, E2F1 inhibition via PHB occurs through a putative coiled-coil domain, and it is this region alone that could hinder the transcriptional activity of E2F1.

Further studies on PHB could unveil mechanisms associating PHB and the regulation of the cell cycle that is vital in uncovering information regarding the initiation of cancer (figure 1.10).

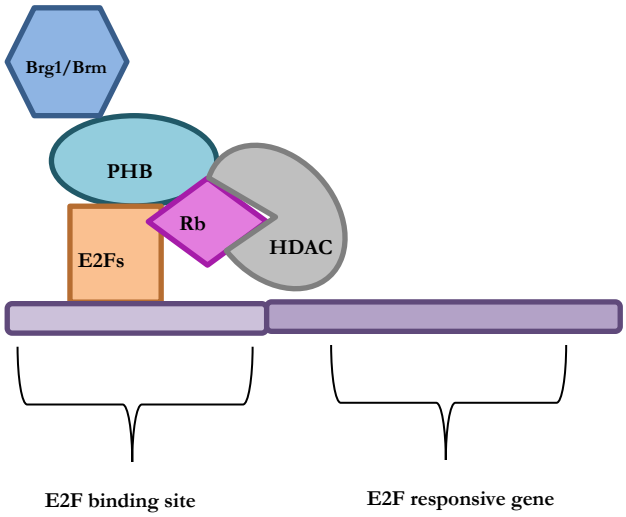

Figure 1.10. Schematic representation of where PHB binds to E2Fs and Rb, causing the recruitment of HDACs.

1.24 PHB and miRNAs

1.24.1 PHB-untranslated region (3'UTR) and miRNAs

The coding region is 95-100% similar in the *PHB* gene across species, however the 3'UTR of the highly conserved *PHB* gene shows high variability across mammals (table 1.2).

Figure 1.11 demonstrates the percentage similarities between species along with the genetic differences between them. The variations in the 3'UTR region of PHB across species and the multiple miRNA target sites suggest it is widely and variably regulated, however this is not the case for the PHB protein, although the UTR could regulate 'fine tuning' of the PHB protein.

Alignment analyses of PHB's 3'UTR across mammals indicate there is variation amongst mammals (figure 1.11).

The human PHB 3'UTR gene has an array of miRNA targets with some similarity to that of the mouse and rat species (Micro-RNA.org).

Many of these miRNA targets on PHB's 3'UTR are classified as oncogenic such as miR-27a (108) (figure 1.12). Therefore, theoretically, administration of the PHB-3'UTR absent of the PHB protein could act as a miRNA 'sponge' (109).

Table 1.2. Similarities of PHB-3'UTR sequence across mammalians.

Species	**Species**	**3' UTR Similarity (%)**	**Coding sequence similarity (%)**
human	chimp	98.93	100
human	mouse	71.44	100
human	rat	68.66	100
human	dog	75.05	100
human	horse	80.36	99.99
human	cow	78.52	100
human	chicken	49.17	99.98

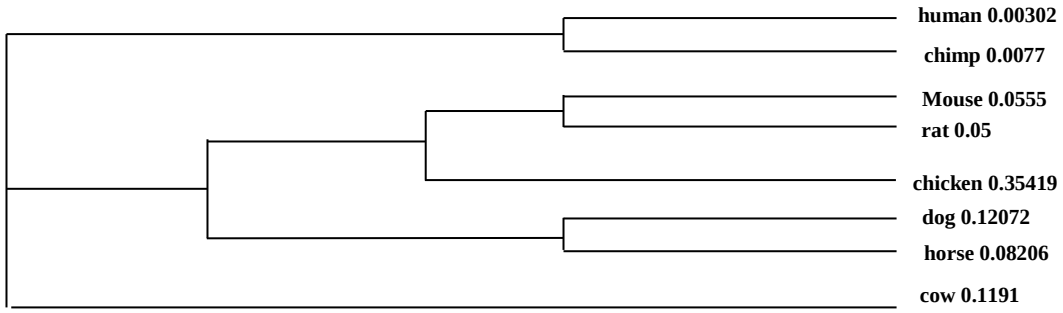

Figure 1.11. Phylogram of 3'PHB-UTR genetic differences between mammalian species. Image adapted from: (NCBI, aligned in ALGGEN).

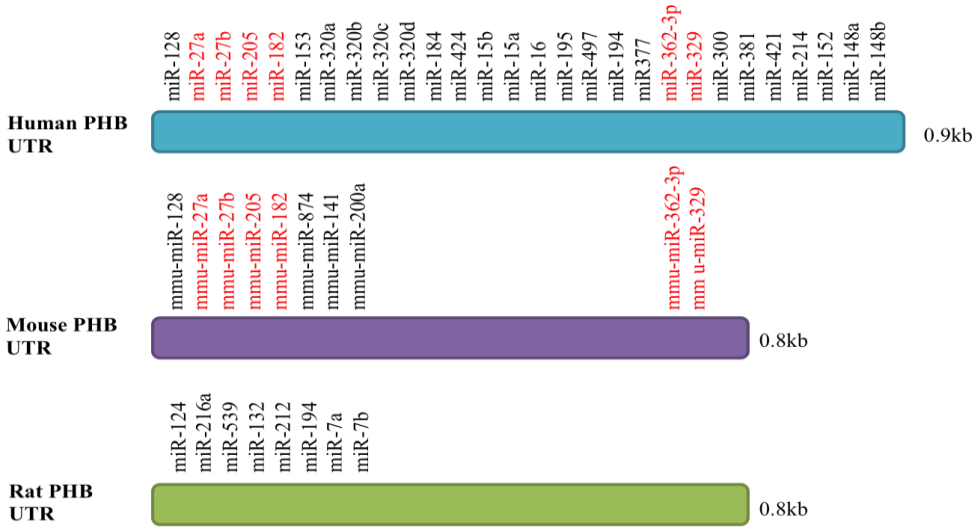

Figure 1.12. miRNA targets within PHB's UTR in humans, mice and rats. Similar targets are indicated in red. Dissimilar targets indicated in black. miR-27a is androgen regulated, showed to be up-regulated in PC (92). However, miR-205 is down-regulated in PC (110).

1.24.2 MicroRNAs and PHB

MicroRNAs are small noncoding strands of RNA, usually around 25 nucleotides long, and can control gene expression by mRNA degradation or inhibition of protein production. Interestingly, microRNA gene locations are often found in cancer associated regions or in fragile sites, making them vulnerable to SNPs, thus can acquire either oncogenic or tumour suppressive characteristics. It is therefore no surprise that microRNAs can become aberrantly activated during prostate carcinogenesis and their acquiring of oncogenic characteristics (OncomiRs). In particular an oncomiR known as MiR-27a located on chromosome 19 position p13.1, is encoded by a intergenic cluster along with both miR-23a and miR-24-2 (92). The expression of this particular cluster has been modified in numerous cancers such as leukaemia and ovarian cancer. Remarkably, its' function can have opposing effects, for example in hepatocellular carcinoma, up-regulation of this cluster can hinder TGFα's ability to suppress tumour growth. On the other hand, in human embryonic kidney cells, it can up-regulate apoptosis. It is probable that post- transcriptional modification plays a role in these clusters' alternative functions within different cellular environments and also on differing gene targets (92). With regards to miR-27a, it was shown by Fletcher, *et al.,* 2012 (92) that this microRNA upon androgen stimulation down-regulates PHB expression, allowing target gene expression and PC cell growth. It was predicted that a binding site for miR-27a was found within the highly conserved 3' UTR of the PHB gene. This was confirmed by a luciferase assay, which confirmed down-regulation of this UTR in response to androgen treatment, suggesting this region's susceptibility to androgen-regulated miRNAs that attach to this position, hindering its activity. Silencing of the AR, resulted in increased PHB activity. It was indeed established by (92) that PHB down-regulation was due to miR-27a binding to the 3'UTR PHB region. The mechanism behind this was said to be due to degradation of the PHB gene transcript rather than post-transcriptional inhibition. To demonstrate that miR-27a possesses characteristics of an oncogene, manipulation of miR-27a caused an upsurge in androgen responsive genes such as *PSA* and *TMPRSS2* (92). Several other targets of miR-27a have been identified such as the tumour suppressor gene *FOXO1*, *ZBTB10*, a repressor of the Sp family of transcriptional factors and *Wee-1* a vital regulator of cyclin B. This highlights the potent oncogenic attribute that miR-27a does indeed have. It is likely that miR-27a only fine tunes PHB protein expression rather than causing complete reduction, and it is likely that miR-27a targets other genes associated with cell

proliferation resulting in growth stimulation (92). Mechanisms understanding the androgen regulation of miR-27a were established by Fletcher *et al,.* 2012 (92). Firstly, the expression cluster region of the primary transcript primiR-23a27a24-2 was shown to rise quickly after androgen treatment and then fall, signifying androgens initially stimulate a high amount of primiR levels.

1.25 PHB in other cancer types

PHB has been showed to have an implication in PC and breast cancer, a functional role has also been noted in ovarian and bladder cancer. Firstly, in line with PHB aiding apoptosis, it was noted that up-regulation of PHB was seen in normal ovarian cells undergoing apoptosis in the presence of gonadotropin releasing hormone (GnRH) (111). As this was seen in the mitochondria, this emphasises that PHB is maintaining the mitochondrial integrity and loss of PHB may be associated with defective apoptosis in ovarian cancer. This may be the reason why PHB accumulation was seen in the peri-nuclear and cytoplasmic regions in the epithelial cells in papillary serous ovarian tumour cells (111). On the other hand, in bladder cancer PHB up-regulation was shown to be associated with the proliferation of bladder cancer cells through PHB1's phosphorylation at thr258 by AKT (112). In the same study it was also observed that up-regulation of PHB, at both a transcriptional and translational levels, in bladder cancer tissue were associated with poorer bladder cancer prognosis when compared to normal adjacent urothelial tissue (112). PHB phosphorylation has also been observed in response to insulin signalling causing PHB to interact to a lesser extent with PIP3 (113). This may disrupt PHB's ability to attenuate the PI3K pathway, which often is aberrant in cancers (113).

As there is an accumulating amount of evidence to suggest that the down-regulation of PHB could be a mechanism involved in androgen independent PC, this thesis will focus on unveiling the mechanism involving PHB in PC.

1.26 Post-translational modifications of PHB

1.26.1 Phosphorylation sites of PHB

Phosphorylation is an essential process involved in post-translational modification. However, improper phosphorylation such as hyper-phosphorylation and de-phosphorylation due to aberrant phosphorylation cascades can lead to the onset of carcinogenesis. Interestingly, PHB1 and its homologue PHB2 were found to be phospho-proteins via orthophosphate labelling in T lymphocytes. Further, Ande *et al,*. 2009 (114) showed that PHB was found to be serine phosphorylated, whereas PHB2 was both tyrosine and serine phosphorylated. Tyrosine phosphorylation of PHB2 was mapped to Tyr^{248}. As these studies demonstrate that PHB and its homologue PHB2 are phosphorylated at different residues, this may relate to their differing functions that they carry out (114). Table 1.3 summarises the phosphorylation sites of PHB. Figure 1.13 illustrates phosphorylation sites of both PHB and PHB2 within different cell types.

Table 1.3. Summary of phosphorylation sites of PHBs (114).

Context	Protein	Phosphorylation site	Known kinase	Function
C2C12	PHB	Tyr^{114}, Tyr^{259}	Receptor tyrosine kinase	Cell signalling
MiaPaCa-2	PHB	Thr^{258}	AKT	Regulation of PHB function
T cells	PHB	Ser (specific site not known)	Not identified	Mitochondrial homeostasis and survival of T cells
T cells	PHB2	Ser(specific site not known)	Not identified	Mitochondrial homeostasis and survival of T cells
Granulosa cells	PHB	Not identified	Not identified	Cell proliferation

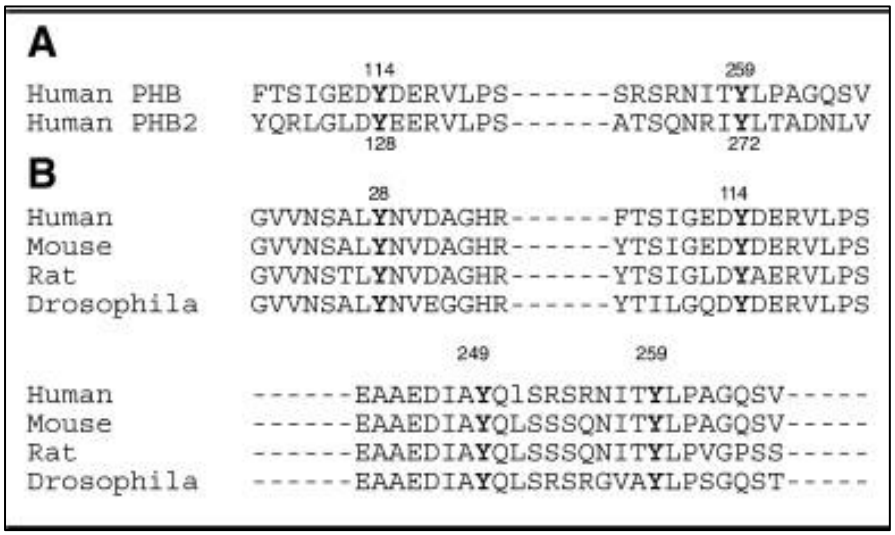

Figure 1.13. Sequence alignments of PHB and PHB2 from human, rat, mouse and *Drosophilia* demonstrating tyrosine residues in the PHB protein are highly conserved across species. **A**, illustrates that PHB and PHB2 are highly conserved in humans. **B**, illustrates that all four Tyr residues are highly conserved across all species. Bold letters indicate probable phosphorylation sites (114).

Further investigation of the tyrosine residues that were phosphorylated in response to insulin was carried out using Human Protein Reference Database (HPRD) server (114). This revealed that it was Tyr^{114} as insulin and EGF receptors kinase motif. NetPhosK 1.0 server also identified this residue as a probable phosphorylation site by insulin receptor kinase. Further studies revealed insulin stimulation causing Tyr^{114} phosphorylation on the PHB protein causes the recruitment of the Shp1 protein (114). This is an interesting signaling cascade that necessitates further investigation.

1.26.2 Ubiquitination of PHB

Research has suggested that some proteins in the mammalian sperm mitochondria are tagged with ubiquitin, a proteolytic peptide that could initiate the destruction of sperm mitochondria inside the fertilised oocyte. A higher molecular weight isoform of PHB was identified in mammalian spermatozoa, along with PHB transcripts' being present in rat spermatogenic cells that were no longer present by the time that spermiation was completed in the testis. This could be due to the degradation of PHB by ubiquitin. Evidence to support this theory includes the accumulation of ubiquitinated PHB in immotile sperm fractions. This suggests ubiquitin-degradation of defective spermatozoa in the epididymis (115). PHB could be tagged with ubiquitin, within the testes, epididymis and in the oocyte cytoplasm. Ubiquitin tagged sperm mitochondria may be hidden by a disulphide bond present during epididymal passage. However, this can then be uncovered by disulfide bond reduction activities during fertilization (115). Therefore, exposed ubiquitin-tagged mitochondria may be able to destroy sperm mitochondria or aid further poly-ubiquitination of other mitochondrial substrates. Ubiquitin-tagged PHB could initiate the signal given during the degradation of sperm mitochondria by the oocyte proteolytic degradation system. Further research into the mechanism of PHB ubiquitination in sperm mitochondria could unveil explanations to male infertility (115).

1.27 The cell cycle

1.27.1 Overview of the cell cycle

Requirements of cell division include DNA replication and the segregation of replicated chromosomes into two distinct separate cells (116). Cell division can be divided into mitosis and interphase. Interphase is then further subdivided into several stages known as G1, S, and G2. The G1 phase precedes the S phase where preparation of DNA synthesis occurs (116). The G2 phase follows on where the cell prepares for mitosis to begin. Interestingly, cells that are in G1 are able to exit the cell cycle and to enter the G0 phase instead of continuing with DNA replication. The majority of non-proliferating cells in the body remain in this phase (116).

1.27.2 Regulation of the cell cycle

Revolutionary studies in yeast have provided the key elements that regulate the cell cycle. In yeast, a single cyclin dependent kinase (CDK) controls the cell cycle, specifically cdc28 in *Saccharomyces cerevisiae* and Cdc2 in *Schizosaccharomyces pombe* (116). Through the process of evolution, the number of cyclins and CDKs identified has increased. On the contrary, only a few key cyclins and CDKs are responsible for the regulation of the cell cycle (figure 1.14).

The 'classical' model of the cell cycle states that specific CDK-cyclin complexes are responsible for events to take place during interphase in a methodical order (116). Firstly, mitogenic signals are received by D-type cyclins that favourably bind CDK4 and CDK6 causing their activation in the G1 phase. The G1 phase is responsible for the preparation of DNA synthesis. The activation of these complexes causes the partial inactivation of pocket proteins such as Rb and RbL1 (116). This allows the expression of E-type cyclins such as cyclin E1 and cyclin E2 that bind to CDK2 causing its activation. This stable complex of cyclin E-CDK2 subsequently causes the complete inactivation of pocket proteins. The expression of E-type cyclins is restricted to the early phase of DNA synthesis (116). This leads to the assumption that CDK2-cyclin E complexes are essential for the G1/S phase transition. Further in the later stages of DNA replication, CDK2 is next activated by cyclin A2 driving the S/G2 phase. To end, CDK1 is activated by A-type cyclins to aid the onset of mitosis, during nuclear envelope breakdown, A-type cyclins are destroyed, allowing the formation of CDK1-cyclin B

complexes. These CDK1-cyclin B complexes are the driving force for the remainder of mitosis (116).

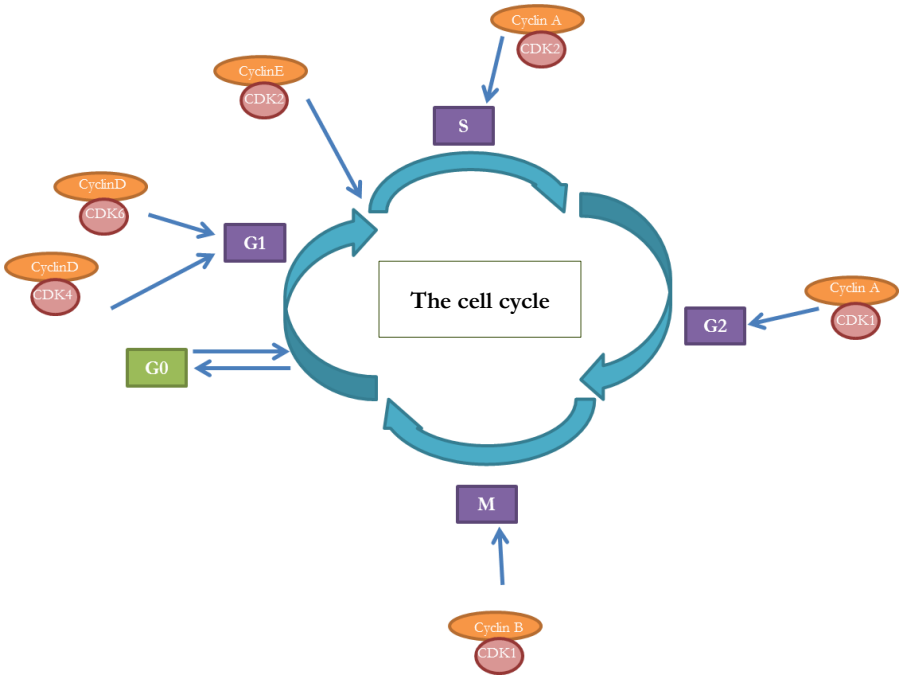

Figure 1.14. Each stage of the cell cycle is regulated by a specific cyclin-CDK complex. M=mitosis. G1-G2=interphase. Image adapted from (44).

1.27.3 Cell cycle inhibitors

The activity of CDKs can be hindered by certain cell cycle inhibitory proteins known as CDK inhibitors. There are two well-defined groups of these inhibitors namely; the INK4 family and Cip/Kip family (116). The INK4 family compromises of p15, p16 and p18 that target CDKs by preventing the binding of cyclins involved in G1 only. Whereas the Cip/Kip family include p21, p27 and p57, that all share a conserved N-terminal domain. They inhibit the G1 CDKs and to a lesser extent CDK1-cylin B complexes. p21 is also known to constrain DNA synthesis by binding to the PCNA (116). p21 contains a binding site for p53 in its promoter region. p21 is therefore under the transcriptional control of p53, the well-known tumour suppressor that is inactivated in more than half of all sporadic cancers (117). In contrast to p21, p27 expression is usually higher in mitogen starved cells and is quickly destroyed as the cell cycle proceeds (118).

1.27.4 The cell cycle and cancer

There is an extensive amount of literature that confirms the deregulation of the cell cycle in cancer biology. Through an accumulation of numerous mutations, tumour cells can acquire a resistance to anti-proliferation signals, resulting in unrestrained proliferation activity. Moreover, most tumours gain genomic instability (GIN) that leads to further mutations and chromosomal instability (CIN) (116). Altogether, un-regulated proliferation, GIN and CIN all lead to the deregulation of the cell cycle. These factors in some way are mediated by the disruption of CDKs.

1.27.5 E2Fs

Accumulating evidence has led to the discovery that E2Fs are involved in cell cycle control. E2Fs are a large family of transcriptional factors that contain one or more conserved DBD. These DBDs are responsible for targeting promoters and regulating expression of certain genes. The Rb pocket protein and its close relatives p107 and p130 are able to directly interact with E2Fs, suppressing their ability to promote gene expression. Evidence of *RB* inactivation in numerous transgenic animal models has shown unregulated control of E2F activity that stimulated aberrant cell proliferation (119).

Since the discovery of the founding member of the E2F family, *E2F1,* seven more genes have been identified in mammals. The unearthing that over-expressing E2F activators led to cells in G0 phase entering G1 phase led to the idea that E2Fs play a role in cell cycle progression and target genes involved in DNA replication (119). Members of the E2F family contain both transactivation and repression domains, thus are able to carry out both activation and repression functions. For example, in order for the activation of transcription, E2Fs are able to form complexes with histone acetyl transferases (HAT), whereas when bound to pocket proteins such as Rb, E2Fs can carry out a repressive activity by interacting with HDACs (120).

There are at least three subtypes of E2Fs. Firstly activating E2Fs: E2F1-3 are well described as promoting progressing of the cell cycle through the S phase when Rb is inactivated. Second repressing E2Fs; E2F4-5 that cause the inhibition of E2F responsive genes by forming a complex with Rb family members. Finally, E2F6-8 work independently of Rb causing the inhibition of the transcription of E2F target genes. Further, it has been found that E2F7-8 are able to form heterodimers and homodimers with one another suppressing the activity of E2F1 (119).

E2F1-6 are able to bind to DNA by forming heterodimers by interacting with a dimerization partner such as DP-1/DP-2 (119).The newer members of the family, E2F7 and E2F8 do not need to bind to either DP-1 or DP-2 (119). There is controversy to suggest that E2F1-3 are solely activators as they are able to bind to Rb, suppressing gene transcription. Especially as E2F1 was first identified to associate with Rb (119). Therefore, one should not distinctly characterise E2Fs into repressors and activators as there appears to be some cross over. However there seems to be a clear difference in the structure between the two groups. For example, E2F1-3 contain their own nuclear localisation signals. On the other hand, E2F4-5 carry nuclear export signals and reside in the nucleus when bound to pocket proteins (119). Figure 1.15 shows how E2Fs are able to progress once the AR causes PHB to dissociate from E2Fs alongside Rb.

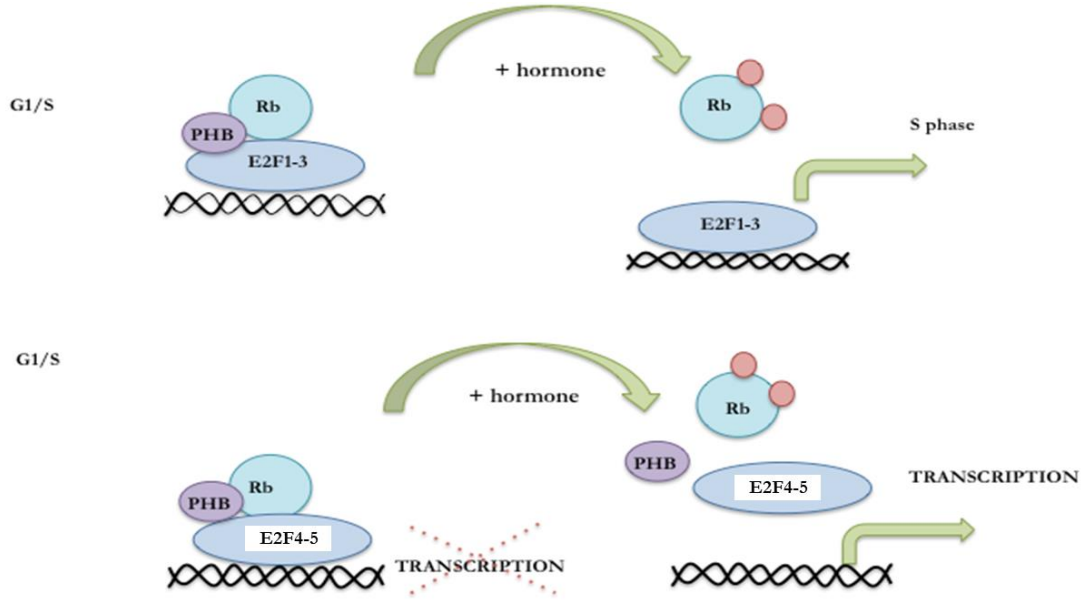

Figure 1.15. The release of PHB when the AR signalling pathway is activated with hormone, allowing transcription of E2Fs, leading to cell cycle progression.

1.27.6 Transcriptional targets of E2Fs

Several microarray studies have demonstrated that E2Fs can regulate a variety of genes involved in many cellular processes such as metabolism and differentiation (121). Interestingly, they have also been identified to regulate the transcription of genes involved in DNA repair, mitosis and the spindle checkpoint. Moreover, E2Fs are able to regulate genes involved in apoptosis and DNA damage checkpoints (121). The simple model of the *Drosophilia* fly has made an ideal system to analyse the genome wide targets of the E2F and Rb protein. Interfering RNA (RNAi) was used to knockdown one activating E2F and one inhibitory E2F. Surprisingly, very few genes were affected by this, suggesting that genes are mostly affected by increasing activating E2F, or decreasing repressing E2Fs as a single event rather than in synergy (121). Genes found to be regulated by decreasing the activating E2F were largely involved in the cell cycle, DNA replication, mitosis and chromosome segregation. Assessing genes regulated in the repression of inhibitory E2Fs were found to be involved in cell development as opposed to cell cycle, including male and female specific genes (121). Table 1.4 displays various gene targets of E2Fs.

1.27.7 Rb

It is well known that Rb is critical in hindering the progression of the G1 and S phase, acting as a tumour suppressor thus playing a pivotal role in cell proliferation. The activity of Rb can act independent or dependent of E2Fs (121). Recently, it has been noted that Rb can send signals from damaged DNA machinery to cell cycle machinery to prevent proliferation in the presence of DNA damage (121).

Table 1.4. E2F gene targets in the G1, S/G2 and DNA synthesis and replication stages (122).

	CELL CYCLE STAGE	**DNA SYNTHESIS AND REPLICATION**
	CCDND1	ASK
	CCND3	CDC14B
G1	JUN	CDC45L
	MYC	CDC6
	MYCN	CDC7L1
G1/S	CCNE1	DCK
	CCNE2	DHFR
	CDC25A	DUT
	CDK2	LIG1
	E2F1	MCM2
	E2F2	MCM3
	E2F3	MCM4
	NPAT	MCM5
	MYB	MCM6
	MYBL2	MCM7
	TFDP1	ORC1L
S/G2		PCNA
	AURKB	POLA
	CCNA1	POLA2
	CCNA2	POLD1
	CDC2	PRIM2A
	CDC20	RFC1
	CKS2	RFC2
	HEC	RFC3
	KI-67	RFC4
	KIF4A	RPA1
	KNSL4	RPA2
	PLK	RPA3
	PRC1	RRM1
	SMC2L1	RRM2
	SMC4L1	TK1
	STK12	TOP2A
		TYMS

1.27.8 Regulation of G1/S phase

Throughout G1, the expression of Rb varies; in the earlier stages of this phase p130 and p107 are highly expressed and associate with E2Fs. For gene expression during the S phase, the Rb family of proteins recruit chromatin remodelling factors such as HDACs and the SWI/SNF chromatin remodelling complex (121). It is known that high levels of cyclin E are found during the G1-S transition, therefore Rb is needed to recruit HDACs in cyclin E transcriptional initiation sites. Rb can also bind to other chromatin remodelling proteins such as Brg1/Brm that are ATP dependent helicases (121). Rb can cause the enlistment of Brg1 to cyclinA promoters stopping its interaction with E2Fs. Regulation of E2F activity by Rb can also be mediated by Rb forming a complex with DNA methyltransferase 1, resulting in the methylation of chromatin (121). Dissociation of Rb occurs during the end of the G1 phase as cyclinD/CDK4 endorses the hyper-phosphorylation of Rb family members, causing the dissociation of Rb from E2Fs permitting the progression of S phase (121). Working independent of E2F, Rb can associate with genes involved in DNA replication such as MCM7, enhancing the idea that Rb plays a role in DNA replication (121).

Finally, Rb is implicated in senescence. Under cellular stress, levels of p16 are increased, heightening the function of Rb. This results in irreversible repressive heterochromatin due to chromatin reorganisation at loci containing E2F targets causing exit from the cell cycle (121).

1.27.9 MCMs

Minichromosome maintenance (MCM) proteins were discovered in the 1980s as being necessary for DNA replication and gene targets of E2Fs. They carry out helicase activity essential for replication elongation. They also participate in other chromosomal activities such as chromatin remodelling, transcription and genome stability (123). The MCM family comprises of 7 members MCM2-8 and are a subgroup of the AAA ATPase family. The structure of MCM family members consists of an ATPase domain and a MCM box that spans around 200 residues. Within the MCM box, two ATPase consensus motifs are found, namely walker A and walker B (123). Walker A consists of a P-loop as an active site with a lysine residue found in all ATP-binding proteins.

However walker B possesses hydrophobic stretches and takes part in ATP hydrolysis. Besides the MCM box, there is little similarity between members of the MCM family (123).

1.27.10 Control of DNA replication

DNA replication is an extremely controlled mechanism that is controlled by members of the MCMs gene family (figure 1.16). The ring structure that MCM proteins form has a central pore that accommodates DNA. In the initial stages of the S phase, MCMs are dispersed onto un-replicated DNA, where it is thought MCMs fasten to the nuclear matrix during the S phase, acting as rotating molecular pumps. As DNA replication advances, CDKs phosphorylate MCMs, freeing them from DNA. The free MCMs continue to reside in the nucleus and remain so until early mitosis (124). They are able to re-bind to chromatin during late M/G1 phase ready for the next G1 phase. The expression of MCMs proteins remains constant throughout the cell cycle in the nucleus. Their recruitment to the chromatin is regulated by CDK activity. The origin recognition complex proteins (ORC) aid both CDC6 and CDT1 (MCM loading factors) that resides on the chromatin to form a pre-replication complex. As the S phase proceeds, CDC6 and CDT1 are phosphorylated causing their displacement from the chromatin. CDC6 is exported to the cytoplasm whereas CDT1 is degraded in the nucleus (124).

1.27.11 MCMs as cancer biomarkers

As the cell cycle is often deregulated in cancer, MCMs are being analysed as biomarkers of cancer. For example, the appearance of MCM positive cells in pre-invasive cervical lesions was higher with increasing histological grade (124). Moreover, disruption of MCM expression was also noted in a range of other malignancies such as colorectal and ovarian cancer (124). So far, Ki67 is used as a proliferation marker, however is ineffective in a clinical setting as it is not as sensitive as MCMs at detecting cells in cycle. MCMs may work better as a biomarker as they are easily stained as their localisation remains in the nucleus, are more abundant and their expression during the cell cycle is unvarying (124). Interestingly, immunohistochemical staining of MCMs has become a useful tool in deciphering survival in patients with breast and prostate cancer (124). Moreover, microarray analysis has identified genes that encode for MCMs to be up-regulated in malignant cancers (124). These genes have also been associated with poor

clinical outcome for breast cancer and mantle cell lymphoma. However, there is not one single MCM that is being overexpressed, rather a few members such as MCM2, 4,5,6 that all work together to form a ring like structure (124).

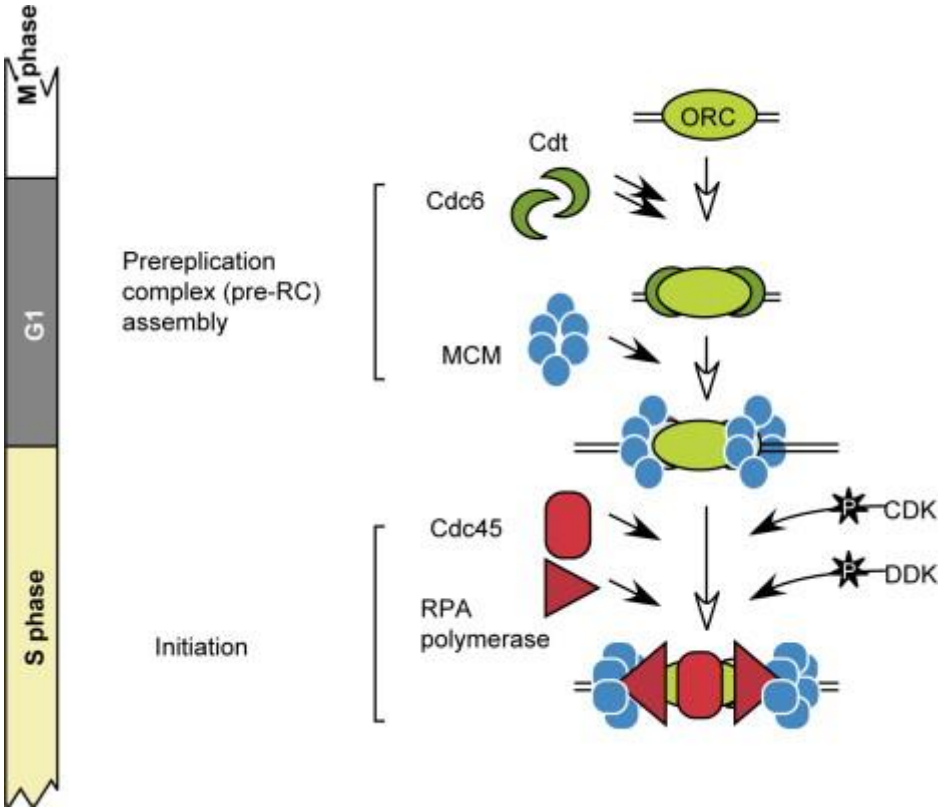

Figure 1.16. Initiation of DNA replication involving ORCs and MCMs, image taken from Tabancay, *et al.,* 2006 (125).

1.28 Summary of key points

PC if diagnosed at an early stage has a good prognosis. However, in many cases patients relapse with anti-androgen treatment currently used in clinics. The cancer usually relapses with a more aggressive phenotype that has sensitised to a low androgen environment, thus is no longer dependent on androgens. This is where current treatment fails, as the cancer is able to survive in the apparent absence of androgen. Aberrant AR pathway activation is essential for the progression and survival of PC. As down-regulation of PHB is seen in more aggressive and metastatic PC, this allows the AR's activation threshold to lower, resulting in minimal androgen stimulation required to stimulate the cascade. Moreover, non-specific androgens such as adrenal androgens are capable of activating the AR. This can progress the cancer from an indolent stage to a metastatic stage.

PHB has been identified to increase the efficacy of breast cancer treatment by increasing the amount of Tamoxifen bound to ERα. This highlights PHB's ability to hold steroid receptors in an inactive state. Moreover, PHB was able to directly repress E2F1 in breast cancer cells, depicting PHB's role in rendering the cell cycle inactive. Therefore it was further investigated if PHB was able to carry and the same repressive role on E2Fs and E2F downstream targets such as MCMs in PC cells. This could aid eluding a mechanism that explains how PC transitions from androgen dependence to androgen independence.

This leads onto my aims and hypothesis.

1.29 Aims and hypothesis

1.29.1 Hypothesis

Androgen activation of the AR rapidly causes PHB to dissociate from the chromatin, leading to PHB's downregulation, allowing cell cycle progression in PC cells.

1.29.2 Aims

- To understand the mechanism of PHB induced cell cycle arrest.
- To understand the dynamics of AR:PHB interaction.
- To understand how the rapid actions of androgens affect PHB.
- To understand how activation of the AR is causing PHB to dissociate from the chromatin.
- To provide a preliminary mechanism to how PHB's tumour suppressive function is lost in aggressive PC.

Chapter II: Materials and Methods.

2 Chapter II. Materials

2.1 Cell culture

The parental LNCaP cell line was obtained from the American Type Culture Collection (ATCC CRL-1740). The LNCaP cell line was cultured in RPMI medium (Sigma), supplemented with 10% (v/v) FBS (Clontech) and 1% (v/v) antibiotics (penicillin-streptomycin 10,000U/mL (Sigma)). The LNCaP cell line modified to over express PHB under the influence of tetracycline (Doxycycline) (10 mM) (*LNCaP/TR2/ PHB*) was developed by Dr Alwyn Dart (58). Refer to figure 3.2 for how the cell line was made. The *LNCaP/TR2/ PHB* cell line was cultured in RPMI supplemented with 10% (v/v) tet-free FBS (Clontech) and 1% (v/v) antibiotics. The PC3 cell line (ATCC CRL-1435) and VCaP cell line (ATCC CRL-2876) were obtained from the American Type Culture Collection. COS-7 cells (ECACC 87021302) were obtained from the European Collection of Authenticated Cell Cultures. PC3, VCaP and COS-7 cells were cultured in DMEM media supplemented with 10% (v/v) FCS and 1% (v/v) antibiotics (penicillin-streptomycin 10,000U/mL). Bicalutamide-resistant LNCaPs (developed by Dr Dart) were made by growing wt LNCaP cells for 6 months in varying concentrations of Bicalutamide (0, 10, 20, 30 μM) until growth was established. 20 μM was the chosen concentration as cells were not healthy with the highest concentration (30 μM).

2.2 Primers

Primer sequences used for the SYBR® Green Q-PCR are shown in table 2.1. In cases where the entire coding sequence was amplified, the primer sequences are shown in table 2.2. All primers used were obtained by Sigma-Aldrich and diluted according to the datasheet provided and were stored at -20°C.

2.3 Antibodies

Primary antibodies used are described in table 2.3. Secondary antibodies used were either horseradish peroxidase (HRP) conjugated anti-mouse (A9044) or anti-rabbit (A0545) IgG antibodies (Sigma-Aldrich).

2.4 Standard reagents and solutions

2.4.1 General laboratory used materials

0.05% DEPC water (Diethylpyrocarbonate)

250 µL of DEPC was added to 500 mL of distilled water, left for 24 h and then autoclaved.

PBS (phosphate buffer saline)

A 10X stock of PBS (Sigma-Aldrich) was diluted to a 1X stock in distilled water. This was then autoclaved and aliquoted accordingly.

2.4.2 Materials used for cell culture

Trypsin-EDTA

10X Trypsin-EDTA (Sigma-Aldrich) was diluted to a 1X solution with PBS.

Antibiotic antimycotic solution

100X antibiotic antimycotic solution containing 10,000 units penicillin, 10 mg streptomycin and 25 µg of amphotericin B per mL was diluted to 1X using distilled water (Sigma-Aldrich).

Charcoal stripped RPMI

In experiments entailing the serum starvation of cells, 25 mL of charcoal stripped FCS (Clontech) was added to 500 mL of phenol-red free RPMI (Sigma-Aldrich) supplemented with 5 mL of antibiotics.

TET-free FBS

The tetracycline inducible cell line; *LNCaP/TR2/ PHB* was cultured with 50 mL of tetracycline-free FBS (Clontech) in 500 mL of RPMI supplemented with antibiotics.

2.4.3 1D and 2D-western blot materials

Lysis buffer

For 100 mL: 0.61 g 50mM TRIS base + 0.19 g 5mM EGTA + 0.87 g 150mM NaCL + 1 mL 1% Triton X-100 (Melford Laboratories, UK). Upon use, a protease inhibitor cocktail tablet (Roche) was added and the solution was aliquoted and stored at -20˚C.

10% APS (ammonium persulphate)

1 g of APS (Melford Laboratories Ltd, UK) was dissolved in 9 mL of distilled water and stored a 4˚C.

TBS (Tris buffered saline)

10X TBS (Sigma-Aldrich) was diluted to 1X using distilled water.

Running buffer

1 L of 10X Tris Gycline SDS buffer (Sigma-Aldrich) was added to 9 L of distilled water.

Transfer buffer

1 L of 10X Tris/Glycine concentrate buffer (Sigma-Aldrich) was added to 2 L of methanol (Fisher Chemical) and 7 L of distilled water.

0.01% TBS-T (TBS-Tween20)

For the washing solution, 500 µL of Tween20 (Melford Laboratories Ltd, UK) was added to 500 mL of 1X TBS and thoroughly mixed.

10% SDS (sodium dodecyl sulfate)

10 g of SDS (Melford Laboratories Ltd, UK) was dissolved in 100 mL of distilled water.

Rehydration buffer

19.82 g urea and 3.81 g thiourea was dissolved in 25 mL of distilled water. Then 0.02 g of CHAPS (Sigma Aldrich) was added to 1 mL of this solution and kept at room temperature.

Reducing solution

0.5 mL of 10X NuPAGE Sample reducing agent (Invitrogen) was added to 4.5 mL of 1X NuPAGE LDS sample buffer (Invitrogen).

Alkylating solution

116 mg iodoacetamide (Sigma Aldrich) was dissolved in 5 mL of 1X NuPAGE LDS sample buffer (Invitrogen).

MOPS running buffer

40 mL of 20X NuPAGE SDS- MOPS buffer (Invitrogen) was added to 760 mL of distilled water to make 800 mL of 1X MOPS buffer.

2.4.4 Materials for bacterial transformation

LB-broth

8 g LB broth (low salt granulated) (Melford Laboratories Ltd, UK) was added to 400 mL of distilled water and autoclaved. 400 µL of 100 mg/mL ampicillin (Sigma-Aldrich) was added to the autoclaved broth to give a 10 mg/mL ampicillin solution.

LB-agar amplicillin plates

LB broth was made according to 2.6.4 with the addition of 6 g of agar (Melford Laboratories Ltd, UK). Once the broth had cooled, the broth was poured in 10 cm^2 dishes to produce LB-agar amplicillin plates.

2.4.5 Materials for immunoprecipitation and cell fractionation

IPH buffer

For 50 mL: 1.88 mL 4M NaCL, 2.5 mL 1M Tris (pH 8), 500 µL 500 mM EDTA, 50 µL 1 mM DTT, 2.5 mL 10% NP40 and a protease inhibitor cocktail tablet (Roche).

Buffer A

For 10 mL: 100 µL 10 mM HEPES (pH7.9), 33 µL 10mM KCL, 15 µL 1.5mM $MgCl_2$, 1.16 g (0.35M) sucrose, 1 mL 10% glycerol, 10 µL 1mM DTT, and a protease inhibitor cocktail tablet (Roche).

Buffer B

For 10 mL: 60 µL 3mM EDTA, 4 µL 0.2mM EGTA, 10 µL 1mM DTT, and a protease inhibitor cocktail tablet (Roche).

2.5 Inhibitors, hormones and anti-androgens

Src-inhibitor-1 (4-(4'-phenox-yanilino)-6,7-dimethoxyquinazoline) (Sigma-Aldrich) was used at a working concentration of 10 nM (stock concentration 10 mM diluted in DMSO). MDV3100 (Enzalutamide) was used as a working concentration of 10 μM. Bicalutamide (CDX Sigma-Aldrich) was diluted in DMSO to produce a stock concentration of 10 mM, and used at a working concentration of 10 μM. R1881 ((17*b*)-17-hydroxy-17-methyl-estra-4,9,11-trien-3-one) (Sigma-Aldrich) was diluted in 100% ethanol to produce a stock concentration of 10 μM. The working concentration used was 10 nM. Ethanol (100% v/v) was used as the vehicle.

Table 2.1. Primer sequences used for the SYBR® Green Q-PCR.

Oligo Name	Sequence (5'-3')
MCM2F	TGCTATGGCGGAATCATCGG
MCM2R	GAGGTGAGGGCATCAGTACG
MCM3F	AGTCATCCTGGGAACCTCCA
MCM3R	TGTTCAGAAGCCTCGTCGTC
MCM4F	CCAGACGCCTCGGAGTGA
MCM4R	TTGGCATCGGCTGCAACT
MCM5F	CACCAAGCAGAAATACCCGGA
MCM5R	GCGAGTCCATGAGTCCAGTG
MCM6F	AGTAAAACGGGGTGTCCTGC
MCM6R	TCCTCCACGTGCTTGAGAAAT
MCM7F	CAGGAGCAAGACCTCTGAGC
MCM7R	ACCTTTTCCTTCTCTAGCGCGT
MCM8F	TGAAGAAGCACAGGAGAGATGA
MCM8R	CCTGAGAAGTTCCCACCACC
MCM9F	GGATCCTGGCACAGGGAAAT
MCM10F	TCCCCTGTAGAGAAGTCTCCC

PHB F	GGCTGAGCAACAGAAAAAGG
PHB R	GCTGGCAGGTAGGTGATGTT
PSA F	GTG TGTGGACCTCCATGTTATT
PSA R	ATATCGTAGAGCCGGTGTGG
GAPDH F	TGC ACC ACC AAC TGC TTA CG
GAPDH R	GGC ATG GAC TGT GGT CAT GAG
RPL19 F	AGC GAG CTC TTT CCT TTC G
RPL19 R	GAG CCT CTT CTG AAG CCT GA

Table 2.2. Primers sequences used for amplification of the coding sequence.

Oligo Name	Sequence (5'-3')
E2F1 F	ATGGCCTTGGCCGGGGCC
E2F1 R	GCCCTGTCAGAAATCCAGGG
PHB F	TGT CAT CTT TGA CCG ATT CCG
PHB R	CTG GCA CAT TAC GTC GTC GAG

Table 2.3. Antibodies used.

Antibody	Code	Company	Dilution
Prohibitin mouse monoclonal IgG	II-14-10	ThermoScientific	1 in 200
Prohibitin rabbit polyclonal IgG	28259	Santa-Cruz	1 in 200
Androgen receptor rabbit polyclonal IgG	816	Santa-Cruz	1 in 200
E2F1 rabbit polyclonal IgG	193	Santa-Cruz	1 in 200
GAPDH mouse monoclonal IgG	32233	Santa-Cruz	1 in 2000
MCM5 rabbit polyclonal IgG	22780	Santa-Cruz	1 in 200
Polyclonal goat anti-rabbit Immunoglobins/Biotinylated	E0432	Dako	1 in 1000

2.6 Methods for cell culture

2.6.1 Cell culture maintenance

All cell lines were incubated at 37˚C, 95% (v/v) humidified atmosphere at 5% (v/v) CO_2 in either a 25cm^2 or a 75cm^2 flask. Media on cells was changed every 3-4 days. All cells were regularly checked for mycoplasma contamination using the EZ-PCR Mycoplasma Test Kit (Biological Industries, Israel). Gene expression of *PSA* was carried out the LNCaP cell line in starvation media using the SYBR® Green Q-PCR technique described in 2.8.3 to validate their androgen responsiveness.

2.6.2 Detachment of adherent cells and cell counting

Adherent cells were detached from the plastic using either 1-2 mL of Trypsin-EDTA (0.01% trypsin and 0.05% EDTA in PBS buffer). Cells were left to detach in an incubator at 37˚C, until detachment of cells were seen under a light microscope. 5-10 mL of serum containing media was added to the cell suspension to quench the trypsin. 10 μL of cell suspension was added to a 0.100mm depth haemocytometer (Neubauer). Cells were counted in four separate squares and averaged.

2.6.3 Freezing cells

Stocks of cells of a low passage number were stored in liquid nitrogen. Cells were trypsinised according to the protocol shown in 2.7.2. The cells were centrifuged at 12,000g for 4 minutes and the cell pellet was resuspended in 1 mL FCS + 10 %DMSO (Sigma-Aldrich). This was placed into a Cyro-tube (Grenier Bio-one) that was then wrapped in protective paper and stored at -80˚C for 24 hours. The vials were then transferred to a liquid nitrogen tank for long term storage.

2.6.4 Resuscitation of cells

Revival of cells was carried out by thawing cell vials from liquid nitrogen in a warm water bath at 37˚C. The cells were then transferred to a sterile universal tube where fresh FCS-containing media was added. The universal tube was centrifuged at 1,000g for 7 minutes. The supernatant was removed and the cell pellet was resuspended in 5 mL of fresh FCS-containing media. The cells were transferred to a 25cm^2 flask where they were left to seed at 37˚C within the incubator.

2.6.5 Mycoplasma test (Biological Industries)

Media from cultured cells was centrifuged at 250 g for two minutes. Next the supernatant was centrifuged for 15000 g for ten minutes. The supernatant was decanted and the pellet was resuspended in 25 μL of Buffer solution. This was then heated to 94˚C for three minutes and stored at -20˚C. A PCR was carried out with the cycling conditions shown in table 2.4. The PCR products were then run on a 0.8% (w/v) agarose gel to visualise DNA products.

Table 2.4. Cycling conditions for mycoplasma PCR.

Stage	**Temperature (˚C)**	**Time**
Holding	94˚C	30 seconds
Cycling (35 cycles)	94˚C	30 seconds
	60˚C	120 seconds
	72˚C	60 seconds
Holding	94˚C	30 seconds
	60˚C	120 seconds
	72˚C	5 minutes

2.7 Methods for molecular biology

2.7.1 RNA extraction

Cells for RNA extraction were lysed in 1 mL of TRI reagent (Ambion) and were scraped down into a sterile Eppendorf tube. 0.2 mL of chloroform (Sigma-Aldrich) was added and the lysates were thoroughly mixed and left to stand for five minutes. The Eppendorf tubes were centrifuged for 15 minutes at 12000 g. The top aqueous layer containing the RNA was removed and placed into a separate sterile Eppendorf tube. 0.5 mL of 2-propanol (Sigma-Aldrich) was added to the aqueous solution and shaken. Samples were left to stand at room temperature for 15 minutes. Eppendorf tubes were then centrifuged at 12000 g for ten minutes to pellet the RNA. The supernatant was decanted and the RNA pellets were washed in 75% (v/v) ethanol and were centrifuged for five minutes at 7500 g. The ethanol was then decanted and the pellet was left to air dry. Once the pellet had dried, the pellet was dissolved in DEPC treated water. The samples were measured on an Implen nanophotometer (UK) to determine the RNA concentrations (ng/μL). Samples were either stored at -80˚C or were immediately reversed transcribed.

2.7.2 Reverse transcriptase reaction (RT)

500 ng of RNA was reverse transcribed (RT) into cDNA with the following protocol: OligodT primer (ABI) (1 μL) was added to RNA and water (total 9 μL). This was heated to 65˚C for 5 minutes. Next 10 μL of the RT mix (ABI) was added. This was heated to 42˚C for 20 minutes followed by 75˚C for 10 minutes. The cDNA was then diluted accordingly.

2.7.3 Quantitative SYBR® green PCR (Q-PCR)

Reactions were plated using MicroAmp Applied Biosystems 96 well plates. Each reaction consisted of 2 μL of the desired cDNA and 8 μL of a master mix. The master mix consisted of 5 μL of Sybr® Green PCR master mix (Applied Biosystems), 1 μL of a primer mix containing both the forward and reverse primers (2.5pmol/μL) and 2 μL of PCR water. Cycling conditions for Quantitative SYBR® green PCR are shown in table 2.5. Gene expression was normalised to housekeeping genes (GAPDH, RPL19).

2.7.4 Quantitative Molecular beacon PCR (Q-PCR)

Reactions were plated using MicroAmp Applied Biosystems 96 well plates. Each reaction consisted of 1 μL of the desired cDNA and 9 μL of a master mix (Primerdesign). Table 2.6 illustrates the contents of the master mix. Table 2.7 illustrates the cycling conditions. All samples were normalised to GAPDH and RPL19 gene expression.

Table 2.5. Cycling conditions for Quantitative SYBR® green PCR.

Stage	Temperature (˚C)	Time
Holding	95˚C	10 minutes
Cycling (40 cycles)	95˚C	15 seconds
	60˚C	60 seconds

Table 2.6. Contents of Quantitative Molecular beacon PCR master mix.

Reagent	Amount
1pM Z reverse primer	0.3 µL
10pM forward primer	0.3 µL
Uniprobe	0.3 µL
Master mix	5 µL
H_2O	3 µL

Table 2.7. Cycling conditions for the molecular beacon Q-PCR.

Stage	**Temperature (˚C)**	**Time**
Holding	95˚C	10 minutes
Cycling (100 cycles)	95˚C	10 seconds
	55˚C	35 seconds
	72˚C	10 seconds

2.8 Methods for proliferation, adhesion and migration assays

2.8.1 Crystal Violet Proliferation assay

96 well plates were plated with the desired cell number and left to adhere overnight. In the case of the doxycycline dose dependent curves, the cells were cultured with fresh medium with the specific concentrations of doxycycline. Plates were left for either 24 hours or 48 hours. At the specific time point, the media was removed from the wells and replaced with 4% (v/v) formalin (Sigma Aldrich) to fix the cells for an hour. The formalin was then washed off gently with tap water and replaced with 0.5% (v/v) Crystal Violet solution (Sigma Aldrich) and left for 30 minutes. The Crystal Violet was then washed off gently with tap water and plates were left to dry. The dye was then dissolved in 10% (v/v) acetic acid (Sigma Aldrich). Absorbance was read at 540nm using an ELx800 plate reading spectrophotometer (BioTek, VT, USA).

2.8.2 Scratch assay

Cells were seeded onto a 24 well plate until a confluent monolayer was formed. Prior to a scratch formation using a p10 pipette tip, the media for each well was changed (1 mL each) with and without doxycycline (10 μM) for 24 hours. In the case of no doxycycline, PBS was added as a control. Once the scratch was made, an image was taken of each well to mark time-point zero. To ensure the same area of the wound was being imaged at every time point, several marks were made underneath the plate as a point of reference. Images were taken every hour using a Leica DMI1 microscope. Semi-quantification of the wound area was measured using Image J software (National Institutes of Health, NY, USA).

2.8.3 Transwell filter migration assay

Cells (500,000) were seeded onto the upper chamber of a 8 μM pore size ThinCert™ insert (Greiner-Bio one) in 500 μL of 1% (v/v) FCS RPMI. The lower chamber of the 24 well plate contained 1 mL of 10% RPMI FCS to create a chemoattractant gradient. Cells were left to migrate for desired time points. At the correct time point, filters were washed with PBS and placed onto a fresh 24 well plate. An enzyme free cell dissociation solution (Millipore) (350 μL) made with calcein AM (Thermo Fisher Scientific) (ratio of 1.2 μL: 1 mL) was placed in the lower chamber of the 24 well plate and left to incubate at 37°C for one hour. The solution was transferred to a black 96 well plate and Fluorescence was measured using the Glomax multi-detection system (Promega) at an excitation and emission wavelengths of 495/515 nm.

2.8.4 FACS (Fluorescence-activated cell sorting)

Cells were fixed with 10 mL of 70% (v/v) ethanol and kept at 4°C. Cells were stained with a propidium iodide/Ribonuclease A (PI/RNase A) solution for 30 minutes. PI was used at a concentration of 50μg/mL and RNase A (Sigma Aldrich) was used at a concentration of 100μg/mL. The samples were then run on a FACSCanto II machine (BD Biosciences). Analysis of the data was carried out using FCS Express 4 Flow research. Gating for live cells was carried out using the FSC-A (forward scatter area) and SSC-A (side scatter area). FCS-A measures the cell size whereas SSC-A measures the cell granularity. Next gating for single cells was carried out by using the FSC-A and FSC-W (forward scatter height) to eliminate doublet cells (figure 2.1). From this gate, the cell cycle histogram was made using the fluorochrome channel PerCP-CY5-5-A against cell count. From here the percentage of cells in G1, S and G2 phase could be calculated.

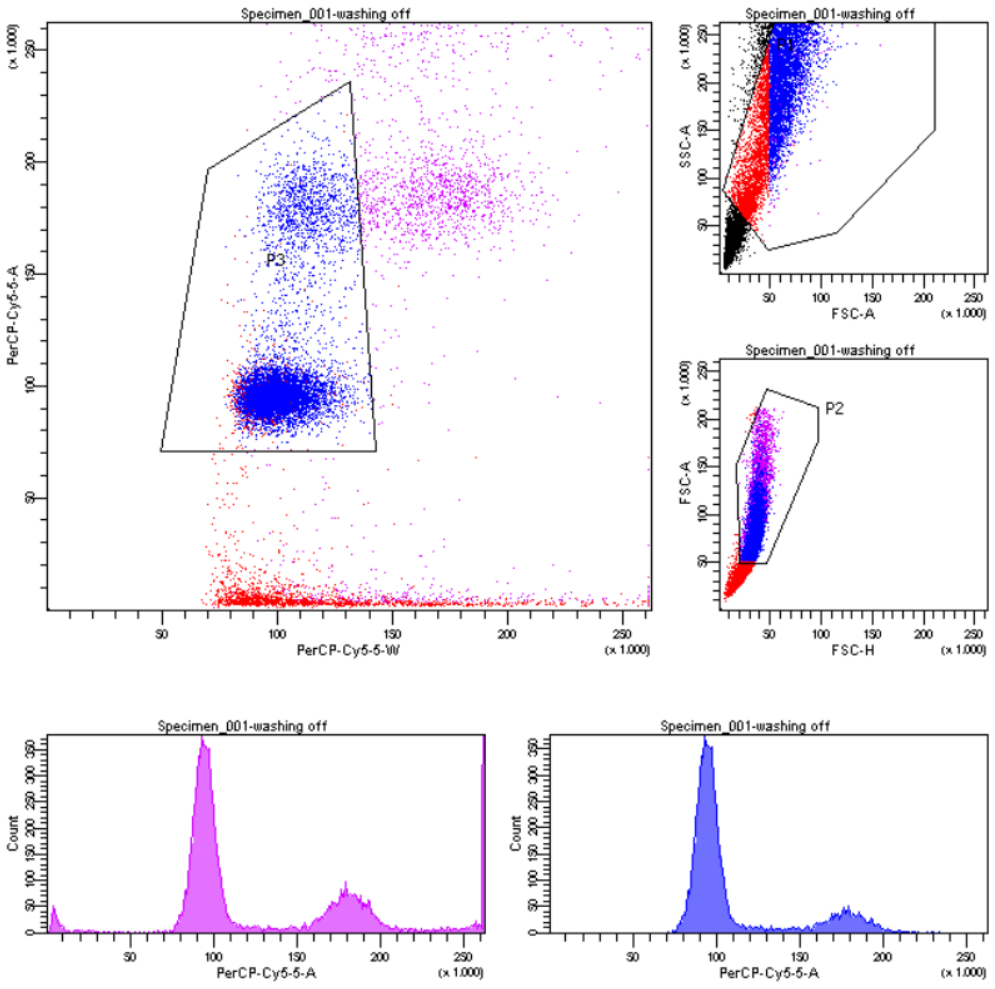

Figure 2.1. Gating on FACSDiva version 6.1.3 for fixed cells stained with propidium iodide (PI).

2.8.5 Adhesion assay

In order to create a surface for the cells to attach to, matrigel was set onto wells of a 96 well plate. Matrigel was made at a working concentration of 5 μg/100 μL in serum free media (stock concentration 9.1 mg/ml). The matrigel was coated onto the wells of the 96 well plate and left to set at 50 °C for 2 hours. The matrigel was then rehydrated in media for 30 minutes, after 30 minutes the media was aspirated off and cells were seeded onto the matrigel (45,000 cells/well). The cells were left at 37°C in the incubator for the desired amount of time. The media was gently removed and the cells on the matrigel were then fixed with 4 % formalin for 30 minutes. The cells were then stained with 0.5 % crystal violet solution for 20 minutes. The cells were gently washed with tap water and left to air-dry overnight. The cells were visualised using a Leica light microscope and pictures were taken using the LAS (Leica Application Suite) 4.4. Each well had 6 pictures taken and the cells seen in the field of view were counted.

2.9 Method for RNA-sequencing

2.9.1 mRNA isolation and cDNA synthesis

The initial stage of RNA sequencing was to isolate polyA mRNA from total RNA, using the Dynabeads mRNA DIRECT kit (Life Technologies). To ensure ribosomal RNA was still intact, any degradation of 18S and 20S (ribosomal peaks) in the RNA samples was identified using a Bio-analyser-2100 (Aligent). Next, the isolated mRNA samples were fragmented using RNAse III and purified to produce a 150-200bp library, using the Total RNA-seq kit (Life Technologies). These fragments were ligated to adaptors to allow cDNA synthesis to occur. The amplified cDNA was carried out using the IonXpress RNA-seq 5' and 3' barcoded primers. Amplified cDNA was then purified and quantified using the Bio-analyser 2100 (Aligent).

2.9.2 Template preparation and RNA-seq

In order to clonally amplify the cDNA library onto Ion Sphere Particles (ISP's) for sequencing, an emulsion PCR was carried out using on an Ion OneTouch2 system and the PI template OT2 200 kit (Life Technologies). Template positive ISP's were recovered using an ion torrent machine (Life technologies) and streptavidin Myone beads. Further, the template positive ISP's were processed using the Ion Proton 200 sequencing kit and loaded onto a P1 chip. This chip was then sequenced on an Ion Proton (Life Technologies). The following parameters were used; single end, forward sequencing. Samples were aligned to the human genome (version Hg19). The torrent Suite version 3.6 (Life Technologies) was utilised for base calling, adaptor trimming, barcode deconvolution, bowtie and cufflinks using STAR aligner. Data analysis was carried out with the Partek Genomic Suite 6.6 (2017 Partek Incorporated). Normalisation was carried out via the RPKM normalisation method (126) along with a 1-way ANOVA test for differential gene expression (n=2). The procedure is displayed in 2.10.3.

2.9.3 Overview of RNA sequencing

1) mRNA is captured using polyT beads

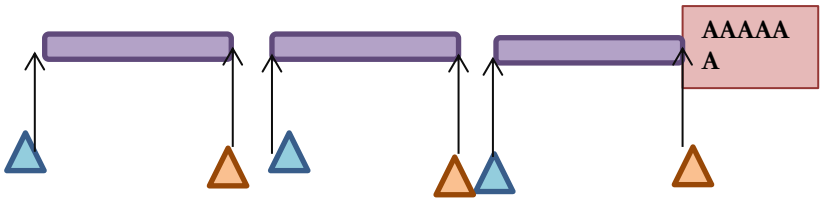

2) mRNA is then fragmented and 5' and 3' adaptors are ligated to fragments

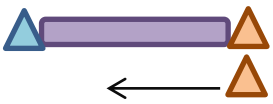

3) RT primer binds and cDNA is synthesised

4) cDNA is amplified and an optional barcode primer (green square) is added to distinguish between samples

5) cDNA is captured and amplified on microbeads during an emulsion PCR

6) Captured DNA is now ready to be sequenced from the A end to the microbead

2.10 Methods for protein detection

2.10.1 Protein extraction

Cells desired for protein extraction were washed with ice-cold PBS. For a T75 flask of confluent cells, 600 µL of the lysis buffer was added to the cells and left on ice for 10 minutes. The cells were then scraped down into a 1 mL Eppendorf tube. The cell lysate was then centrifuged at 20,000g for 20 minutes. The supernatant containing the protein was then transferred to a clean sterile Eppendorf tube ready to be quantified.

2.10.2 Protein quantification (BSA assay)

Quantification of protein samples for loading onto a SDS-PAGE gel, was carried out using the BioRad DC Protein Assay kit (BioRad Laboratories) against a BSA (bovine serum albumin) standard curve. Firstly, a serial dilution of BSA was made, starting with the highest concentration of 10 mg/mL down to 0.15625 mg/mL. Each dilution (5 µL) was pipetted into a 96 well plate. Reagent S (20 µL) was added to each mL of reagent A (Biorad). This solution (25 µL) was added onto the 5µL of standards and protein samples. Reagent B (200 µL) (Biorad) was then added to each well and left to stand until a blue colour developed. Absorbance was read at 630 nm using an ELx800 plate reading spectrophotometer (BioTek, VT, USA). Excel was used to calculate protein concentrations using the generated standard curve. The proteins were diluted to a concentration of 20 µg/µL with lysis buffer. This was then further diluted with 2X Llaemeli sample buffer concentration (Sigma-Aldrich) at a ratio of 1:1. The samples were then denatured at 95 °C for 3 minutes, before loading onto the SDS-PAGE gel.

2.10.3 SDS Polyacrylamide Gel Electrophoresis (SDS-PAGE)

The percentage of the gel used was dependent on the size of desired protein to be detected. For a 10% resolving gel, table 2.8 depicts the components and volumes used. For the 5% stacking gel, table 2.9 depicts the components and volumes used. Gels were set between two glass plates held in place by a loading cassette. Once both the resolving gel had set, the stacking gel was prepared according to the guidelines set in table 2.9 and a well-forming Teflon comb was inserted and the gel was allowed to polymerise. The loading cassette was then placed into a gel electrophoresis tank filled with running buffer. The comb was removed and the appropriate amount of heat-denatured protein was loaded (concentrations of protein determined via BSA assay). 5 µL of a BLUeye prestained protein ladder (Geneflow) was loaded as a marker. Samples were electrophoresed at 120V for 90 minutes.

2.10.4 Transfer of proteins onto polyvinylidene fluoride (PVDF) membrane

Once the SDS- PAGE was complete, a wet transfer was carried out to transfer the proteins onto an Immobilon®-P PVDF membrane (Merck Millipore, MA, USA). Prior to transfer, the PVDF membrane was activated in methanol for 5 minutes. The resolving gel was gently removed and placed in transfer buffer, alongside filter papers. On the negative side of the 'sandwich' cassette, two filter papers were placed onto a sponge, the resolving gel was placed onto the filter papers. This was followed by the activated PVDF membrane alongside two more filter papers and a sponge. Electro-blotting was carried out at 250mA for 2 hours. Once transfer was complete, membranes were incubated at room temperature in 5 % (w/v) blocking buffer (5 g of milk powder (Marvel) in 100 mL of TBS) for 1 hour to ensure non-specific binding of the primary antibody. Membranes were kept on a rolling platform (Wolf Laboratories).

2.10.5 Immuno-blotting of proteins

The primary antibody was diluted in 5 % blocking solution according to table 2.3. Membranes were incubated overnight with the primary antibody at 4˚C with constant rotation. Membranes were then washed three times (5 minutes each) with 0.1 % (v/v) TBS-T at constant rotation. The HRP-conjugated secondary antibody secondary was diluted 1 in 1000 in 5% blocking solution and incubated with the membranes for 1 hour at room temperature with constant rotation. Membranes were washed twice with TBS-T and the final time with TBS. Development of membranes was carried out by mixing a 1:1 ratio of EZ-ECL solution A and solution B (Biological Industries) and incubating this solution on the membrane for 5 minutes. Images were processed using the G-BOX by Syngene. Semi-quantitative analysis of protein expression was carried out using Image J software (National Institutes of Health, NY, USA).

Table 2.8. Volumes and components for a 10% resolving gel.

Solution	Component volume (mL)
H_2O	5.9
30% acrylamide mix	5.0
1.5M Tris (pH 8.8)	3.8
10% SDS	0.15
10% ammonium persulfate	0.15
TEMED	0.006

Table 2.9. Volumes and components for a 5% stacking gel.

Solution	Component volume (mL)
H_2O	3.4
30 % acrylamide mix	0.83
0.5 M Tris (pH 6.8)	0.63
10 % SDS	0.05
10 % ammonium persulfate	0.05
TEMED	0.005

2.10.6 2D western blot

In order to assess both the molecular weight and the isoelectric point of proteins, a 2D western blot assay was carried out. Firstly, a 2D clean up procedure (GE healthcare) was carried out to remove interfering contaminants such as salts and lipids. To 100 µL of protein sample, 300 µL of precipitant was added and left on ice for 15 minutes. Next 300 µL of co-precipitate was added and the sample was centrifuged at 12,000g for five minutes. The supernatant was removed and 40 µL of co-precipitant was added to the pellet. The sample was then left on ice for five minutes. The sample was centrifuged at 12,000g for 5 minutes and the supernatant was discarded. Next 25 µL of dH_20 was added onto the pellet and vortexed to disperse the pellet. 1 mL of chilled wash buffer (-20˚C) was added with 5 µL of wash additive. This was vortexed every ten minutes for half an hour. Next, the sample was centrifuged at 12,000g for five minutes and the pellet was left to air-dry once the supernatant had been discarded. The pellet was resuspended in 116 µL of rehydration buffer, 1 µL of bromophenol blue, 2 µL of IPG buffer and 6.25 µL of Dithiothreitol (DTT).

Next the total sample was loaded onto a coffin (Amersham Biosciences). An Immobiline DryStrip (IPG) pH 3-10, 7 cm (GE healthcare Life Sciences) was placed on top of the sample with the anode facing the positive end of the strip. The sample and IPG strip was covered with 0.5 mL of DryStrip cover fluid. The coffin was then placed onto the isoelectric focusing unit (IPGPhor Pharmacia Biotech). The protocol was as follows;

Rehydration: 12 hours at 20˚C

Step 1: Step and hold 500V for 1 hr

Step 2: Gradient 1000V for 2 hr

Step 3: Step and hold 1000V for 1 hr

Step 4: Gradient 8000V for 2 hr

Step 5: Step and hold 8000V for 8 hr

Once the isoelectric focusing was complete the IPG strip needed to be equilibrated. First the IPG strip was placed in 5 mL of reducing solution in a Falcon tube and placed on a rolling platform for 15 min. The reducing solution was then decanted and replaced with 5 mL of alkylating solution and left to rotate for 15 min. The IPG strip was then placed into the IPG well of NuPAGE 4-12% Bis-Tris Zoom Gel (Invitrogen). 1X MOPS running buffer was added to the centre chamber and external chamber. The gel was electrophoresed at 200V for 5 min and then 150V for 55 min. The transfer of proteins onto PVDF membrane and immunoblotting of the membranes were carried out following the guidelines in 2.11.4 and 2.11.5.

2.10.7 Cell fractionation and chromatin isolation

Cells were seeded at a specific cell number and hormonally starved for 72 hr. Cells were either treated with R1881 (10 nM) or the vehicle (100% ethanol). Cells were washed in PBS once and scraped down in PBS. Cells were pelleted and resuspended in 400 µL of hypertonic buffer A and 50 µL of 1% (v/v) Triton-X100 (Melford Laboratories UK). Cells were left on ice for five minutes. Next cells were centrifuged at 1300g for four minutes to isolate the cell nuclei. The supernatant was collected into a separate tube as the cytoplasmic fraction. The pellet was resuspended in 200 µL of buffer B and left on ice for ten minutes to lyse the nuclei. This was then centrifuged at 1700g for four minutes to isolate the chromatin. The supernatant was collected as the soluble nuclear fraction. The pellet was resuspended again in buffer B and centrifuged at 1700g for four minutes. The pellet was collected as the chromatin fraction. All fractions were diluted in 2X Laemmli sample buffer. The fractions for each condition; +/- R1881 was then electrophoresed on an SDS PAGE gel and immunoblotting was performed for desired proteins as described in 2.11.5.

2.10.8 Immunoprecipitation

Once the nuclear fraction of the cell lysate had been isolated as described in 2.11.7, the pellet was resuspended in IPH buffer. Next 50 µL of the lysate was mixed with 450 µL of IPH buffer. The primary antibodies (3 µg) were added to each sample. As a control, a polyclonal rabbit (or monoclonal mouse) anti-rabbit IgG antibody (3 µg) was added to each sample, depending on the species of the primary antibody used. Samples were left on a shaker for two hours at 4°C. The required amount of Dynabeads® protein G (Invitrogen Life technologies) were placed on a DynaMay2 magnetic stand (Life Technologies) and the supernatant was removed. The beads were then resuspended in IPH buffer. Dynabeads® (15 µL) were added to each sample and left on a shaker for one hour at 4°C. Samples were placed onto a magnetic stand, supernatant was removed and Dynabeads® were washed three times with 200 µL of washing solution. Antigen-antibody complexes were eluted off the beads in 20 µL of elution buffer. Elutes were mixed with 2X llaemmli sample buffer and a western blot was carried out as described in 2.11.3.

2.10.9 Kinexus protein array

LNCaP cells were hormonally starved for 72 hr. Cells were treated with R1881 (10 nM) or ethanol as a vehicle control. Cells were lysed with 300 µL of lysis buffer and centrifuged at 20,000g for twenty minutes. The samples were then sent to Kinexus (Canada) where both total protein changes and phosphorylated proteins were recorded. The array consisted of 518 pan-specific antibodies and 359 phosphosite-specific antibodies in duplicate. Data was received as an Excel spreadsheet. The fold change was calculated from the z score of the vehicle and R1881 treatment. The full Kinexus antibody microarray contains 877 antibodies. Kinexus provided both semi-quantitative and qualitative analyses of expression of signalling proteins and also their phosphorylation status. The signal strength of each antibody spot was measured by its size and also its density. The fluorescent signal was quantified and presented in duplicates in a Microsoft Excel spreadsheet, alongside the average percentage change from control, Z scores and fold change ratios.

2.11 Methods for bacteriology

2.11.1 Cloning

The desired coding sequence for a gene or DNA sequence of interest was amplified from its original plasmid or cDNA using the components and volumes shown in table 2.10. The cycling conditions are shown in table 2.11. The amplified gene was then purified and cloned into desired plasmids as described in 2.12.3 and 2.12.4.

2.11.2 DNA gel extraction

DNA fragments were electrophoresised on an agarose gel and were excised, weighed and solubilised using the gel solubilisation solution (Sigma Aldrich). 1X volume of Isopropanol (Sigma Aldrich) was then added to the gel volume and mixed until homogenous in colour. The solubilised gel mixture was loaded onto a prepared binding column and centrifuged for one minute. The flow through was discarded and the column was washed with wash solution (diluted from Wash solution Concentrate G) and centrifuged for one minute. Any residual wash solution was removed by another centrifugation step. The DNA was then eluted, by adding 25 µL of the elution solution onto the binding column and centrifuging for one minute. All centrifugation steps were carried out at 12000 g.

Insertion of DNA into the pEF6/V5-His TOPO vector was carried out in compliance with table 2.12. Contents were incubated for five minutes, then place on ice, ready for transformation of competent cells.

2.11.3 Transformation of competent cells

One vial of One-Shot® TOP10 chemically competent *E.coli* (Invitrogen) was thawed on ice (25-50µL). *E.coli* was aliquoted for each plasmid. The DNA plasmid and insert (0.5 µL) was placed directly into the middle of the cells. The contents of the tubes was flicked to mix and left on ice for thirty minutes. As a positive control, the pUC19 plasmid was added another aliquot of cells. The cells were then heat shocked for 30 s at 42°C and then placed on ice. Pre-warmed S.O.C medium (Invitrogen) (250 µL) was added to each tube. The tubes were incubated at 37°C on a shaking platform for one hour. Each transformation was spread onto a pre-warmed selective plate and incubated overnight.

Table 2.10. PCR reactions.

Components	**Amount (µL)**
GoTaq®G2 green master mix	12.5
PCR water	12
cDNA template	2
Forward primer	0.25
Reverse primer	0.25

Table 2.11. Cycling conditions for PCR.

Stage	**Temperature (˚C)**	**Time**
Holding	95˚C	5 minutes
Cycling (25 cycles)	95˚C	30 seconds
	55˚C	30 seconds
	72˚C	180 seconds
Extension	72 ˚C	10 minutes
	4 ˚C	Until taken off machine

Table 2.12. Components for ligation of DNA into the pEF6 vector.

Component	**Amount**
DNA	3µL
Salt solution	1µL
Vector (pEF6/V5-His TOPO)	1µL
water	1µL

2.11.4 Colony selection and overnight culture

Once the LB-ampicillin agar plates had been incubated overnight with *E.coli*, colonies were picked and inoculated with 5 mL of LB media and left overnight with constant shaking at 37°C.

2.11.5 Plasmid purification

Once recombinant *E.coli* cultures were grown overnight in liquid LB media, 2 mL of the culture was centrifuged at 12,000g. The pellet was resuspended in 200 µL of resuspension solution until cells appear homogenous. The cells were then lysed using 200 µL lysis solution. The solution was immediately mixed. Neutralisation solution (250 µL) was added and centrifuged for ten minutes at 12000g. The lysate was then loaded onto a prepared Miniprep binding column and centrifuged for 30 s. The flow through was discarded and 750 µL of diluted wash solution was added to the column and centrifuged for one minute. The columns were further centrifuged to remove any excess liquid. The DNA was eluted by adding 50 µL of elution solution. The DNA concentration was measured using the spectrophotometer. To ensure the plasmid has taken up the DNA insert of interest, a single and double restriction digestion was carried out according to table 2.13. Each reaction was incubated at 37°C for one hour. Alternatively a PCR reaction was carried out. The kit used for plasmid purification was GenElute® Plasmid Miniprep kit (Sigma-Aldrich).

Table 2.13. Single and double restriction enzyme digestions.

	Single Digest (BamH1)	**Double digest (BamH1 and EcoRV) (Sigma-Aldrich)**
DNA	5 µL	5 µL
Buffer (x10)	3 µL	3 µL
Enzyme	0.5 µL	0.5 µL + 0.5 µL
PCR water	21.5 µL	21 µL

Table 2.14. Ligation reaction.

Ligation reaction	**Amount**
10X DNA T4 DNA ligase buffer with 10mM ATP	5 µL
Desired vector	X
Insert	X
T4 DNA ligase	1 µL
Water	Up to 10 µL if reaction is less

2.11.6 Ligation of vector and insert

The ligation of the desired insert into a linearized plasmid was carried out using 10X DNA T4 DNA ligase buffer with 10mM ATP (New England Biolabs) and a T4 DNA ligase enzyme (New England Biolabs).

The equation used for the ligation reaction was:

(ng of vector x kb of insert)/ kb of vector x ratio =ng of insert (x3)

This formula gave the ng of insert needed for a 1:1 ratio of vector to insert. However the preferred ratio is 3:1, therefore the final number was multiplied by three to increase the likelihood of ligation. The reaction was left at 16-18°C for two hours to ligate. The ligation reaction was then transformation into *E.coli*. Table 2.14 demonstrates the contents for each ligation reaction. Ligation controls consisted of reactions with no enzyme, no insert and no insert or enzyme. Sequencing of plasmids was carried out in house at CBS (Central Biotechnologies Services).

2.11.7 Lipofectamine Transfection

In order to transfect plasmids of interest into cell lines, Lipofectamine 2000 (ThermoFisher Scientific) was the transfection agent used. Firstly, DNA up to 500 ng was diluted in 25 µL of serum free media. Next 2 µL of Lipofectamine 2000 was diluted in 25 µL of serum free media. Each tube was left to stand for 5 minutes. The two tubes were then mixed together and left to stand for twenty minutes. The DNA-lipid complex was then added to the cells dropwise and left for 48-72 hours.

2.11.8 Luciferase assay

Cells were seeded in a 24 well plate and transfected with specific luciferase reporter plasmids. Cells were lysed with 1X sample buffer, diluted in PBS from the 5X reporter lysis buffer (Promega) and were left to freeze at -20˚C. Each lysate (15 µL) was transferred to a white microfluor 96 well plate. Bright-Glo™ luciferase assay substrate (Promega) (15 µL) was added to each sample and mixed. The luminescence was read on a glomax multi detection system (Promega).

2.11.9 β-galactosidase assay

β-galactosidase transfection assay (Invitrogen) was used following a luciferase assay as a control for transfection efficiency. In any transfection assay a bos-β-galactosidase plasmid was transfected into the cells. At the end of the experiment, half of the lysate was used for the luciferase assay and half for the β-galactosidase assay. β-galactosidase assay 1X cleavage (50 µL) buffer with β-mecaptoethanol was added to each lystate (30 µL) along with 17µL of ONPG. The plate was left at 37˚C for one hour, until a yellow colour developed. The reaction was stopped by the addition of 125 µL of stop buffer to each well. Absorbance was read at 405nm using an ELx800 plate reading spectrophotometer (BioTek, VT, USA).

2.12 QuikChange lightening Site-directed mutagenesis

2.12.1 Primer design

First primers were designed for mutating targeted gene of interest using ORF finder (NCBI, U.S.A). ORF finder (Open Reading Frame Finder- NCBI) was used to analyse specific codons for different amino acids. Amino acid codons for specific serine or tyrosine residues were then single nucleotide substituted for codons for alanine. Primers were synthesised by Eurofins Genomics and were diluted according to the datasheet. Sequences for primers designed for the mutagenesis of PHB and the E2F binding site in the promoter region of MCM6 are shown in table 2.17.

2.12.2 Mutant strand synthesis reaction

Components from the QuikChange lighting Site-directed mutagenesis kit (Agilent Technologies) were used. Firstly, mutant strand synthesis reaction involved both a positive control reaction and target gene reaction. Components of both reactions are shown in table 2.15. QuikChange lighting enzyme (1 μL) was added to each reaction that were then put in a thermocycler with the cycling conditions shown in table 2.16.

Table 2.15. Mutant strand synthesis reactions.

Control reaction	**Sample reaction**
2.5 µL 10X reaction buffer	2.5 µL 10X reaction buffer
2.5 µL pWhitescript 4.5Kb control plasmid	100ng of dsDNA template
0.625 µL oligonucleotide control primer 1	125ng of oligonucleotide primer
0.625 µL oligonucleotide control primer 2	0.5 µL dNTP mix
0.5 µL dNTP mix	0.75 µL QuikSolution reagent
0.75 µL QuikSolution reagent	H_2O up to 25 µL
17 µL H_2O	

Table 2.16. Cycling conditions for mutant strand synthesis reactions.

Segment	**Cycles**	**Temperature (˚C)**	**Time (seconds)**
1	1	95	120
2	18	95	20
		60	10
		68	30/Kb of plasmid length
3	1	68	300

Table 2.17. Primer sequences for the mutagenesis of *PHB* and the promoter of *MCM6*.

Oligo Name	**Primer sequence (5'-3')**
MCM6 promoter mutation 1	CCAGAAGGGCTTTGCA
MCM6 promoter mutation 2	GTTCATTGGTCAGGGTAG
PHB S82	GTAATGTGCCAGTCATCACTGGTGCCAAA
PHB T91	CAGAATGTCAACATCGCACTGCGCATCCTCTTC
PHB S101	TTCCGGCCTGTCGCCGCCCAGCTTCCTCGCATCTT
PHB S213	GGCGGCCATCATCGCTGCTGAGGGCGACT
PHB S106	CGCATCTTCACCGCCATCGGAGAGGACTATGA

2.12.3 *Dpn* I digestion of amplication products

Dpn I restriction enzyme (1 µL) was added directly to each amplification reaction and immediately incubated at 37˚C for five minutes to digest the parental DNA strand.

2.12.4 Transformation of XL10-Gold Ultracompetent cells

The XL10-Gold Ultracompetent cells (Agilent Technologies) were thawed on ice. For each control and sample reaction, 22 µL of cells were aliquoted. To each aliquot, 1 µL of β-Mercaptoethanol (β-ME) was added and incubated on ice for two minutes. Following this, 2 µL of the *Dpn* I treated DNA from the control and sample reactions were transferred to each aliquot of the competent cells. The samples were mixed and left on ice to transform for thirty minutes. The samples were heat pulsed at 42˚C in a water bath for thirty seconds. The samples were then placed on ice for two minutes. To each sample, 0.5 mL of SOC media was added and the tubes were incubated at 37˚C for one hour, shaking at 225 rpm.

An appropriate volume of each transformation was then plated onto a pre-warmed LB-agar ampicillin plate.

2.13 Methods for cytotoxicity assays

2.13.1 MTT assay

Cells were seeded into a 96 well plate and treated with increasing concentrations of doxycycline for 24 hr. Thiazolyl Blue Tetrazolium Bromide (MTT) (Sigma Aldrich) solution was made by diluting 100 mg of MTT in 20 mL of PBS and was filter sterilised through a minisart 0.2 µm sterile filter (Sartorius Stedim Biotech) to produce a working concentration of 5 mg/mL. 100 µL of the MTT solution was added to 900 µL of media to produce a 10% solution. The cells were incubated for 4 hr at 37˚C in the incubator. At the end point, the media was aspirated off gently, and the cells were mixed with 200 µL of acidifed isopropanol. Absorbance was read at 540 nm using an ELx800 plate reading spectrophotometer (BioTek, VT, USA).

2.13.2 RealTime-Glo™MT Cell Viability assay

LNCaP/TR2/ PHB cells were seeded onto a white microplate 96 well and treated with increasing concentrations of doxycycline for 24 hr. The RealTime-Glo™MT Cell Viability assay kit was used (Promega). First, the 2X RealTime-Glo™ reagent was made by diluting the MT cell viability substrate and NanoLuc® Enzyme in cell culture media. An equal volume of the 2X RealTime-Glo™ reagent to the media on the cells was added to each well. The cells were incubated for 60 minutes in an incubator ay 37˚C. The luminescence was read on a glomax multi detection system (Promega), once the Photomultiplier Tube (PMT) had been activated for 5 minutes.

2.13.3 CellTox™Green Cytotoxicity Assay

LNCaP/TR2/ PHB cells were seeded onto a white microplate 96 well and treated with increasing concentrations of doxycycline for 24 hr. The CellTox™Green Cytotoxicity Assay (Promega) was used. The CellTox™ Green reagent was made diluting the CellTox™ Green dye in the assay buffer (1:500). 100 µL of the CellTox™ Green reagent was added to each well and mixed on an orbital shaker for 1 minute. The plate was incubated for 15 minutes at room temperature, shielded from light. The fluorescence was measured at 485-500nm_{ex} on a glomax multi detection system (Promega).

2.13.4 CellTitre-Glo®Luminescent Cell Viability Assay

LNCaP/TR2/ PHB cells were seeded onto a white microplate 96 well and treated with increasing concentrations of doxycycline for 24 hr. The CellTitre-Glo®Luminescent Cell Viability Assay (Promega) was used. First an equal volume of CellTitre-Glo® reagent to the media in the well was added, and the contents were left to shake on an orbital shaker for two minutes to induce lysis. The plate was equilibrated at room temperature for 10 minutes to stabilise the luminescent signal. The luminescence was read on a glomax multi detection system (Promega), once the Photomultiplier Tube (PMT) had been activated for 5 minutes.

2.14 Checkmate ™ Mammalian two-hybrid assay

In order to assess protein-protein interaction, a Checkmate ™ Mammalian two-hybrid assay was carried out. The assay contained two primary plasmids, pBIND and pACT. The pBIND plasmid contains the yeast Gal4 DNA binding domain upstream of a multiple cloning site. The pACT plasmid has the herpes simplex virus VP16 activation domain that is upstream of a multiple cloning site. The genes of interest (PHB and E2F1) were cloned into these vectors to produce fusion proteins with the DNA binding domain of Gal4 and VP16 respectively (refer to 2.12). The fusion constructs were transfected alongside pGL5 into mammalian cells (refer to 2.12.8). pGL5 has five GAL4 binding sites upstream of a TATA box, that is upstream of the firefly luciferase reporter gene. In the absence of protein interaction, there is a background level of luciferase production. However, upon protein-protein interaction, an increase in luciferase production is seen above the threshold limit. Cells were left to transfect for up to 48 hours and then lysed. The amount of luciferase was measured as compared to the negative controls. The luminescence was read on a glomax multi detection system (Promega). Two positive control plasmids were provided. pBIND-ID and pACT-myo. They both expressed proteins that are known to interact *in vivo*.

2.15 Statistical analysis

GraphPad Prism (GraphPad Software, Inc., CA, USA) for used for all statistical analysis. Each experiment was repeated a minimum of three times (n=3), to give three independent biological repeats, unless otherwise stated. Error bars represent the standard deviation or standard error of mean of all three experiments which is stated in each figure legend. An unpaired student T test, or a one way ANOVA test was used to test statistical significance on data that was normally distributed. On non-normal data, a Kruskal–Wallis one-way statistical test was carried out. Asterisk (*) notation was used to denote p values; *<0.05, **<0.01,***<0.001.

Chapter III: Characterisation of the LNCaP cell lines used in this study.

3 Chapter III: Characterisation of the LNCaP cell lines used in this study.

3.1 Introduction

As this thesis is focusing on PC, the main cell lines used were derived from PC patients. The first step was to identify that the cell lines used throughout this thesis were verified for their hallmark characteristics and their AR responsiveness. The main cell model used in this project was the parental cell line, LNCaPs. Table 3.1 describes its main features.

The LNCaP cell model was first isolated from a human metastatic prostate adenocarcinoma found in a lymph node. The original cell line is androgen responsive and is positive for both gene and protein expression of prostate specific antigen (PSA) and the androgen receptor (AR). Although LNCaP cells are androgen sensitive, they harbour a mutation within the ligand binding domain of the AR, allowing non-specific ligands to activate the AR, thus are beginning to become less androgen dependent. This is the T877A mutation, that gives the cell line its unique promiscuous binding affinity for a broad range of steroids such androgens as well as adrenal androgens (127). Expression of EGF/TGF-α-R and IGF-1-R are seen. Inactivation of both *PTEN* and *P53* are seen in this cell line, along with the expression of cytokeratin 8, 18 and 20. Xenografts using this cell model have a 80% success rate with a tumour doubling time of 86 hours when implanted with Matrigel™ in nude mice (127).

Table 3.1 Characteristics of wt LNCaP cells.

	Description
Organism	*Homo sapiens,* human
Tissue	prostate, derived from metastatic site: left supraclavicular lymph node
Disease	carcinoma
Age	50 years old
Gender	male
Morphology	epithelial
Growth properties	adherent, single cells and loosely attached clusters
AR	Positive
PSA	Positive

3.2 Methods

- Cell culture of LNCaPs and LNCaP/TR2/PHB cells (refer to 2.1).
- SYBR® green Q-PCR (refer to chapter 2.8.3).
- Western blot (refer to chapter 2.11.1-2.11.5).
- Cell cycle FACS analysis (refer to chapter 2.9.4).
- Crystal violet proliferation assay (refer to chapter 2.9.1).
- Cell cytotoxic assays (MTT assay, RealTime-Glo™MT Cell Viability assay and CellTox™Green Cytotoxicity Assay). Refer to chapter 2.14.1-2.14.3.

3.3 Results

3.3.1 Verifying the characteristics of the parental LNCaP cell line

To confirm that the cell line LNCaP was androgen responsive and that the methods of hormone manipulation used were robust, we verified the androgen sensitivity and responsiveness of the cells.

Firstly, the LNCaP cell line was plated at a cell number of 250,000 cells (in a 6 well plate) and left to adhere. The cells were washed with PBS and the media was then replaced with 1 mL of charcoal stripped media and the cells were left to hormonally starve for 72 hr. Cells were then treated with either R1881 (10 nM) as a synthetic androgen or ethanol (vehicle) and left for 24 hr. The RNA was then extracted, reverse transcribed and SYBR® green Q-PCR was used to analyse the fold increase in the AR regulated gene; *PSA (KLK3)*. Figure 3.1 illustrates a 286 fold increase in PSA expression when compared to ethanol treated cells.

It has also previously been reported that androgen treatment downregulates PHB at the RNA level. Figure 3.1 illustrates a 6 fold decrease in *PHB* expression in cells treated with R1881 (10 nM). This confirms that the wt LNCaP cell line is in accordance with characteristics such as production of *PSA* gene expression upon AR stimulation (with the addition of R1881) and a decrease in *PHB* expression as previously published (128).

3.3.2 Verifying characteristics of the LNCaP/TR2/PHB cell line

The LNCaP cell line was used to derive a doxycycline-inducible cell line over-expressing PHB cDNA that was carried out prior to the beginning of this project and published (129).

Firstly, an introduction into the production of the *LNCaP/TR2/PHB* cell line. The T-REX system by Invitrogen Life Technologies was adopted according to the manufacturer's guidance. The pcDNA6/TR expression plasmid was transfected in LNCaP cells to express the Tet repressor. Successful transfection was identified by Blasticidin (12 mg/mL) selection. Positive colonies were expanded and a luciferase assay was used to determine doxycycline (dox) inducibility using a control pcDNA4/TO/luc plasmid (tet-inducible luciferase). Choosing a sub clone was dependent on being highly inducible with non-leaky expression of luciferase (129). Following this, LNCaP/TR2 cells were stably transfected with pcDNA4/TO/PHB (tet-inducible *PHB* cDNA). Now only in the presence of doxycycline, the cell line produces ectopic *PHB* cDNA. The schematics of how this system works is shown in figure 3.2. Validation of the hallmarks of this doxycycline inducible cell line was carried out using Q-PCR, western blot and FACs.

Firstly in order to verify that the inducible cell line used was producing an ectopic over-expression of *PHB* cDNA only in the presence of doxycline (dox). The cells (250,000 cells per well in a 6 well plate) were treated with 10 μM of dox for a minimum of 16 hr in TET-free RPMI media. PBS was used as the vehicle. The RNA was extracted, reverse transcribed and SYBR® green Q-PCR was carried out to assess gene expression. Figure 3.3 demonstrates that with the addition of dox there is a significant increase in *PHB* gene expression.

Further, the expression level of *PSA* was also assessed in the LNCaP/TR2/PHB cell line. The cells were hormonally starved for 72 hr (charcoal stripped FBS), R1881 (a potent synthetic androgen 10 nM) was then added to the cells for 24 hr. Ethanol was used as the vehicle control. Figure 3.3 shows that in the absence of dox and with the addition of R1881 there is a 16 fold increase in *PSA* expression when compared to ethanol. However, with the addition of dox, there is no androgen induction of *PSA* expression. Figure 3.3 illustrates no difference in *PHB* expression with and without R1881 in the absence of dox. However, when dox is added, the expression of *PHB* increases, indicating the dox inducibility of *PHB*, and with the addition of R1881 the *PHB* expression decreases in the presence of dox but is not statistically significant.

As a control to ensure dox was not inducing an increase in *PHB* on its own in the absence of the inducible plasmid, the LNCaP cells (250,000 cells in a 6 well plate) were also treated with 10 μM of dox for a minimum of 16 hr. Figure 3.3 demonstrates no significant change in the expression of *PHB* in the presence of doxycycline. This signifies that dox is only producing *PHB* cDNA over-expression in the inducible cell line.

The protein expression of PHB was also assessed in the LNCaP/TR2/PHB cell line. Figure 3.4 demonstrates that there is a 6 fold increase in PHB protein expression in the presence of doxycycline. Indicating that doxycycline (16 hr) induced etopic *PHB* cDNA is being translated into a functional protein.

3.3.3 PHB over-expression halts the cell cycle

Previous reports have identified that PHB has a repressive role on the cell cycle (128), thus further investigations were taken forward. FACs analysis was carried out to identify at what cell cycle stage PHB's over-expression was having an effect. Cells were left to seed to 70% confluency and incubated with 10 μM doxycycline for two time points, 24 hr and 48 hr. Significance was seen at the 48 hr time point. Figure 3.5 shows PHB over-expression increases the cell population in the G1 phase and decreases the cell population in the S phase and G2/M phase. This confirms that PHB carries out a repressive role in the cell cycle by halting the cell population in the G1 phase. In synergy with this experiment, a proliferation assay was carried out at the same time points, 24 hr and 48 hr using the crystal violet assay on the LNCaP/TR2/PHB cell line (figure 3.6). Different concentrations of doxycycline were used to identify the optimum

concentration. Significance was seen at 10 μM of doxycycline at 24 hr and at 2.5 μM, 5 μM and 10 μM at 48 hr. This again confirmed that PHB suppressed the proliferation of the LNCaP cells.

As PHB has an important role in the mitochondrial membrane, supporting proteins involved in the electron transport chain, it was important to verify that PHB over-expression caused only cell cycle arrest and not cell death or mitochondrial dysfunction that could have halted the cell cycle. Various assays were used to assess mitochondrial activity, membrane integrity and number of live cells (Figure 3.7). Firstly, an MTT assay was carried out on the LNCaP/TR2/PHB cell line treated with various concentrations of doxycycline (0 μM, 0.312 μM, 0.625 μM, 1.25 μM, 2.5μM, 10 μM) for 24 hr. The MTT assay indicated there was no significant effect on mitochondrial activity with increasing concentrations of doxycycline, suggesting ectopic PHB over-expression was not causing cellular stress. Further, a CellTox Green assay was carried under the same experimental conditions. The assay showed no changes in cell membrane integrity - disruption of membrane integrity is indicative of cell death. Next, the cell Titer-Glo assay determined the number of viable cells based on ATP production, an indicator of metabolic activity. Increasing concentrations of doxycycline had no significant effect on the amount of ATP produced suggesting cells are still viable at the highest concentration of doxycycline. Finally a RealTime-Glo™ MT Cell Viability assay was carried out. This assay depends on the reducing ability of cells that in turn depicts metabolic activity. Increasing concentrations of doxycycline had no significant effect on the luminescence produced, suggesting metabolism within the cells were unaffected with the presence of PHB over-expression.

Further, cells pre-treated with doxycycline (16 hr) were then washed with PBS and left to grow for either 48 hr or 72 hr in full media. The cell population in the S phase was measured via FACs analysis. After 96 hr, slowly the cell population began to re-enter the S phase. This suggests that PHB over-expression is causing a temporary suppression of the cell cycle and not permanent quiescence. Accumulating these assays together, PHB over-expression is only causing cell cycle arrest. This is also confirmed by the FACS analysis showing no apoptotic cell population (figure 3.5).

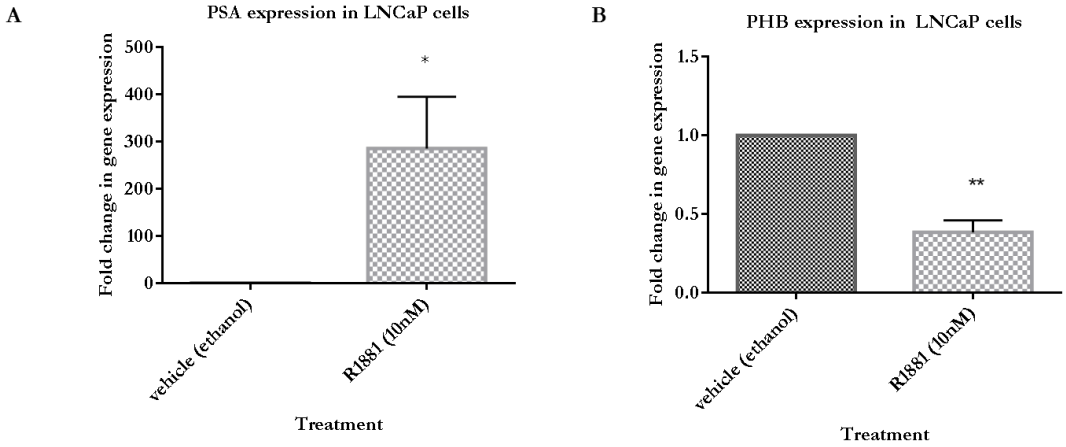

Figure 3.1. Characterisation of the LNCaP cell line**. A,** SYBR green Q-PCR results of *PSA (KLK3)* gene expression. The LNCaP cells were grown in charcoal stripped media (72hr) and then treated with 10 nM of R1881 or vehicle (ethanol) for 24hr. Fold increase is shown compared against cells treated with ethanol. **B**, SYBR green Q-PCR results of *PHB* gene expression. LNCaP cells were grown in charcoal stripped media (72hr) and then treated with 10 nM of R1881 or vehicle (ethanol) for 24hr. p value <0.05*, <0.01**. n = 3. Fold decrease is shown compared against cells treated with ethanol. Data was normalised to housekeeping genes; RPL19 and GAPDH. Error bars depict the SEM.

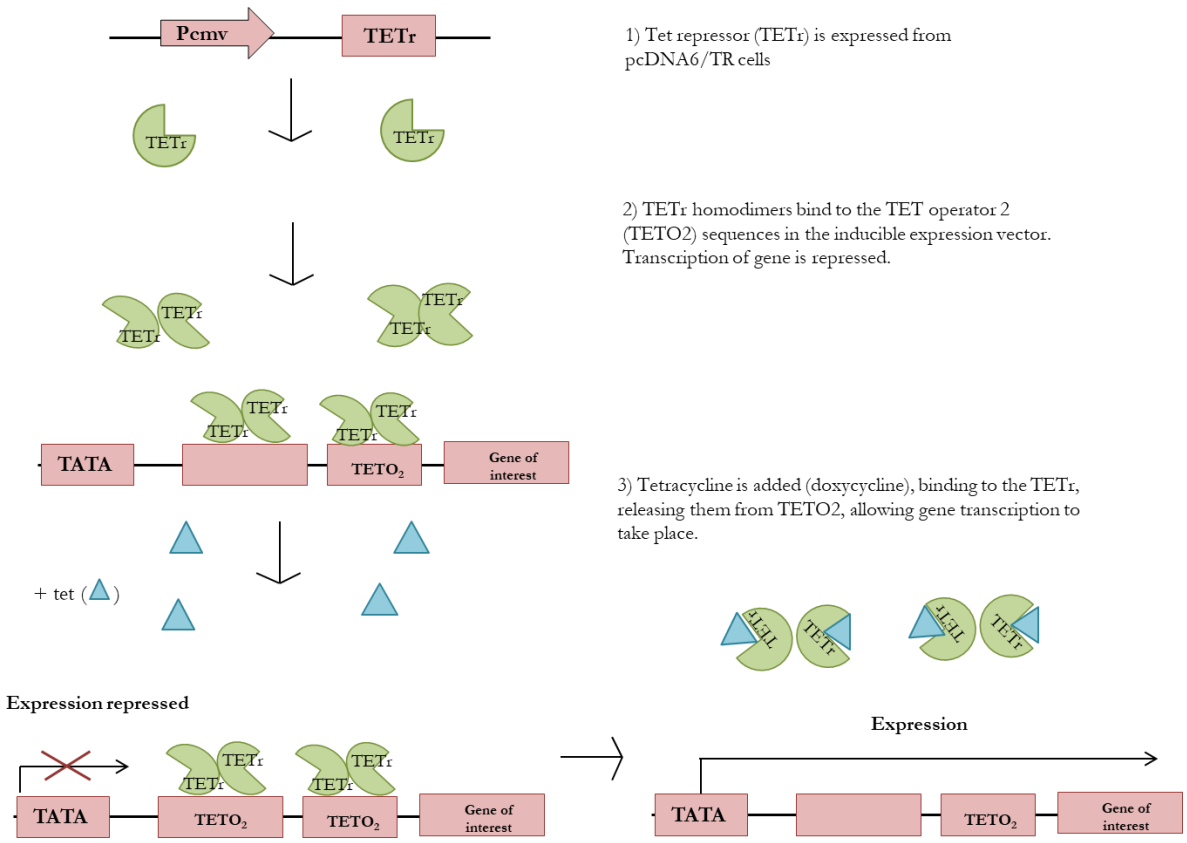

Figure 3.2. Schematic representation of how a tetracycline inducible cell line works. Image adapted from the protocol of life technologies T-REx™ System. A Tetracycline-Regulated Expression System for Mammalian Cells.

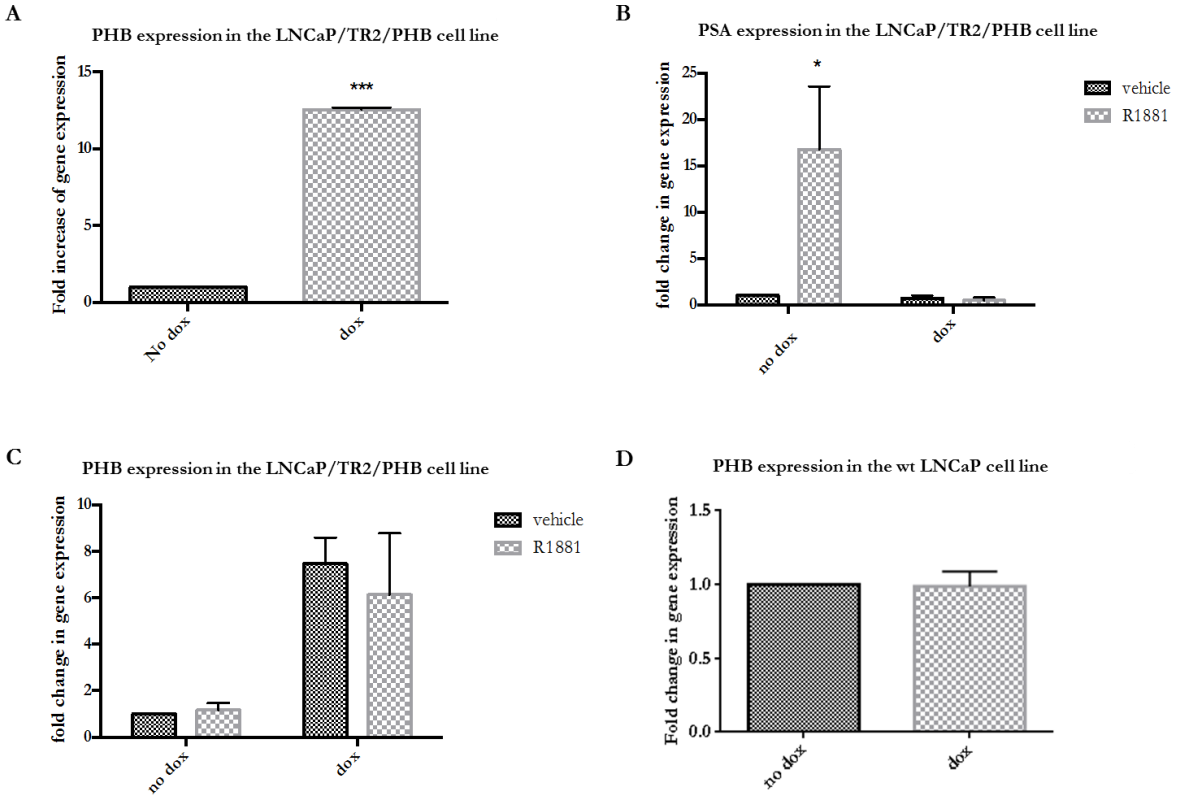

Figure 3.3. Characterisation of the inducible cell line LNCaP/TR2/PHB by analysing gene expression of *PHB* and *PSA (KLK3)*. **A**, *PHB* expression in LNCaP/TR2/PHB cells grown in TET free media with and without 10 μM of dox (16hr). Fold increase compared against cells with no dox (PBS). **B**, *PSA* gene expression in LNCaP/TR2/PHB cells grown in charcoal stripped media (72hr) with and without 10 nM of R1881for 24hr and with and without 10 μM of dox. Fold increase compared against cells with ethanol and cells without dox. **C**, *PHB* gene expression in *LNCaP/TR2/PHB* cells in charcoal stripped media (72hr) with and without 10 nM of R1881 for 24hr and with and without 10 μM of dox. Fold increase is shown compared against cells treated with ethanol and cells without dox. **D**, *PHB* gene expression in wt LNCaP cells. No significant difference in *PHB* expression in LNCaP cells treated with and without 10 μM of dox (16 hr). Data was normalised to housekeeping genes; RPL19, GAPDH and βactin. p value <0.05*, p value <0.001***. n=3. Error bars represent SEM.

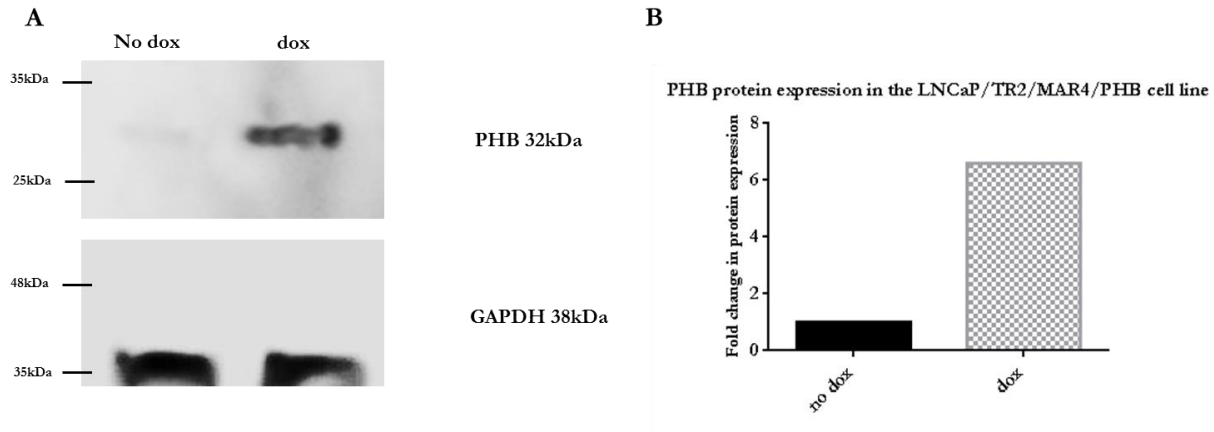

Figure 3.4. Protein verification of PHB expression with dox in LNCaP/TR2 /PHB cells. **A**, western blot analysis showing PHB expression in LNCaP/TR2/PHB cells treated with dox (16hr, 10 μM). **B**, a bar graph illustrating the densitometry values of the bands shown in A. Values were normalised to GAPDH values. Approximately a 7-fold increase in PHB protein expression is seen with dox. n=1.

A

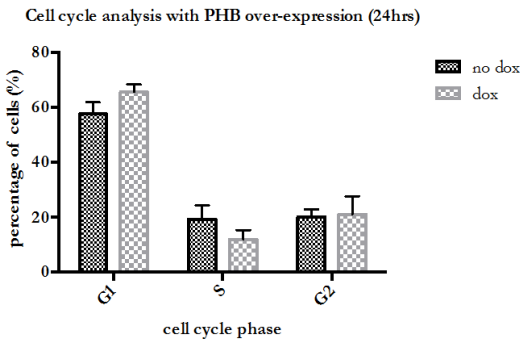

B

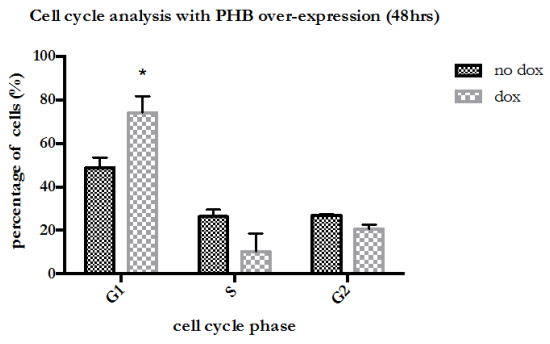

24 hours	G1 (%)	S(%)	G2(%)	48 hours	G1 (%)	S(%)	G2(%)
No dox	58 ± 4	19 ± 4	20 ± 2	**No dox**	49 ± 3	28 ± 3	27 ± 2
Dox	66 ± 2	12 ± 3	21 ± 6	**Dox**	74 ± 4	21 ± 6	11 ± 2

C

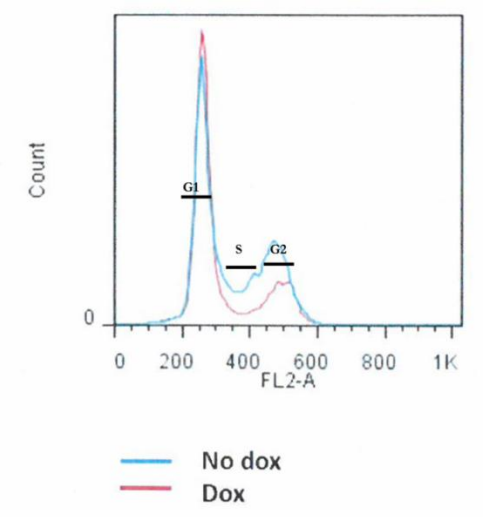

Figure 3.5. Cell cycle analysis of LNCaP/TR2/PHB cells treated with and without doxycycline (10 μM) for 24 hr and 48 hr. **A**, bar graph indicating number of cells in each phase, measured by FACs in LNCaP/TR2/PHB cells treated with dox (24hr). **B**, bar graph indicating number of cells in each phase, measured by FACs in LNCaP/TR2/PHB cells treated with dox (48hr). % of cell population in each phase of the cell cycle is seen below each respective graph (± standard error of mean) and was calculated using FlowJo® analysis. **C**, histogram showing the number of cells in each phase measured by FACs in LNCaP/TR2/PHB cells treated with dox (24hr). The blue line represents cells with no PHB over-expression. The red line represents cells with ectopic PHB over-expression (dox). $p<0.05$* n=3.

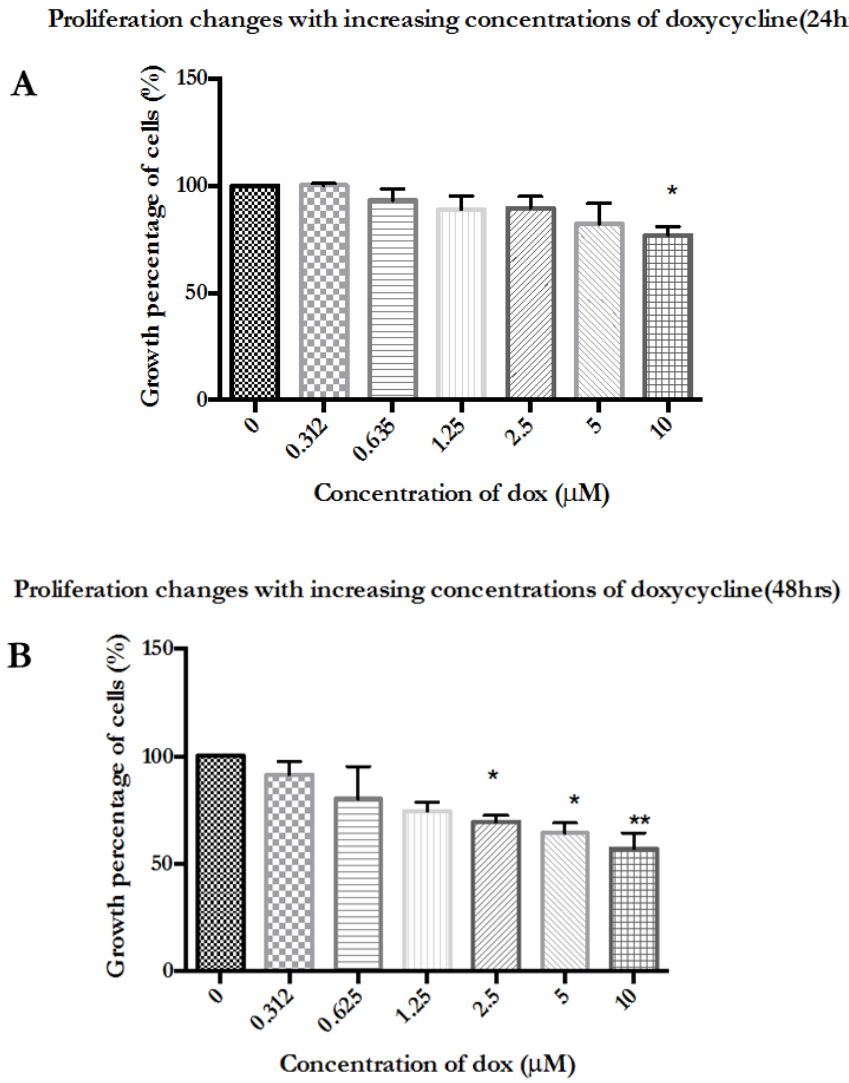

Figure 3.6. Crystal violet proliferation assay. **A**, Proliferation of LNCaP/TR2/PHB cells treated with increasing concentrations of dox for 24 h (0.312 µM - 10 µM). **B**, Proliferation of LNCaP/TR2/PHB cells treated with increasing concentrations of dox for 48 h (0.312 µM - 10 µM). $p<0.05$*, $p<0.01$** n=3. Absorbance was read at 540nm.

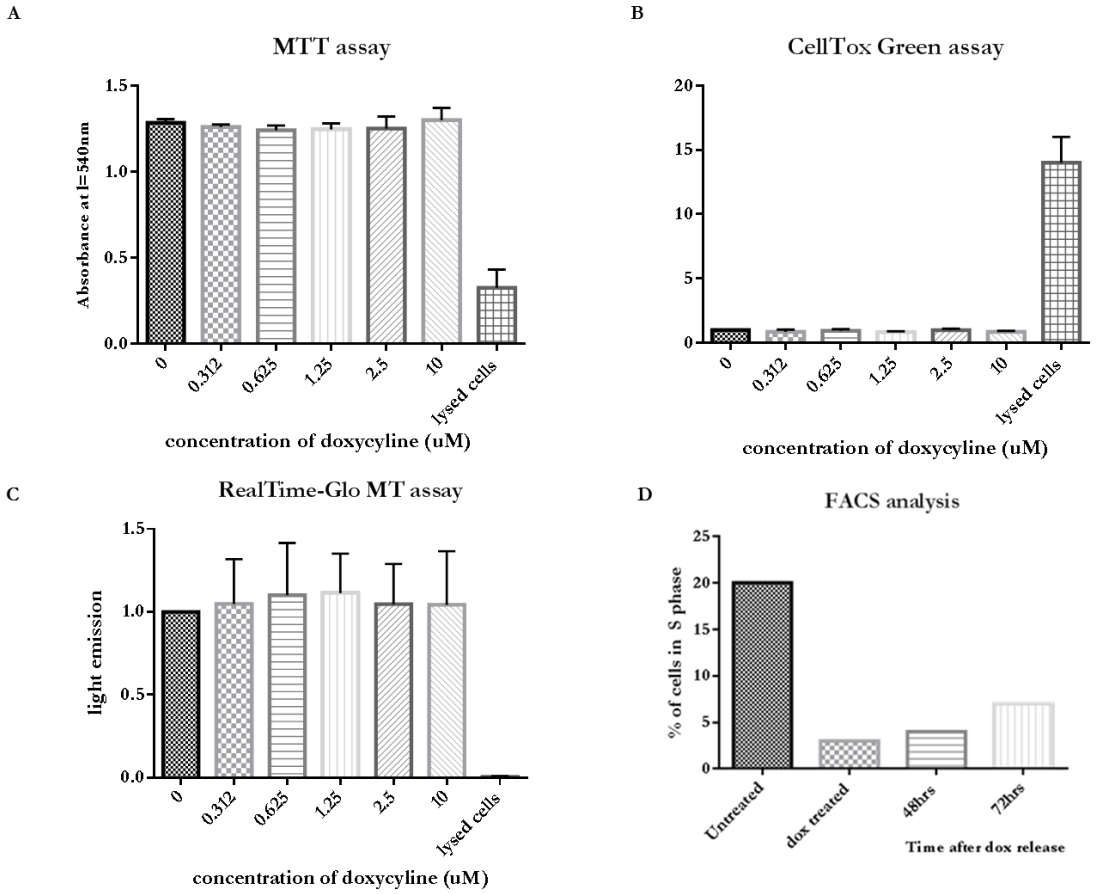

Figure 3.7. Cytotoxicity assays on the LNCaP/TR2/PHB cell line. **A**, MTT assay, mitochondrial activity of LNCaP/TR2/PHB cells treated with increasing concentrations of doxycycline. **B**, CellToxGreen assay, cell membrane integrity of LNCaP/TR2/PHB cells treated with increasing concentrations of doxycycline. **C**, Realtime-Glo MT assay on LNCaP/TR2/PHB cells treated with increasing concentrations of doxycycline n=2. As a control for cell cytotoxicity, cells were lysed. **D**, bar graph showing % of LNCaP/TR2/PHB cells that re-enter the S phase after doxycycline was washed off and left for 48 hr and 72 hr. n=1.

3.4 Discussion

Accumulating both data presented here and previous literature, it is clear that PHB is a repressor of the AR. This was due to a strong repression of *PSA* gene expression seen in the presence of *PHB* ectopic over-expression. Both the AR and PHB are in dynamic opposition in controlling androgen-mediated gene activation in prostate cancer cells. According to(130), androgen stimulation of LNCaP cells led to a down-regulation of PHB protein expression, allowing progression of the cell cycle. However, the over-expression of PHB led to a repression of AR signalling and cell cycle arrest. This agrees with data from Gamble, *et al,*. (130), whereby transfection of LNCaP with a PHB expression plasmid led to the failure of cells entering the cell cycle, even in the presence of the potent androgen; DHT. It was verified that the cell cycle arrest was not due to cell death, as various cell cytotoxicity assays indicated that PHB over-expression had no effect on mitochondrial activity or function, alongside no change in membrane integrity. This is of particular importance as mitochondrial dysfunction plays a key role in activating apoptosis in mammalian cells, especially as mitochondria are essential for cell viability (131). Mitochondria undergo structural and functional changes upon apoptotic initiation. First mitochondria incur a decrease in their membrane potential followed by membrane permeability. Moreover, the cytotoxicity assays assessed the metabolism of viable cells. If nutrients in the cell environment are lacking, metabolic checkpoints are activated leading to the intrinsic apoptotic pathway through the activation of the Bcl-2 family of proteins (132). As PHB over-expression showed no effects on the metabolism of the cells, the apoptotic pathway was not activated. Further evidence that PHB has no role in activating cell apoptosis, FACs analysis showed no sub G0/G1 population left to the G1 peak, indicating no DNA fragmentation or apoptotic cell population. Additionally when doxycycline-induced PHB was removed, cells began to re-enter S phase of the cell cycle, indicating no permanent damage or quiescence. Thus, PHB over-expression was having a prominent effect on arresting the cells in the G1 phase. There is an array of genes or proteins that PHB could be interacting with to cause cell cycle arrest that will be further investigated.

3.5 Conclusion

To summarise, characterisation of the predominantly used cell lines throughout this project were validated prior to further experiments. Data collected supported that PHB over-expression repressed the AR and led to a halt in the cell cycle that in turn led to reduced cell proliferation. This was not a result of cellular stress, apoptosis or cell death. Therefore, PHB mediated cell cycle arrest is specific and further experiments were set out to investigate this mechanism.

3.6 Summary points

- Validation of the androgen responsive LNCaP cell line was confirmed by assessing the androgen responsive gene; *PSA* when cells were treated with a synthetic androgen (R1881).
- Validation of the LNCaP/TR2/PHB cell line was confirmed as in the presence of doxycycline, an increase in ectopic *PHB* cDNA and protein expression was seen.
- *PHB* expression is down-regulated in LNCaP cells stimulated with hormone (R1881).
- PHB has a significant repressive role on the cell cycle – this in turn significantly decreased the proliferation of the LNCaP/TR2/PHB cells.
- PHB causes cell cycle accumulation in the G1 phase.
- PHB's repressive role on the cell cycle is not due to causing cellular stress or cell death.

Chapter IV. The repression of E2Fs is mediated through PHB binding to MCMs' promoter region.

4 Chapter IV: The repression of E2Fs is mediated through PHB binding to MCMs' promoter region.

4.1 Introduction

Chapter III showed that PHB halted the cell cycle by increasing the cell population in the G1 phase whilst decreasing the cell population in S phase. From previous literature, it has been identified that PHB is able to repress the cell cycle through interactions with genes that progress the cell cycle. Gene families that are known to regulate and progress the cell cycle include cyclins, CDKs, and E2Fs. Cyclins and CDKs work together to form complexes that are essential for the regulation of interphase during the cell cycle. E2Fs are a family of transcriptional factors that have one or more conserved DNA-binding domains that play a role in the progression of the cell cycle. E2Fs are regulated by the Retinoblastoma (Rb) proteins and are often deregulated in carcinogenesis (133). Numerous E2F targets have been identified, such targets include *c-jun, myc, POLA* and *MCMs*. Members of the *MCM* and *POLA* gene family are responsible for DNA replication. Interestingly, PHB has been shown to interact with E2F1 by binding to Rb, rendering E2F's function inactive. This led to the inhibition of the cell cycle. This interaction was established in a breast cancer cell line; T47D. Moreover, PHB is a strong gene repressor (e.g. the *AR* gene) and can recruit histone modifying proteins such as HP1 and HDAC to the chromatin. Previous evidence of PHB's repressive mechanism on the cell cycle is limited and not fully understood in PC.

The aim was to identify a mechanism by which PHB arrests the cell cycle. We investigated if this repression was regulated through major cell cycle pathways such as E2F, CDKs or PI3K or whether any other novel pathways could be found. To assess how PHB's over-expression mediated cell cycle arrest in PC cells, a RNA sequencing (RNA-seq) experiment was carried out as PHB has a strong role in repressing gene expression. Therefore gene repression could indicate a novel mechanism. This allowed the analysis of the entire transcriptome that was affected by PHB over-expression. Methods used to carry out these aims included an unbiased analysis of the RNA sequencing database through bioanalysis platforms and biased data mining into the RNA sequencing database. Q-PCR was also carried out to validate gene expression alterations seen with PHB over-expression, from targets identified in the RNA-seq.

Key genes that were significantly altered with PHB over-expression were then isolated for further study and a hypothesis was proposed as how PHB causes cell cycle arrest.

4.2 Methods

- RNA sequencing (refer to chapter 2.10).
- SYBR® Green Q-PCR (refer to chapter 2.8.3).
- Metacore, IPA-Ingenuity and DAVID gene ontology analysis. Here a gene list from the RNA-seq database was created using genes that had a significant fold change (<0.05) with a fold change >-2/2. This gene list was inputted into online programs to assess for associated networks, pathways and transcription factors.
- Luciferase reporter assay (refer to chapter 2.12.8).
- Western blot (refer to chapter 2.11.1-211.5).
- Site-directed mutagenesis (refer to chapter 2.13).

4.3 Results

4.3.1 Gene expression changes in response to PHB over-expression in the LNCaP/TR2/PHB cell line

In order to identify how PHB over-expression in the LNCaP/TR2/PHB cells affected gene expression, an unbiased RNA-seq experiment was carried out. Firstly, the total RNA samples from LNCaP/TR2/PHB cells (+/dox, 10μM, 16 hr) were assessed for their quality and integrity using a Bio-analyser. Next, isolation of polyA mRNA from total RNA using polyT beads was carried out (figure 4.1A). The mRNA was then fragmented by RNaseII digestion, purified and again run on a Bio-analyser to confirm the fragmented mRNA was within the correct base pair size region (figure 4.1B). Purified fragmented mRNA was then amplified to cDNA fragments, 150-300bps long (figure 4.1C) these were then amplified onto Ion Sphere Particles (ISPs) by an emulsion PCR. Next ISPs were loaded onto a P1 chip and sequenced on the Ion Torrent Proton sequencer. Figure 4.2A illustrates the percentage of ISP loading onto the chip (88%). The total number of reads sequenced was 68,303,495 as the final library (figure 4.2B) per experiment of four samples. Each read length was in the correct base pair size region (50-200) as shown in figure 4.2C. 72% of reads were aligned to the human genome 19 as shown in figure 4.3 with a mean raw accuracy of 96.6%. The reason why the software used had Bowtie and Cufflinks integrated with automatic settings. Data output was in the form of a BAM file format.

Analysis of the RNA-seq data with Partek Genomics suite software was carried out using a workflow as shown in figure 4.4. Firstly, A RPKM (reads per kilobase million) normalisation step was carried out to account for sequencing depth and gene length of the two replicates for no dox vs dox. The final step was a one way ANOVA analysis of the untreated sample vs the doxycycline treated sample, that produced a transcripts list of significantly differentially expressed transcripts in each sample set. The list produced contained transcripts that either had no change, or an increase or decrease in expression in response to doxycycline.

Firstly, to ensure the inducible cell line was producing an over-expression of ectopic *PHB* cDNA in the presence of doxycycline, the location of the *PHB* gene was analysed. Figure 4.5 depicts the chromosomal location of *PHB* (chromosomal location 17q21.33) and its exons. Two replicates can be seen of the histogram of read pile-ups. Within each replicate, at each exon there is an increase in *PHB* transcript pile-ups in cells treated with doxycycline when compared to untreated cells. As the software is unable to detect the *PHB* cDNA is from an exogenous source (an integrated plasmid), the pile ups are seen on the hg19 chromosomal location was seen. Therefore, as the two replicates show, *PHB* cDNA was being ectopically over-expressed in the presence of doxycycline and the cell line LNCaP/TR2/PHB was working accordingly, as previously described. Q-PCR analysis was carried out to verify that *PHB* was being over-expressed in the presence of doxycycline (n=3) (figure 4.5).

Partek software was used to create a heatmap, clustering genes from both replicates in order of log2 expression (p value <0.05). The parameters used were; each gene expression was normalised to zero with a standard deviation of 1. Genes that were unchanged were displayed as a grey colour with a value of zero, down-regulated genes were displayed as blue with a negative value, whereas up-regulated genes were displayed as red with a positive value. Around 2000 genes were significantly altered in the presence of *PHB* over-expression (figure 4.6). The top ten most significantly up-regulated and down-regulated transcripts from the RNA-seq database are shown in figure 4.7.

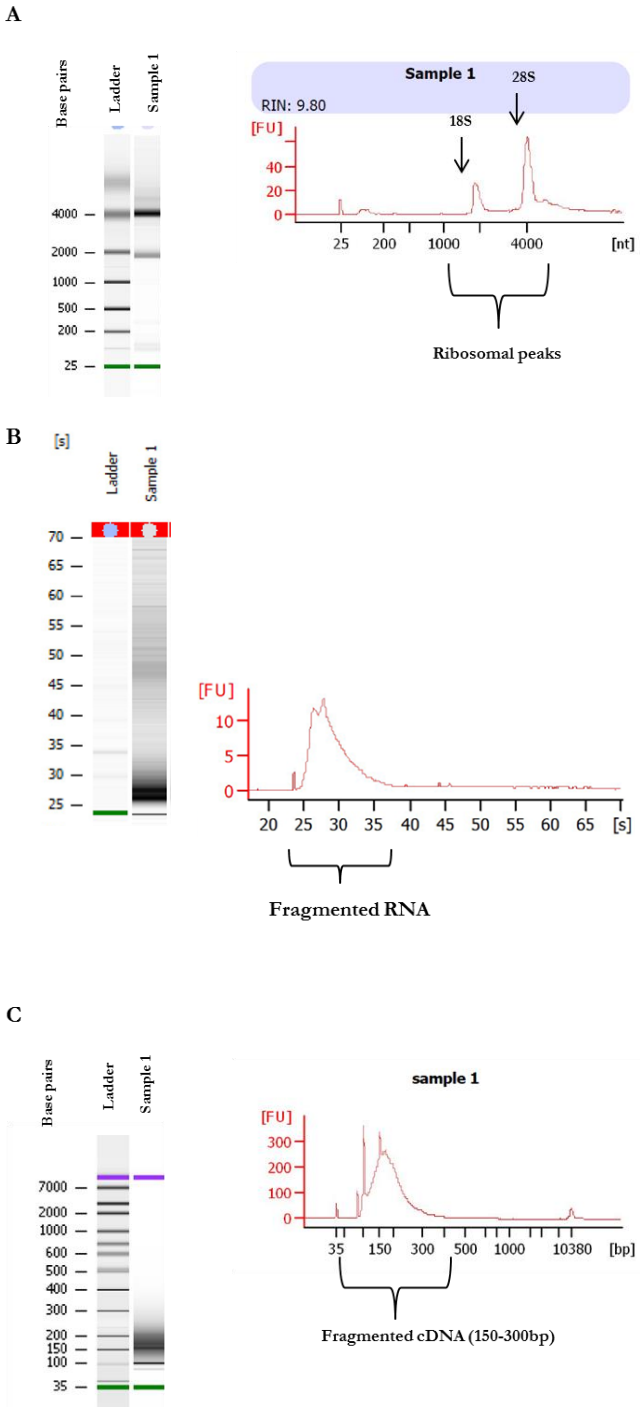

Figure 4.1. RNA-library preparation. **A**, an example of an electrogram from total RNA extracted from LNCaP/TR2/PHB cells provided by a Bioanalyser. RIN (RNA integrity) number is 9.8, highest RIN number a sample can get is 10. (FU = fluorescence, nt=nucleotides, bp = base pairs, RIN= RNA integrity number). **B**, Bioanalyser results showing fragmented mRNA after RNAse II digestion. **C**, Purified amplified cDNA with a base pair range of 150-300.

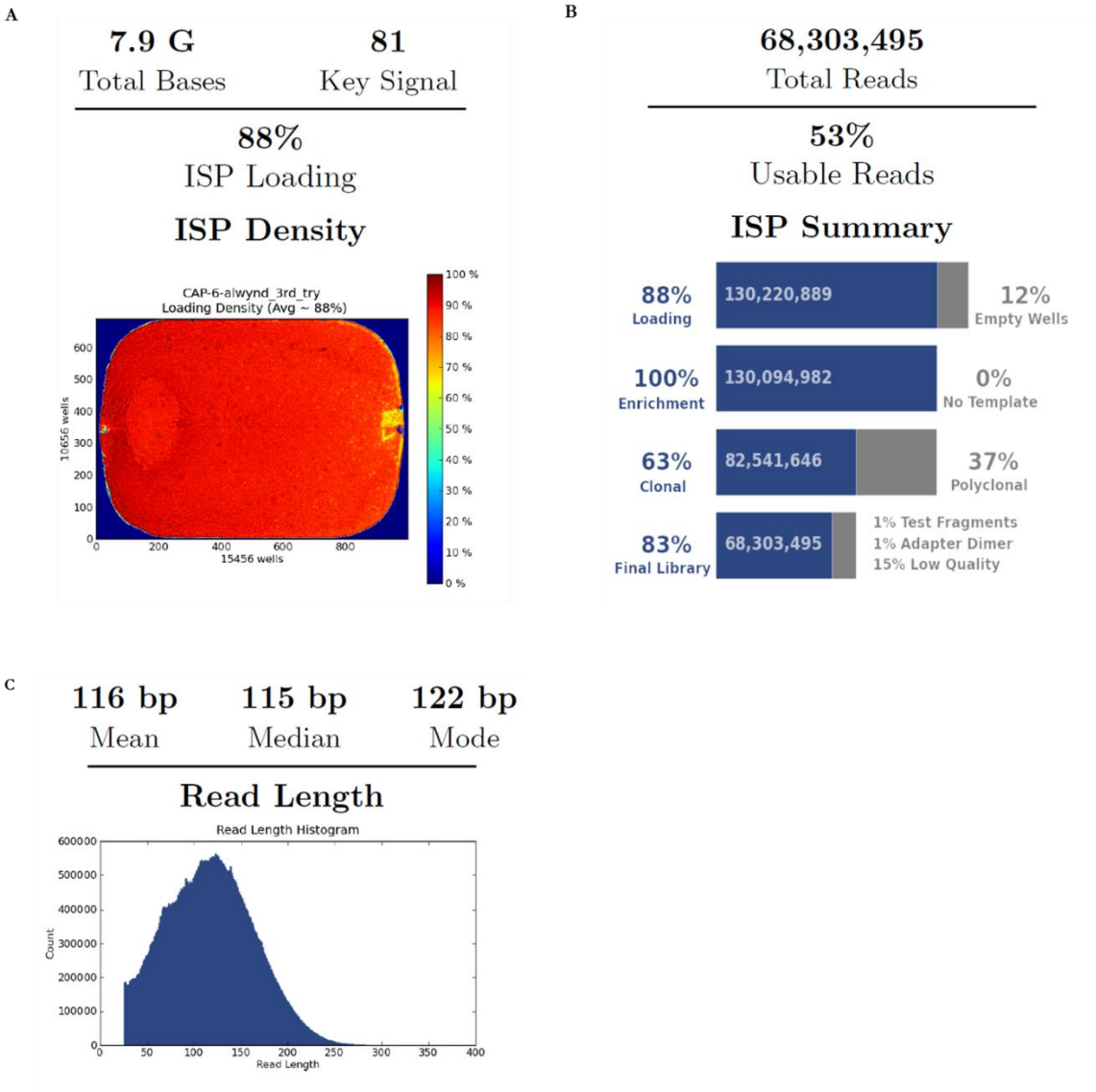

Figure 4.2. Run report summary for the RNA-sequencing experiment. **A**, 88% of the P1 chip was successfully loaded with the ISP beads as shown by ISP density. **B**, 100% enrichment of successfully loaded beads, with a 83% final library including 68,303,495 total sequencing reads. **C**, illustrates a histogram of global read lengths, reads had a mean length of 116 base pairs.

A

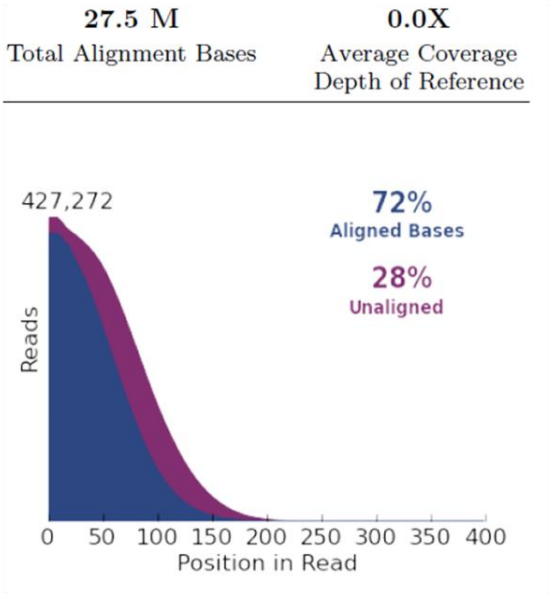

B

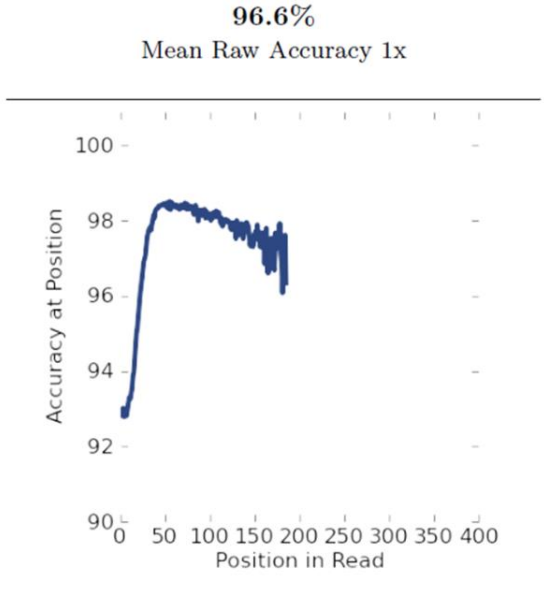

C

Barcode Name	Sample	Bases	≥ Q20	Reads	Mean Read Length
IonXpressRNA_011	lncap no dox	1,874,006,260	1,569,650,091	18,471,773	101 bp
IonXpressRNA_012	lncap dox phb	1,926,656,082	1,589,643,934	15,418,861	125 bp

Figure 4.3. Alignment report summary for the RNA-sequencing experiment. **A**, alignment to Hg19 genome. 72% of bases were successfully aligned to the human genome version Hg19. **B**, illustrates alignment was successfully achieved with a 96.6% mean raw accuracy. **C**, shows the number of reads per sample (LNCaP/TR2/PHB (+/- dox, 10μM, 16 hr).

A

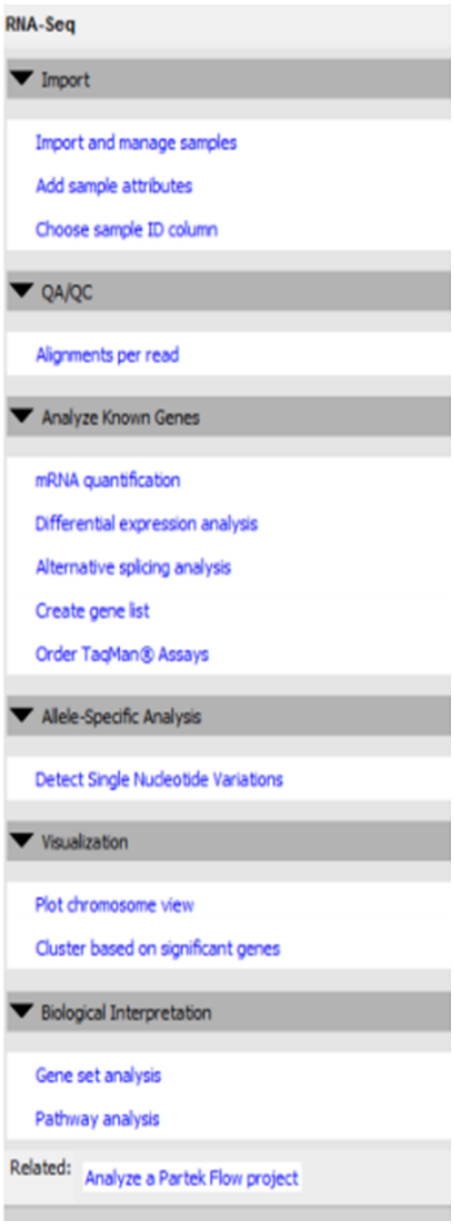

B

Step 1: samples are run on a ion proton sequencer. The software uses STAR aligner and Bowtie and Cufflinks settings

↓

Step 2: Importing the aligned BAM file. Sample ID's are then given to each file, e.g. no doxycycline and doxycycline. Reads are aligned to the Hg19 genome. RPKM normalisation.

↓

Step 3: Visualisation. Once imported the mapped reads can be visualised with gene information. The annotation source is known as RefSeq Transcripts. Here visualisation of each chromosome with the gene location can be seen with the transcript pile ups at each exon.

↓

Step 4: Analysis of known genes. Detection of differential expressed genes by mRNA quantification. a mapping summary spreadsheet is a quality control check giving a summary of reads.

↓

Step 5: A gene list is created. The Partek software is able to create a gene list that summaries genes that are significantly differentially expressed and alternatively spliced (on a separate file) amongst the two sample sets.

Figure 4.4. Partek Genomics suite software RNA-seq workflow. **A,** Screenshot of the workflow. **B**, description of the main steps resulting in a final gene list.

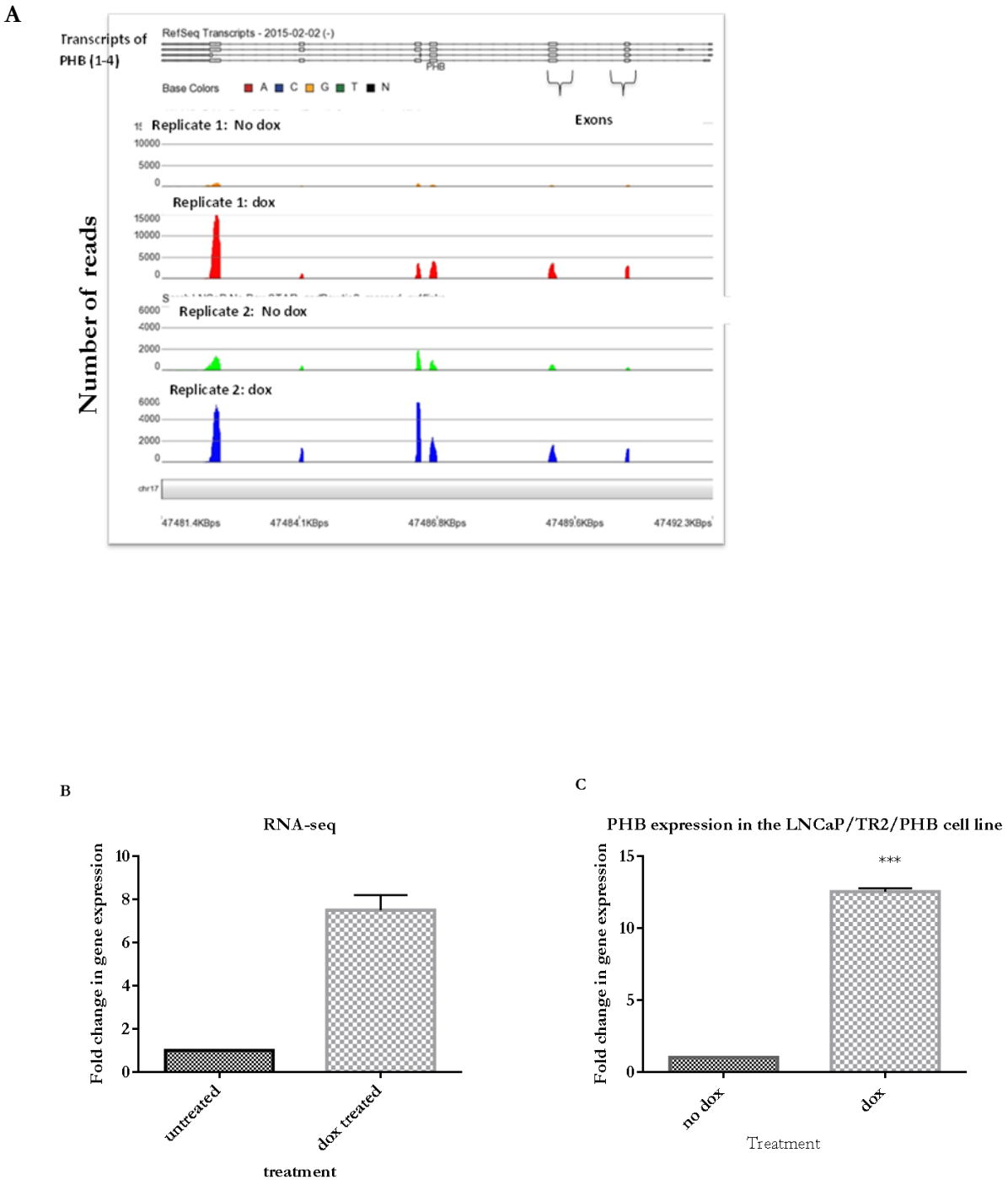

Figure 4.5. Identification that doxycycline is producing ectopic *PHB* cDNA in the RNA-seq data. **A**, Histogram of transcript pile-ups on chromosome 17 where the *PHB* gene is found. At each exon there is an increase in transcript pile-ups in the presence of dox when compared to no dox. **B**, RNA-seq data showing PHB expression is increased in cells treated with dox. **C**, Q-PCR validation showing *PHB* gene expression is significantly increased when dox is added to LNCaP/TR2/PHB cells, values normalised to GAPDH and RPL19. n=3 $p<0.001$***.

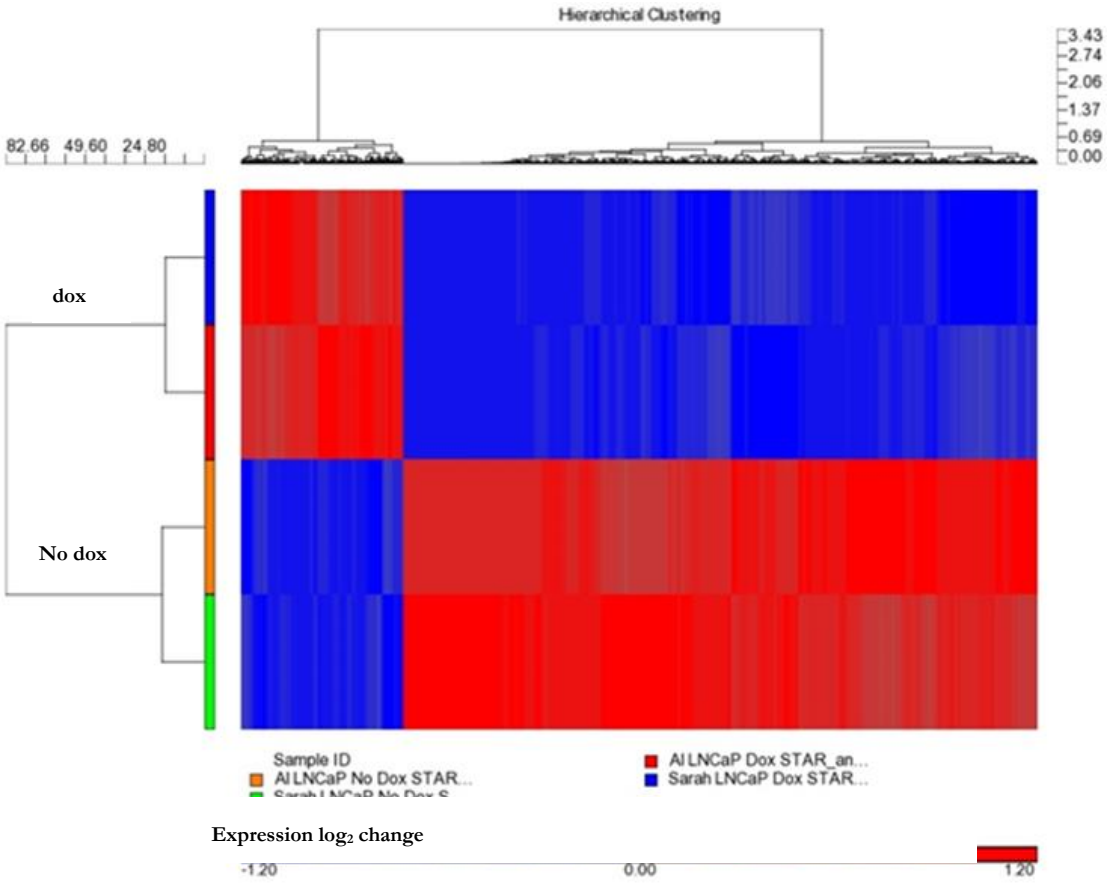

Figure 4.6. Significantly altered genes identified by Partek software and organised into hierarchical clustering and log_2 transformed ($p < 0.05$) with PHB over-expression in the LNCaP/TR2/PHB cell line. n=2.

A

Gene name	Fold change(Dox vs. No Dox)	p-value(Dox vs. No Dox)
GPR1	20.254	0.0115446
IL2RB	13.2214	0.0104991
PARP6	10.1765	0.0144475
FIBIN	10.1722	0.0439402
CNGA3	9.6886	0.0176946
IRF4	8.65874	0.01947
APOL6	7.51019	0.0161344
RSAD2	7.01736	0.00335991
PHB	6.99994	0.013963

B

Gene name	Fold change(Dox vs. No Dox)	p-value(Dox vs. No Dox)
GAGE8	-15.6726	0.00370352
RASA4B	-17.3827	0.0294307
ADORA2A	-17.4916	0.0410437
SNORD86	-20.6807	0.0328174
KCNN3	-21.4214	0.00239767
OR2A20P	-26.9244	0.0280263
LOC101929829	-52.2134	0.000817677
LOC100289561	-8676.95	0.0260481
MIR3652	-11124	0.0105543
NPY4R	-213023	0.0348247

Figure 4.7. Top ten significantly altered transcripts from the RNA-seq data. **A**, top ten most significantly up-regulated transcripts from the RNA-seq database. **B**, top ten most significantly down-regulated transcripts from the RNA-seq database.

4.3.2 Metacore analysis for gene ontology

From the list produced by Partek software with approximately 42,000 transcripts, all transcripts with a p value > 0.05 were removed. This left 2327 transcripts. Of these, transcripts with no change in expression in response to doxycycline were removed. Further, the fold change of 2 was deemed to be within error and any fold change in expression 2/-2 was removed. This left 1208 transcripts that were $p<0.05$ and a fold change in expression >2/>-2.

To further analyse the data retrieved from the RNA-seq data, a pathway analysis program, Metacore was used. Metacore is an integrated software suite for the functional analysis of RNA-seq or expression data. The program searches for shared biological pathways within the gene list. It carries this out utilising a database made of; transcriptional factors, receptors, ligands, kinases, drugs and endogenous metabolites. Finally, signalling pathways were embodied onto maps and networks. Firstly, the excel spreadsheet consisting of transcripts that had a significant p value <0.05 and a fold change higher than or equal to 2/-2 was saved as a tab-delimited text file and imported into Metacore. Annotation statistics showed if any errors occurred during the upload and how many transcripts were correctly identified in the transcript list.

Figure 4.8 shows the data from the RNA-sequencing interpreted into biological processes, pathways and networks by Metacore. The pathways illustrated are a two-dimensional representation of the data as it links genes together, rather than just a transcript list. The cell cycle, regulation of the cell cycle and cell cycle progression appear within the top ten biological processes associated with PHB over-expression. Interestingly, cell cycle G1-S growth factor regulation, cell cycle G2-M and cell cycle meiosis are within the top 10 biological networks. This emphasises that PHB has an effect at each stage of the cell cycle. This agrees with the FACs analysis, showing that PHB causes a decrease in cell population within the S and G2 phase, whilst increasing the cell population in the G1 phase. Figure 4.9 shows insight into the cell cycle network through a multi-dimensional analysis of the data. Here it depicts PHB over-expression has a repressive role on the E2F/Rb pathway. Further, the top most up-regulated process showed by Metacore was cellular metabolic processes. Moreover, the Wnt-signal transduction pathway was also within the top ten altered processes, alongside

integrin-mediated cell adhesion, these processes will be discussed in proceeding chapters.

4.3.3 DAVID analysis of gene ontology

The Database for Annotation, Visualization and Integrated Discovery (DAVID) pathway analysis is a platform where a large gene database can be analysed such as RNA-seq data, however DAVID does not take into account fold change. It discovers enriched functional-related gene groups and biological themes. The gene list from RNA-sequencing was also inputted into this system. Figure 4.10 illustrates that E2F3 and E2F6 were in the top ten functional related genes list. This agrees with the Metacore analysis that members of the E2F family are associated with PHB over-expression. Moreover, cyclin H and forkhead box E transcriptional factor were within the top most functional related genes with PHB over-expression. Cyclin H plays a role in progression of the cell cycle, whereas forkhead box E is involved in cellular proliferation and growth. These are all key pathways involved in PC progression.

4.3.4 IPA analysis of gene ontology

Finally, a third platform was used to analyse the gene list, namely Ingenuity® Pathway Analysis (IPA). IPA is a software designed for the analysis and interpretation of data retrieved from 'omics experiments such as RNA-seq but is compiled by human knowledge. Figure 4.10 illustrates the top 5 associated networks with the imported gene list. Interestingly, the cell cycle appears at the top of the list. This agrees with the Metacore and DAVID analysis. Moreover, cellular growth and cancer were found within the top five networks associated with PHB over-expression, highlighting PHB's impact on tumorigenesis. All three bioanalysis platforms conclude that PHB over-expression is associated with cell cycle regulation and progression, and this could be due to regulation of key genes from the E2F transcription factor family.

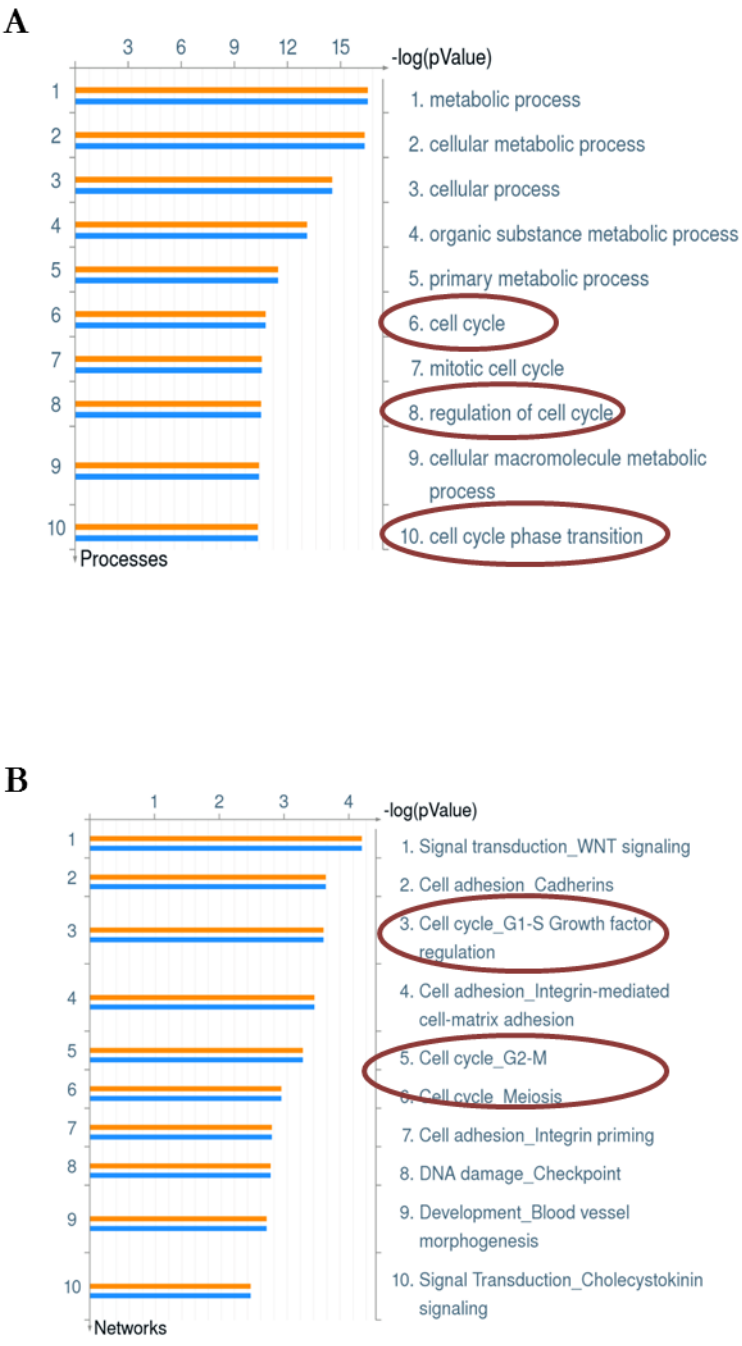

Figure 4.8. Pathway analysis of RNA-sequencing data by Metacore. **A**, a list of the top 10 biological processes influenced by PHB over-expression produced by Metacore analysis. **B**, Describes the top ten networks produced by Metacore. Cell cycle regulation, cell cycle G2-M phase transition and meiosis all are shown within the top ten.

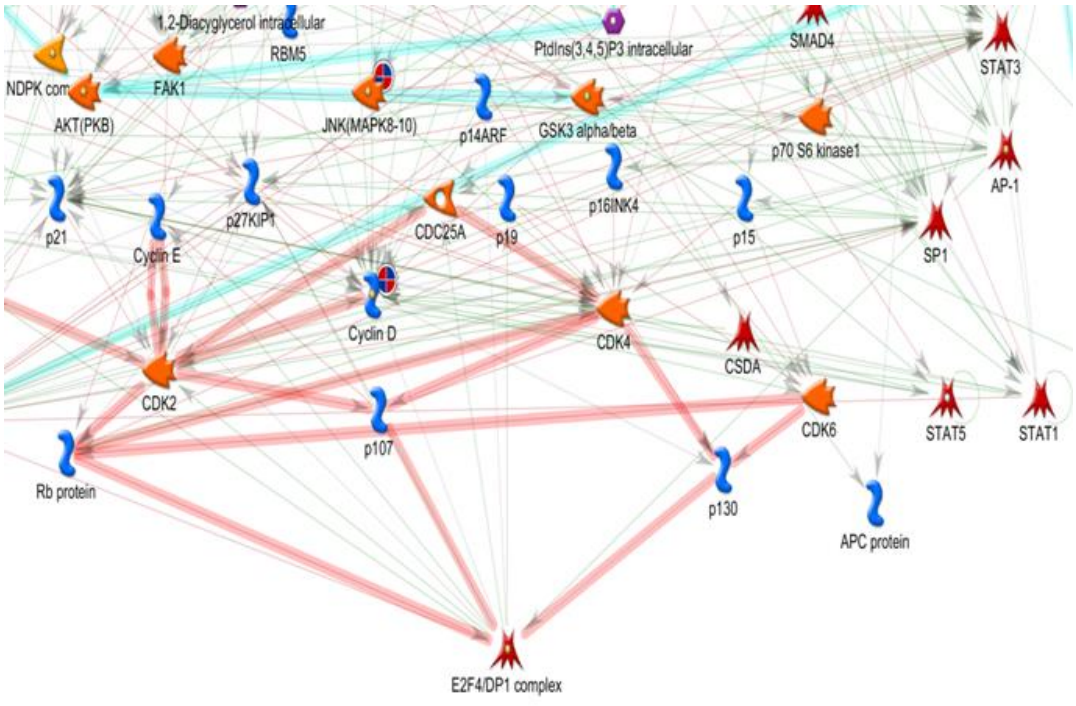

Figure 4.9. Network analysis of RNA-sequencing data drawn by Metacore. Network shown is of the cell cycle regulation. Highlighted in red depicts inhibitory pathways. Members of the Rb family; Rb, p107 and p130 inhibit E2F4/DP1 functions. Highlighted in green depicts activation pathways.

A

Top Networks

ID	Associated Network Functions
1	Cell Cycle, Cellular Development, Cellular Growth and Proliferation
2	Cellular Development, Cellular Growth and Proliferation, Cell Cycle
3	Cellular Development, Cellular Growth and Proliferation, Tissue Development
4	Auditory Disease, Cell-To-Cell Signaling and Interaction, Cellular Assembly and Organization
5	Cancer, Cellular Development, Organismal Injury and Abnormalities

B

#	Functionally Related Gene
1	E2F transcription factor 3
2	mediator complex subunit 17
3	general transcription factor IIF, polypeptide 1, 74kDa
4	cyclin H
5	TEA domain family member 4
6	BRF1 homolog, subunit of RNA polymerase III transcription initiation factor IIIB (S. cerevisiae)
7	forkhead box E3
8	T-box 19
9	E2F transcription factor 6
10	transcription factor Dp-1

Figure 4.10. DAVID and IPA bioanalysis of the gene list derived from the RNA-sequencing experiment. Screenshots describe top 5 associated networks and top 9 functionally related genes. **A**, DAVID bioanalysis platform describes the cell cycle and development and cell growth to be in the top 5 network functions. **B**, IPA bioanalysis platform describes E2F3 and E2F6 to be in the top 9 functionally related genes.

4.3.5 RNA-seq identifies PHB over-expression represses genes involved in the cell cycle and in DNA replication

The Bioanalysis programs confirmed that PHB over-expression strongly influences genes involved in the regulation and progression of the cell cycle, which correlates to the data shown in chapter III. Selection of genes to be assessed was carried out by previous literature stating PHB's role in interacting with E2Fs, consequently causing cell cycle arrest. Therefore, gene families involved in t cell cycle regulation, alongside DNA synthesis and DNA replication were assessed via the RNA-seq database as a biased analysis (figure 4.11). Interestingly, cyclin-dependent kinases (CDKs) that were down-regulated with a fold change higher than 2 in response to PHB over-expression included *CDK1, CDK2, CDK14, CDK17, CDK20*. As it has already been established that PHB has a unique inhibitory interaction with certain E2Fs (107), data also pertaining to E2Fs, were retrieved from the RNA sequence database. *E2F1,2,7,8* were all down-regulated in response to PHB over-expression. Although figure 4.10 describes *E2F3* as the top transcriptional factor to be affected by PHB's over-expression, the *E2F1* gene was taken forward for further analysis as it is a representative of the 'activating E2Fs' and often there is interplay and redundancy between E2F1 and E2F2/3. Moreover, figure 4.12 shows Metacore analysis depicting *E2F1* within the top transcriptional factors altered by PHB over-expression. Previous data has established an interaction between E2F1 and PHB in breast cancer, thus the same interaction was investigated in PC. Similarly, members of the *MCM* family *MCM2,4,5,6,7,10* that play a vital role in DNA replication, were down-regulated with PHB over-expression. This suggests PHB also has a repressive role in DNA replication. Further, the cell cycle inhibitor known as *CDKN1A* (*p21/WAF/CIP1*) showed opposite regulation and was seen to be up-regulated in response the PHB over-expression. As the RNA-seq was n=2, SYBR ® Green Q-PCR was carried out in triplicate to validate the expression changes in key members in the gene families of interest. Screening of all the members of the *E2F* and *MCM* family were carried out. A significant decrease was seen in *E2F1* and *E2F4* with PHB over-expression and *MCM2,3,4,6,7* (figure 4.13). Q-PCR validation was also carried out for the cell cycle inhibitors *CDKN1A* (*p21*) and *CDKN1B* (*p27*). Both cell cycle inhibitors showed a significant up-regulation in the presence of PHB over-expression.

4.3.6 PHB represses MCM5&6 promoter activity

Previously data collected from a low density array screen (through personal communications, Dr Dart) showed that members of the *MCM* gene family, *TK1* and the *CDK* gene family were down-regulated with PHB over-expression. However, *p21*, *p27,* and *GADD45a* were all up-regulated with PHB over-expression. *TK1* is a DNA biosynthetic precursor gene, and plays a role in DNA replication. Therefore this data suggests that PHB over-expression down-regulates genes involved in DNA replication, an essential step in the S phase of the cell cycle. Both p21 and p27 are cyclin dependent kinase inhibitors, stopping cell cycle progression. This agrees with the data produced from the RNA-seq. Q-PCR was carried out to valid these targets (figure 4.13).

Previous literature states that E2F binding sites are located in MCM promoter regions and thus potentially, MCMs are E2F-regulated (134) (135). In particular, promoter activity of MCM5 and MCM6 were seen to be regulated by E2F by its binding to multiple E2F recognition sites in their promoter regions (136). This was also confirmed by previous work carried out by Dr Alwyn Dart, entailing the transfection of LNCaP cells and COS-7 cells with an E2F1-overexpression construct, resulting in an increase in MCM5&6 gene expression (figure 4.16D) (137). This suggests that MCM5&6 are regulated by E2F1. It was thought that potentially, PHB is able to bind to E2F1, repressing E2F1 from interacting with DNA binding sites within the promoter regions of MCM5&6. Thus the promoter activity of both *MCM5*&*6* were assessed in the presence of PHB over-expression.

Previously, 1Kb of the promoter sequence of both *MCM5*&*6* was cloned into pGL4-luciferase plasmids to produce reporter plasmids by Miss Georgia Economides (figure 4.14). 1 Kb of the proximal promoters was chosen as the E2F binding sites were found within this DNA sequence via *in silico* analysis (-40, -56, -118). Firstly, COS-7 cells were transfected with either 400 ng of pGL4-MCM5 luciferase plasmid or pGL4-MCM6 luciferase plasmid. The pSG5-PHB plasmid was also transfected into COS-7 cells at an increasing concentration (0-400 ng). In the absence of pSG5-PHB, a pSG5-empty plasmid was transfected into the cells as a control in an equal quantity. In both cases, increasing concentrations of the pSG5-PHB plasmid led to a significant decrease in the promoter activity of *MCM5*&*6* (figure 4.15). This was monitored by luciferase production. A constitutively active Bos-β-galactosidase plasmid was transfected into

the COS-7 cells alongside the reporter plasmids to control for transfection efficiency. The β-galactosidase assay results were used to normalise the luciferase values.

The same experiment was also carried out in the LNCaP/TR2/PHB cell line. However, instead of transfecting the pSG5-PHB plasmid into the cells, doxycycline was used at increasing concentrations to produce PHB over-expression. 0,2.5,5 and 10 μM of doxycycline was used with 400 ng of both *MCM5*&*6* reporter plasmids. The cells were left to transfect for 48 hr rather than 24 hr as transfection in LNCaP cells is less efficient. Data retrieved agreed with the COS-7 cell transfections, and PHB was shown to have a repressive function on both the *MCM5*&*6* promoter regions.

4.3.7 Mutating a predicted E2F binding site in the MCM6 promoter region

In order to identify if PHB was repressing E2F directly at the MCM promoter, one-site directed mutagenesis was carried out. *In silico* analysis highlighted no predicted E2F binding sites in the mutated sequences. Interestingly, transfection of COS-7 cells with the mutated *MCM6* reporter plasmid, abolished the repression of the promoter with increasing concentrations of the pSG5-PHB plasmid, when compared to the wild-type MCM6 reporter plasmid (figure 4.16). A similar experiment was carried out on the *TK1* promoter by mutating predicted E2F binding sites by Dr Alwyn Dart. PHB repression of the *TK1* promoter was abolished upon base changes within the predicted E2F binding sites. This mirrors the same effect seen in the mutated *MCM6* promoter. ALLGEN *in silico* analysis showed no significant E2F1 potential sites in the mutated sequences (supplemental figure 2). Accumulating this data together, PHB is able to repress the activity of E2F-regulated genes such as *MCM*s, through a mechanism that is discussed in proceeding chapters.

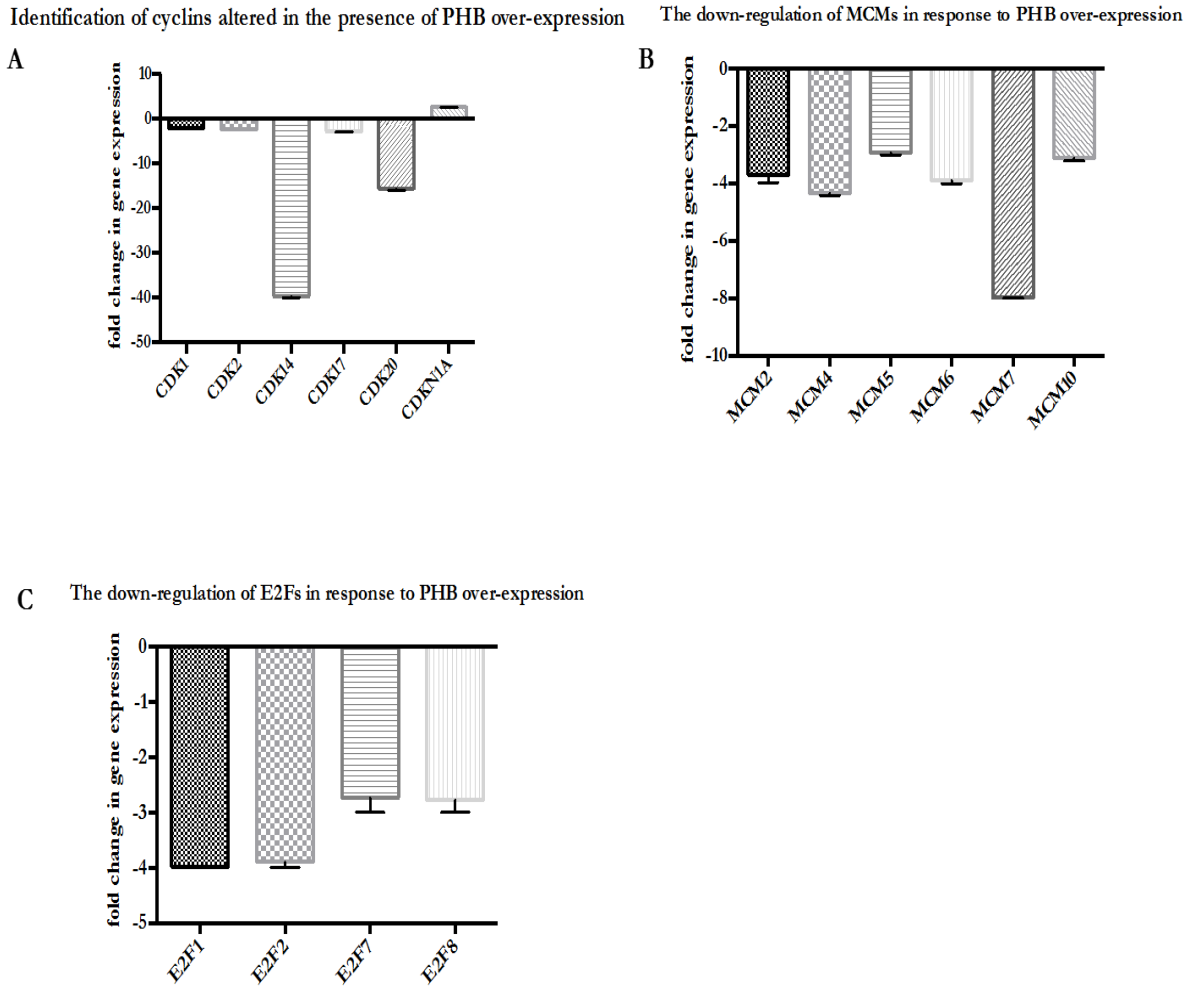

Figure 4.11. RNA-sequencing data analysis. The down-regulation of *CDKs*,*MCMs*,*E2Fs* with PHB over-expression in LNCaP/TR2/PHB cells. **A**, The down-regulation of *CDK1*, *CDK2*, *CDK14*, *CDK17* and *CDK20* with PHB over-expression. A cell cycle inhibitor known as *CDKN1A* (*p21*) was up-regulated with *PHB* over-expression. **B**, *MCM2,4,5,6,7,10* showed downregulation with PHB over-expression. **C**, *E2F1,2,7,8* were down-regulated with PHB over-expression. n=2.

No	Key network objects	GO Processes
1	CREB1	macromolecule metabolic process (61.2%), metabolic process (74.1%), cellular metabolic process (65.6%), cellular macromolecule metabolic process (55.1%), primary metabolic process (66.0%)
2	c-Myc	regulation of primary metabolic process (64.5%), regulation of cellular metabolic process (65.1%), regulation of metabolic process (69.9%), cellular metabolic process (78.5%), regulation of macromolecule metabolic process (62.4%)
3	SP1	positive regulation of cellular metabolic process (49.6%), positive regulation of cellular process (62.2%), positive regulation of metabolic process (52.8%), positive regulation of biosynthetic process (37.8%), positive regulation of biological process (65.4%)
4	ESR1 (nuclear)	negative regulation of nucleic acid-templated transcription (30.2%), positive regulation of cellular process (60.3%), negative regulation of RNA biosynthetic process (30.2%), negative regulation of cellular process (56.9%), positive regulation of cellular metabolic process (46.6%)
5	p53	positive regulation of cellular process (62.9%), positive regulation of cellular metabolic process (47.4%), positive regulation of biological process (64.7%), positive regulation of nucleobase-containing compound metabolic process (35.3%), positive regulation of cellular biosynthetic process (36.2%)
6	Oct-3/4	regulation of metabolic process (70.6%), positive regulation of cellular metabolic process (45.0%), regulation of primary metabolic process (63.3%), positive regulation of cellular process (57.8%), regulation of cellular metabolic process (64.2%)
7	YY1	macromolecule metabolic process (76.1%), regulation of macromolecule metabolic process (63.3%), organic substance metabolic process (80.7%), negative regulation of biological process (56.9%), negative regulation of cellular process (54.1%)
8	GCR-alpha	positive regulation of cellular metabolic process (48.6%), positive regulation of metabolic process (53.3%), positive regulation of cellular process (61.0%), positive regulation of biosynthetic process (37.1%), regulation of cellular metabolic process (66.7%)
9	Androgen receptor	positive regulation of cellular process (67.7%), positive regulation of biological process (71.7%), positive regulation of cellular metabolic process (51.5%), positive regulation of metabolic process (56.6%), positive regulation of macromolecule metabolic process (48.5%)
10	c-Jun	positive regulation of macromolecule metabolic process (52.3%), positive regulation of cellular metabolic process (53.5%), response to organic cyclic compound (36.0%), response to oxygen-containing compound (41.9%), positive regulation of metabolic process (55.8%)
11	E2F1	mitotic cell cycle (39.3%), cell cycle (46.4%), cell cycle process (42.9%), mitotic cell cycle process (35.7%), positive regulation of macromolecule metabolic process (56.0%)

Figure 4.12. A screenshot of the transcription workflow report from Metacore showing *E2F1* and the *AR* within the list of transcriptional factors affected by PHB over-expression.

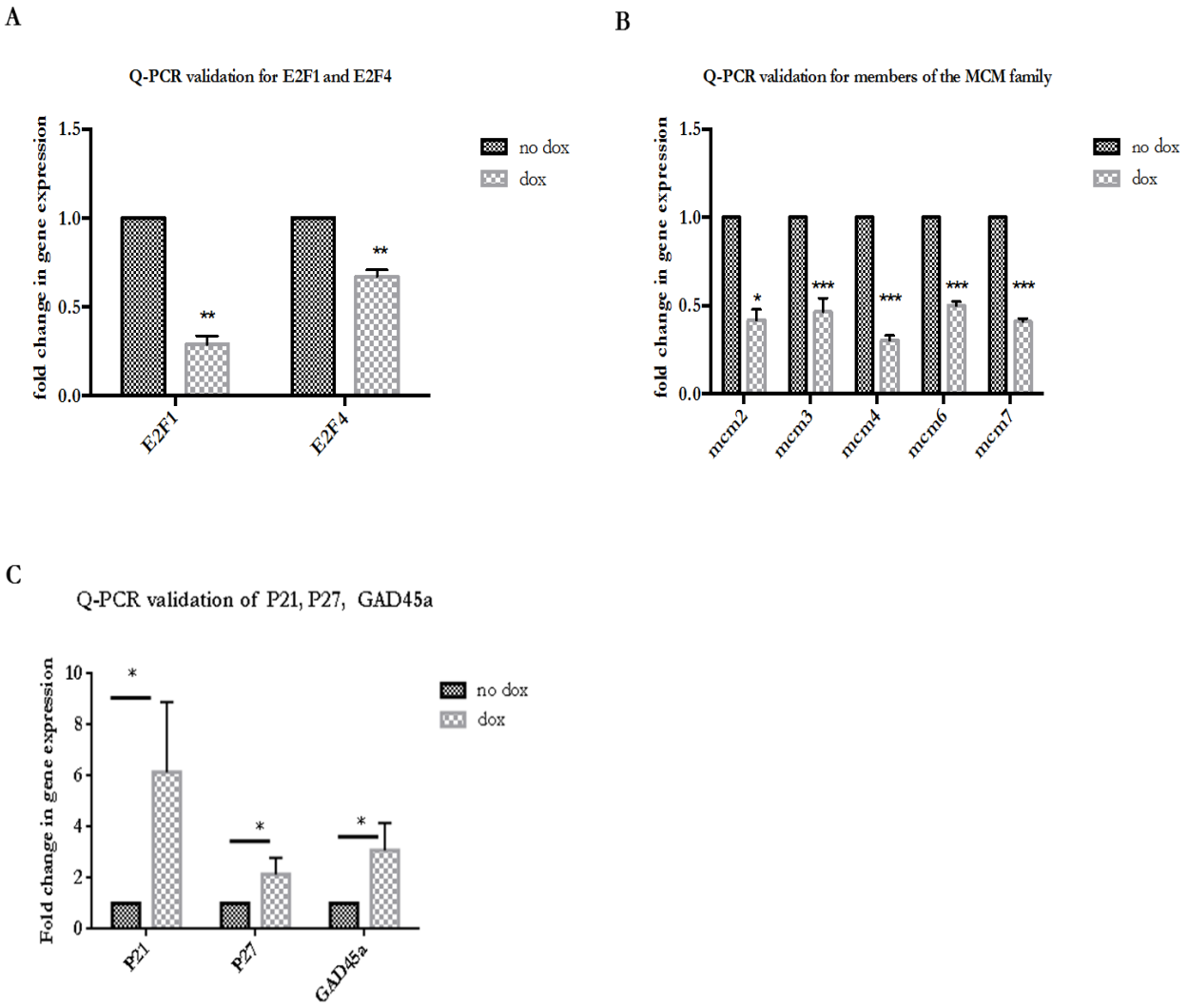

Figure 4.13. SYBR ® Green Q-PCR validation of the gene targets identified with a fold change >2/-2 from the RNA-seq database. **A**, *E2F1* and *E2F4* were significantly downregulated with PHB over-expression. **B**, *MCM2,3,4,6,7* were significantly downregulated with PHB over-expression. **C**, the upregulation of cell cycle inhibitors, *p21* and *p27* with PHB over-expression, and the stress induced gene *GADD45a.* Values were normalised to GAPDH, RPL19 and β-actin. , $p<0.05$*, $p<0.01$**, $p<0.001$***.n=3.

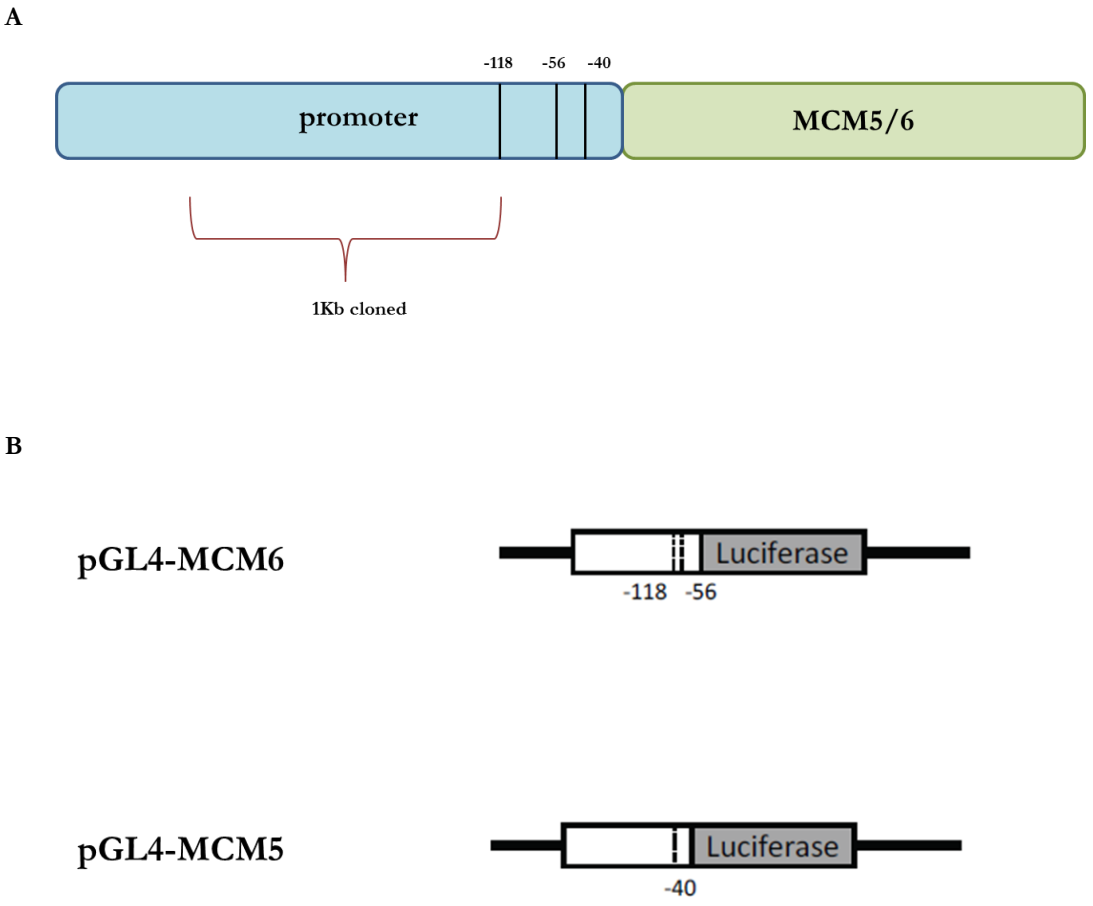

Figure 4.14. Schematic of the *MCM5&6* promoter. **A**, Schematic of the cloned promoter region of MCM5&6 with predicted E2F binding sites (-56 & -118 for *MCM6*) and (-40 for *MCM5*). **B**, Schematic diagram of the promoter-reporter fusion plasmids generated linked to luciferase. 1Kb of the proximal gene promoter cloned upstream of luciferase. Numbered lines indicate the position of predicted strong E2F1 binding sites (ALGGEN software).

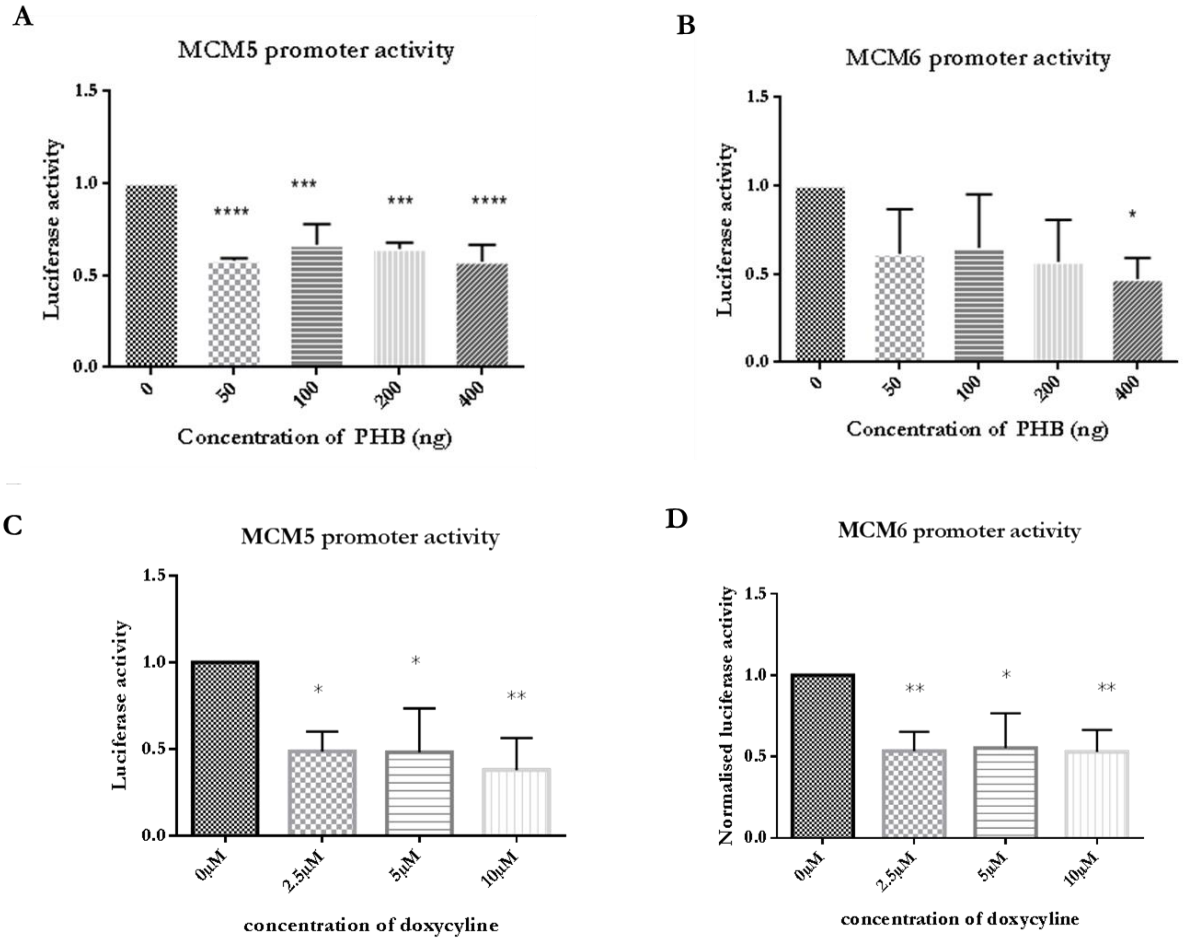

Figure 4.15. The activity of the promoter regions of pGL4-MCM5&6 is reduced with PHB over-expression. **A**, Bar graph showing luciferase activity for *MCM5* promoter activity from COS-7 cells transfected with pSG5-PHB for 24 hr. **B**, Bar graph showing luciferase activity for *MCM6* promoter activity from COS-7 cells transfected with pSG5-PHB for 24 hr. **C**, LNCaP/TR2/PHB cells treated with doxycycline (16 hr) and monitoring *MCM5* promoter activity. **D**, LNCaP/TR2/PHB cells treated with doxycycline (16 hr) and monitoring *MCM6* promoter activity. Luciferase signal normalised to β-galactosidase values. $p<0.05$*, $p<0.001$***, $p<0.0001$****. n=3.

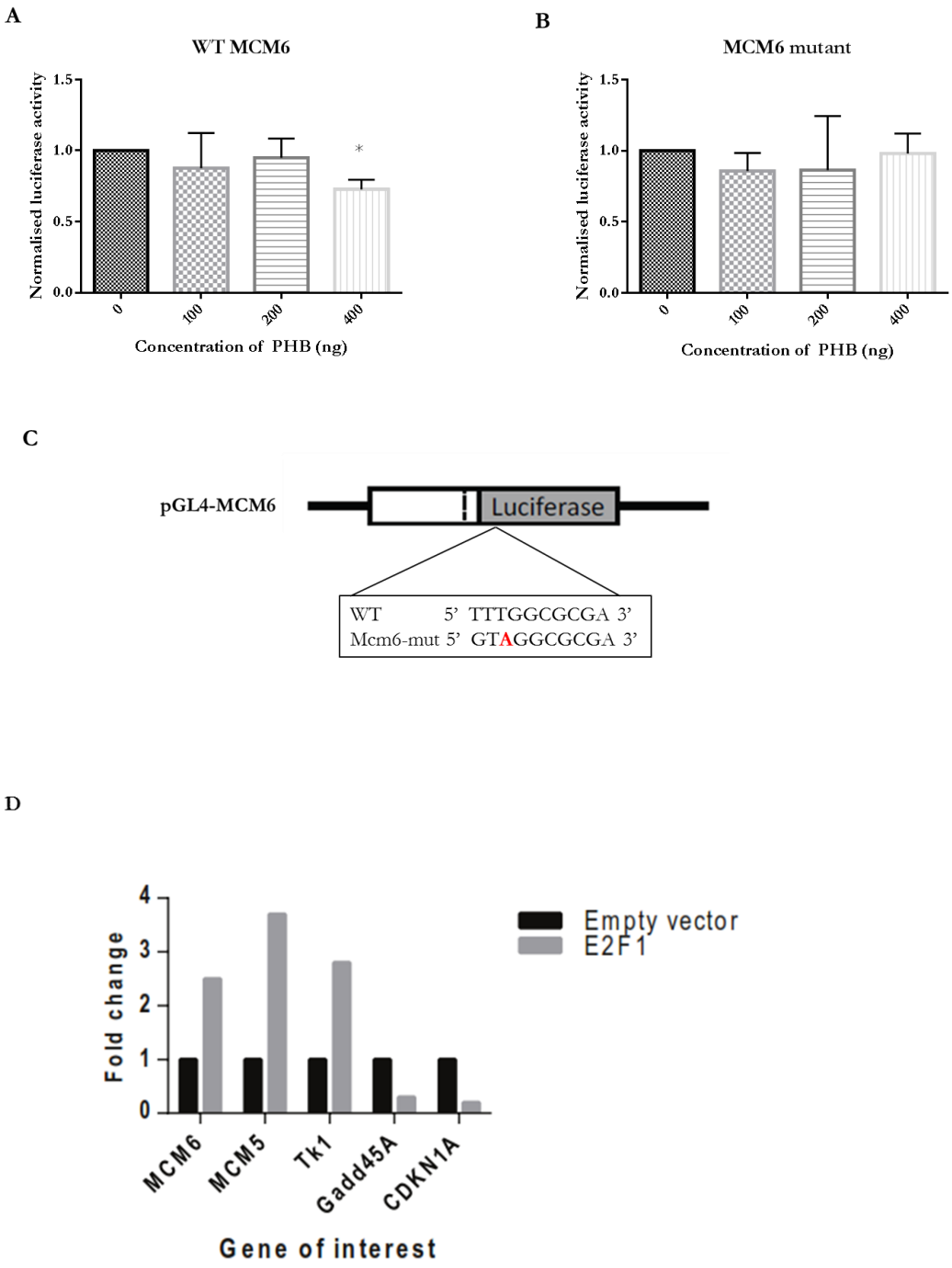

Figure 4.16. Mutagenesis of the *MCM6* promoter abolishes PHB repression. **A**, wt *MCM6* reporter plasmid is repressed with increasing concentrations of pSG5-PHB plasmid (0-400ng). n=3, $p<0.05$*. **B**, mutated *MCM6* reporter plasmid. Repression is not seen in the presence of PHB, n=3. **C**, schematic of the *MCM6* reporter plasmid with the predicted E2F binding site. This site was mutated with a single base substitution of T>A. **D**, Q-PCR analysis of LNCaP cells transfected with an E2F1-overexpression construct.

4.4 Discussion

The aim of this chapter was to identify how PHB over-expression caused cell cycle arrest in PC cells as shown in chapter III. Therefore, an RNA-seq experiment was carried out as PHB has been documented to have a profound effect on gene expression. Revealing information about a particular transcriptome is essential in understanding the development of diseases such as cancer. In this case, the transcriptome of LNCaP/TR2/PHB cells treated with and without doxycycline, to produce ectopic *PHB* cDNA over-expression, was analysed. There are a few technologies available to quantify the transcriptome included hybridisation and sequence based approaches, in this case an RNA-seq was carried out.

RNA-seq showed how PHB over-expression influenced the transcriptome of androgen sensitive cells, LNCaPs. It was vital to perform both unbiased and biased analysis with the data produced to yield an in-depth and comprehensive analysis. Unbiased analysis of the RNA-seq data entailed inputting the data into pathway analysis programs such as METACORE, DAVID and IPA. METACORE depicted that several stages of the cell cycle were heavily influenced with PHB over-expression. DAVID in particular, is a high-throughput data-mining program that analyses gene expression data. Analysis demonstrated that the key networks associated with the inputted datasheet were cell cycle and the regulation of the cell cycle. The IPA pathway analysis showed that *E2F3* was the top transcriptional factor associated with the inputted gene list. Accumulating both gene ontology analysis and RNA-seq data, lead to the assumption that PHB has a repressive function on the cell cycle through interactions of genes associated with the progression of the cell cycle. The unbiased data also depicted that cellular metabolism, cell adhesion and Wnt signalling were within the top ten processes to be altered with PHB over-expression. Interestingly, altered cellular metabolism is an essential initiator in prostate adenocarcinoma. Without metabolism transformation, neoplastic cells are unable to survive. Moreover, altered cell adhesion, particular altered expression of integrin proteins has been documented in 'castration-resistant PC'. Similarly, over-activated Wnt signalling has been seen in aggressive PC(138). Both these processes will be discussed further in proceeding chapters. However, the biased analysis entailed data-mining for genes associated with the regulation and progression of the cell cycle and DNA replication. Previous data has suggested that PHB has a direct influence on E2F1 in breast cancer cells (139). Moreover, Dart *et al.,* (128) described PHB that over-

expression induced androgen responsive LNCaP cells to accumulate in the G0/G1 phase of the cell cycle. E2F binding sites have been identified in promoter regions of the *MCM* gene family that are responsible for DNA replication, genes essential for S phase progression (136). Thus gathering this data together, *PHB*'s role on the *E2F*, *CDK*s and *MCM* gene families was investigated.

Interestingly, PHB over-expression caused an up-regulation of *p21* alongside a down-regulation of *CDK*s, *E2F*s and *MCM*s. Data pertaining to a p21-promoter luciferase reporter plasmid, showed that increasing concentrations of PHB lead to heightened promoter activity through an increase in luciferase production (137). Whereas increasing concentrations of PHB led to the repression of a TK1-promoter luciferase reporter plasmid (137). This highlights PHB's role in suppressing the activity of genes involved in DNA replication, whilst enhancing the function of cell cycle inhibitors such as p21. p21 initiates the arrest of the cell cycle through stimuli such as anti-proliferative signals (140). Whereas CDK1 forms a complex with cyclin A and B to create the maturation-promoting factor, essential for early phase mitosis (141). Thus, accounting for the above data, one can assume that the over-expression of PHB causes a synergic effect of both the down-regulation of cell cycle activators with an increase in cell cycle inhibitors. Interestingly, the Growth Arrest and DNA Damage-inducible 45 (*GADD45a*) was up-regulated with PHB over-expression. GADD45a plays a role in senescence and genotoxic stress (142), suggesting PHB is able to hinder uncontrolled damage cellular proliferation through the up-regulation of GADD45a as it was previously reported that PHB induces senescence in yeast, limiting their proliferative life span (143).

The mechanism of how PHB influences key genes involved in the regulation of the cell cycle was investigated. Binding sites for members of the E2F family have been identified in promoter regions of both *MCM5* and *MCM6*. This was evidenced by mutations within the E2F binding sites causing failed promoter regulation even in the presence of exogenous E2F expression (136). Therefore the activity of these promoters was assessed with PHB over-expression. Data revealed that PHB can significantly reduce the activity of the promoter region of *MCM5*&*6*. Interestingly, upon mutating the predicted E2F binding site within the promoter region of *MCM6*, this repression was not seen. It has been reported that the recruitment of PHB to the promoters leads to HDAC1-dependent transcriptional repression which resembles Rb's

mode of repression (144). Interestingly, previous work demonstrates that with the addition of cyclin dependent kinases (CDKs), PHB's repressive function on gene promoters is not affected (144). This potentially could be due to PHB's being part of a larger repressive complex (144). Further analysis could potentially provide a preliminary mechanism linking PHB, MCMs and E2Fs to the inhibition of the cell cycle (figure 4.17).

Interestingly, ectopic expression of E2F1,2,3 is sufficient to induce the S-phase of the cell cycle in serum starved cultured cells, unlike E2F4 and E2F5 that are unable to carry out the same function. Therefore E2F1,2,3 are the main instigators of cell cycle progression. The DNA binding sites of E2F have been identified in promoters of genes that are responsible for DNA replication and cell cycle control. Such genes include; dihydrofolate reductase (*DHFR*), DNA polymerase α, and regulatory molecules for the initiation of DNA replication, such as HsOrc1 and HsCdc6. As shown by (Ohtani, *et al.,* 1999) both promoter regions of *MCM5* & *MCM6* containing E2F binding sites were regulated by E2Fs and that endogenous expression of E2F1 led to the expression of all the members of the MCM family in REF52 cells (136).

Collectively, these results indicate that *MCM* and *E2F* genes were downregulated by over-expression. It was seen that PHB has a repressive effect on the promoter regions of both *MCM5&6* that was abolished when predicted *E2F* binding sites were mutated. PHB's repressive function on E2F1 is further explored as it has such a prominent role in controlling the progression of the cell cycle. Moreover, both gene expression analysis and bio-analysis indicated that *E2F1* was the main E2F transcriptional factor affected by PHB over-expression.

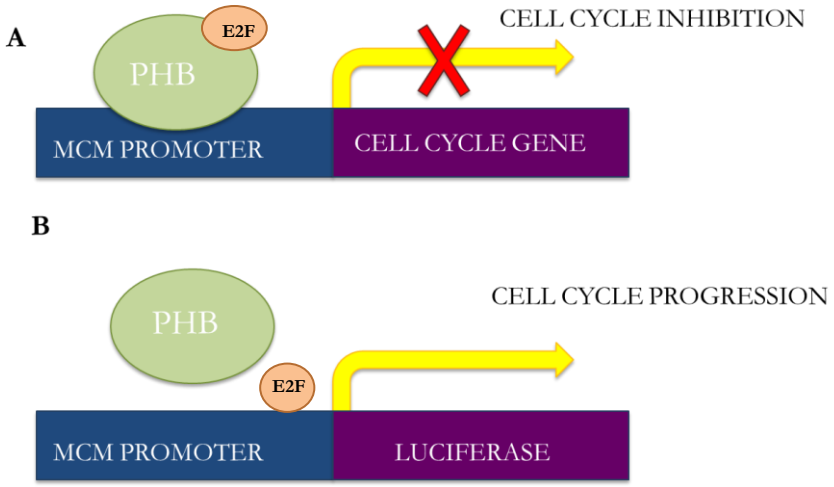

Figure 4.17. Schematic representation of a preliminary mechanism involving PHB, *MCM* promoters and cell cycle progression. **A**, PHB can repress E2F activity on E2F binding sites, preventing the downstream transcription of genes associated with the cell cycle. **B**, through some mechanism, potentially by AR signalling activation, PHB can no longer bind to the *MCM* promoter regions, thus cell cycle progresses.

4.5 Conclusion

RNA-seq showed an array of genes that were altered as a result of PHB over-expression. Analysis of this gene list gave insight that the cell cycle GO pathway was heavily influenced by PHB over-expression. This was supported by the evidence that key genes involved in the cell cycle were down-regulated as a result of PHB over-expression. Specifically, members of the *E2F* and *MCM* gene family with the validation of Q-PCR were significantly downregulated. RNA-seq confirmed that PHB arrests the cell cycle via E2F-repression.

4.6 Key points

- RNA-seq showed PHB over-expression caused the down-regulation of E2Fs, MCMS and CDKs.
- RNA-seq showed PHB over-expression caused the up-regulation of cell cycle inhibitors such as *p21* and *p27*.
- Bioanalysis programmes such as METACORE, DAVID and IPA, all suggested that PHB over-expression heavily influenced the regulation of the cell cycle.
- The bioanalysis programmes also indicated that *E2Fs* were the main transcriptional factor associated with PHB over-expression.
- PHB was able to reduce the activity of both *MCM5* and *MCM6* promoter regions via E2F binding sites.
- Accumulating data, it is theorised that PHB is able to suppress the cell cycle repressing E2F from binding to *MCM* promoter regions, preventing *E2F* gene transcription that in turn causes cell cycle arrest.

Chapter V. The interaction of PHB and E2F1 is lessened with AR activation.

5 Chapter V. The interaction of PHB and E2F1 is lessened with AR activation.

5.1 Introduction

It was established that PHB's role in causing cell cycle arrest may be mediated through E2F repression and down-regulation. In particular, both RNA-seq and bio-informatic analysis indicated that E2F transcription factors were down-regulated with PHB over-expression. Moreover, PHB was able to regulate E2F responsive genes such as *MCM*'s and *TK1* reducing their promoter activity. This repressive response was abolished upon mutation of the E2F binding site within the *MCM* promoter. As *MCM* genes are involved in DNA replication, this could explain why fewer cells were seen in S phase and an accumulation of cells was seen in the G1 phase, with PHB over-expression.

Specifically, as the Q-PCR data indicated *E2F1* was the most significantly down-regulated member of the E2F gene family and *E2F1* targets *E2F3*'s gene transcription (122) which was the most affected gene according to IPA and DAVID analysis, further experiments were carried out with this key gene. There is evidence to suggest that in breast cancer PHB directly interacts with E2F1 within the nucleus of T47D and MCF7 cells where it also co-localises with p53 (89). Therefore, it was of interest to evaluate whether PHB can directly interact with E2F1 in androgen sensitive PC cells. This could be key in unveiling a mechanism to how PHB is able to repress the cell cycle and how androgens may influence it.

Two key methods were adopted to observe if there was a direct interaction between PHB and E2F1 in the LNCaP cell line; the Checkmate ™ Mammalian two-hybrid assay and co-immunoprecipitation. As the AR is the main pathogenic signalling pathway in PC, the role the AR pathway plays in the interaction of E2F1 and PHB was investigated.

The aim was to identify if there was an interaction between E2F1 and PHB in the LNCaP cell line. As activation of the AR signalling pathway results in PHB dissociating from the chromatin, it was investigated if PHB's interaction with E2F1 was influenced by androgens and the AR. This could then lead to a preliminary mechanism alluding to how PHB is down-regulated as PC progresses, leading to an increased E2F activity and progression of the cell cycle.

5.2 Methods

- Molecular cloning (refer to chapter 2.12).
- Checkmate ™ Mammalian two-hybrid assay (refer to chapter 2.15).
- Co-immunoprecipitation assay (refer to chapter 2.11.8).
- Cell fractionation and chromatin isolation of protein lysates (refer to chapter 2.11.7).

5.3 Results

5.3.1 Checkmate™ Mammalian Two-hybrid system

In order to assess if there was a physical interaction between E2F1 and PHB, a CheckMate™ Mammalian Two-Hybrid assay was carried out. In this system, interaction of two proteins results in the transcription of the firefly luciferase reporter gene. Firstly, production of plasmids expressing fusion proteins was carried out.

5.3.2 Production of pACT-E2F1 and pBIND-E2F1 plasmids

Firstly, the fusion plasmids were made via a two-step cloning procedure (figure 5.4). The coding sequence of *E2F1* was amplified from the pCMV6- E2F1 plasmid (Origene) by PCR, using primers with attached restriction sites for *BamH1* and *Xba1* (figure 5.1A). Next the PCR product was cut out of the 0.8% (w/v) gel and purified using a gel purification kit. The purified PCR product was ligated into the pEF6 vector. Transformation of *E.coli* was carried out using this pEF6-E2F1 plasmid. The *E.coli* was spread onto an LB-ampicillin agar plate to grow overnight. Colonies were checked for a positive orientation of the insert using PCR (figure 5.1B). Plasmids that had a positive orientation of the *E2F1* insert were sent for sequencing. BLAST was used to align the sequence produced by the PCR product to *Homo sapiens* E2F transcriptional factor 1 (*E2F1*) mRNA (Figure 5.1C).

Following on from confirming the PCR product was E2F1, the insert was cut out of pEF6 using the restriction enzymes *BamH1* and *Xba1*. These restriction enzymes were used as the Checkmate™ assay plasmids pACT and pBIND contain these restriction sites in the multiple cloning sites (figure 5.3). Next the insert of *E2F1* was ligated into linearised pBIND and pACT plasmids (figure 5.1D) and left to ligate for 2 hours at room temperature.

Both pACT-E2F1 and pBIND-E2F1 were transformed into *E.coli* and left to grow overnight on LB-ampicillin agar plates. Colonies were picked and were grown overnight in LB-ampicillin broth. The plasmids extracted from these colonies were screened for the *E2F1* insert using the orientation check. Plasmids with positive orientations that were sequenced, were re-transformed and DNA was extracted using a

maxiprep DNA extraction kit to ensure a high DNA concentration needed for the Checkmate™ assay.

5.3.3 Production of pBIND-PHB and pACT-PHB

The Checkmate™ assay involves assessing the interaction of two proteins, thus the next step was to create a PHB plasmid that could interact with either the pACT-E2F1 or pBIND- E2F1 plasmid. Firstly, the coding sequence of PHB was amplified from the pSG5-PHB plasmid (figure 5.2A). Next, the *PHB* PCR product was cut out of the 0.8% (w/v) gel and purified using a gel extraction kit. This purified PCR product was then ligated into the pEF6 vector. The ligated pEF6-PHB plasmid was used to transform *E.coli*. Colonies grown were chosen and amplified in LB-ampicillin broth. The DNA was extracted using a miniprep DNA extraction kit. A single and double restriction enzyme digest was carried out to check if the *PHB* insert had successfully ligated into the pEF6 plasmid (figure 5.2B). The enzymes used were *BamH1* and *EcoRV*.

Subsequently the *PHB* insert cut out of the pEF6-PHB plasmid was ligated into the linearised pACT and pBIND plasmids for the CheckMate™ assay. The *PHB* insert was cut with *Xba1* and *BamHI* as these were the enzymes used to linearize both pACT and pBIND. Next the ligation reaction was performed to successfully ligate the insert into both vectors. The reactions were transformed into *E.coli*. Colonies were picked and the plasmids extracted which were sent for sequencing. The sequencing data was inputted into BLAST and the results indicated 99% identify with *Homo sapiens* prohibitin (*PHB*) transcript variants 1-4 (figure 5.2C). As the checkmate ™ assay relies on two complementary plasmids interacting, pACT-E2F1 and pBIND-PHB were chosen.

5.3.4 Confirming PHB and E2F1 physically interact

Once the fusion plasmids were made, COS-7 cells were transfected with the Checkmate™ plasmids, as their transfection efficiency are much higher than that of LNCaP cells. Firstly, cells were transfected with the pGL5 plasmid to monitor luciferase production. As a positive control, pBIND-ID and pACT-Myo were transfected into the cells. As a negative control, pBIND-empty and pACT- E2F1 was used. The two positive plasmids (pBIND-ID and pACT-Myo), producing the two proteins with a known interaction, produced a high luciferase activity as predicted (figure 5.5). The negative controls used produced little luciferase activity, indicating this as the baseline luciferase production was from pGL5. Cells transfected with pACT-E2F1 and pBIND-PHB produced luciferase activity significantly higher than the negative controls, indicating a positive interaction (figure 5.5).

5.3.5 PHB dissociates from the chromatin in response to androgen

Previous literature suggests PHB dissociates from the chromatin when the AR signaling pathway is stimulated with androgen (4 hr) (94). This experiment was carried out in androgen dependent cell lines; VCaP and LNCaP cells. Figure 5.6 illustrates that when R1881 (10 nM) was added to these hormonally starved cells, thus stimulating downstream AR signaling events, the AR associated with the chromatin while PHB dissociated from the chromatin (4hr). The reason why there are two bands for PHB in VCaP and PC3 cells is yet to be investigated, potentially PHB2 was also present on the chromatin. To make sure that the AR signaling cascade was activated in the presence of R1881, figure 5.6 shows an increase in chromatin bound AR, where the AR is presumably binding to sites within promoter regions of androgen responsive genes, amongst others. It was then analysed to see if the AR null line cell; PC3 would respond similarly. PC3 cells no longer express the AR nor are they androgen dependent. Figure 5.6 illustrates that in PC3 cells no AR was bound to the chromatin in the cells as expected, when they were stimulated with ethanol (vehicle) or the hormone R1881 (10 nM). Moreover, PHB levels were very low in comparison to the wt LNCaP cells and were unaffected by hormone treatment in PC3 cells. Thus figure 5.6 demonstrates no change in the little chromatin bound PHB with or without R1881 stimulation.

5.3.6 The novel interaction of PHB and E2F1 in LNCaP cells

Luciferase signal produced by the Checkmate™ assay showed an interaction between the pACT-E2F1 and pBIND-PHB fusion proteins. Therefore immunoprecipitation assays were also carried out to determine if a direct protein:protein interaction existed between PHB and E2F1 in *wt* LNCaP cells within the nuclear fraction. Figure 5.7 shows the immunoprecipitation of PHB when probed with PHB primary antibody. Further, the AR rabbit polyclonal IgG, was seen to co-immunoprecipitate PHB in the in hormonally starved cells (figure 5.7). Interestingly, although PHB is a well-established co-repressor of the AR, it has not previously been shown to directly interact with the AR. However in the presence of androgen, the interaction of PHB and the AR in the LNCaP cell is lessened (R1881 10nM, 4 hr). Figure 5.6 also depicts a novel interaction between PHB and E2F1 in the LNCaP cells. Significantly, this novel interaction was reduced when the cells were treated with R1881.

5.3.7 PHB is potentially dephosphorylated in response to androgen

Since the chromatin dissociation was so rapid (4 h), it was assumed that a movement of proteins within the cell was occurring, which are frequently regulated by post-translational modifications of proteins. Such modifications include phosphorylation, ubiquitination and acetylation that can alter the size and overall charge of PHB. Thus, analysis of post-transcriptional modification by 2D western blot was carried out, in order to assess if the isoelectric point of PHB was affected in presence of hormone. Figure 5.8 illustrates that with the addition of hormone (R1881, 10 nM, 4 hr), *wt* LNCaP cells that had been serum starved for 72 hr showed a pattern change in PHB's isoelectric point. In the presence of hormone, the immunoblot detected spots for PHB shifted more towards pH 10. The same pattern was seen in the VCaP cell line that was serum starved for 72 hr and treated with hormone (R1881, 10 nM, 4 hr), VCaPs are also AR positive, thus signifying the pattern is not cell line specific. The shift change was thought to be potentially a post-transcriptional modification. In particular as there was no size change, it was speculated that the stimulation of the AR pathway was causing PHB to become dephosphorylated. The suggestion that it could be a dephosphorylation event was due to the isotypes of PHB shifting towards pH 10, thus the isoforms are less acidic as phosphate groups are acidic. The same experiment was carried out on PC3s, a cell model representative of androgen independent PC. The isoelectric spots for PHB were the same pattern as the isoelectric spots of PHB in the

LNCaP cells treated with R1881 (figure 5.9). This pattern is also seen in Hela cells that are AR negative and non-prostate cancer cells (94).

5.3.8 PHB is likely to be dephosphorylated in response to androgen

An immunoprecipitation assay was carried on protein lysates that had been treated with calf intestinal phosphatase (CIP). This was to confirm that the post-transcriptional modification was a dephosphorylation event. CIP is an enzyme that removes the phosphate group from the protein and other molecules. Removal of a phosphate group, resembling dephosphorylation led to the reduced interaction of E2F1:PHB in wt LNCaP cells (figure 5.10). Thus, potentially, androgen stimulation of the AR could be leading to the dephosphorylation of PHB, leading to its dissociation from E2F1.

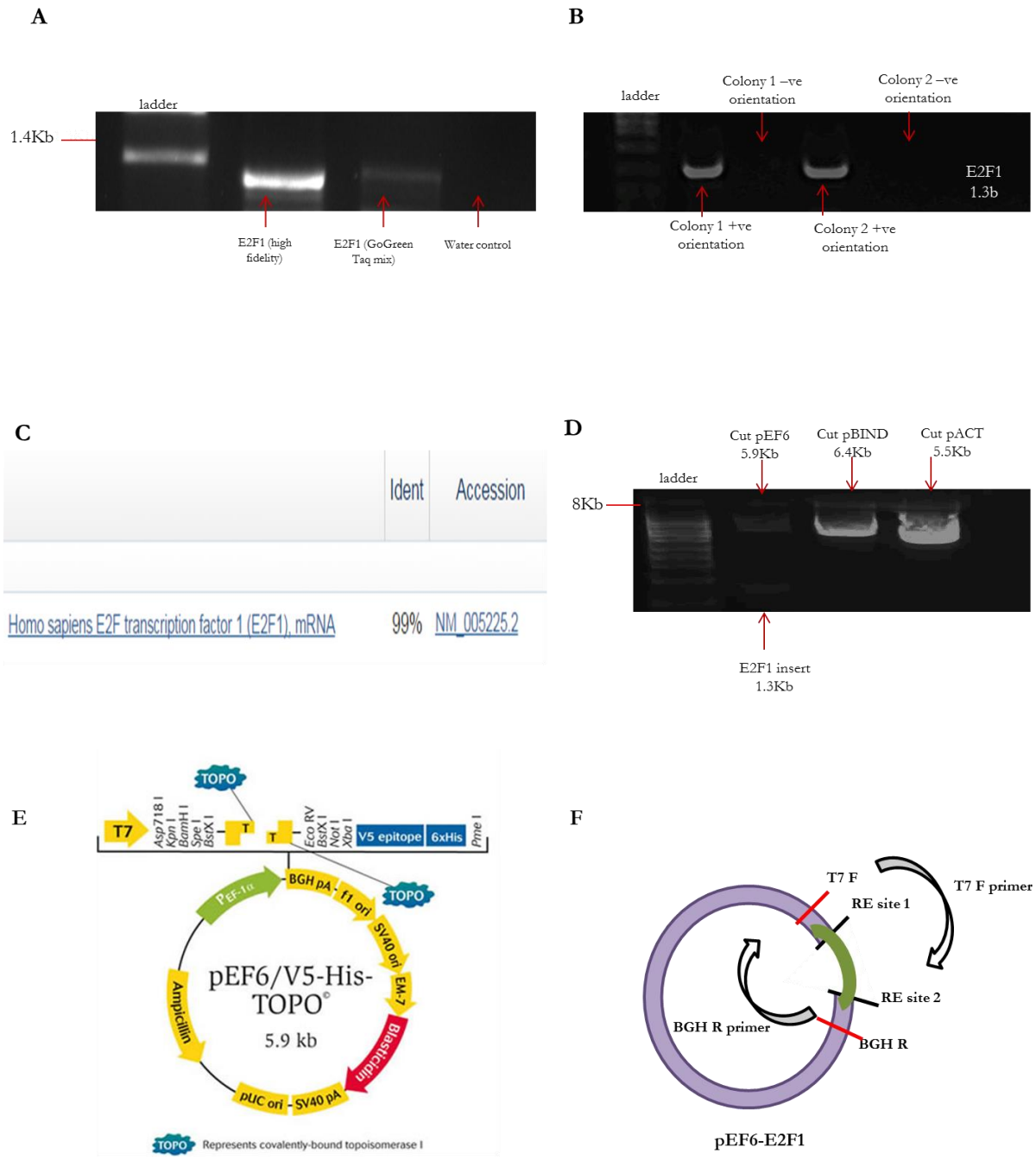

Figure 5.1. Cloning of *E2F1* into the plasmids pACT and pBIND. **A**, PCR amplification of *E2F1* coding sequence using a high fidelity enzyme (Pfu) and GoGreen Taq enzyme. **B**, orientation check of pEF6-E2F1. **C**, screenshot of BLAST (NCBI) results of E2F1-PEF6 sequencing result. **D**, the digestion of pEF6-E2F1 with *BamH1* and *Xba1*, illustrating the insert of E2F1 free of the pEF6 backbone. pACT and pBIND were also digested with the same enzymes. **E**, pEF6 vector circle map (image taken pEF6/V5-His TOPO®, ThermoFisher Scientific) used for the first step of the cloning procedure. **F**, schematic of the pEF6 ligated with the *E2F1* insert, and how the orientation check is carried out using the T7 forward and BGH reverse primers.

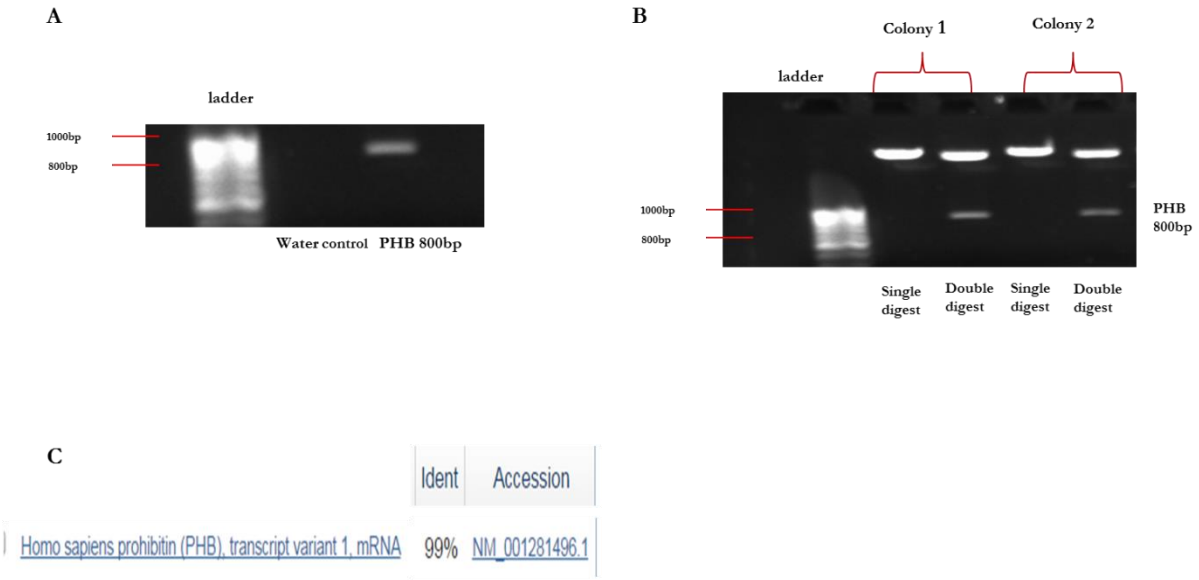

Figure 5.2. Cloning of the *PHB* insert into pEF6. **A**, PCR product of PHB's coding sequencing from pSG5-PHB. **B**, Restriction digest of pEF6-PHB plasmid with *BamH1* and *EcoRV*. Single digest represents the plasmid being cut with only *BamHI* to give a linearized plasmid. In the case of the double digest, both restriction enzymes (*BamH1* and *EcoRV*) were used, dropping out the PHB insert (800bp) and producing a smaller linearized plasmid. **C**, screenshot of BLAST results representing the sequence of pBIND-PHB aligned to *Homo sapiens* PHB mRNA.

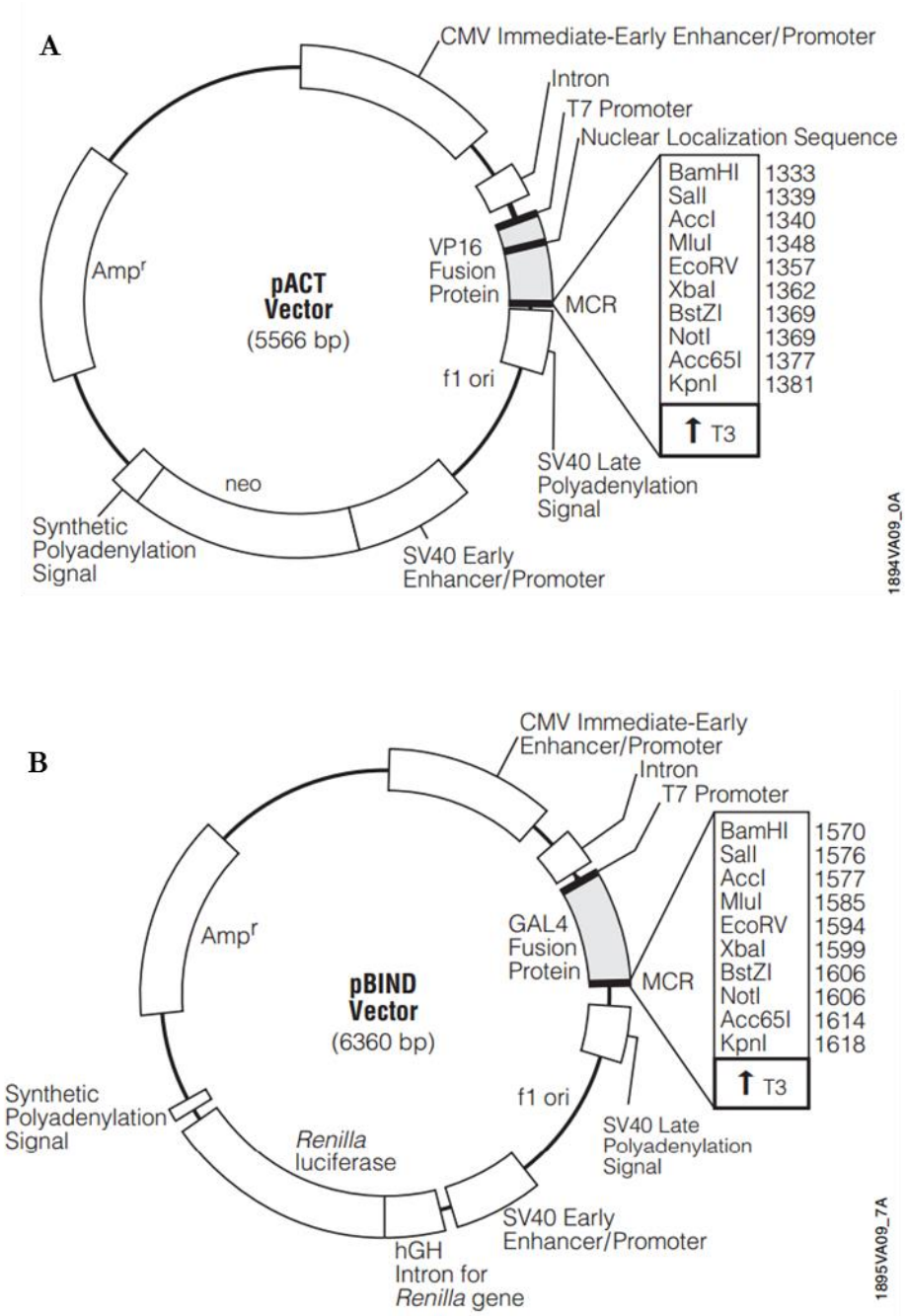

Figure 5.3. Plasmid maps for pACT and pBIND. **A**, pACT vector circle map and sequence reference points (image taken from Promega CheckMate™ Mammalian Two-Hybrid System). **B**, pBIND vector circle map and sequence reference points (image taken from Promega CheckMate™ Mammalian Two-Hybrid System). In the MCR (multiple cloning region) of pACT, the insert of *E2F1* was ligated in. In the MCR of pBIND, the insert of *PHB* was ligated in.

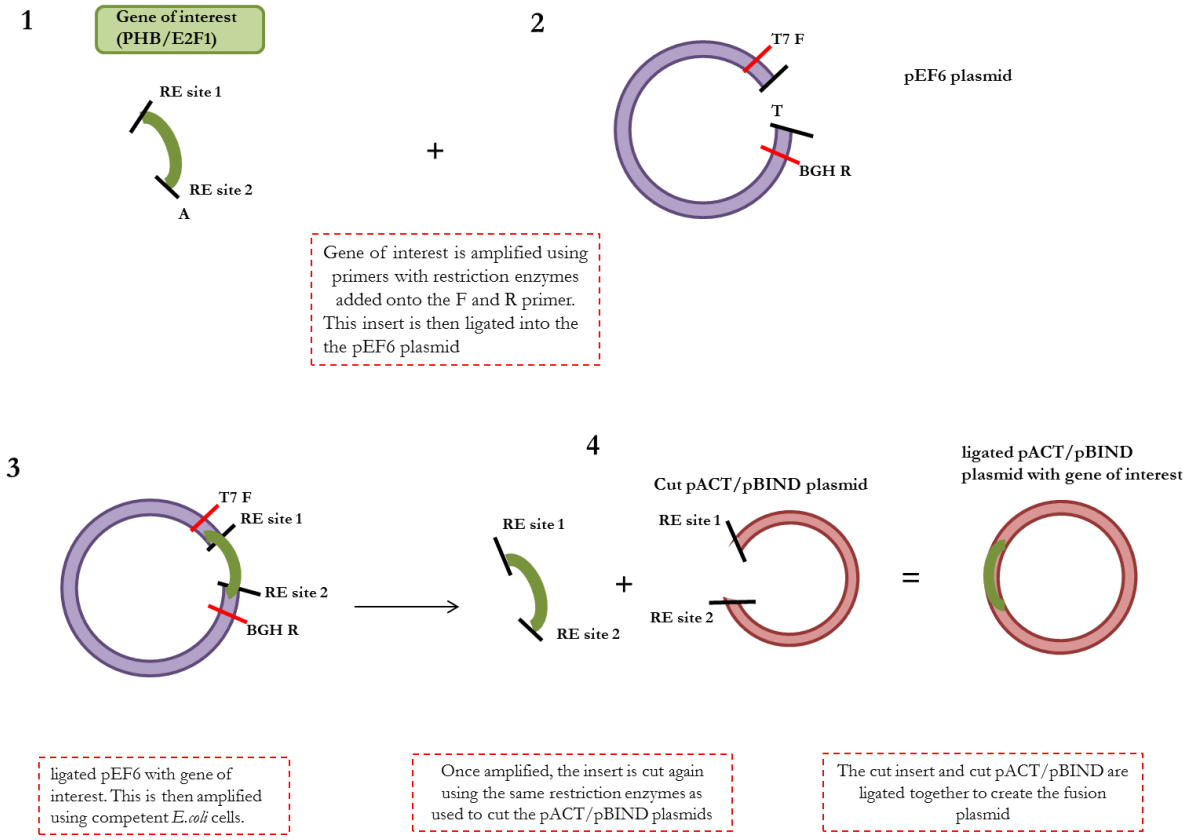

Figure 5.4. Schematic representation of the two-step cloning procedure. First the coding sequence of the gene of interest is amplified using primers with added restriction enzyme (RE) sites. This PCR product is then ligated into the cut pEF6 plasmid via a T-A ligation. This plasmid is then amplified via competent *E.coli* cells. The PCR insert is then cut out of the plasmid using restriction enzymes compatible to those used in the Checkmate™ plasmids. The insert is now ready to ligate into either pBIND or pACT to create the fusion plasmids needed for the Checkmate™ Mammalian two-hybrid assay.

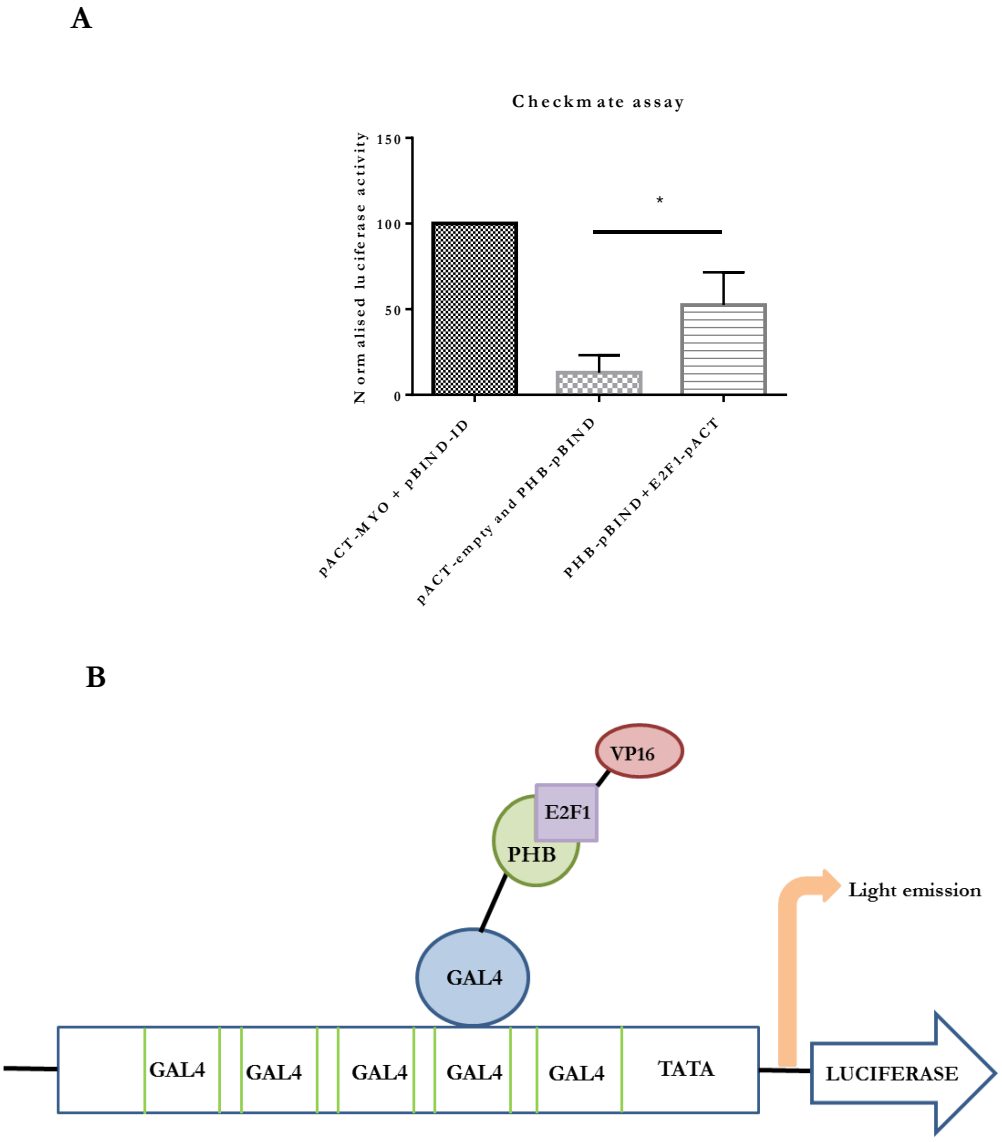

Figure 5.5. The interaction of PHB and E2F1. **A**, The CheckMate™ Mammalian Two-Hybrid assay carried out in the COS-7 cell line. Positive control where luciferase production was highest between pACT-MYO and pBIND-ID. Negative control was pACT-empty and PHB-pBIND. Interaction was seen with the fusion plasmids; pBIND-PHB and pACT-E2F1. Luciferase production was normalised to the positive control. n=3, $p < 0.05$*. **B**, schematic of the interaction of E2F1 and PHB leading to luciferase activity (137).

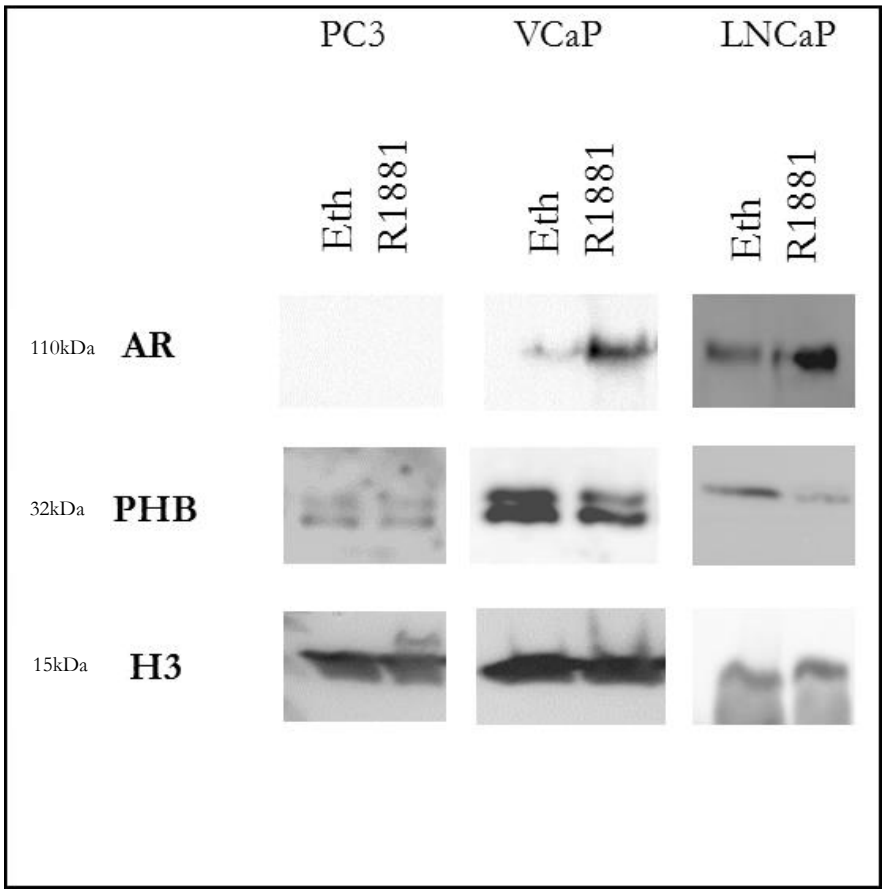

Figure 5.6. The AR and PHB are in dynamic opposition on the chromatin. Western blot for the AR, PHB, H3 from the chromatin cell fraction of PC3, VCaP and LNCaP cells for the AR, PHB and H3. PC3s, VCaPs and LNCaPs were serum starved for 72 hr and treated with R1881 (10 nM,4 hr). As a loading control, chromatin histone H3 was assessed. n=1.

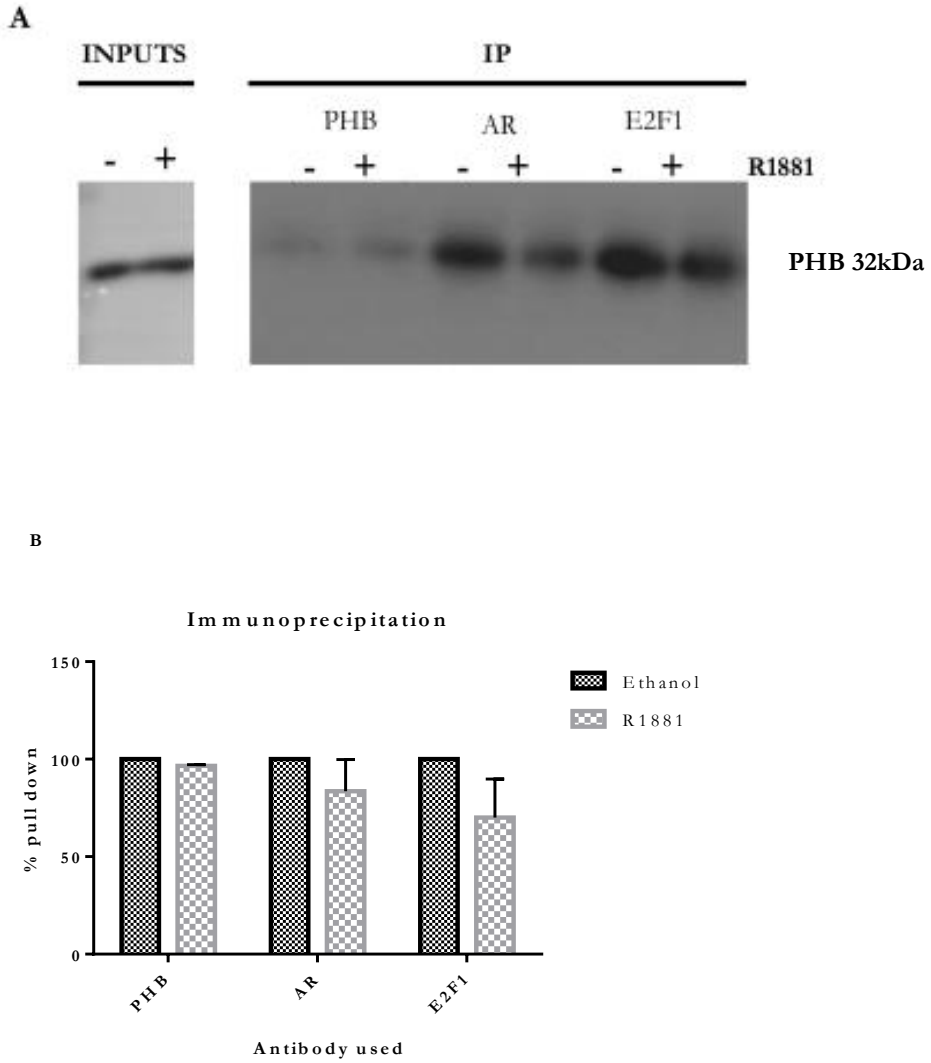

Figure 5.7. The interaction of E2F1 and PHB in the *wt LNCaP* as shown by co-immunoprecipitation. **A**, immunoblot for PHB from nuclear cell lysates +/-R1881 (4 h, 10 nM). Inputs are total nuclear PHB, pull-down of each protein was normalized to its input counterpart. **B**, relative percentage pull-down of PHB, AR and E2F1 with PHB. n=3. Error bars represent SEM.

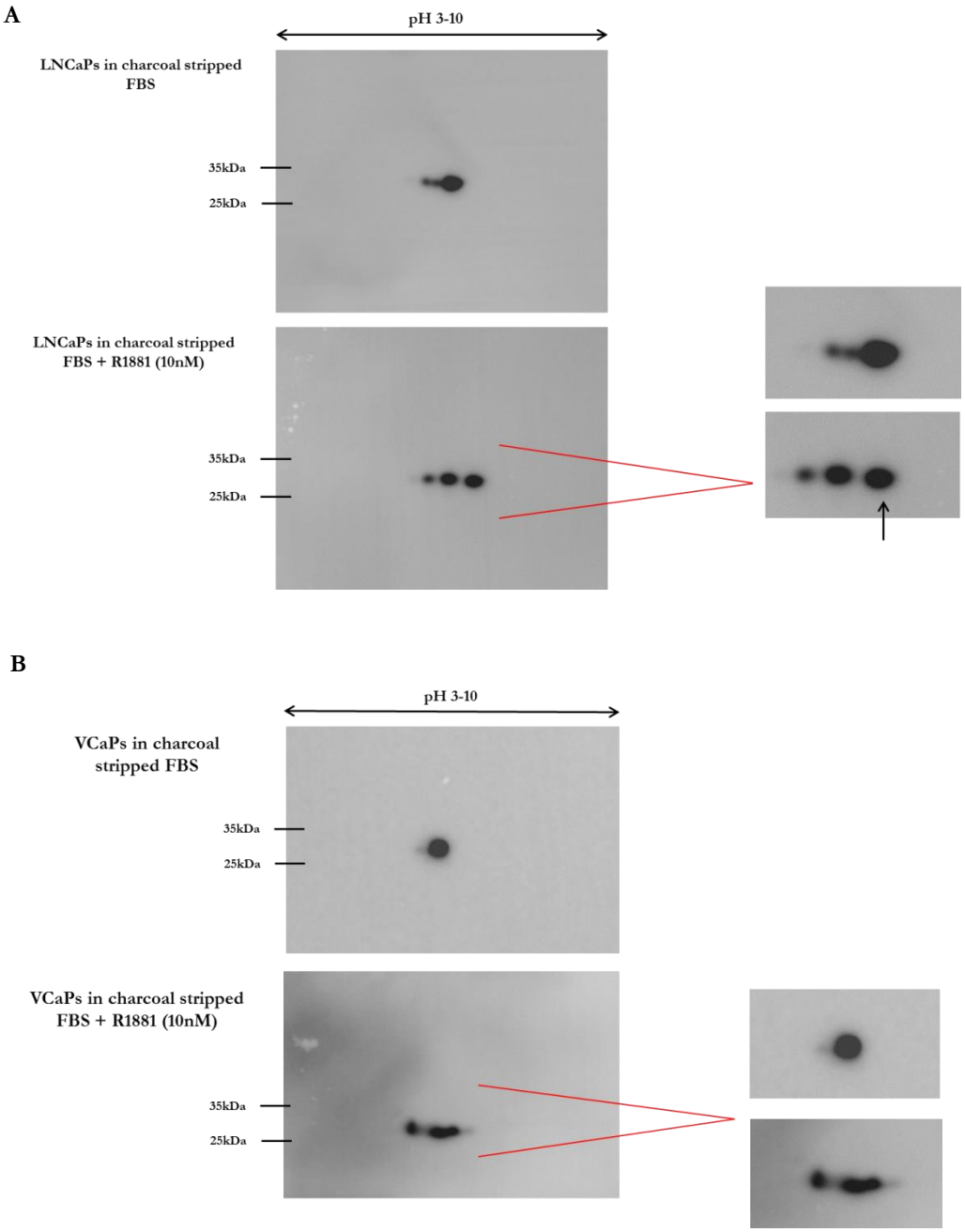

Figure 5.8. 2D western blot of PHB in androgen dependent cell lines. **A**, *LNCaP* cells serum starved for 72 hours and treated with ethanol or R1881 (10 nM,4 hrs). **B**, *VCaP* cells serum starved for 72 hours and treated with ethanol or R1881 (10 nM,4 hrs). *VCaP* cells stimulated with R1881 displayed a basic shift change of PHB isotypes (isotypes are shifted towards pH 10). Right hand side shows a magnified image.

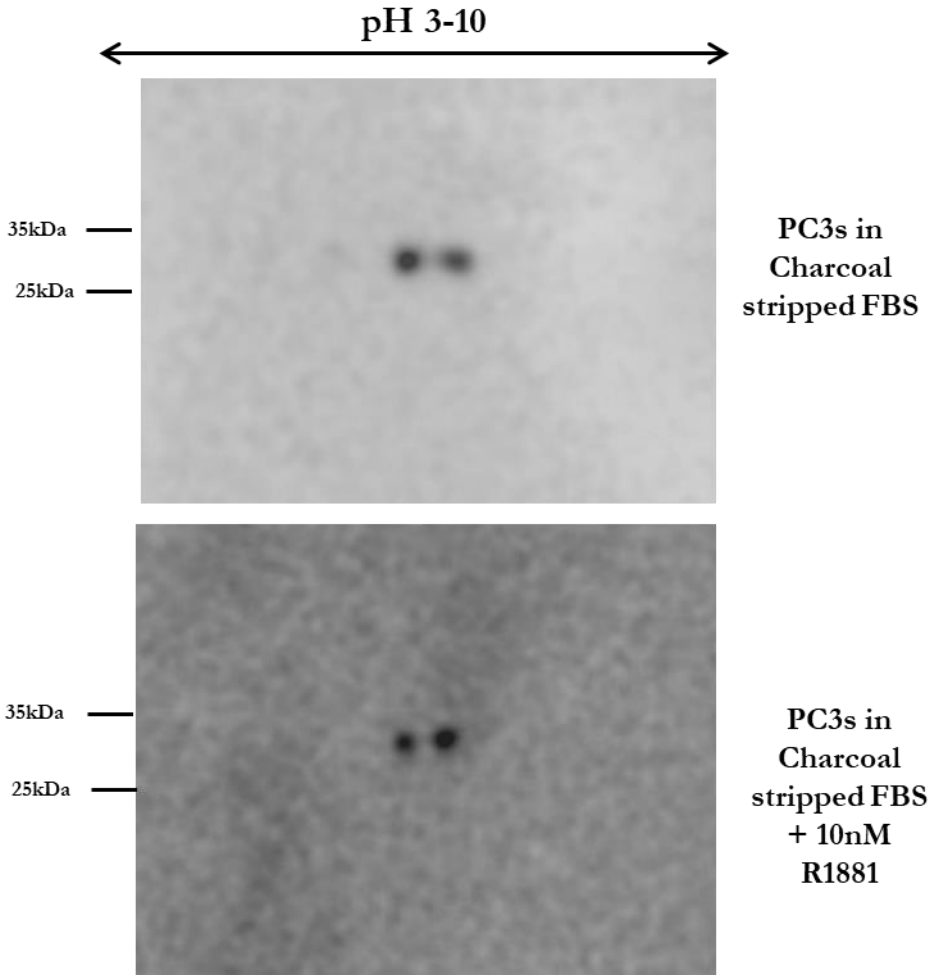

Figure 5.9. 2D western blot of PHB in wt PC3 cells serum starved for 72 hours and treated with ethanol or R1881 (10 nM,4 hrs).

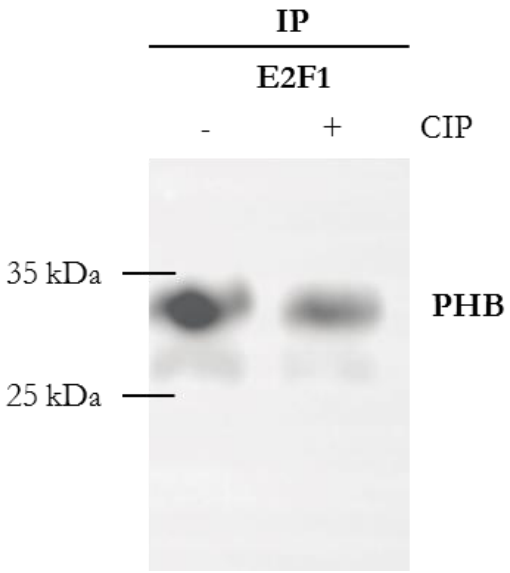

Figure 5.10. Western blot showing PHB interaction with E2F1 the *LNCaP* hormonally starved for 72 hrs (+/- CIP) via co-immunoprecipitation. Hormonally starved LNCaP cells were treated with CIP for 1 hour prior to immunoprecipitation at 37°C before immunoprecipitations with E2F1. Pull down of E2F1 is seen when immunoblotted for PHB.

5.4 Discussion

PHB has pleiotropic roles within the cell depending upon its localisation with the cell compartments. Within the nucleus, PHB carries out its repressive function via interaction with retinoblastoma (Rb) and nuclear co-repressor (NCoR) that then form a complex with E2Fs, rendering their function inactive within the cell cycle (107). However, within the mitochondria, PHB is essential for the dynamics and integrity of the mitochondria as it interacts with SLP-2, a protein essential for mitochondrial biogenesis (79). The novel interaction between PHB and the transcriptional factor; E2F1 in the androgen dependent LNCaP cell line was depicted by immunoprecipitation and the Checkmate ™ Mammalian two-hybrid assay. Although novel in PC, this interaction was also seen in experiments carried out by Wang *et al,*. (107) that describes PHB as an Rb binding protein that is able to suppress E2F (1-5) activity in T47D breast cancer cells. Within the nucleus PHB recruits histone deacetylases such as histone deacetylase 1 (HDAC1) to aid the repression of E2Fs, similar to how Rb represses E2F activity. However, one way in which PHB differs from Rb in its repressive function is that PHB can recruit N-CoR. Moreover, PHB's repressive function on E2F1, was not overcome when T47D cells were stimulated with adenovirus E1A protein. E1A protein is able to inactive Rb and its two family members; p107 and p130, thus allowing transactivation of E2F target genes, even in the absence of growth factor stimulation. This deregulation of E2F activity can contribute to tumour development. Therefore, PHB's ability to repress the activity of E2F1-5 even in the presence of E1A protein, perhaps due to PHB forming a large repressive complex involving other proteins that are able to withstand stimulation of the cell cycle (107). This could explain why the signal for the CheckMate™ Mammalian Two-Hybrid assay was not relatively high as PHB interacting with E2F1 may be a part of a larger protein complex involving Rb and N-CoR and potentially other histone deacetylases.

Interestingly, PHB was found to be complexed with either Rb or E2F1 in an array of cells. Such include Ramos cells (B lymphocyte cell line) (139) and from this data, LNCaP cells. Distinct binding sites of E2F1 (amino acids184-214) and Rb (amino acids 74-116) are found on PHB, thus it is possible that all three proteins bind together at the same time to form a large complex. Work carried out by (107) also described PHB's ability to repress the transcriptional activity of E2F2-5 by binding to the highly conserved marked box region. As Rb can only influence the activity of E2F1-3, this

suggests that PHB may interact with other proteins to render the activity of E2F4-5 inactive, independent of Rb.

Previous data carried out by D Dart, from a Nanobit assay that assesses protein:protein interaction in real time, showed that the interaction of PHB and E2F1 was diminished with androgen within 1 hour (137). Data shown here by the co-immunoprecipitation and the CheckMate™ Mammalian Two-Hybrid assay agrees with the Nanobit assay, confirming that PHB can directly interact with E2F1 in the *wt* LNCaP cell line. This could explain how PHB causes cell cycle arrest as shown in chapter III. This also confirms how PHB is able to repress the promoter activity of MCM5&6. Interestingly, as the immunoprecipitation experiment illustrates, the interaction between E2F1 and PHB was reduced when the AR signaling cascade is stimulated with hormone. The dynamic opposing interaction between PHB and the AR has been well established, particularly as androgen stimulation causes a down-regulation of PHB at both an mRNA and protein level (at 16-24 hr), however this is too slow to account for chromatin changes (seen at 4 hr) (58). However with data presented here, hormone stimulation of the AR caused PHB to rapidly dissociate from the chromatin. Although PHB has no specific DNA binding motifs, it does strongly associate with chromatin as shown here and also in serum starved HeLa cells (94). However, the mechanism to how PHB dissociates from the chromatin is still not well understood. Therefore it was interesting to find that a potential post-translational modification seen on a 2D western blot could be the reason to why PHB dissociates from the chromatin and E2F1. It was theorized that the activation of the AR signaling cascade was causing PHB to undergo a post-translational modification, the main likely event being dephosphorylation, as phosphate groups are acidic, removal of the phosphate group by a phosphatase enzyme resulted in a more basic protein. A more basic species of PHB was seen after androgen stimulation upon 2D western blotting. Phosphorylation of proteins is a fundamental process that governs protein activity, location and degradation and when aberrantly regulated can lead to diseases such as cancer. Mutation analysis of the human *PHB* gene (by the Human Gene Mutation Database, Institute of Medical Genetics, Cardiff), stated no recorded mutations in PC (figure 5.11) only one recorded mutation in breast cancer, stressing that only post-translational modification of PHB governs its intracellular movement, as mutations within the *PHB* gene may be lethal. This is evidenced by *PHB* knockout in mice resulted in embryonic lethality (97).

The entire PHB protein comprises of 17 serine, 14 threonine and 4 tyrosine residues all of which could serve as phosphorylation sites (114). There are only four tyrosine phosphorylation sites found within the PHB protein; Tyr^{28}, Tyr^{114}, Tyr^{249} and Tyr^{259} all that are highly conserved from human, rat, mouse and *Drosophila.* Results collected from Ande *et al,*. (114) suggest that at least two of these tyrosine residues on PHB are phosphorylated in response to insulin treatment in C2C12 cells. The 2D western blot analysis showed 2 isoelectric spots of PHB with a third small, spots possibly indicating several phosphorylation changes. However, there are also 23 sites that are ubiquitination, acetylation, methylation or glycosylation sites.

Ubiquitination involves the attachment of ubiquitin (8.5kDa) to a target protein by an isopeptide bond on a lysine residue (145). As the molecular weight of ubiquitin is small (8.5kDa) and does not bear a charge, this post-translational modification was ruled out as there was no size change observation. Moreover, acetylation involves the transfer of one acetyl functional group from one protein to another. Acetyl groups are polar, thus addition of this group to a positive amino acid would incur a shift change of PHB to give an overall negative charge. Numerous proteomics studies concur that acetylation occurs on approximately 2,500 proteins and is as widespread as phosphorylation. In human cells, acetylated proteins are involved not only in the cell cycle but also chromatin remodeling, membrane trafficking and RNA metabolism. Therefore, acetylation of PHB could be a potential post-translational modification occurring upon AR signaling pathway activation (146). Methylation of non-histone proteins can also occur. It is now known that lysine, arginine and histidine residues can be post-transcriptionally methylated by methyltransferases. This modification has been impacted in gene regulation and signal transduction (147). However, the addition of a methyl group to PHB bears no relevance as it carries a neutral charge. Therefore no shift change in PHB would occur. Finally, glycosylation involves the attachment of sugar side chains to a protein and is considered the most complicated post-transcriptional modification. Glycosylation has been identified in an array of organisms that leads to a production of mature carbohydrate units on glycoproteins that either become a part of the cell itself or is secreted (148). As a mature carbohydrate unit attached onto PHB would significantly alter the molecular weight, glycosylation as a post-translational modification occurring to PHB was ruled out.

Compiling evidence together, either a dephosphorylating, neutralising or an acetylating, or all at the same time, may be occurring to PHB in response to hormone stimulation of the AR pathway in the *wt LNCaP* cells, as PHB underwent only a shift charge change and not a molecular weight change. PHB is often phosphorylated in response to various stimuli such as insulin, insulin-like growth factor and epidermal growth factor (EGF). In particular aberrant tyrosine phosphorylation of PHB is implicated in an array of diseases such as type I diabetes, irritable bowel syndrome and different types of cancers. Thus as it was likely that it was a dephosphorylation event happening to PHB as removal of a phosphate group led to a reduced interaction between PHB and E2F1, the likelihood that PHB could be acetylated was reduced. This needs to have further validation.

To relay this information back to understanding how PC transitions from androgen dependent to an androgen independent disease, PHB's status within PC3 cells (an androgen independent cell line) and VCaP cells (androgen dependent) was also assessed. PHB's isotypes pattern within the VCaP cells resembled the same pattern as identified in the LNCaP cell line, thus signifying the shift pattern of PHB in response to hormone is dependent on the AR. As PHB bears no charge shift change with or without hormone stimulation in the androgen independent cell line; PC3s, but resembles the same PHB isotype pattern of that found in *wt LNCaP* cells stimulated with hormone, it can be argued that in PC3 cells, PHB has already undergone a permanent post-transcriptional modification without androgen stimulation or the AR. Therefore potentially as PC progresses to a more advantaged stage, PHB perhaps is dephosphorylated by an unknown pathway and is no longer able to bind to chromatin, and is no longer able to repress genes associated with the regulation of the cell cycle. This unknown pathway may be a novel mechanism of the development of unregulated cell cycle activation in PC and androgen independence.

The main therapeutic intervention for PC is androgen deprivation (149). However, this type of treatment often leads to transition of the cancer to an eventual androgen independent state, where the androgen receptor signaling cascade is no longer required for cell survival. There are several mechanisms that could allude to how advanced PC is able to survive without androgen stimulation. One explanation could be that the AR is non-specifically activated by a non-specific ligand due to mutations within the ligand binding domain of the AR. Such non-specific ligands include adrenal androgens.

This is due to ligand bound AR being able to associate with molecular substrates within the cytoplasm and the cell membrane to activate intracellular kinase cascades. This is known as rapid non-genomic actions of the AR that lead to enhanced cell proliferation and survival. Non genomic actions of the AR normally occur within minutes, preceding transcriptional events (150). Non-genomic activation of the AR can lead to activating cAMP response element-binding protein (CREB), promoting cell survival. Loss of ligand specificity could explain receptor activation, thus tumour growth in the absence of androgen, resulting in therapy failure. One such signaling pathway known to be elevated in androgen independent PC cases is Src-family kinases. In particular, *FGR* is the only Src family member to be elevated in androgen independent PC (37%) (151). Post-transcriptional modification of the AR may be responsible for its constant activation in the absence of hormone. For example, phosphorylation of the AR by Src at Y534 was identified by mass spectrometry (152). To highlight that the AR may be a SRC-target, inducing PC cells with a Src-AR complex led to heightened cell proliferation (153). Moreover, with the use of a Src kinase inhibitor, transactivation of the AR was inhibited (153). On the contrary, expression of activated Src was able to induce growth of androgen independent cells *in vivo* (151).

5.5 Conclusion

Gathering both previous literature alongside novel data presented here, PHB was seen to directly interact with E2F1 in LNCaP cells as shown by immunoprecipitation and the Checkmate™ assay. This could explain how PHB is able to repress the cell cycle, as it directly interacts with a cell cycle regulator; E2F1, thus hindering its activity. Highlighting the dynamic opposing interaction between the AR signalling pathway and its co-repressor; PHB, the interaction between E2F1 and PHB was lessened when LNCaP cells were stimulated with hormone. This shows that the activated AR signalling pathway can override PHB's repressive function on the cell cycle, as it induces PHB to dissociate from the chromatin. The dissociation of PHB from the chromatin was thought to be due to a post-transcriptional modification. This was due to observing a basic shift change of PHB protein in response to hormone stimulation of the LNCaP cell line. The post-transcriptional modification was narrowed down to likely be a dephosphorylation event occurring to PHB. To conclude, PHB's repressive function on the cell cycle could be due to a direct interaction with E2F1; a key cell cycle regulator. However this interaction was disrupted once the AR signalling pathway was

activated, causing PHB to dissociate from the chromatin due to a potential dephosphorylation event.

5.6 Key points

- Interaction between E2F1 and PHB was established by a CheckMate™ Mammalian Two-Hybrid assay in COS-7 cells.
- Interaction between E2F1 and PHB was established by a co-immunoprecipitation assay in LNCaP cells.
- The interaction between E2F1 and PHB was reduced when the LNCaP cells were stimulated with hormone, activating the AR signalling pathway.
- PHB dissociated from the chromatin once the AR signalling pathway was activated.
- A 2D western blot showed a basic shift charge change of PHB protein when the AR signalling cascade was stimulated with hormone in an androgen dependent cell line; LNCaPs.
- The post-translational modification was thought to likely be a dephosphorylation event.
- A 2D western blot showed no net shift change of PHB isotypes when the AR signalling cascade was stimulated with hormone in an AR-negative cell line; PC3s.
- However, the isotypes of PHB seen in PC3 and HeLa cells resembled a similar pattern to PHB isotypes found in the LNCaP cells that had been stimulated with hormone.
- This suggests that as PC transitions to an androgen independent state, PHB may be post-transcriptionally modified aberrantly and thus can no longer carry out its tumour suppressor activities

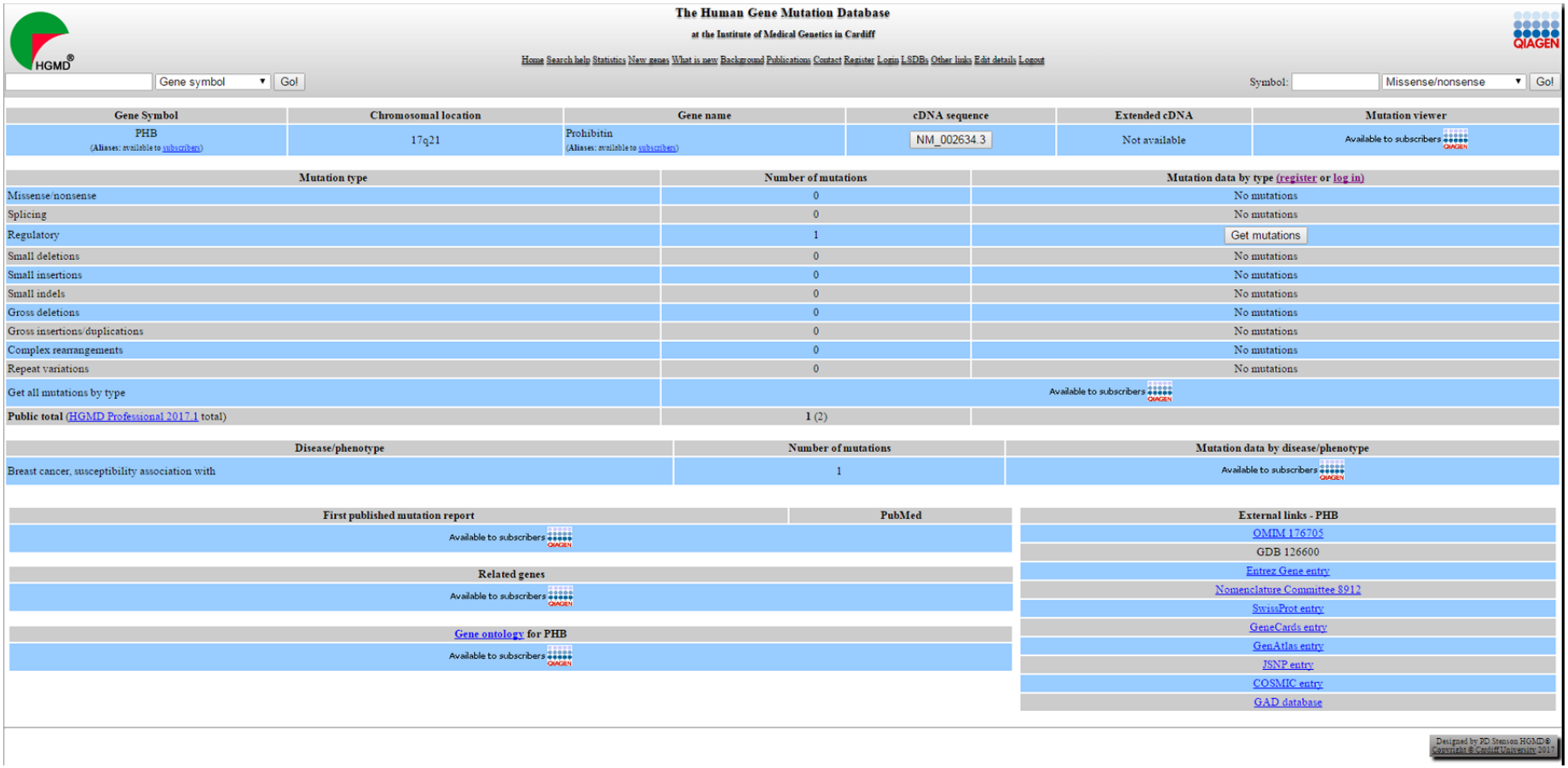

The Human Gene Mutation Database

at the Institute of Medical Genetics in Cardiff

Home Search help Statistics New genes What is new Background Publications Contact Register Login LSDBs Other links Edit details Logout

Gene symbol Go! Symbol: Missense/nonsense Go!

Gene Symbol	Chromosomal location	Gene name	cDNA sequence	Extended cDNA	Mutation viewer
PHB (Aliases: available to subscribers)	17q21	Prohibitin (Aliases: available to subscribers)	NM_002634.3	Not available	Available to subscribers

Mutation type	Number of mutations	Mutation data by type (register or log in)
Missense/nonsense	0	No mutations
Splicing	0	No mutations
Regulatory	1	Get mutations
Small deletions	0	No mutations
Small insertions	0	No mutations
Small indels	0	No mutations
Gross deletions	0	No mutations
Gross insertions/duplications	0	No mutations
Complex rearrangements	0	No mutations
Repeat variations	0	No mutations
Get all mutations by type	Available to subscribers	
Public total (HGMD Professional 2017.1 total)	1 (2)	

Disease/phenotype	Number of mutations	Mutation data by disease/phenotype
Breast cancer, susceptibility association with	1	Available to subscribers

First published mutation report	PubMed
Available to subscribers	

Related genes
Available to subscribers

Gene ontology for PHB
Available to subscribers

External links - PHB
OMIM 176705
GDB 126600
Entrez Gene entry
Nomenclature Committee 8912
SwissProt entry
GeneCards entry
GenAtlas entry
JSNP entry
COSMIC entry
GAD database

Designed by PD Stenson HGMD® Copyright © Cardiff University 2017

Figure 5.11. Screenshot of mutations in the human *PHB* gene from the Human Gene Mutation Database (Institute of Medical Genetics, Cardiff University).

Chapter VI. Inhibiting the Src-pathway heightens PHB's function.

6 Chapter VI. Inhibiting the Src-pathway heightens PHB's function.

6.1 Introduction

Castration resistant PC has very limited treatment options, often with a poor prognosis (32). As the dissociation of PHB from chromatin was too quick to account for transcriptional changes in response to androgen stimulation (4hr), it was thought that PHB protein was being post-transcriptionally modified in response to androgen. It was identified that in response to androgen, a dephosphorylation event was the likely event occurring to PHB. Potentially, it was this phenomenon occurring to PHB that leads to its dissociation from E2F1 and the chromatin, allowing the progression of the cell cycle. However, in castration resistant PC, the cancer has developed mechanisms to survive in the absence of androgen stimulation of the AR. One such mechanism is known as non-genomic activation of the AR. Non-genomic activation of the AR has been documented to progress PC in an androgen depleted environment (150). Here, non-specific ligand (adrenal androgens, growth factors and cytokines) activate the AR leading to activation of intracellular signaling cascades (Src, cAMP, PI3K) that occurs within minutes (150). It is these signaling cascades that can propagate AIPC, causing patient relapse to anti-androgen therapy. Moreover, it is likely that the non-genomic activation of the AR, leading to the activation of these signaling pathways can lead to the deactivation of PHB's tumour suppressive functions. To assess and identify AR non-genomic pathways we aimed to study what proteins were phosphorylated in response to AR activation.

6.2 Methods

- 2D western blot (refer to chapter 2.11.6).
- Kinexus array (refer to chapter 2.11.9).
- Chromatin isolation (refer to chapter 2.11.7).
- Luciferase assay (refer to chapter 2.12.8).
- SYBR® Green Q-PCR (refer to chapter 2.8.3).

6.3 Results

6.3.1 Src phosphorylation is the most significant change in response to androgen treatment in LNCaP cells

As the discovery that androgen activation of the AR led to the post-translational modification of PHB (as shown in chapter V), was rapid (4 hours), signalling pathways were investigated in response to androgen treatment in an androgen dependent cell line. There are a huge amount of post-translational modifications happening to proteins with the cell at one time, proving too complex to study. However, here a Kinexus protein array was used as they offered the most numerous targets and phosphorylation changes available in one screen. LNCaP cells were hormonally starved for 72 hours (using charcoal stripped FCS-media) and treated with R1881 (10nM, 4hr). As a vehicle control, 100% ethanol was used. Protein lysates were extracted and sent to Kinexus (Canada). Results were presented as a KinexTM Antibody Microarray Data Report on an Excel file sheet (figure 6.1). The data was sorted in Excel by the highest % CFC (percentage change from control) in response to androgen treatment. The data was separated into the top ten total and specific phosphorylated proteins (figure 6.2). Figure 6.2 describes that ROCK1/ROKB was the most total phosphorylated protein. Whereas Src-Y418 was the top most specific phosphorylated protein. This was validated by a western blot showing that androgen stimulation led to an increased phosphorylation of Src-Y418 (supplemental figure 3).

6.3.2 Inhibiting the Src pathway leads to reduced AR activity

The activation of the Src pathway is heavily influenced in the non-genomic activation of the AR. Data from figure 6.2 demonstrated that Src-Y418 was the most phosphorylated protein changed from the control, alongside several protein components having Src as their apical kinase (ErbB2, FAK). Therefore, the Src pathway was further investigated. To assess the inhibitory effects of blocking the Src signalling pathway, a Src inhibitor was used; Src-inhibitor-1 (SrcI-1) (20μM working concentration). LNCaP cells were hormonally starved for 72 hours and stimulated with R1881 (10nM, 4hr). Alongside, Src-inhibitor-1 was added to the cells with and without R1881. SYBR® Green Q-PCR was carried out to assess if inhibiting the Src pathway influenced the androgen responsive genes, *PSA*. As seen in figure 6.3 with the addition of the Src-inhibitor-1, the *PSA* fold expression was significantly reduced when compared to cells stimulated with

R1881 (figure 6.3). Moreover, cells treated with the Src-inhibitor-1 had a slight increase in *PHB* gene expression, when compared to cells treated with R1881. Figure 6.3 illustrates a trend but it was not statistically significant.

6.3.3 Inhibiting the Src pathway increases chromatin-bound PHB

As it has been previously described, treatment of cells with R1881 results in PHB dissociating from the chromatin. However, cells treated with the Src-inhibitor-1 (20 μM) demonstrated an increase in chromatin-bound PHB, as shown in figure 6.4. An increase in chromatin-bound PHB was also seen in cells with simultaneous activation of the AR with hormone and inhibition of the Src pathway with Src-inhibitor-1. This suggests that potentially activation of the Src pathway by the AR leads to the dissociation of PHB from the chromatin.

6.3.4 Inhibiting the Src-pathway stops the likely dephosphorylation event on PHB in response to androgen

As it has been previously shown in Chapter V that hormone activation of the AR results in a likely dephosphorylation event on PHB, it was assessed if inhibition of the Src pathway could stop this from happening. A 2D western blot was carried out on LNCaP cells treated with the Src-inhibitor-1. LNCaP cells were hormonally starved for 72 hr, and treated as follows; +/-R1881 (10nM), +/-Src-inhibitor-1 (20μM) for 4 hr. The pattern of the PHB protein in cells stimulated with R1881 only, demonstrated a shift towards pH 10 as seen in chapter V, resembling a dephosphorylation event occurring to PHB upon AR activation. Interestingly, cells stimulated with Src-inhibitor-1 alone illustrated that the PHB protein had no longer shifted towards pH 10 (figure 6.5). This suggests that inhibiting the Src-pathway alone, inhibits PHB from potentially being dephosphorylated, thus PHB can still retain its tumour suppressive functions. This pattern was also mirrored for the cells treated simultaneously with R1881 and Src-inhibitor-1. This signifies that blockade of the Src-pathway even upon AR activation is enough to inhibit PHB from becoming dephosphorylated. This could allude to how inhibiting the Src pathways leads to more PHB bound chromatin.

6.3.5 Down-regulation of PHB is seen in an anti-androgen resistant cell line

A cell model for an anti-androgen resistant phenotype was derived from the wt LNCaP cell line. First, the LNCaPs were grown in the presence of a clinically approved anti-androgen drug (Bicalutamide) for up to 6 months at varying concentrations (as described in chapter 2.7.1). Conferring to the Geodatasets presented in chapter VII, it was identified that in chemotherapy-resistant cell lines (docetaxel-resistant DU-145 and PC3) , *PHB* was significantly down-regulated at a gene level. Therefore, RNA extracted from a Bicalutamide-resistant LNCaP (Bicalutamide-R) cell line was reverse transcribed and analysis of *PHB* gene expression was carried out. SYBR® Green Q-PCR results depicted that *PHB* gene expression was significantly down-regulated in the Bicalutamide-R cell line when compared to LNCaP cells (figure 6.6A). Moreover, RNA extracted from wt PC3 cells was reversed transcribed and analysed for *PHB* gene expression. Figure 7.4 describes a significant down-regulation of *PHB* gene expression in PC3 cells when compared to LNCaP cells. This also emphasises that *PHB* is down-regulated in androgen independent cells. Moreover, a 2D western blot analysis compared the difference in PHB protein isoelectric points in wt LNCaP and Bicalutamide-R LNCaPs. Figure 6.6B depicts that the isoelectric point of PHB in the Bicalutamide-R LNCaPs has shifted more towards pH 10 than the wt LNCaP cells. This suggests that in an anti-androgen resistant phenotype, PHB has already undergone a post-translational modification, a similar trend since when the AR is activated.

6.3.6 Anti-androgen treatment heightens PHB's repression of the MCM promoter

LNCaP/TR2/PHB cells were transfected with the pGL4-MCM6 reporter plasmid as described in chapter IV. However, the efficacy of PHB over-expression was assessed in the presence of another anti-androgen drug; enzalutamide (MDV3100). Interestingly, the activity of the MCM6 promoter was significantly reduced in the presence of enzalutamide. However, the biggest significant decrease in MCM6 promoter activity was seen in cells treated with both doxycycline and enzalutamide (3 fold decrease) (figure 6.7A). This highlights that PHB heightens the function of the anti-androgen treatment; enzalutamide, repressing AR responsive genes such as *MCM6*.

6.3.7 Anti-androgen treatment prevents the likely dephosphorylation event on PHB

As inhibiting the Src pathway inhibited the likely dephosphorylation event on PHB, it was investigated if enzalutamide (MDV3100) could also mirror the same pattern. LNCaP cells were hormonally starved for 72 hr and treated with (+/-R1881 10nM, 4hr) (+/-MDV3100 10μM, 4hr). Cells treated with MDV3100 illustrated the isoelectric point of PHB had no longer shifted towards pH 10, resembling inhibition of a dephosphorylation event (figure 6.7B). This suggests that the likely dephosphorylation on PHB is due to an AR related event, as enzalutamide inhibits AR activity.

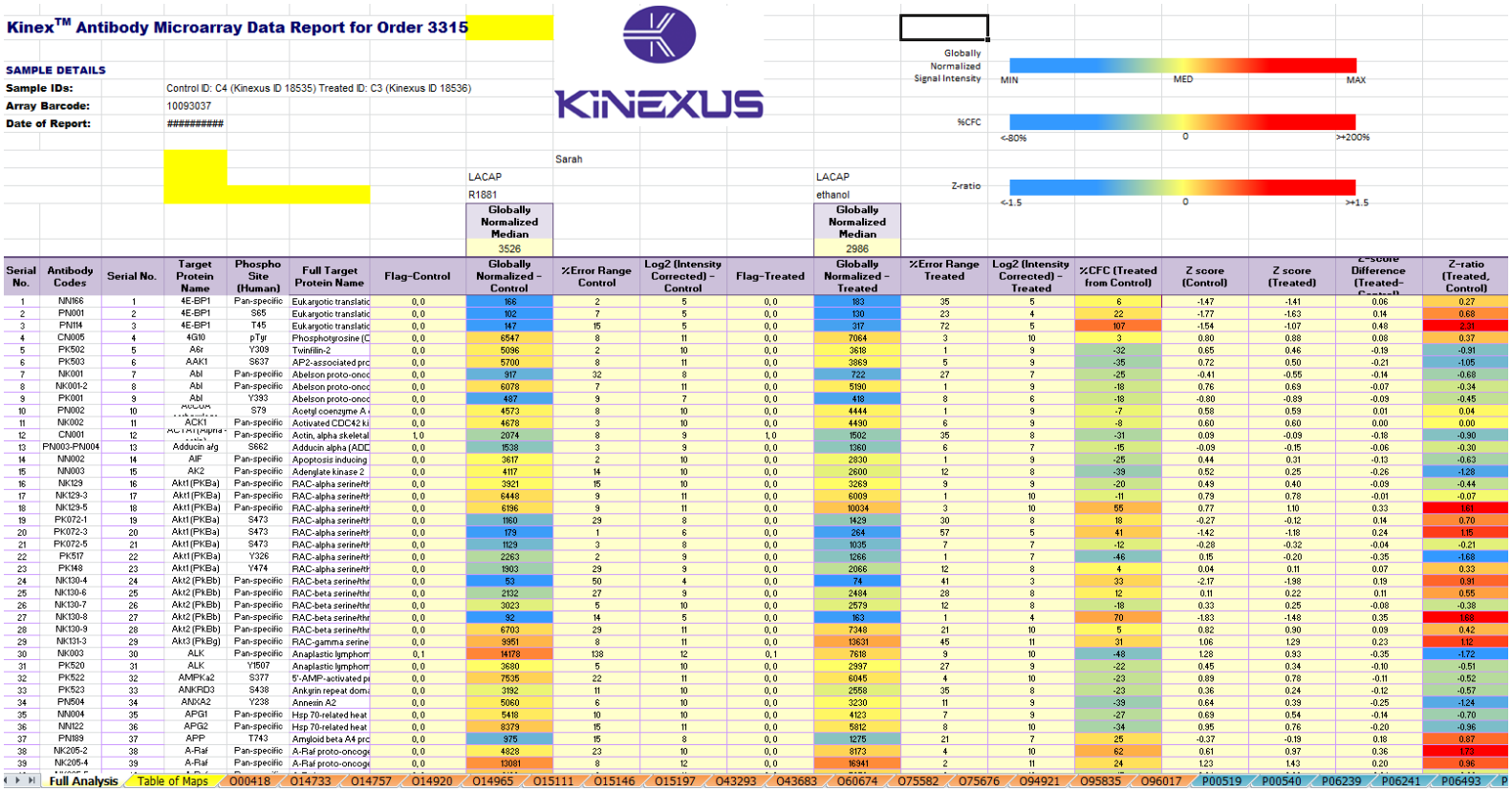

Kinex™ Antibody Microarray Data Report for Order 3315

KINEXUS

SAMPLE DETAILS

Sample IDs:	Control ID: C4 (Kinexus ID 18535) Treated ID: C3 (Kinexus ID 18536)
Array Barcode:	10093037
Date of Report:	##########

Sarah

LACAP
R1881
Globally Normalized Median
3526

LACAP
ethanol
Globally Normalized Median
2986

Globally Normalized Signal Intensity: MIN MED MAX
%CFC: <-80% 0 >+200%
Z-ratio: <-1.5 0 >+1.5

Serial No.	Antibody Codes	Serial No.	Target Protein Name	Phospho Site (Human)	Full Target Protein Name	Flag-Control	Globally Normalized – Control	%Error Range Control	Log2 (Intensity Corrected) – Control	Flag-Treated	Globally Normalized – Treated	%Error Range Treated	Log2 (Intensity Corrected) – Treated	%CFC (Treated from Control)	Z score (Control)	Z score (Treated)	Z-score Difference (Treated–Control)	Z-ratio (Treated, Control)
1	NN168	1	4E-BP1	Pan-specific	Eukaryotic translatic	0, 0	166	2	5	0, 0	183	35	5	6	-1.47	-1.41	0.06	0.27
2	PN001	2	4E-BP1	S65	Eukaryotic translatic	0, 0	102	7	5	0, 0	130	23	4	22	-1.77	-1.63	0.14	0.68
3	PN114	3	4E-BP1	T45	Eukaryotic translatic	0, 0	147	15	5	0, 0	317	72	5	107	-1.54	-1.07	0.48	2.31
4	CN005	4	4G10	pTyr	Phosphotyrosine (C	0, 0	6547	8	11	0, 0	7064	3	10	3	0.80	0.88	0.08	0.37
5	PK502	5	A6r	Y309	Twinfilin-2	0, 0	5096	2	10	0, 0	3618	1	9	-32	0.65	0.46	-0.19	-0.91
6	PK503	6	AAK1	S637	AP2-associated prc	0, 0	5700	8	11	0, 0	3869	5	9	-35	0.72	0.50	-0.21	-1.05
7	NK001	7	Abl	Pan-specific	Abelson proto-onoc	0, 0	917	32	8	0, 0	722	27	7	-25	-0.41	-0.55	-0.14	-0.68
8	NK001-2	8	Abl	Pan-specific	Abelson proto-onoc	0, 0	6078	7	11	0, 0	5190	1	9	-18	0.76	0.69	-0.07	-0.34
9	PK001	9	Abl	Y393	Abelson proto-onoc	0, 0	487	9	7	0, 0	418	8	6	-18	-0.80	-0.89	-0.09	-0.45
10	PN002	10	ACCOA	S79	Acetyl coenzyme A (	0, 0	4573	8	10	0, 0	4444	1	9	-7	0.58	0.59	0.01	0.04
11	NK002	11	ACK1	Pan-specific	Activated CDC42 ki	0, 0	4678	3	10	0, 0	4490	6	9	-8	0.60	0.60	0.00	0.00
12	CN001	12	ACTA1 (Alpha	Pan-specific	Actin, alpha skeletal	1, 0	2074	8	9	1, 0	1502	35	8	-31	0.09	-0.09	-0.18	-0.90
13	PN003-PN004	13	Adducin a/g	S662	Adducin alpha (ADC	0, 0	1538	3	9	0, 0	1360	6	7	-15	-0.09	-0.15	-0.06	-0.30
14	NN002	14	AIF	Pan-specific	Apoptosis inducing	0, 0	3617	2	10	0, 0	2830	1	9	-25	0.44	0.31	-0.13	-0.63
15	NN003	15	AK2	Pan-specific	Adenylate kinase 2	0, 0	4117	14	10	0, 0	2600	12	8	-39	0.52	0.25	-0.26	-1.28
16	NK129	16	Akt1 (PKBa)	Pan-specific	RAC-alpha serine/th	0, 0	3921	15	10	0, 0	3269	9	9	-20	0.49	0.40	-0.09	-0.44
17	NK129-3	17	Akt1 (PKBa)	Pan-specific	RAC-alpha serine/th	0, 0	6448	9	11	0, 0	6009	1	10	-11	0.79	0.78	-0.01	-0.07
18	NK129-5	18	Akt1 (PKBa)	Pan-specific	RAC-alpha serine/th	0, 0	6196	9	11	0, 0	10034	3	10	55	0.77	1.10	0.33	1.61
19	PK072-1	19	Akt1 (PKBa)	S473	RAC-alpha serine/th	0, 0	1160	29	8	0, 0	1429	30	8	18	-0.27	-0.12	0.14	0.70
20	PK072-3	20	Akt1 (PKBa)	S473	RAC-alpha serine/th	0, 0	179	1	6	0, 0	264	57	5	41	-1.42	-1.18	0.24	1.15
21	PK072-5	21	Akt1 (PKBa)	S473	RAC-alpha serine/th	0, 0	1129	3	8	0, 0	1035	7	7	-12	-0.28	-0.32	-0.04	-0.21
22	PK517	22	Akt1 (PKBa)	Y326	RAC-alpha serine/th	0, 0	2263	2	9	0, 0	1266	1	7	-46	0.15	-0.20	-0.35	-1.68
23	PK148	23	Akt1 (PKBa)	Y474	RAC-alpha serine/th	0, 0	1903	29	9	0, 0	2066	12	8	4	0.04	0.11	0.07	0.33
24	NK130-4	24	Akt2 (PkBb)	Pan-specific	RAC-beta serine/thr	0, 0	53	50	4	0, 0	74	41	3	33	-2.17	-1.98	0.19	0.91
25	NK130-6	25	Akt2 (PkBb)	Pan-specific	RAC-beta serine/thr	0, 0	2132	27	9	0, 0	2484	28	8	12	0.11	0.22	0.11	0.55
26	NK130-7	26	Akt2 (PkBb)	Pan-specific	RAC-beta serine/thr	0, 0	3023	5	10	0, 0	2579	12	8	-18	0.33	0.25	-0.08	-0.38
27	NK130-8	27	Akt2 (PkBb)	Pan-specific	RAC-beta serine/thr	0, 0	92	14	5	0, 0	163	1	4	70	-1.83	-1.48	0.35	1.68
28	NK130-9	28	Akt2 (PkBb)	Pan-specific	RAC-beta serine/thr	0, 0	6703	29	11	0, 0	7348	21	10	5	0.82	0.90	0.09	0.42
29	NK131-3	29	Akt3 (PkBg)	Pan-specific	RAC-gamma serine	0, 0	9951	8	11	0, 0	13631	45	11	31	1.06	1.29	0.23	1.12
30	NK003	30	ALK	Pan-specific	Anaplastic lymphom	0, 1	14178	138	12	0, 1	7618	9	10	-48	1.28	0.93	-0.35	-1.72
31	PK520	31	ALK	Y1507	Anaplastic lymphom	0, 0	3680	5	10	0, 0	2937	27	9	-22	0.45	0.34	-0.10	-0.51
32	PK522	32	AMPKa2	S377	5'-AMP-activated pr	0, 0	7535	22	11	0, 0	6045	4	10	-23	0.69	0.78	-0.11	-0.52
33	PK523	33	ANKRD3	S438	Ankyrin repeat dom	0, 0	3192	11	10	0, 0	2558	35	8	-23	0.36	0.24	-0.12	-0.57
34	PN504	34	ANXA2	Y238	Annexin A2	0, 0	5060	6	10	0, 0	3230	11	9	-39	0.64	0.39	-0.25	-1.24
35	NN004	35	APG1	Pan-specific	Hsp 70-related heat	0, 0	5418	10	10	0, 0	4123	7	9	-27	0.69	0.54	-0.14	-0.70
36	NN122	36	APG2	Pan-specific	Hsp 70-related heat	0, 0	8379	15	11	0, 0	5812	8	10	-34	0.95	0.76	-0.20	-0.96
37	PN189	37	APP	T743	Amyloid beta A4 prc	0, 0	975	15	8	0, 0	1275	21	7	25	-0.37	-0.19	0.18	0.87
38	NK205-2	38	A-Raf	Pan-specific	A-Raf proto-oncoge	0, 0	4828	23	10	0, 0	9173	4	10	62	0.61	0.97	0.36	1.73
39	NK205-4	39	A-Raf	Pan-specific	A-Raf proto-oncoge	0, 0	13081	8	12	0, 0	16941	2	11	24	1.23	1.43	0.20	0.96

Full Analysis | Table of Maps | O00418 | O14733 | O14757 | O14920 | O14965 | O15111 | O15146 | O15197 | O43293 | O43683 | O60674 | O75582 | O75676 | O94921 | O95835 | O96017 | P00519 | P00540 | P06239 | P06241 | P06493 | P

Figure 6.1. Screenshot of Kinexus™ antibody Microarray data report. CFC (change from control) was used to sort data. Data is alphabetical. This is the original data file prior to sorting into top ten most and least phosphorylated proteins.

A

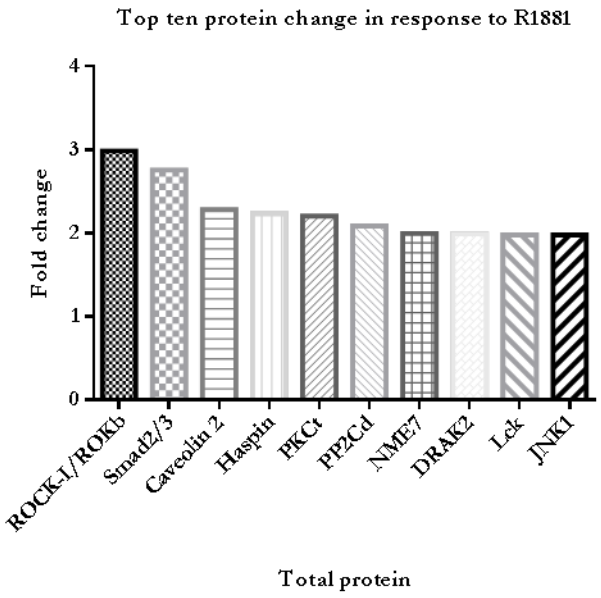

B

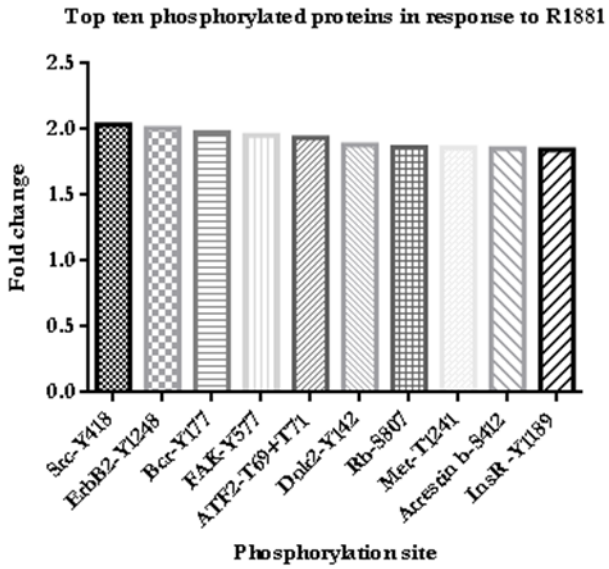

Figure 6.2. Kinexus protein array data of the top ten total and specific phosphorylated proteins in response to androgen stimulation in the LNCaP cells. **A**, the top ten total protein changes in response to R1881 treatment (10 nM, 4hr) from LNCaP cells (72 hr serum starved). **B**, the top ten phosphorylated proteins in R1881 treatment (10 nM, 4hr) from LNCaP cells (72 hr serum starved).

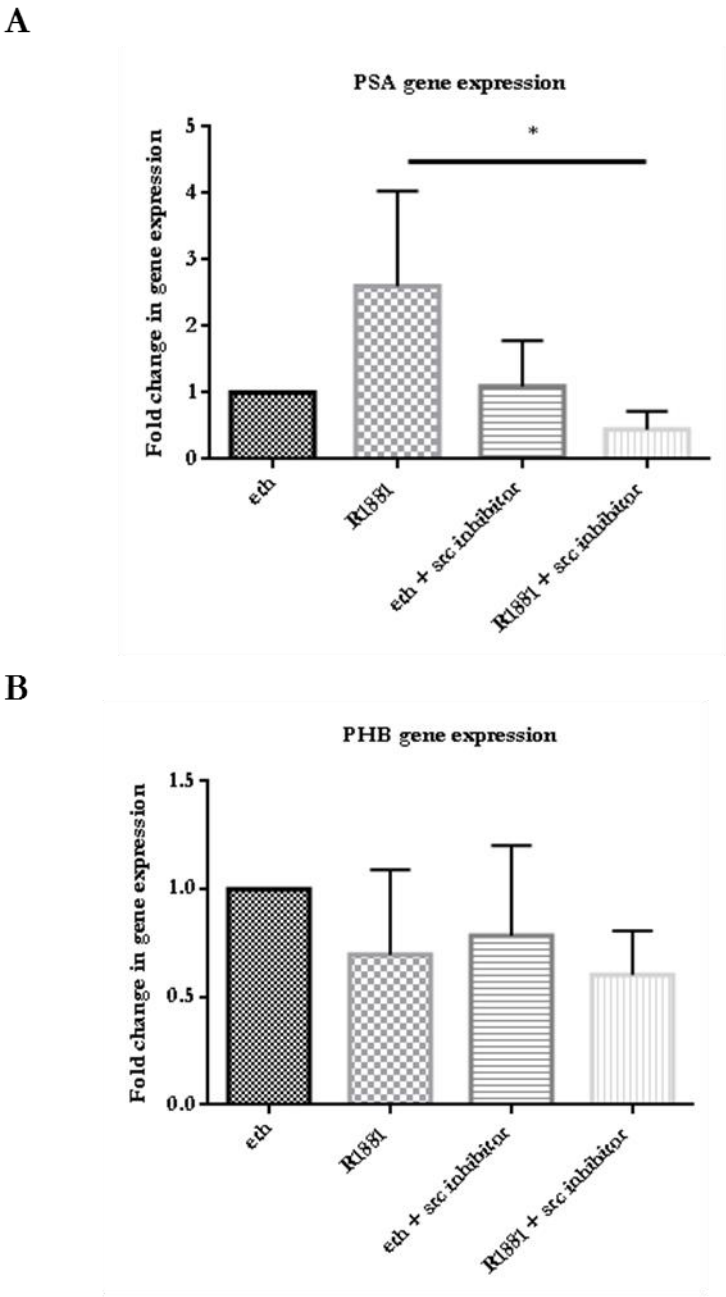

Figure 6.3. Gene expression of *PHB* and *PSA* in the LNCaP cell line. **A**, SYBR® Green Q-PCR data showing *PSA* expression +/-R1881 (10 nM, 4 hr) +/-Src inhibitor 1 (20 μM,4 hr). **B**, SYBR® Green Q-PCR data showing *PHB* expression +/-R1881 (10 nM, 4 hr) +/-Src inhibitor 1 (10 μM,4 hr) n=3, p <0.05*. A one-way ANOVA statistical test was used. Error bars represent standard error of mean.

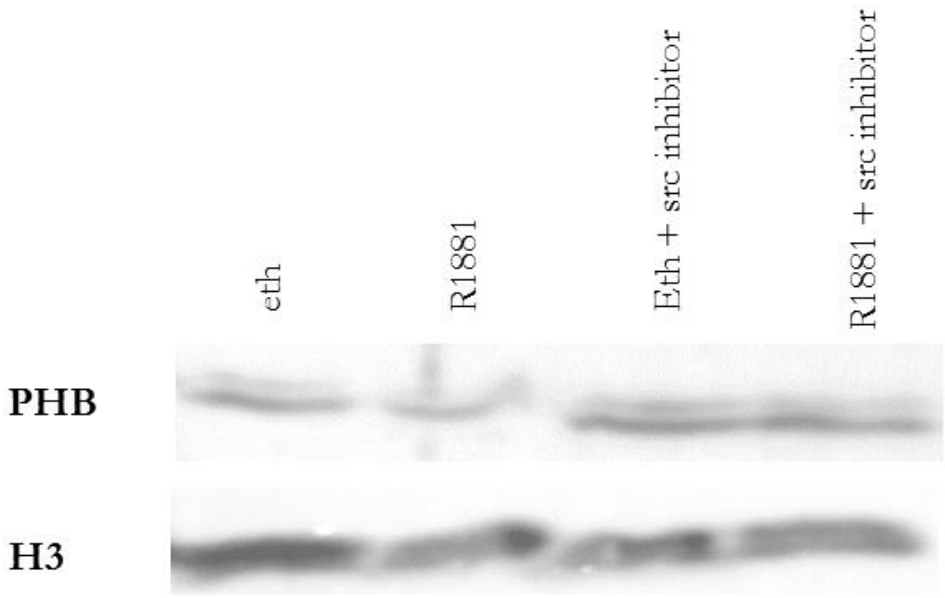

Figure 6.4. Chromatin isolation and western blot of PHB (+/-R1881 (10nM, 4h), (+/-Src-inhibitor-1 (20μM, 4h). PHB dissociates from the chromatin in the presence of R1881. As a loading control, histone H3 was used, n=1.

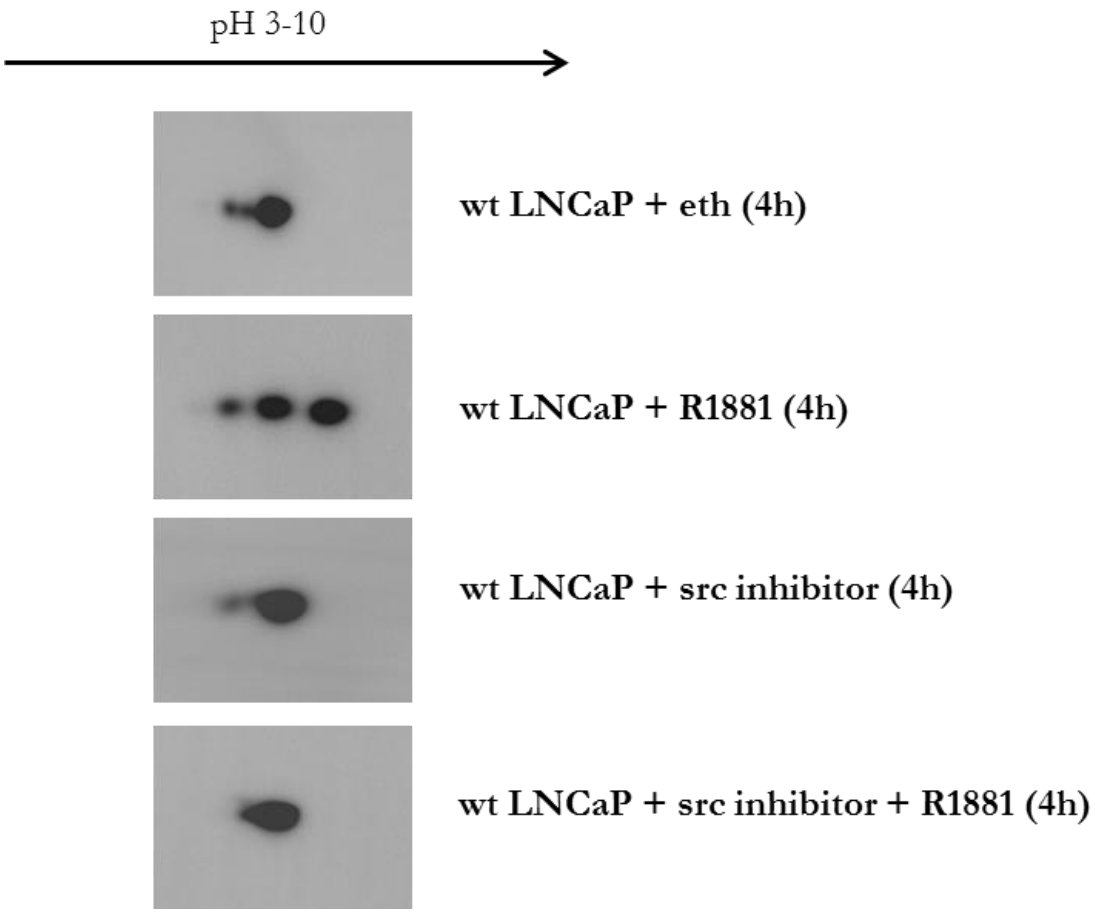

Figure 6.5. 2D western blot of PHB. LNCaP cells were hormonally starved for 72 hours and treated with (+-R1881(10nM), +/-Src-inhibitor-1(20μM), 4h) n=1.

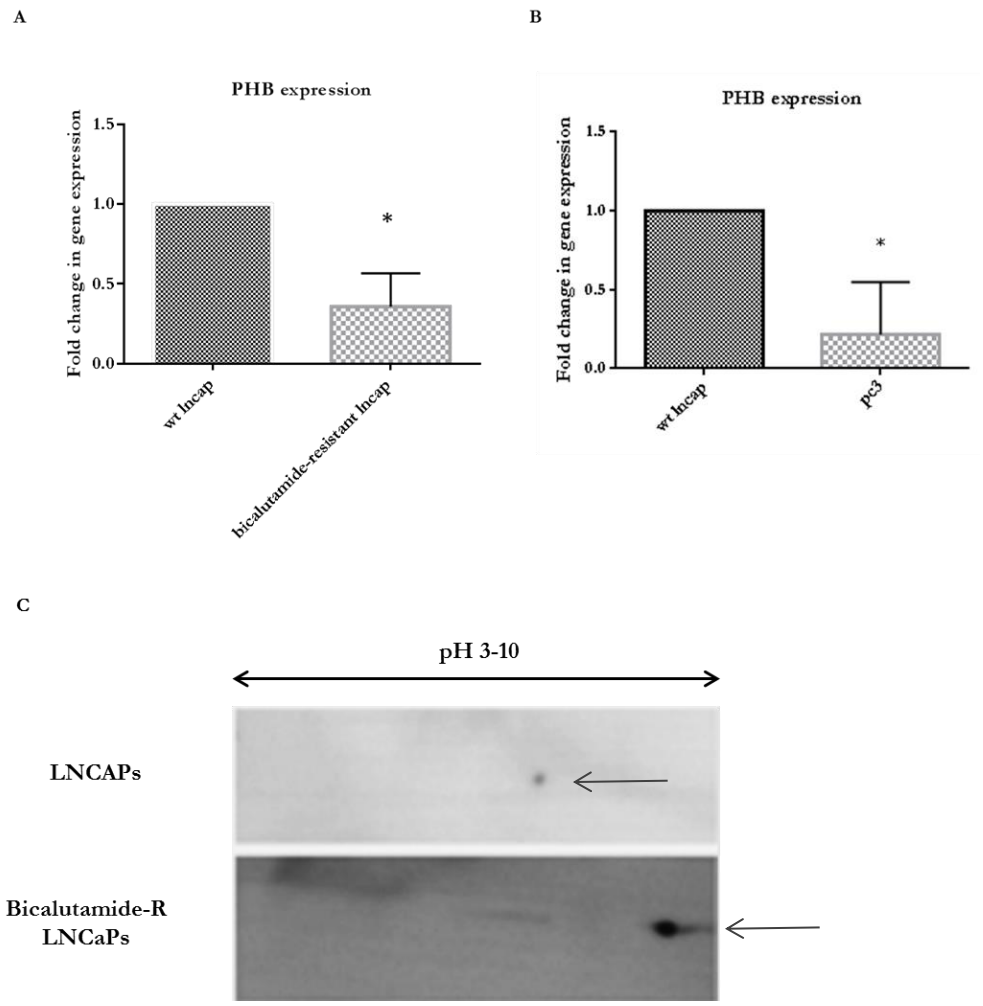

Figure 6.6. SYBR® Green Q-PCR analysis of *PHB* in Bicalutamide-R LNCaP cells and PC3 cells. **A**, *PHB* gene expression in Bicalutamide-R LNCaP cells, n=3 *p<0.05. **B**, *PHB* gene expression in PC3 cells, n=3 *p<0.05. **C**, 2D western blot analysis of the PHB protein in the wt LNCaP cell line and the Bicalutamide-R LNCaP cell line. n=1.

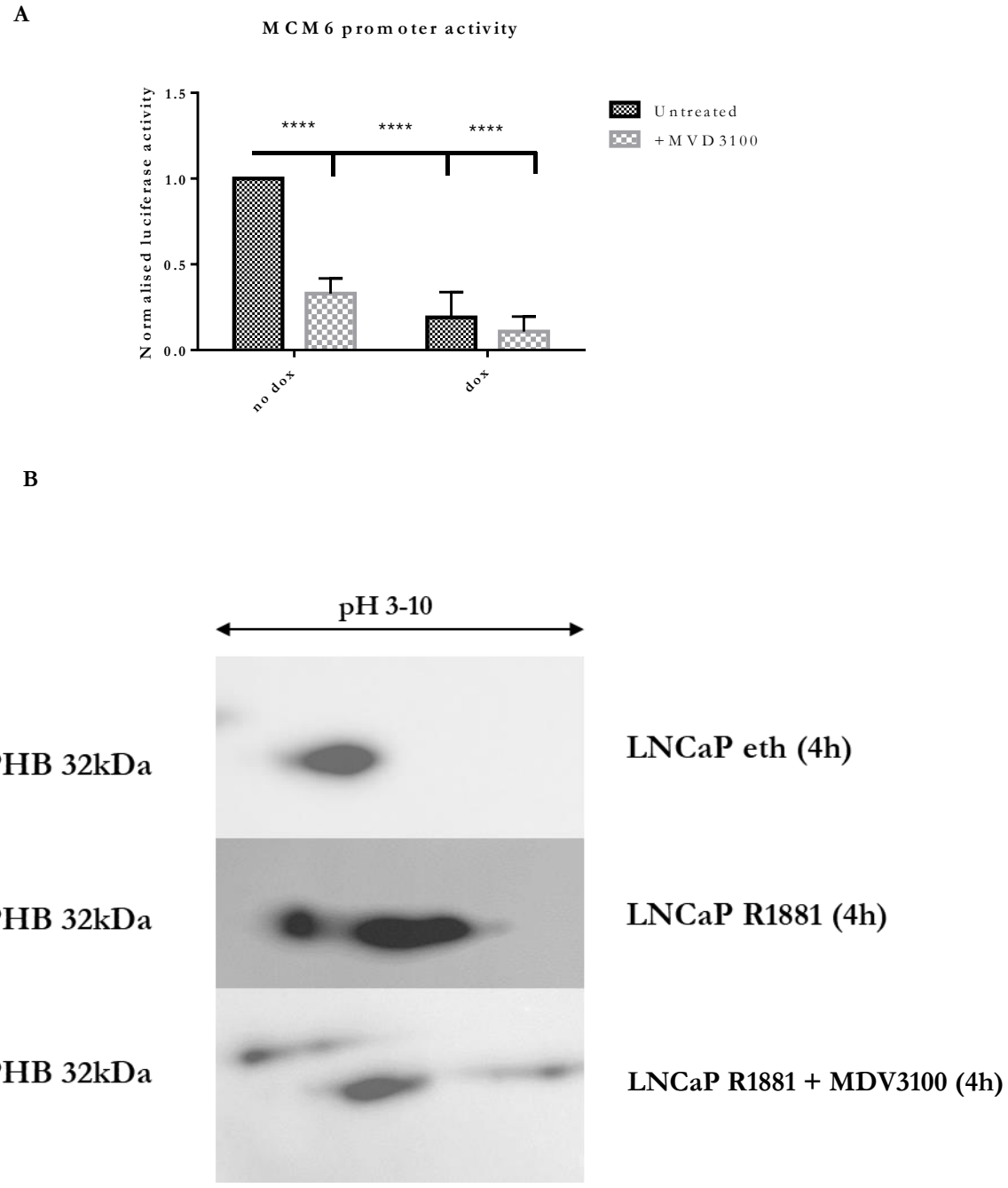

Figure 6.7. *MCM6* promoter activity in the presence of PHB over-expression and enzalutamide (MDV3100). 2D western blot of PHB +/-R1881 (10nM), +/-MDV3100 (10μM), 4hr. **A**, Reduction of *MCM6* promoter activity is seen in cells treated with doxycycline and MDV3100, n=3, $p<0.001$****. **B**, MDV3100 inhibits the dephosphorylation of PHB isotypes.

6.4 Discussion

Treating metastatic, castration resistant PC with androgen deprivation therapy (ADT) remains controversial, as relapse often ensues. It is the first line therapy for patients with symptomatic metastatic PC, however it is also used as a neoadjuvant to radiotherapy and clinically localised PC (154). Unfortunately, with the use of ADT overtime, it is inevitable that a majority of patients relapse due to the propagation of androgen independent PC (154). Patients receiving androgen deprivation therapy alongside chemotherapy with docetaxel and prednisone have a medium survival rate of 18.9 months. Worryingly, progression of the disease following a docetaxel containing treatment plan leads to a drop in medium survival to 15.1 months (155). This highlights a need for treatment that inhibits the progression of the cancer to an androgen independent state. Firstly, PHB's expression in aggressive chemotherapy resistant and androgen independent cell line was shown to be significantly down-regulated. A potential mechanism for patient relapse could be due to the down-regulation of PHB, allowing deregulated AR activity. Assessing the effects of a clinically used anti-androgen treatment; enzalutamide in the presence of PHB showed an increased efficacy, especially in reducing the activity of the MCM6 gene, a key instigator in DNA replication. Enzalutamide (MDV3100) is approved for patients with metastatic castration resistant. One of its mechanisms of actions is inhibiting the translocation of the AR to the nucleus. Remarkably, PHB's role in increasing the efficacy of clinically used treatment has already been seen in breast cancer, whereby the growth suppression of breast cancer cells is PHB mediated, through the recruitment of Brg1/Brm remodelling proteins (59). Thus, targeting the down-regulation of PHB could heighten the efficacy of anti-androgen therapy, currently used for PC treatment.

As the change in PHB localisation was rapid (4 hr), investigations into kinase pathways were carried out. Previous data showed phosphorylation changes on PHB, identified by co-immunoprecipitation and 2D western blot, therefore Kinexus array analysis was carried out. Although the Kinexus array is not exhaustive, there was a good indication that the Src pathway was activated by androgen treatment. Data presented here indicate that activation of the AR lead to the rapid phosphorylation of Src on tyrosine^{418}. Tyrosine 418 is located within the catalytic domain of Src and is one of the auto-phosphorylation sites. Phosphorylation of Tyrosine 418 is essential for full catalytic activity of Src (156).

Inhibiting the Src-pathway led to an increase in PHB bound chromatin, perhaps through an inhibition of the AR signalling pathway. This could potentially allow PHB to recruit chromatin-modelling proteins such as HDACs to repress the transcription of genes associated with the cell cycle, e.g E2Fs and MCMs (as previously described). Moreover, inhibiting the Src pathway prevented the PHB protein shifting towards pH 10 in response to androgen, thus preventing PHB's likely dephosphorylation event.

It has been well established that c-Src drives the development of castration-resistant PC and bone metastasis (157). The family of Src kinases comprises of 9 structurally similar non-receptor protein tyrosine kinases. The amino acid composition of Src kinases are made of four distinct peptide domains, known as Src homology domains (SH), alongside a regulatory sequence. SH4 regulates membrane attachment, kinase activity and intracellular stability (157) Whereas SH2 and SH3 domains allow the interaction of Src with signalling proteins. Negative regulation of Src is mediated through the phosphorylation of Y530 that resides in the catalytic domain (SH1) that is joined to the carboxyl terminal. Upon phosphorylation, Src undergoes a 'closed' molecular conformation with low enzyme activity (157). Under the closed conformation, Y530 interacts with SH2. Disruption between these interactions allows the activation of Src and undergoes an open conformation. The open conformation is aided by SH2 having a higher affinity for other tyrosine phosphorylated proteins than Y530 (157). Consequently, the c-terminal phosphate becomes available for phosphatases that dephosphorylate Y530, stabilising Src's active form. Src can also be activated by cytoplasmic proteins such as focal adhesion kinase (FAK) (158). In the active form, Src is able to bind to ATP and substrates to induce signal transduction and regulation of the cytoskeleton. Src kinase activity is increased in the majority of solid tumours including PC, and is often found to be over-activated in more malignant stages of cancer (157).

Normal prostate epithelium expresses six of the Src kinase family members (Src, Lyn, Fyn, Yes, Hck, Fgr). However, their expression increases during PC tumorigenesis. For example, Lyn (a family member of Src kinase) is expressed in 95% of primary PC, and worryingly in 100% of metastatic cases (159). Moreover, (Goldenberg *et al.,* 2004), showed that as the Gleason score increased in the primary tumours, the expression of Lyn also increased (159). Src, Lyn and Fyn all have been shown to participate to the development of PC in mouse models. Constitutively active Src is correlated with increasing the chance of transforming the prostate epithelium, followed by

constitutively active Fyn and Lyn. Evidence supports that not only does Src kinases promote tumourigenesis, they also partake in increasing the proliferation and growth of cancer cells. Src kinase inhibitors such as Dasatinib can cause a 50% reduction in cell proliferation of both LNCaP and PC3MM2 cells (157). Moreover, another Src inhibitor known as Saracatinib also led to a 50% reduction in the proliferation of PC3 and DU145 cells (157). Although inhibitors of Src have a profound effect on the proliferation of PC cells, the cytotoxic effects are minimal.

Ligand activation of the AR causes the autophosphorylation of Src, however this autophosphorylation does not occur in LNCaPs grown in serum starved media (160). Progression of the cell cycle to the S phase was noted in cells with AR-induced Src activation. *In vivo* studies demonstrated that the synergic over-expression of both the AR and Src induced the transformation of prostate epithelium to invasive adenocarcinoma. There is a positive feedback loop between the AR and Src, as Src phosphorylation induces the phosphorylation at tyrosine, serine and threonine residues (160) Phosphorylation of Src leading to the phosphorylation of AR can feed back to further phosphorylation of Src-eventually resulting in the down-regulation of PHB. Growth factors (IGF-1 and EGR), interleukins (Il-6 and IL-8) and neuropeptides (bombesin) have been associated with ligand-independent phosphorylation of the AR (160). Activation of all of these pathways lead to the activation of Src, highlighting the vast amount of signalling pathways that can activate Src, thus leading to the direct phosphorylation of the AR. Moreover, Src activation has also been shown to repress the interaction of co-repressors such as LCoR and the AR (160). This could also be the case with PHB, non-genomic activation of the AR leading to the phosphorylation of Src, thus inhibiting the interaction of PHB and the AR, facilitating AR function and cell growth.

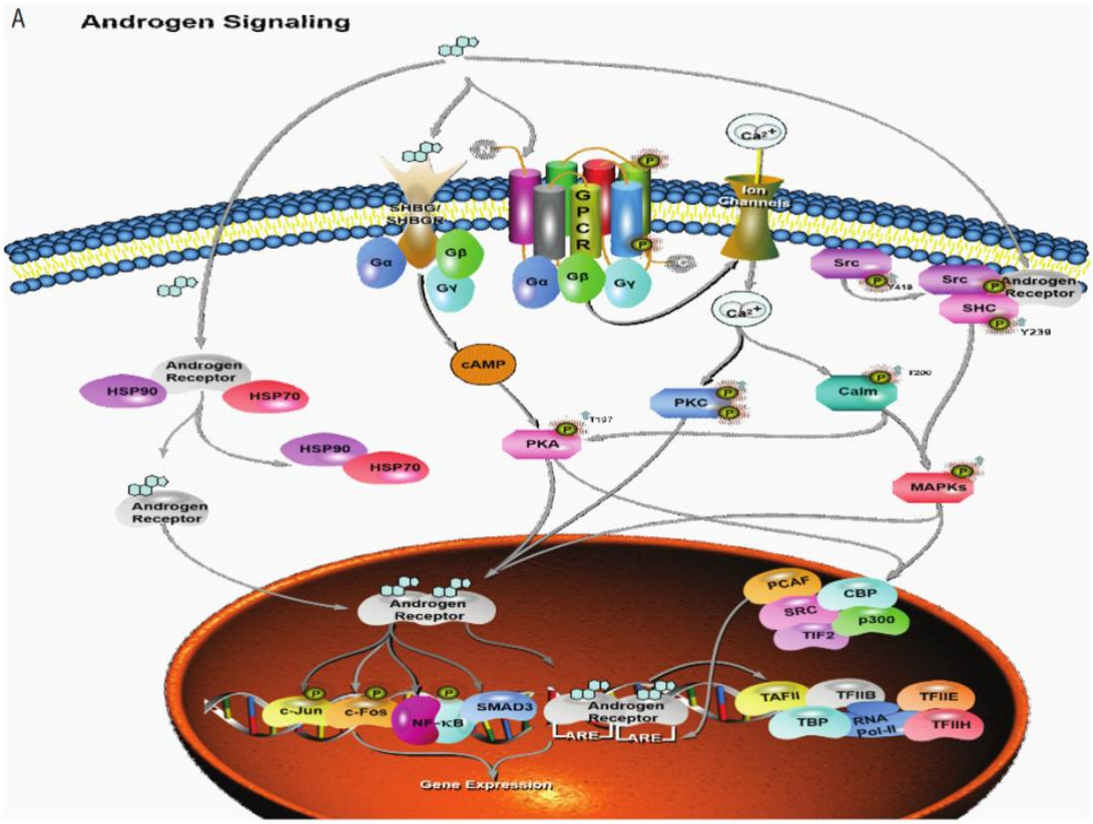

Figure 6.8. Image provided by Dr Alwyn Dart. Androgen induced phosphorylation of cellular signalling pathways. Src appears upstream of PKC, MAPKs and AR activation (137).

6.5 Conclusion

Since the discovery that PHB is likely to be dephosphorylated in response to AR stimulation in a short amount of time (4 hr), signalling pathways were investigated. Interestingly, Src was the top most phosphorylated protein in response to androgen. There is a large amount of evidence to indicate that Src can activate the AR in the absence of ligand, therefore targeting the Src pathway was carried out. Inhibition of the Src pathway led to an array of effects, and activation of the AR led to Src phosphorylation. Firstly, androgen responsive genes were significantly down-regulated such as *PSA* whereas *PHB* was increased. Moreover, inhibition of the Src pathway led to more PHB bound chromatin, potentially because inhibition of the Src pathway prevented the likely dephosphorylation on PHB that in turn could prevent PHB dissociating from the chromatin and E2F1 in response to androgen. Thus a preliminary mechanism was propagated, phosphorylation of Src, leads to the activation of the AR leading to the dissociation of PHB from the chromatin due to a potential dephosphorylation event (figure 6.9). Finally, the role PHB had in increasing the efficacy of anti-androgen therapy was assessed. Interestingly, the repressive function of PHB on the MCM promoter was heightened in the presence of an anti-androgen treatment; enzalutamide. Therefore, potentially during the development of androgen independent/castration resistant PC, aberrant Src signalling leads to independent AR activation leading to the dephosphorylation of PHB causing PHB to dissociate from the chromatin.

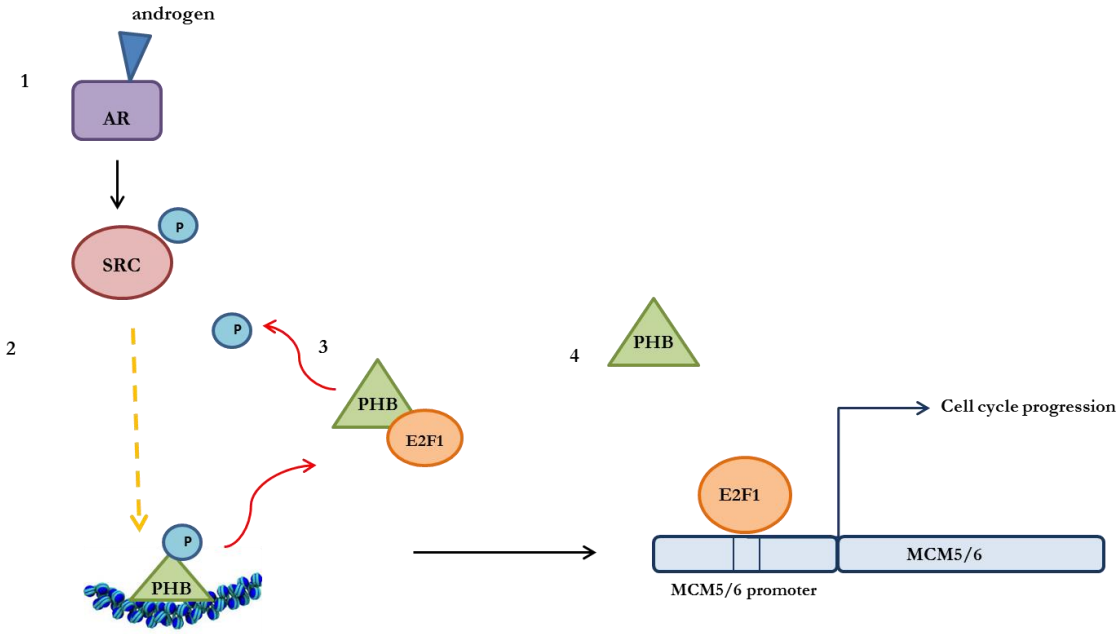

Figure 6.9. Preliminary mechanism involving Src, the AR and PHB. **1,** ligand binding of the AR leads to the phosphorylation of Src. **2,** phosphorylation of Src leads to an unknown mechanism leading to PHB dissociating from the chromatin, potentially through a dephosphorylation event. **3,** PHB dissociates from the chromatin and E2F1 due to AR signalling. **4,** E2F1 is free from PHB to bind to E2F binding site within the promoter region of MCM5/6. This leads to transcription of genes associated with cell cycle progression (E2Fs, CDKs, Cyclins, MCMs).

6.6 Key points

- Activation of the AR in LNCaP cells leads to the phosphorylation of Src at tyrosine 418.
- Inhibiting the Src pathway reduces AR activity as measured by a reduced *PSA* expression.
- Inhibiting the Src pathway stops the dissociation of PHB from the chromatin.
- The inhibition of the Src pathway also prevents the likely dephosphorylation PHB.
- *PHB* gene expression is significantly down-regulated in Bicalutamide-resistant LNCaP cells and also androgen independent cells; PC3s.
- The efficacy of PHB repressing the MCM6 promoter is increased in the presence of an anti-androgen treatment; Enzalutamide.
- Enzalutamide prevents the likely dephosphorylation on PHB-demonstrating the dephosphorylation of PHB is AR regulated-potentially through Src signalling.
- A preliminary mechanism: ligand binding of the AR leads to Src phosphorylation, activating cascades that led to the dissociation of PHB from the chromatin potentially through a dephosphorylation event.

Chapter VII. PHB inhibits the migration of both androgen dependent and androgen independent PC cells.

7 Chapter VII. PHB inhibits the migration of both androgen dependent and androgen independent PC cells.

7.1 Introduction

The androgen dependent subtype of PC, if diagnosed at an early stage where the cancer is confined with the prostate gland, displays little or no metastasis and is 100% treatable (161). However, as the cancer progresses to a more malignant state through adapting to a low androgen environment, the transition of the cancer to an 'androgen independent' state can occur. Once the cancer has progressed to an androgen independent state (AI), the survival rate is less than 30% for 5 years.

Although recently, there has been a steady decline in the cases of newly diagnosed metastatic PC, the risk of clinically localised PC transitioning to extra-prostatic disease is still high (30-60%) (162). If left untreated, metastatic PC is more than likely to become resistant to therapy.

Cells migrating to the pelvic lymph nodes is one of the initial stages of PC metastasis, where the bloodstream spreads the cells to distant organs such as the bones (37). Worryingly, PC cells have a strong affinity for the bone environment as the majority of patients diagnosed with advanced stage PC have histological skeletal involvement. The prognosis given from the initial identification of bone metastases and death has a median value of 3-5 years (37). Complications that ensue with PC bone metastasis are bone pain, resultant from the stimulation of periosteum pain receptors and spinal cord compression.

The mechanism of PC cells migrating and invading out of the prostate gland is poorly understood. Analysing PHB's role in PC metastasis could allude to a novel mechanism. Previous data showed that *PHB* knockout increased PC xenograft growth in mice, and also increased metastasis of LNCaP cells, a cell line that rarely metastasises (supplemental figure 3). As data presented in chapter III, IV and V indicate PHB has a prominent role in inhibiting the proliferation of androgen dependent cells and also halting the cell cycle, mediated by E2F-repression. Therefore, it was investigated if PHB down-regulation was associated with the migration of PC, as the cell cycle and cell motility are related mechanisms. Thus, over-expression of PHB in PC cells was carried

out in several functional assays to depict its role in migration, invasion and adhesion assays in both androgen dependent and androgen independent PC cell lines.

7.2 Methods

- Analysis of data retrieved from RNA-sequencing (refer to chapter 2.10).
- Scratch assay (refer to chapter 2.9.2). In the case of PC3 cells, after the scratch formation, the well plate was placed into an incubation chamber onto an Evos FL auto machine (life technologies). Each well had three beacons assigned, and each condition was carried out in triplicate. Cells were incubated at 5 % CO_2 at 37°C. At the end of the experiment, the percentage of wound closure was analysed as stated in chapter 2.4.2.
- Transwell assay (refer to chapter 2.9.3).
- SYBR®Green Q-PCR (refer to chapter 2.8.3).
- Geodatabase analysis (data available from GSE6919, GDS3973 geodatasets). Data was taken from freely available Geodatasets and was analysed via GraphPad Prism 6.
- Adhesion assay (refer to chapter 2.9.5).

7.3 Results

7.3.1 Geodatabase data of PHB

Supplemental figure 4 entailed *PHB* knock-down in LNCaP xenografts injected 8-week male BALB/c strain nude mice. *PHB* knockdown led to growth in xenografts of PC cells in mice (data provided by Dr D Dart), therefore PHB's status within malignant metastatic cancer was assessed via a geodatabase (GSE6919) (163, 164). This study involved a comprehensive gene expression analysis of 152 human samples. These samples were divided into normal tissue, PC tissue, normal adjacent tissue and metastatic tissue. Here analysis in this dataset was carried out using the Affymetrix U95a, U95b and U95c chip sets. Firstly, figure 7.1A illustrates a graph representing the gene expression levels of *PHB* in normal and tumour tissue. There was a significant decrease in *PHB* expression in tumour tissue when compared to normal tissue. This highlights PHB is down-regulated in tumour tissue and in advanced stages of PC.

The groups were further subdivided into normal adjacent tissue and metastatic tissue derived from patients. Figure 7.1B represents the data analysis of the four groups. A Man U Whitney test was carried out and a significant decrease in *PHB* expression was seen in metastatic tissue. This highlights that potentially *PHB's* loss is also linked to the migration and invasion capacity of PC cells. Interestingly, figure 7.1C (GDS1439) depicts the significant down-regulation of PHB as the PC transitions from a normal state to a malignant state, that agrees with the data presented in figure 7.1A-B. Moreover, Figure 7.1D illustrates that when two metastatic PC cell lines; DU145 and PC3 were compared with their docetaxel resistant counterpart a down-regulation of *PHB* was observed. This could link *PHB* down-regulation with chemotherapy resistant PC cases.

Moreover, analysis of 70 primary gastric tumors representing 3 subtypes (invasive, metabolic, and proliferative) from the Australian patient cohort (figure 7.2) also showed some differences in PHB expression. The invasive subtype displayed the lowest expression of PHB, whereas the proliferative subtype showed the highest. This may link to there being higher levels of PHB in the earlier stages of gastric cancer that then diminishes as the cancer progresses to an invasive type.

7.3.2 Metacore analysis describes Wnt-signalling as a top network affected by PHB over-expression

The analysis carried out by the bioanalysis platform, Metacore is described in chapter IV. The top network that was affected by PHB expression was the Wnt-signal transduction pathway (figure 7.3A). This agrees with figure 7.3B-C that depicts PHB over-expression down-regulating key non-canonical Wnt genes (*Wnt10B* and *Wnt7B*). Moreover, expanding into the Wnt-signalling network, the pathway is highlighted in red showing that this signalling pathway is being suppressed. Consequently, there is an inhibition of an accumulation of the transcriptional factor; β-catenin shown in figure 7.4. This is relevant as β-catenin has been documented to activate the AR in the absence of androgen (165).

7.3.3 RNA-seq identified genes involved in migration are down-regulated with PHB over-expression

As Metacore analysis highlighted that the Wnt-signalling pathway was the top most affected pathway in response to PHB over-expression, data mining into the RNA-seq transcript list was carried out. This identified that members of the Wnt family were down-regulated in response to PHB over-expression. Interestingly, Wnt10B and Wnt7B were both down-regulated with PHB over-expression with a fold change greater than -2 (figure 7.3B). To validate these genes, a SYBR® Green Q-PCR was carried out. LNCaP/TR2/PHB cells were treated (+/-dox) for 16 hr prior to RNA extraction. The RNA was reverse transcribed and the gene expression of *Wnt10B* and *Wnt7B* were analysed against untreated cells. Both genes were significantly down-regulated by more than 2 fold with PHB over-expression (figure 7.3C).

7.3.4 Over-expression of PHB leads to decreased migration in an androgen dependent and androgen independent cell line

Two experiments were carried out to assess the role of PHB in migration of PC cells. Firstly, a scratch assay was carried out. The LNCaP/TR2/PHB cell line was left to seed in a 24 well plate until a confluent monolayer was formed. After the scratch formation (or wound), the migration across the wound was monitored. Figure 7.5A illustrates that at the 24 hr time point, cells with PHB over-expression had 40 % less of the wound closed when compared to control cells. At 48 hr when complete wound closure was seen, there was a significant decrease in the migration of cells with PHB

over-expression (approx. 50 % decrease). In synergy with this experiment, a transwell filter migration assay was carried out. The LNCaP/TR2/PHB cells (+/-dox 10 μM) were left to migrate for 24 hr. At the 24 hr time point, cells with PHB over-expression had a 50% decrease in migration when compared to control cells (p value < 0.05) (figure 7.5B). This has the same pattern as the scratch assay at the 24 hr time point. Moreover, the same experiments were carried out on the androgen independent cell line; PC3. 48 hours prior to the scratch formation, PC3s were transfected with either pSG5-empty or pSG5-PHB. The cells were then left on the evos FL auto machine for 24 h. At 24 hr PC3's with PHB over-expression had a significant decrease in migration (approx. 20%) (Figure 7.5C). Further, the transwell filter migration assay displayed a similar trend. In 4 hr, PC3's over-expressing PHB has a significant decrease in migrating cells when compared to the control cells (Figure 7.5D). Figure 7.5E-F confirms the over-expression of PHB in LNCaP/TR2/PHB cells treated with dox (10 μM) and PC3 cells transfected with pSG5-PHB at a protein level.

7.3.5 Over-expression of PHB leads to a decreased adhesion of cells

To assess the adhesion of cells to a basement membrane in the form of Matrigel™, an adhesion assay was carried out. LNCaP/TR2/PHB cells were treated with doxycycline (10 μM) 24 h prior to the assay. 45,000 cells were then seeded onto a Matrigel™, coated 96-well plate. The cells were left to adhere to the Matrigel™ at 37°C for 1 hour 15 minutes. Cells that had adhered to the Matrigel™ were counted in each field of view. There was a significantly large difference in adhesion in dox-treated cells and control cells. PHB over-expression led to a reduced amount of Matrigel™-adhered cells as shown in figure 7.7. Quantitative analysis highlighted that with PHB over-expression there was a 5.8 fold decrease in the adhesion of cells when compared to control cells as highlighted by figure 7.7. Interestingly, this data agrees with the Metacore analysis (figure 7.3). Cadherin-mediated adhesion, integrin-mediated cell matrix adhesion and integrin priming were all depicted as networks associated with PHB over-expression. Thus highlighting PHB does play a role in the adhesive and motility behaviour of androgen dependent cells.

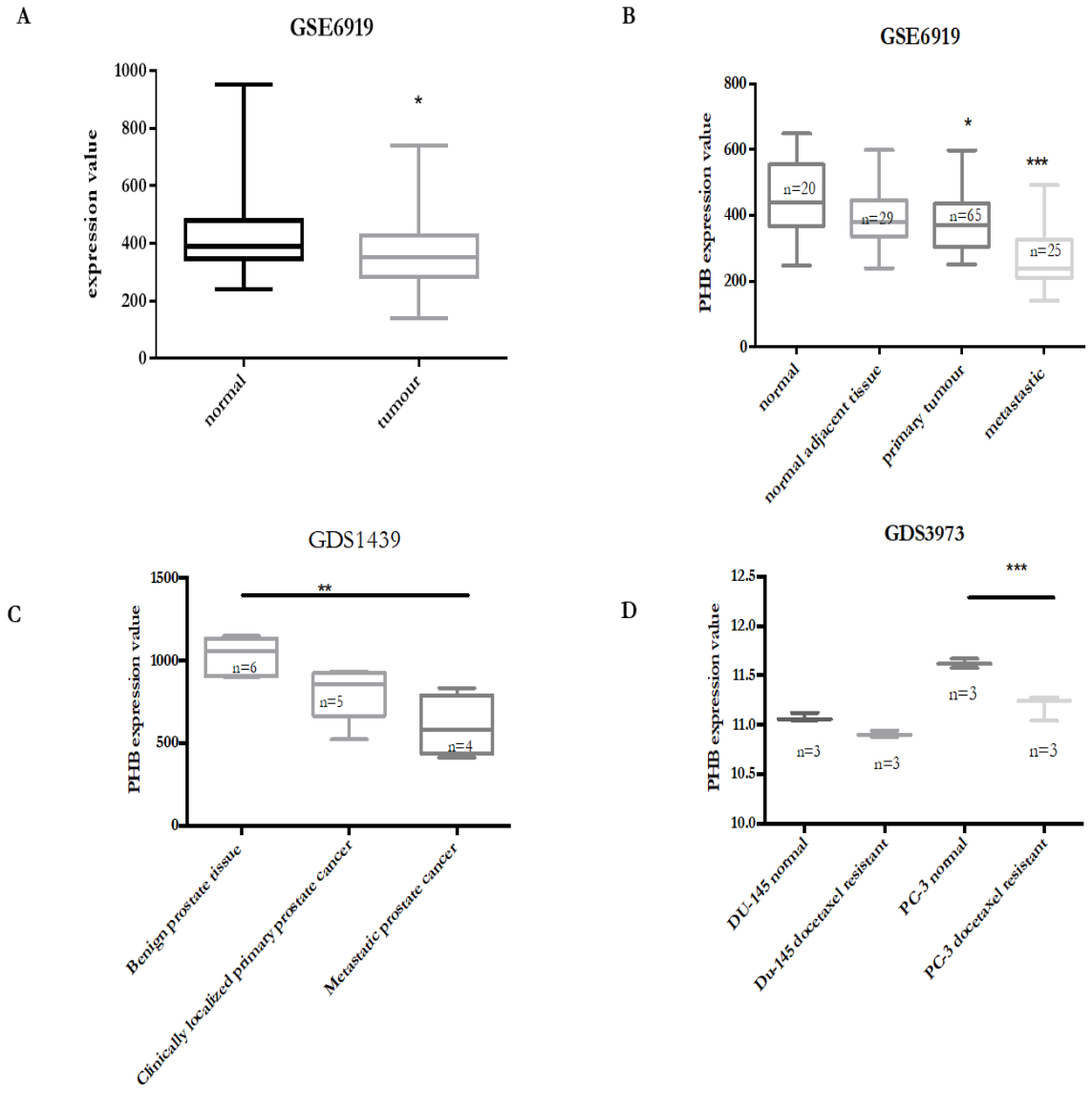

Figure 7.1. Geodataset analysis (GSE6919, GDS1439, GDS3973) of *PHB* gene expression. **A**, Expression analysis of *PHB* gene levels between normal tissue and PC tissue, n=171. **B**, expression analysis of PHB levels between normal tissue, PC tissue, primary tumour and metastatic tissue n=171. **C**, expression profiling of prostate cancer tumors that are benign, clinically localized and metastatic, n=19. **D**, Analysis of prostate cancer cell lines resistant to docetaxel chemotherapy, DU-145 resistant and PC-3 resistant, which were derived from cell lines DU-145 and PC-3, respectively, n=12. p value <0.05*, <0.01**, <0.001***. All geodatasets were analysed by a Kruskal–Wallis one-way statistical test.

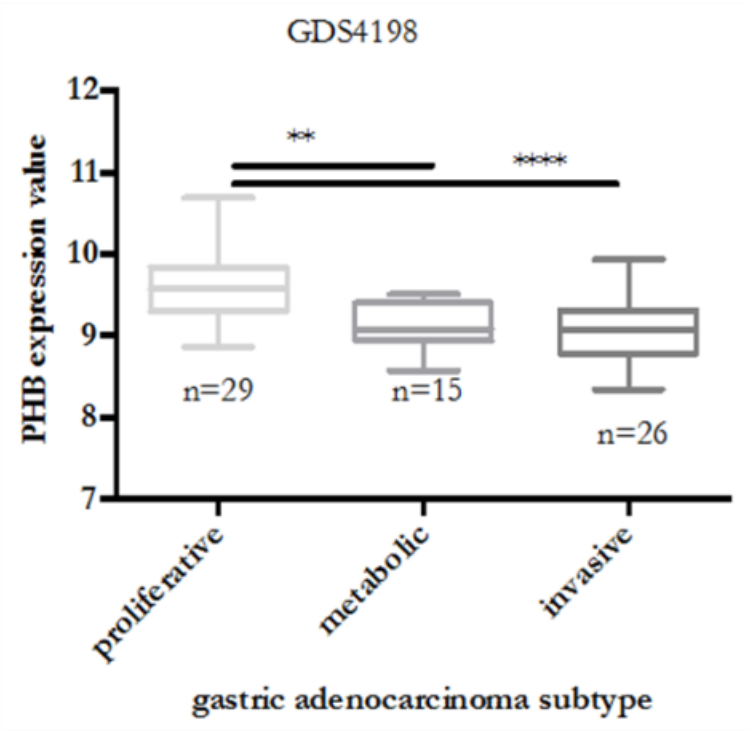

Figure 7.2. *PHB* gene expression in gastric cancer. GDS4198 geodataset displaying 70 primary gastric tumors representing 3 subtypes (invasive, metabolic, and proliferative) from the Australian patient cohort. p value <0.01**, <0.0001**** between proliferative and metabolic and proliferative and invasive.

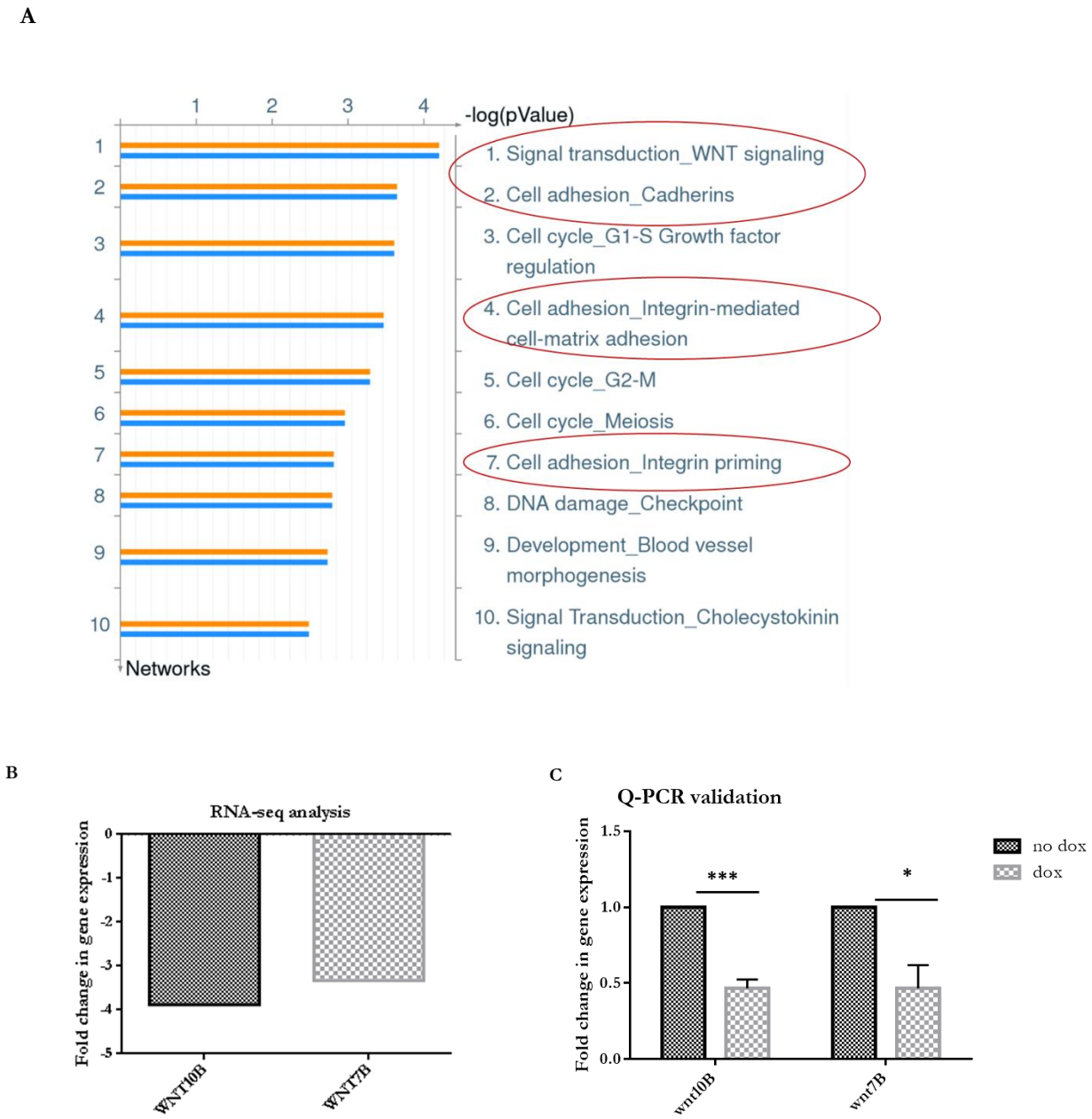

Figure 7.3. The Wnt signalling pathway is associated with PHB over-expression. **A**, Metacore analysis showing that the Wnt signalling pathway is the top most affected network with PHB over-expression. **B**, RNA-seq data illustrating members of the Wnt family; *Wnt10B* and *Wnt7B* are down-regulated with PHB over-expression. **C**, Q-PCR validation that *Wnt10B* and *Wnt7B* are significantly down-regulated with PHB over-expression, n=3 *p<0.05, ***p<0.001.

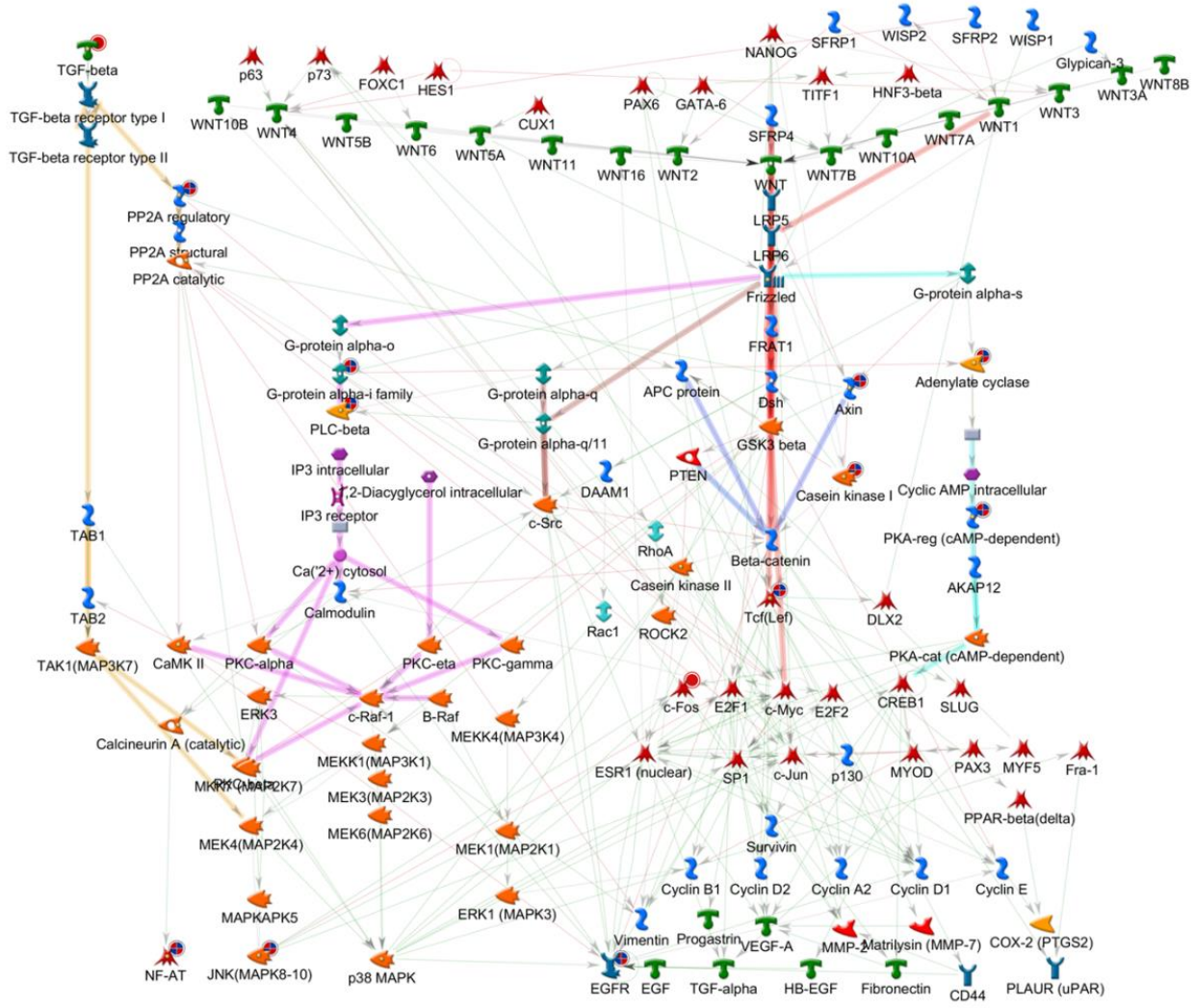

Figure 7.4. Metacore analysis of the top network associated with PHB over-expression. The Wnt signalling pathway shown in red is being inhibited.

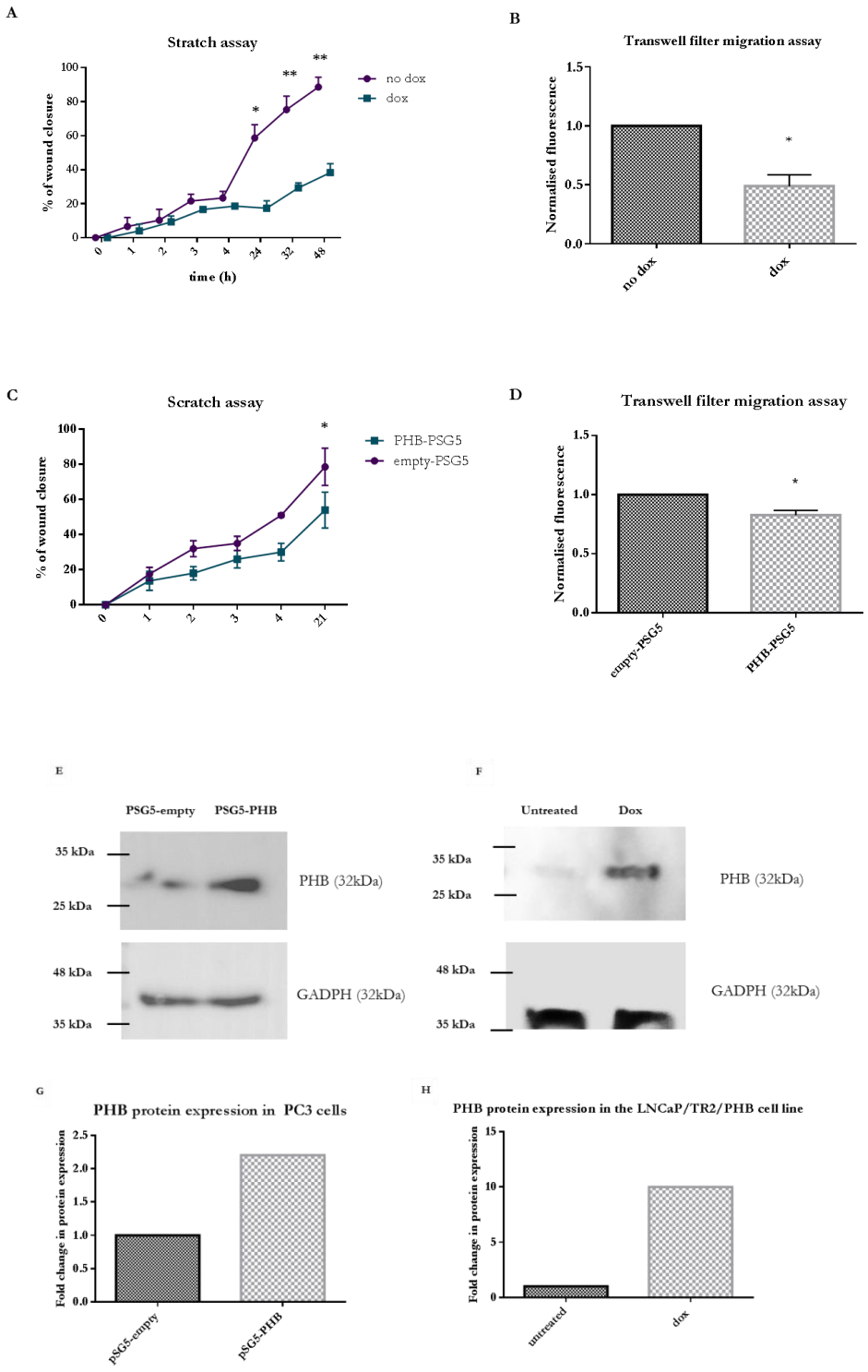

Figure 7.5. Migration assays for LNCaP and PC3 cells. **A**, scratch assay for LNCaP/TR2/PHB cells (+/- dox 16 hr) for 48 hr. **B**, Transwell filter migration assay for LNCaP/TR2/PHB cells (+/-dox 16 hr) for 24 hr. **C**, scratch assay for PC3 cells (+/-pSG5-PHB) for 21 hr. **D**, Transwell filter migration assay for PC3 cells (+/- pSG5-PHB) for 21 hr. **E**, western blot of PHB over-expression in cells treated with pSG5-PHB in PC3 cells. **F**, over-expression of PHB in LNCaP/TR2/PHB cells treated with dox (10 μM). GAPDH was used as a loading control. **G**+ **H** densitometry values for E + F. n=3, $p<0.05$*, $p<0.01$**.

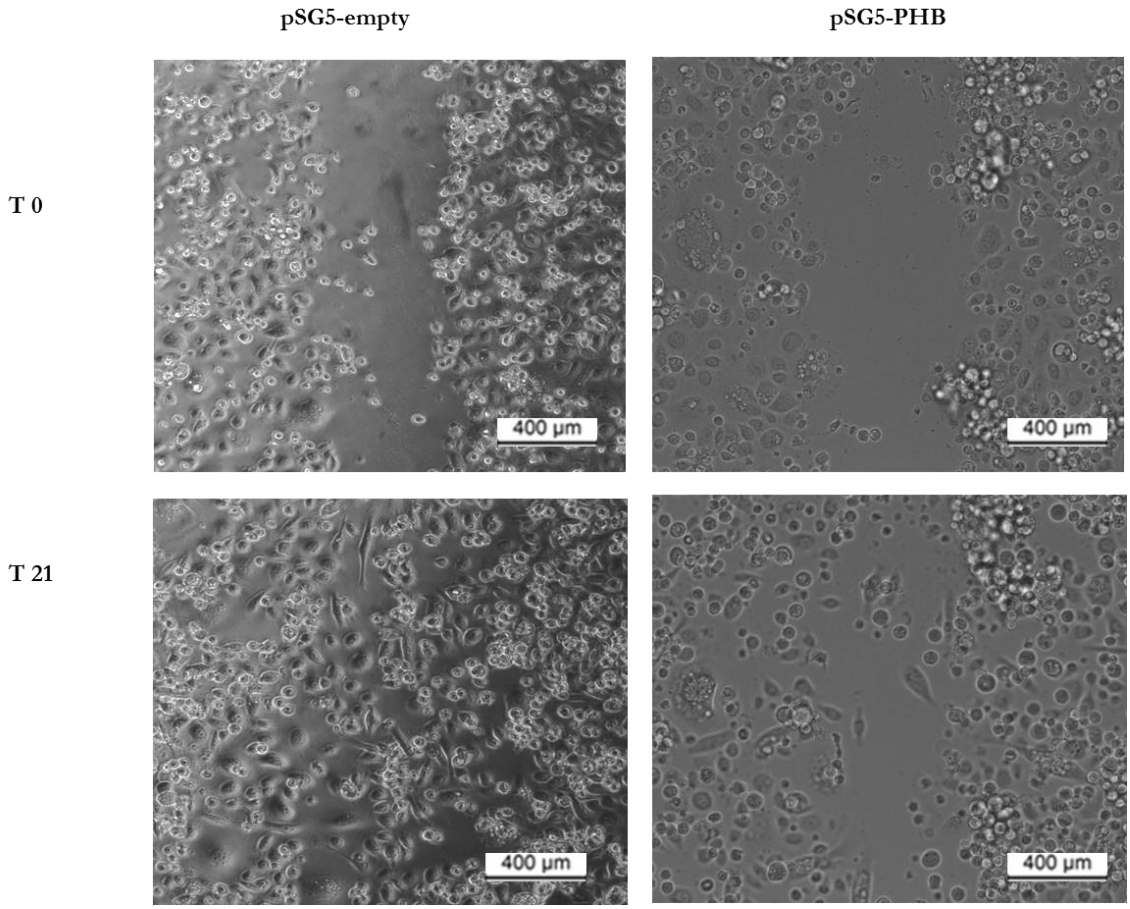

Figure 7.6. Scratch assay showing wound closure of PC3 cells after scratch was made +/- pSG5-PHB. At T0 (time 0) cells were imaged after wound was made. At T21 (time 21) wound closure was seen. Images are representative of n=3.

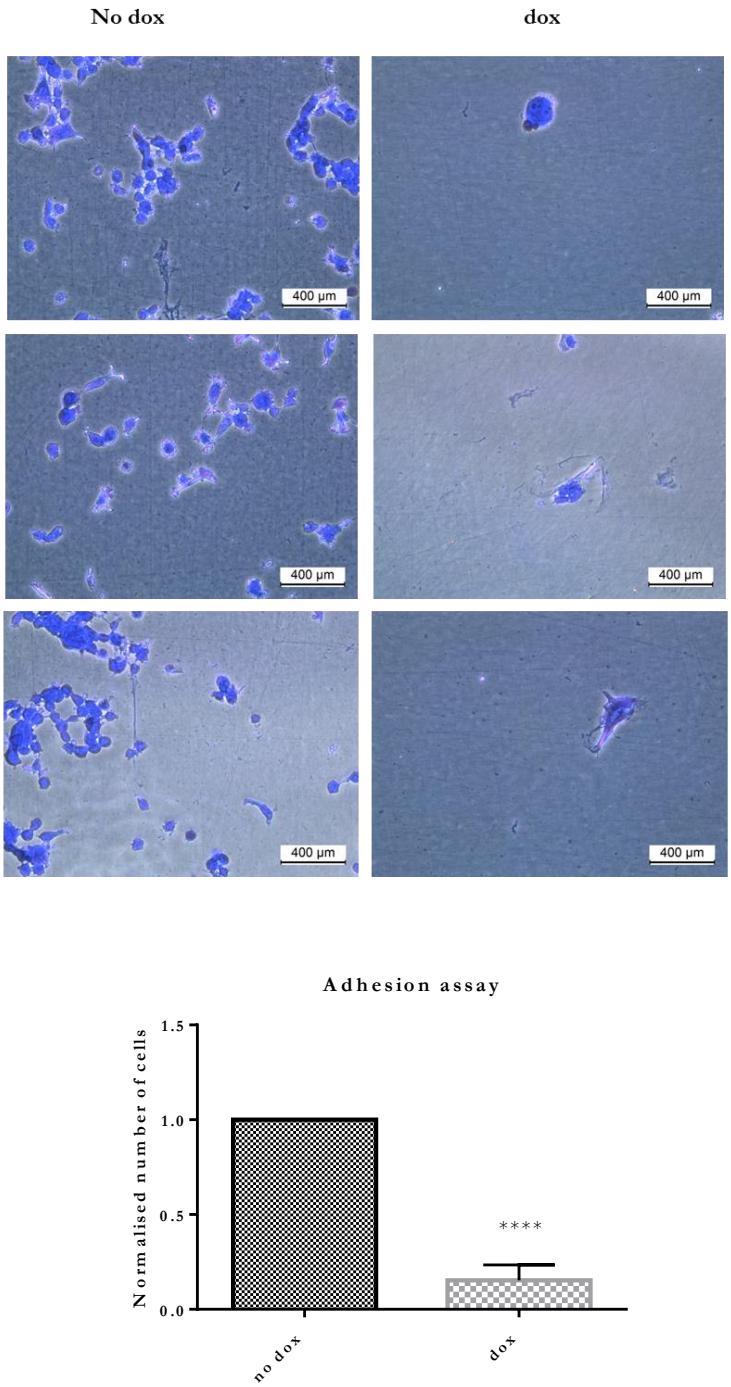

Figure 7.7. Adhesion assay for LNCaP/TR2/PHB cells. Cells were stained with crystal violet after adhering to a Matrigel™ basement membrane. p<0.0001****. Images are representative of n=3. Error bars represent SEM.

7.4 Discussion

The high rate of mortality and morbidity caused by PC is due to metastasis of the primary tumour (166). Information on how PC metastasises from the primary tumour to sites such as the bone is lacking. The course of PC migration from the primary tumour entails several stages. Firstly, tumour cells acquire the ability to invade the surrounding tissues by passing through the basement membrane and extracellular matrix (167). This is where the cells invade the lymphatic or circulatory system. The tumour cells will eventually settle in a secondary site, proliferate and form a secondary tumour. Loss of cell to cell adhesion is essential for tumour cells to dissociate from the primary tumour and begin migrating but ability to adhere to distant organs is essential for successful metastasis, therefore there is a fine balance involved in adhesion of cells (167). Changes in the cell matrix interactions allow the tumour cells to invade the surrounding stroma, this is known as cell invasion. The degradation of the basement membrane and extracellular matrix is necessary for invasion to secondary sites alongside up-regulation of proteins or signalling pathways associated with cell motility (167). Therefore the metastasis cascade is reliant on loss of cell adhesion, and the ability of the tumour cell to acquire a phenotype that is motile through changes of cell to matrix interactions.

Although PHB's role in repressing the cell cycle has been hypothesised as being E2F-mediated (refer to chapter V), PHB's role in the migration of PC cells has yet to be identified. It was interesting to note, that analysis of Geodatasets showed *PHB*'s down-regulation at a gene level as prostate cancer advances to a metastatic state. This highlighted PHB's role in suppressing migration from the primary tumour. As PC3's display more aggressive characteristics of PC, they are more malignant and metastatic, thus potentially accounting for PHB's ability to only inhibit the migration by 20 %. According to chapter V, in PC3 cells, PHB already has been post-translationally modified (a likely dephosphorylation event) thus already hold the mechanism in place allowing the down-regulation of PHB. Therefore, trying to counteract this mechanism by inducing PHB over-expression may be difficult.

Analysing the RNA-sequencing, data revealed that genes involved in migration such as *wnt* genes were down-regulated with PHB over-expression. Moreover, Metacore analysis showed that integrin-mediated cell adhesion was affected by PHB over-expression. This data was confirmed by carrying out functional assays. It appeared that PHB over-expression plays a key role in suppressing the migration of both androgen dependent and androgen independent cell lines.

However, although there is documented evidence to suggest there is cross-over between components that regulate the cell cycle and cell migration, PHB could also be suppressing the migration of PC cells through down-regulation of genes involved in cell migration. Such genes include *Wnt7B* and *Wnt10b* identified by RNA-seq. Moreover, Wnt-signalling was identified as the top most affected network by PHB over-expression.

Interestingly, Wnt signalling plays a role both in developmental and oncogenic processes. Binding of Wnt proteins to the frizzled receptor causes the activation of either the canonical or non-canonical pathway (168). The canonical pathway causes the down-stream transcription of Wnt-associated genes by preventing the phosphorylation-mediated degradation of β-catenin by a destruction complex. In the canonical pathway β-catenin acts as a co-activator for transcriptional factors TCF/LEF (168). Whereas activation of the non-canonical pathway leads to the activation of intracellular signalling pathways such as c-*Jun*-NH_2 kinase (JNK), protein kinase C (PKC) and Ca^{2+} dependent protein kinase II (CaMKII). The accumulation of β-catenin within the nucleus, caused by the activation of the canonical pathway has been identified in advanced PC (169). Metastatic PC cells found in bone showed homogenous expression of β-catenin in 77% of patients (169). Moreover, β-catenin has been shown to activate the AR in the presence of androgens, leading to the heightened transcription of androgen regulated genes. Transcriptional factors AR and TCF/LEF both compete for β-catenin. Both pathways once activated, promote cell growth (168).

Wnt signalling has been documented to play a role in the initiation of castration resistant PC (CRPC)(168). Aberrant Wnt-signalling allows the progression and survival of PC cells in an androgen deprived environment. Thus Wnt-signalling could be a key pathway contributing to relapse to anti-androgen therapy. Particularly as β-catenin, a downstream target of Wnt signalling, increases AR-mediated transcriptional activity in

androgen deprived conditions (170). Moreover, the interaction of AR and Wnt signalling pathway is heightened in castration-resistant mice when compared to non-castrated mice (171). Moreover, sequencing of exomes revealed mutations in Wnt signalling components in castration resistant tumours when compared to castration sensitive tumours (172). Wnt signalling is involved in castration resistant PC, however the key components of the pathway are yet to be identified. However, Wnt7B has been shown to be androgen-regulated and remains at a high expression in CRPC cells (168). Wnt7B activates the non-canonical pathway leading to an increased PC growth and survival in an androgen deprived environment (168). Moreover, Wnt7B was identified to promote osteoblastic responses in the bone. Thus Wnt7B plays a vital role in the progression of castration-resistant PC to bone metastasis (168).

Interestingly, supplemental figure 5 demonstrates that both *Wnt7B* and *Wnt10B* have predicted binding sites of E2F within their promoter regions. This could explain how PHB is causing a decrease in migration. As documented in chapter V, PHB has a direct interaction with E2F1, preventing progression of the cell cycle. This could also be the case for how PHB prevents migration of PC cells. PHB could prevent E2F binding to the predicted E2F binding sites in the promoters of Wnt7B and Wnt10B, preventing down-stream transcription of the Wnt genes associated with migration. A preliminary mechanism is shown in figure 7.8.

Recently, it has been established that the cell cycle and migration of tumour cells are interlinked at a molecular level (173). For example, for cells to begin migrating, formation of actin arrays at the leading edge of the cell is needed, thus forming lamellipodia. Proteins that regulate the formation of lamellipodia include the Arp2/3 complex and the WAVE regulatory complex (173). Inhibiting the lamellipodia suppresses the proliferation of normal fibroblasts however it cannot arrest cancerous cell proliferation. Depletion of the Arp2/3 protein in normal fibroblasts causes an inhibition in cell migration. Moreover, they also cannot proliferate, unless loss of the p16INK4a/p14Arf tumour suppressor locus has also occurred. This locus is essential to initiate cell cycle arrest in response to cellular stress. Loss of Arp2/3, leading to inhibition of migration therefore acts as a stress signal causing cell cycle arrest through transcription of p16INK4a/p14Arf (173). Interestingly, linking loss of Arp2/3 with the cell cycle, a mechanism was suggested. Firstly, extracellular signals stimulate lamellipodial machinery through integrin-mediated activation of Rac1 (a small GTPase)

Activated Rac1 can then activate the cell cycle through activation of cyclin D1 (173). Therefore, mechanisms are in place that link the cell cycle and cell motility via the cross-talk of signalling pathways.

Moreover, another study carried out by Kagawa, *et al,*. 2013 (174), analysed the spatiotemporal properties of both cell cycle and cell motility simultaneously *in vivo*. The molecular components that regulate the cell cycle also play a vital role in cellular functions such as motility. Particularly ARHGAP11A, a potential E2F1 regulated gene that alters its expression through a cell cycle dependent manner. ARHGAP11A induced cell mobilisation through activation of Rac1 (174). Fuci-green cells expressing high levels of ARHGAP11A exhibited elongated shapes, consistent with previous work that elongated migration is mediated through Rac1 (174). This leads to the assumption that perhaps PHB inhibiting E2F1's function could inhibit the transcription of ARHGAP11A, leading to less cell motility. What is more, it was identified that key genes that regulate the cell cycle such as p27 and p21 also influence cell motility. p27 was shown to bind to RhoA whilst p21 was shown to bind to ROCK (174). Interestingly chapter IV depicted that both p21 and p27 were significantly up-regulated with PHB over-expression. Regulation of cell motility by Rho-family proteins has been extensively studied. Both ROCK mediated and Rho mediated signalling play a crucial role in cancer metastasis (174).

Adhesion of circulating PC cells to a microvascular endothelium and low adhesion to the primary tumour is critical for cancer metastasis. This highlights the importance of PHB over-expression significantly reducing the adhesion of androgen dependent cells. Metastasis from the primary tumours is one of the leading causes of cancer-related mortality (175). Two events coordinate PC cell dissemination into the blood stream to distant sites; anoikis and cell adhesion to vessel endothelium (175). For circulating tumour cells to survive within the blood stream, firm adhesion to the vessel endothelium is essential in an organ microenvironment. PC cells tend to adhere to vessel endothelia that express E-selectin. E-selectin ligands include PSGL-1, ESL-1 and other adhesive molecules such as α2-integrin and β1-integrin (175). Interestingly, Metacore analysis described integrin-mediated cell-matrix adhesion as one of the top networks associated with PHB over-expression. It could be that PHB is decreasing the cell adhesion of PC cells by down-regulating integrins that in turn could reduce the amount of cell-basement membrane adhesion.

Both cell proliferation and metastasis need continuous interaction with ECM (extracellular matix) components. ECM is mainly made of tissue components such as fibronectin, laminin and collagen IV. The adhesion signal of these molecules is essential for successful metastasis (175). This response is dependent on the activation of various signalling pathways such as Rho GTPases, JNK and FAK that are recruited to the ECM ligand/integrin binding site. In PC, integrins are expressed abnormally with aberrant ECM (138). Integrins particularly play a role in PC primary tumour growth and are heavily implicated in the ability of cancer cells to grow and survive in distant sites. PC3 and DU145, both metastatic PC cell lines, express integrin $\alpha_{IIb}\beta_3$, suggesting a role for integrin $\alpha_{IIb}\beta_3$, in PC metastasis. Studies showed a higher expression of integrin $\alpha_{IIb}\beta_3$ in DU145 cells derived from the prostate when compared to the subcutis-depicting integrin $\alpha_{IIb}\beta_3$ role in the progression of prostate adenocarcinoma (176). Bone metastasis is one of the lethal outcomes of PC. Targeting integrin αV with siRNA in xenografts inhibited the growth of PC tumours in the bone, whilst increasing the number of cancerous cells undergoing apoptosis. Further, the expression of functional integrin $\alpha_v\beta_3$ promoted tumour growth in the bone, whereas mutated forms did not (138). This data suggests integrin $\alpha_v\beta_3$ plays a key role in bone metastasis. It is clear that integrins subunits are involved in the progression of PC that then go on to activate down-stream signalling pathways. Although the exact molecular mechanism of how integrins contribute to the cancer progression still needs to be identified, it is interesting to note that PHB does play a role in decreasing the adhesion of PC cells, probably through the alteration of integrin expression.

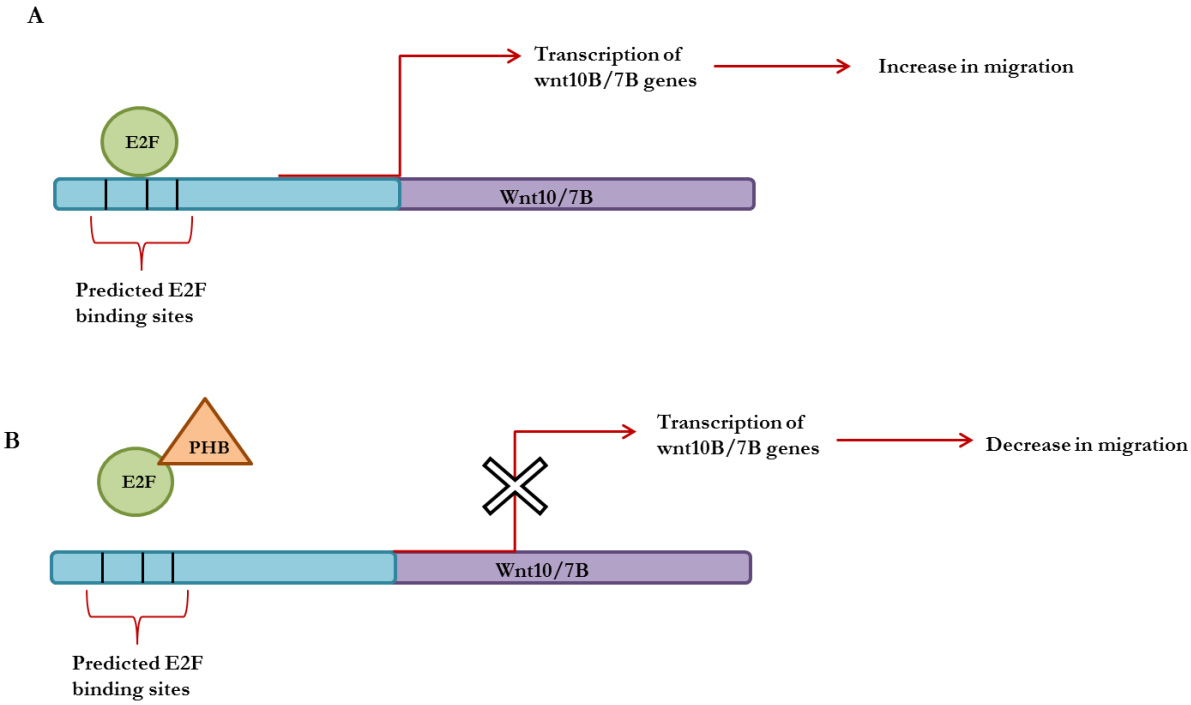

Figure 7.8. Preliminary mechanism to how PHB decreases migration of PC cells. **A**, in the absence of PHB, E2F binds to the predicted binding sites in the promoters of Wnt10B/Wnt7B causing downstream transcription of genes associated with migration. **B**, in the presence of PHB, E2F is inhibited from binding to the promoter region-migration is reduced.

7.5 Conclusion

PHB's role in the migration of PC cells is yet to be defined. However previous data reported that *PHB* knockdown increased PC xenograft growth in mice, and also increased metastasis of LNCaP cells. Data presented here highlights that *PHB* is down-regulated at a gene level as PC metastasises from the primary tumour. PHB over-expression was seen to significantly reduce the adhesion and migration of PC cells, both functions essential for local and distant migration of tumour cells. Interestingly, Wnt genes; *Wnt10B* and *Wnt7B* were significantly down-regulated with PHB over-expression. Wnt genes are heavily involved in the progression and migration of PC cells. *Wnt7B* is androgen regulated and is highly expressed in castration-resistant PC cells. Thus PHB inhibiting Wnt7B could provide a therapeutic option for castration resistant PC. Finally, a preliminary mechanism involving PHB, E2F, Wnt10B/Wnt7B and migration is described in figure 7.8.

7.6 Key points

- Geodatasets show that PHB is lost at a gene level as PC progresses to a malignant aggressive state.
- Q-PCR identify that PHB over-expression decreases two Wnt genes; *Wnt10B* and *Wnt7B*.
- Wnt genes are heavily influenced in the progression and migration of PC.
- Metacore analysis depicted that both Wnt-signalling and integrin-mediated adhesion are in the top 10 most affected networks by PHB over-expression.
- The migration of androgen dependent cells; LNCaP and androgen independent cells; PC3 is significantly decreased with PHB over-expression.
- PHB over-expression significantly decreases the adhesion of androgen dependent PC cells to a basement membrane Matrigel™ coating.
- Adhesion of tumour cells to the basement membrane is essential for primary tumour metastasis.
- E2F binding sites are predicted in the promoter regions of *Wnt10B* and *Wnt7B* genes.
- A preliminary mechanism of how PHB decreases migration: PHB binds to E2F preventing its interaction with predicted E2F binding sites in the promoters of

Wnt10B/Wnt7B. This inhibits downstream transcription of genes associated with migration.

Chapter VIII. General discussion.

8 Chapter VIII. General discussion.

PC still remains a debilitating disease, with disease progression and metastasis remaining the main obstacles for new treatment options. Typically, PC relies on androgen stimulation for its survival and proliferation. The identification that the prostate requires hormone stimulation was observed in the 1940s by Charles Huggins, where castrated canines had a reduced prostate gland size and a reduction in acid phosphatase secretion. However addition of testosterone counteracted these effects. PC's survival is based upon the ratio of cells proliferation to cells undergoing apoptosis. Androgen stimulation results in a synergic effect of heightening proliferation whilst inhibiting apoptosis in PC cells. Thus the clinically used androgen ablation treatment essentially increases the cells undergoing apoptosis whilst inhibiting proliferation, thus causing cancer cell regression (177). As PC is heavily regulated by hormone stimulation, blockade of the AR with current treatment options such as anti-androgens are often used in clinics. An example of anti-androgen therapy is gonadotropin-releasing hormone agonists. The hypothalamus releases gonadotropin-releasing hormone that acts on the anterior lobe of the pituitary. In response, the pituitary releases luteinizing hormone that acts on the testes to produce testosterone. Long-term treatment with gonadotropin-releasing hormone agonists leads to castration levels of testosterone within 3 weeks (178). While androgen deprivation therapy (ADT) improves overall survival, relieves bone pain and suppresses the PSA levels by up to 90% in patients suffering with malignant PC, it is often used as palliative treatment. Subsequent expected survival rates drops to 16-18 months from the time of progression. Many patients undergoing ADT eventually relapse as the cancer has sensitised to a low androgen environment, thus transitioning to androgen independence. AIPC is a lethal form of PC, and unfortunately there is no effective treatment available at present.

Firstly, AIPC can arise through several different pathways. For example, non-specific ligand activation of the AR. Adrenal androgens and growth factors such as insulin like growth factor-1(IGF-1) can cause activation the AR in the absence of androgen. This is due to mutations within the LBD domain of the AR that can arise through the use of anti-androgen therapy. This results in the current treatment of androgen ablation becoming less effective, increasing the likelihood of patient relapse. Further, AR gene and protein amplification has been documented in 25-30 of AIPC cases (69). An increase in AR co-activators has been identified in AIPC cases, causing an increased

recruitment of transcriptional machinery, enhancing the transcription of AR-regulated genes. Another proposed mechanism leading to aberrant AR activation is the down-regulation of AR co-repressors. One well established co-repressor of the AR is known as PHB, and PHB has been shown to be down-regulated at both a gene and protein level in PC. PHB can co-repress the AR by recruiting chromatin remodifying proteins such as HDAC, N-CoR and BRG1/Brm, repressing transcription of AR sensitive genes, such as *PSA*. However in PC, once the AR signalling cascade has been activated, PHB dissociates from the AR, allowing downstream transcription of genes with androgen responsive elements in their promoter regions. This leads to heightened proliferation, a decrease in apoptosis and an overall increased survival of the cancer. Therefore, it was explored whether PHB over-expression had any adverse effects on the cell cycle, proliferation and migration of both androgen dependent and androgen independent cell lines. Investigating how PHB is down-regulated in PC could provide a novel mechanism involving the transition of PC from androgen dependence to true androgen independent PC (AIPC).

Accumulating the data collected throughout this project and previous literature has shown that PHB is a ubiquitously expressed pleiotropic protein. Along with its homologue; PHB2, it carries out a varied role within the cell. Within the mitochondria, it serves as a chaperone for newly synthesised proteins. Within the nucleus it interacts with transcriptional factors that regulate genes essential for cell cycle regulation and DNA replication. More importantly, relevant to this project, PHB serves as a co-repressor to the AR, whereby it represses the translocation of the AR to the nucleus, inhibiting the transcription of androgen responsive genes (130). PHB localises in the nucleus in a variety of diseases such as irritable bowel syndrome (IBS), inflammatory disorders and cancers. Such cancers include gastric, breast and prostate (179). Online analysis of the *PHB* gene highlighted no detected mutations in prostate adenocarcinoma (The human gene mutation database).

Previous work that led onto this project identified that *PHB* gene levels are seen to be reduced with high grade cancer and metastasis, demonstrated by both *in vivo* models and geodatasets analysis. Stimulation of the AR in androgen dependent PC cells (LNCaPs) led to a 50% reduction in PHB protein levels (24 hr) (128). The same effect was seen in the androgen independent cell line PC3s, when they were stably transfected with the AR (30% decrease) (128). Further, PHB over-expression was able to inhibit the

progression of the cell cycle in LNCaP cells by increasing the sub-population of cells in the G1 phase, whilst decreasing the number of cells entering the S phase (130).

PHB's role in the cell cycle has been identified in breast cancer, whereby interaction of Rb family proteins with PHB was seen, alongside repression of E2F transcriptional activity. One of the aims of this thesis was to identify how PHB modulates the cell cycle and how this regulation is influenced by AR activation. As PHB has been found to have a profound effect on gene expression an RNA-sequencing experiment was carried out. Data provided from the RNA-sequencing experiment and Q-PCR data showed that PHB renders the cell cycle inactive via an E2F-dependent mechanism, downregulating genes involved in DNA replication (MCMs). The RNA-seq data was also subjected to analysis from bioanalysis programs. IPA and Metacore analysis determined E2F to be one of the top ten transcriptional factors to be regulated by PHB. Gene ontology pathways were also centred on E2F3/4. There is a large amount of redundancy in the *E2F* gene family, their functions switching between repression and activation during different stages of the cell cycle. The role PHB has on E2F3/4 has yet to be investigated. The members of the E2F gene family are vital for the regulation of the cell cycle, especially in the G1/S transition phase. E2F transcription factors are bound by members of the retinoblastoma (Rb) family, rendering their functions inactive during early G1 phase. Supplemental figure 6 depicts that LNCaPs stimulated with androgen incur a cyclinA/D phosphorylation leading to the phosphorylation of Rb, freeing E2F1 to progress the cell cycle. Over-expression of E2F1 in mesangial cells induced the protein expression of cyclinD1 and cyclinE, both crucial for cell cycle progression (180). When bound to phosphorylated Rb (pRb), E2Fs function as transcriptional repressors, whereas in free form, E2Fs act as activators of transcription (135). The repression of E2Fs by pRb is enhanced by their phosphorylation by cyclinD, and this repression is inhibited by cyclinD inhibitors. Rb has a vital role cell cycle progression as well as regulating apoptosis, differentiation of myoblasts and adipocytes and their development (135). To highlight Rb's role as a tumour suppressor, mice carrying a one mutant *Rb1* allele were predisposed to cancer development. pRb role within the terminal differentiation of certain cell types can be divided into two mechanisms. Repression of E2F dependent promoters such as those found in the *MCM*s genes, allows the regulation of the cell cycle and apoptosis.

Secondly, pRb family members can interact with transcriptional regulators such as MyoD and HBP1 that aid the regulation of differentiation (135).

It was then investigated if PHB was able to repress E2F activity on the promoters of E2F-regulated genes e.g. the *MCM* gene family. MCMs encode for proteins with DNA helicase activity that is vital for replication elongation during DNA replication. They also participate in other chromosomal activities such as chromatin remodelling, transcription and genome stability. Data established in this project highlighted that with increasing concentrations of PHB measured by Q-PCR and luciferase production, the promoter activity of both *MCM5* and *MCM6* were reduced. This led to a preliminary mechanism that PHB physically interacts with E2F1, repressing its function, leading to the repression of the cell cycle. Mutating a single amino acid in a predicted E2F binding site within the *MCM6* promoter region 1Kb upstream of the starting codon, abolished PHB's repressive function on the promoter. Moreover, PHB in combination with Enzalutamide (anti-androgen treatment) led to heightened efficacy in repressing the *MCM6* promoter activity.

An exciting and novel interaction was found between E2F1 and PHB in hormonally starved LNCaP cells by a co-immunoprecipitation assay. This interaction was reduced upon AR activation (cells stimulated with androgen) suggesting that the AR pathway hinders PHB's repressive function on E2F1. This could allude to how PHB is able to inhibit the cell cycle, through direct protein interaction with E2F1. The two hybrid assay (Checkmate™) determined a weak interaction between E2F1 and PHB, suggesting that the two proteins do not interact in a 1:1 ratio, but rather part of a larger complex of proteins such as HP1, Brg1/Brm and Rb. This then led to the assumption that PHB is able to interact with E2F1, preventing its transcriptional activity on the *MCM* genes, leading to cell cycle arrest.

The next step was to identify the effect androgen signalling had on the PHB protein. The PHB protein is known to undergo a variety of post-translational modifications (PTM) such as, palmitoylation, ubiquitation, phosphorylation, *O*-GlcNAc modification and cysteine oxidation, however androgens effect on PHB was unknown (181). The PHB protein contains four tyrosine residues at positions 28, 114, 249 and 259 that are highly conserved among different species (182). PHB can undergo tyrosine phosphorylation by activation of various stimuli. Stimuli include insulin, insulin-like

growth factor and epidermal growth factor. Insulin receptor can phosphorylate PHB at tyrosine-114, which creates a binding site for SH2 domain containing protein tyrosine phosphatase-1 (Shp1), that in turn phosphorylates Akt and glycogen synthase kinase-3β (183). Unfortunately, the only commercially available phosphorylated PHB antibody available is at the position Y-259. Therefore 2D western blot analysis was carried out.

A novel finding that could explain how androgen-independent PC occurs, is depicted in the 2D western blot analysis of PHB. Firstly, as PHB dissociates rapidly from the chromatin when the AR is activated with hormone (2-4 hr), this suggested that post-translational modifications were occurring as opposed to transcriptional changes. This led onto studying the non-genomic actions of androgens on the LNCaP cell line. Hormonally starved LNCaP cells that had been treated with androgen (4hr) showed a pattern change of the isoelectric point of PHB with a shift towards pH 10, as opposed to hormonally starved LNCaP cells where PHB had an isoelectric point of pH 6 (approximately). This indicated that upon AR activation, PHB loses a negative charge, suggesting that PHB is being dephosphorylated. The conjugation of a ligand or protein to PHB was ruled out as there was no protein size change seen. The same isoelectric point pattern of PHB was seen with androgen treatment in the AR positive VCaP cell line, highlighting it is an AR related event. Interestingly, the charge shift of PHB (the dephosphorylation event) was inhibited when the LNCaP cells were treated with Enzalutamide; a clinically used anti-androgen therapy. Moreover, PC3 cells that are AR null and represent androgen independent PC, displayed no charge shift of PHB in the presence of hormone. However, the isoelectric point of PHB in the PC3 cells resembles the same pattern of PHB in the androgen-treated LNCaP cells. This insinuates that in androgen independent PC, PHB has already undergone this post-translational modification, inhibiting the repressive function of PHB through its dissociation from the chromatin. This could allude to a novel mechanism that may have allowed PC to transition from androgen dependence to androgen independence. Particularly as it was shown that *PHB* gene expression was significantly lower in Bicalutamide-resistant LNCaP cells when compared to control LNCaP cells. This together with the down-regulation of PHB through this potential dephosphorylation event could be involved in current PC treatment resistance.

Further investigations were carried out to assess the non-genomic actions of androgens, as it was too rapid to account for gene expression changes, by using a Kinexus array on hormonally starved LNCaP cells treated with androgen (4 hr), the same amount of time that it takes for PHB to dissociate from the chromatin in the presence of androgen. Firstly, the Kinexus protein array identified that Src was phosphorylated at tyrosine 418 in response to AR activation. Moreover, focal adhesion kinase (FAK) was also phosphorylated at tyrosine Y577. Src is a known up-stream regulator of FAK and Src-mediated phosphorylation of FAK is essential for actin and adhesion dynamics and survival signalling, which is turn aids the migration of cancerous cells (184). Cells lacking FAK demonstrated impaired migration and displayed large focal adhesion structures. Moreover, cells lacking the three members of the Src family; Src, Lyn and Yes, also displayed impaired migration and altered dispersal of focal adhesions (184). Activation of Src is essential for tyrosine phosphorylation of focal adhesion substrates such as FAK that in turn aids cell motility and focal adhesion turnover. How the relationship between Src and FAK aid cell motility still remains vague. However, signalling cascades activated through FAK have been identified to play a role in cell migration. Such pathways include the PI3K pathway (phosphatidylinositol 3-kinase), or phosphorylation of paxillin or various other focal adhesion substrates (184). Interestingly, FAK's expression and not its kinase activity, is essential for platelet derived growth factor and epidermal growth factor stimulated cell motility. FAK also plays a role in apoptosis, by preventing cells from undergoing apoptosis in response to anoikis. A study entailing mutating each of the putative Src-induced tyrosine phosphorylation sites (Tyr 407, 576, 577, 861, and 925) highlighted that Src-induced phosphorylation of FAK is essential for calpain-mediated focal adhesion turnover during cell migration and cell transformation (184). Moreover, Src-induced phosphorylation of FAK is necessary for survival and anchorage-independent growth of transformed cells. Therefore this evidences that both Src and FAK are essential for cell motility, and androgen-activation of the AR leads to activation of these signalling cascades (184). Data collected in this thesis showed that PHB up-regulation reduced the activity of the AR, thus this could potentially stop the rapid phosphorylation of $Src^{tyr\text{-}418}$ that is essential for Src's full catalytic activity. This in turn could prevent the phosphorylation of FAK, leading to reduced downstream effects such as cell migration. A Src-inhibitor that was in use in clinical trials for metastatic castration resistant PC is known as Dasatinib. However, Dasatinib failed to be translated into clinical benefit in

combination therapy alongside Docetaxel for castration resistant PC, as no improved survival was seen with the combination therapy when compared to patients treated with Docetaxel alone (185). However targeting the Src pathway still is a promising target for PC treatment, as treating Bicalutamide-resistant LNCaP cells with a Src-inhibitor led to reduced proliferation of these cells in response to Bicalutamide, suggesting targeting the Src pathway can reverse some aspects of current anti-androgen therapy resistance.

Growth factors and downstream tyrosine kinases are notably increased during androgen ablation (IL-6, IGF-1, Src, MAPKs,PKC) and can induce the tyrosine phosphorylation of the AR, which can sensitise the AR to a low androgen environment, increasing the likelihood of PC developing an androgen independent phenotype. Studies carried out by Guo, *et al.,* 2006 (152) showed that levels of AR tyrosine phosphorylation were higher in samples from castration-resistant prostate xenograft tumours when compared to their hormone sensitive counterparts. Src kinase activity was identified to be elevated in the same castration-resistant prostate xenograft tumours, highlighting Src kinase to be responsible for the AR tyrosine phosphorylation (152). A kinase-inactive mutant SrcK295M failed to induce the tyrosine phosphorylation of the AR in LNCaP cells, suggesting that Src kinase induces the EGF induced AR tyrosine phosphorylation (152). Vandetanib, a dual inhibitor of both the EGF receptor and the vascular endothelial growth factor receptor-2 (VEGFR-2) failed to improve the efficacy over Bicalutamide alone in castration resistant PC patients.

The next aim of the study was to address PHB's role in PC metastasis. It has been established that if diagnosed early, local stage PC has a 100% survival rate for more than 5 years. Once the cancer progresses to a distant site, this survival rate drops to 28% for more than 5 years(186). Therefore, it is essential to uncover mechanisms that evolve the cancer from an indolent local stage to an aggressive distal stage. There is limited literature linking the role PHB has in the migration and metastatic potential of PC. However, data collected in the thesis via Geodatasets analysis showed that PHB is downregulated in advanced PC, particularly in distant metastatic sites. Further *in vivo* work carried out by Dr.D.Dart, demonstrated that knock-down of *PHB* led to local and distal metastases of LNCaP xenografts in a mouse model (supplemental figure 4). Moreover, data collected here, indicate that up-regulation of PHB inhibited the migration of both androgen dependent and androgen independent cell lines. Therefore, by targeting the down-regulation of PHB in PC, there could be a synergic effect of

inhibiting both the proliferation of the PC cells and their migration from the primary tumour. Bio-analysis of the RNA-seq data showed that migration and adhesion were pathways affected by PHB over-expression. Mechanistically, up-regulation of PHB could, thus, have a negative effect on genes associated with PC migration. Interestingly, data mining into the RNA-sequencing database revealed that PHB up-regulation caused members of the *Wnt* gene family to be down-regulated. After validation of key genes via Q-PCR, both *Wnt10B* and *Wnt7B* were significantly down-regulated. The Wnt proteins are secreted as glycosylated and palmitoylated peptides. The family of Wnt proteins are involved in migration, stem cell differentiation and integrity of the stem cell niche (187). Deregulated Wnt signalling has been documented in the development and progression of cancer. For example, in acute myeloid lymphoma (AML), β-catenin, a downstream target of canonical Wnt signalling can progress pre-leukaemia initiating cells to a leukemic initiating state. In chronic lymphocytic leukaemia (CLL) canonical Wnt signalling is up-regulated and upon inhibition of the signalling pathway, apoptosis of CLL cells ensues *in vitro* (188). Moreover, somatic *Wnt* gene mutations were found in 14% of studied cases. Targeting these mutated *Wnt* genes led to a decrease in cell viability whereas non-mutated *Wnt* genes were unaffected when targeted. There is strong evidence to suggest that aberrant canonical Wnt signalling has a prominent role in the progression subtypes of leukaemia. Heightened Wnt signalling has also been documented in both melanoma and breast cancer (188). Firstly, in 50% of breast cancer cases, Wnt signalling is activated leading to reduced overall survival rate. Worryingly, Wnt antagonists are silenced whereas Wnt ligands and receptors are over-expressed in breast cancers (188). Moreover, in melanoma the non-canonical Wnt5A led to increased motility as well as causing a pseudo-senescent phenotype. This pseudo-senescent phenotype consists of melanoma cells that are increasingly chemo resistant (188). Therefore Wnt5A mediated signalling leads to an invasive and resistant phenotype within melanomas.

Wnt signalling has been implicated in cancer metastasis. One of the hallmarks in cancer metastasis is epithelial to mesenchymal transitioning (EMT). Here polarised epithelial cells transform into migratory mesenchymal cells (189). One of the transcriptional factors associated with EMT is known as *SNAI2* (190). Activation of the non-canonical Wnt pathway leads to the stabilisation of SNAI2 by preventing GSK3β kinase activity, thus instigating EMT in breast cancer cells (188). However in colon cancer, over-

activation of the canonical Wnt pathway leads to nuclear accumulation of β-catenin resulting in cancer metastasis (188). This highlights that both non-canonical and canonical Wnt signalling are implicated in cancer metastasis, and thus PHB over-expression having a negative effect on their gene expression resulting in reduced migration could prevent local and distal PC metastasis. Moreover, Kinexus data revealed that ROCK-1 was the most phosphorylated total protein in response to androgen stimulation. Interestingly, ROCK-1 plays a pivotal role in tumour cell motility. ROCK proteins are a downstream target of the small GTPase Rho. The Rho family of small GTPases are integral for the metastatic potential of cancerous cells (191) Interesting, Rho proteins can interact with Src proteins, ultimately leading to actin cytoskeleton remodelling and increased cell motility. This is of particular importance as it was shown here that activation of the AR pathway leads to Src phosphorylation. A specific Rho GTPase protein; Rac1 can induce growth of androgen independent PC cells in cell culture and *in vivo,* suggesting that Rac1 is an important mediator of ligand-independent AR activation in PC progression (192). Therefore, inhibition of the AR through PHB up-regulation could prevent the activation of Rho GTPase proteins, leading to inhibition of PC progression and metastasis.

This thesis supports an accumulating amount of evidence to suggest that up-regulating PHB hinders malignant characteristics of PC. Such functions include cell cycle arrest, inhibition of cell proliferation, adhesion and migration. Stopping these functions in PC is critical in reducing the malignancy of the cancer, and improving prognosis. However, therapeutically it is difficult to induce the over-expression of PHB within the cells due to its protein size (32kDa). However, there are ways in which PHB is down-regulated at a genetic level. For example, it is well known that microRNAs (miRNAs) are able to fine tune its gene expression. miRNAs are single stranded RNAs around 22 nucleotides long that are able to bind to mRNA, silencing their expression (193). They are able to negatively regulate their gene targets one of two ways. Firstly, miRNAs that bind to their gene target with almost 100% complementarity induce the RNA-mediated interference pathway. Secondly, miRNAs that bind to their targets with less complementarity occurs in the 3' untranslated regions (UTR), inhibiting translation of mRNA through a RISC complex similar to the RNA-mediated interference pathway (193). Work carried out by Kang *et al.,* 2013 (194) identified that miR-27a and miR-128 were predicted to be conserved miRNA families among vertebrates that target human

PHB by using the TargetScan Database. Interestingly, miR-27a has been seen to down-regulate PHB both in prostate and gastric cancer. Firstly, in gastric cancer studies carried out by Lui, *et al.,* 2009 (195) identified miR-27a as an oncomiR and knockdown of miR-27a could suppress cancer cell growth. Interestingly, further studies revealed that the 3-UTR of *PHB* contained a binding site for miR-27a. Blocking the function of miR-27a led to an increase in both *PHB* mRNA and PHB protein. Therefore, it was identified that miR-27a can bind to *PHB*'s 3'UTR inducing the cleavage of *PHB* mRNA, resulting in PHB's loss of function. A similar effect was also seen in PC, whereby it was detected that AR activation led to an increase in miR-27a, leading to the down-regulation of PHB in a positive feedback system (92). miR-27a down-regulation of PHB could therefore propagate PC's oncogenic phenotype, through aberrant AR signalling. Therefore, therapeutically targeting miR-27a could prevent the down-regulation of PHB that in turn could prevent the progression of PC. Inhibiting oncomiRs using antisense oligomers is emerging as a therapeutic strategy. However, in order to target such oncomiRs, certain information is needed. Firstly, to understand the miRNAs mechanism of action, what is the most efficient form of delivery of miRNA therapy, and its action *in vivo*. Once this information has been discovered, targeting miRNA-27a's downregulation of PHB may be a therapeutic option of PC.

8.1 Future work

The data collected throughout this thesis has lead onto promising mechanisms that could explain how androgen independent PC arises through the use of anti-androgen therapy. However, although complete knockout of PHB is lethal in embryonic cells, experiments can be carried out using a knock-down ribozyme plasmid targeted to the 3'UTR of PHB to induce the partial knockdown of PHB (approx. 30%). Functional experiments carried out in this thesis could then be repeated using the *PHB* targeted ribozyme plasmid, to note if the reciprocal pattern occurs. Mass spectrometry could aid identifying the residue or residues on PHB that is being dephosphorylated, that could lead to raising an antibody specific to this residue. Further protein:protein interaction assays could be carried out to further validate if PHB directly or indirectly interacts with E2F1. Chromatin immunoprecipitation (ChIP) could validate regions on the chromatin where PHB is binding, and how hormone activation of the AR could disrupt this binding.

Moreover, analysis into the expression of the *Wnt* genes throughout the phases of the cell cycle could be carried out. If *in silico* analysis predicts *E2F* binding sites within the promoter regions of *Wnt10b* and *Wnt7b,* an E2F1 plasmid could be transfected into LNCaP cells, and promoter activity of both *Wnt10b* and *Wnt7b* could be analysed to identify if they are E2F-regulated. If they appear to be E2F regulated this could link to PHB's direction interaction with E2F1, repressing E2F1s activity on the *wnt* genes, leading to an inhibition of down-stream effect of *wnts* such as cell migration in PC. More PC cell lines could be used for validation.

Identifying the amino acid residue or residues of PHB that is targeted for the dephosphorylation in response to androgen treatment, would be the next step. This sequence could then be used to identify the phosphatase responsible for the dephosphorylation. This phosphatase could then be therapeutically targeted, to prevent the dephosphorylation of PHB leading to its dissociation from the chromatin. Moreover, an antibody for this residue could be manufactured, and a screening procedure for PC biopsies could be made available. If the PC biopsy is positive for the dephosphorylated PHB in patients that are undergoing anti-androgen therapy, it is a good indication that the therapy is not effective and can be stopped preventing the patients from suffering unnecessary side effects and can be used as a prognostic indicator. Once in vitro validation was complete, use of animal models and primary tissue samples would be obtained to prove proof of principle.

8.2 Conclusion

To conclude this thesis, there is a large body of data to suggest PHB down-regulation is a mechanism that aids the development of 'androgen independent' or 'castration-resistant PC'. This is due to the novel identification that androgen stimulation of the AR leads to the potential dephosphorylation of PHB. This in turn may lead to the dissociation of PHB from the chromatin, and dissociation of PHB from promoters that contain *E2F* binding sites such as MCM genes that are responsible for DNA replication. A novel interaction of E2F1 and PHB was identified in the LNCaP cell line. This interaction was disrupted upon androgen stimulation, allowing E2F1 to carry out its function in cell cycle progression. PHB's repressive role on the cell cycle was due to causing the down-regulation of several members of the *E2F* gene family and the *MCM* gene family, alongside causing an up-regulation of cell cycle inhibitors such as *p21*

and *p27*. Moreover, up-regulation of PHB was also seen to play a role in hindering the cellular adhesion and cellular migration of both androgen dependent and androgen independent PC cells. Mechanistically this was narrowed down to PHB causing the down-regulation of *Wnt* genes that are predominantly influenced in cell motility and PC progression. To confirm this, bioanalysis data verified that Wnt signalling and integrin signalling were within the top networks to be effected by PHB over-expression. Both of these pathways are essential for progression of the PC from the primary tumour, leading to local and distant metastasis. Thus, accumulating the data presented here, PHB is a multi-functional protein that upon up-regulation leads to an inhibition of several cascades of events that eventually leads to a regression of malignant PC. This thesis has provided data that has alluded to a novel suggested mechanism involved in androgen independent PC as shown in figure 8.1.

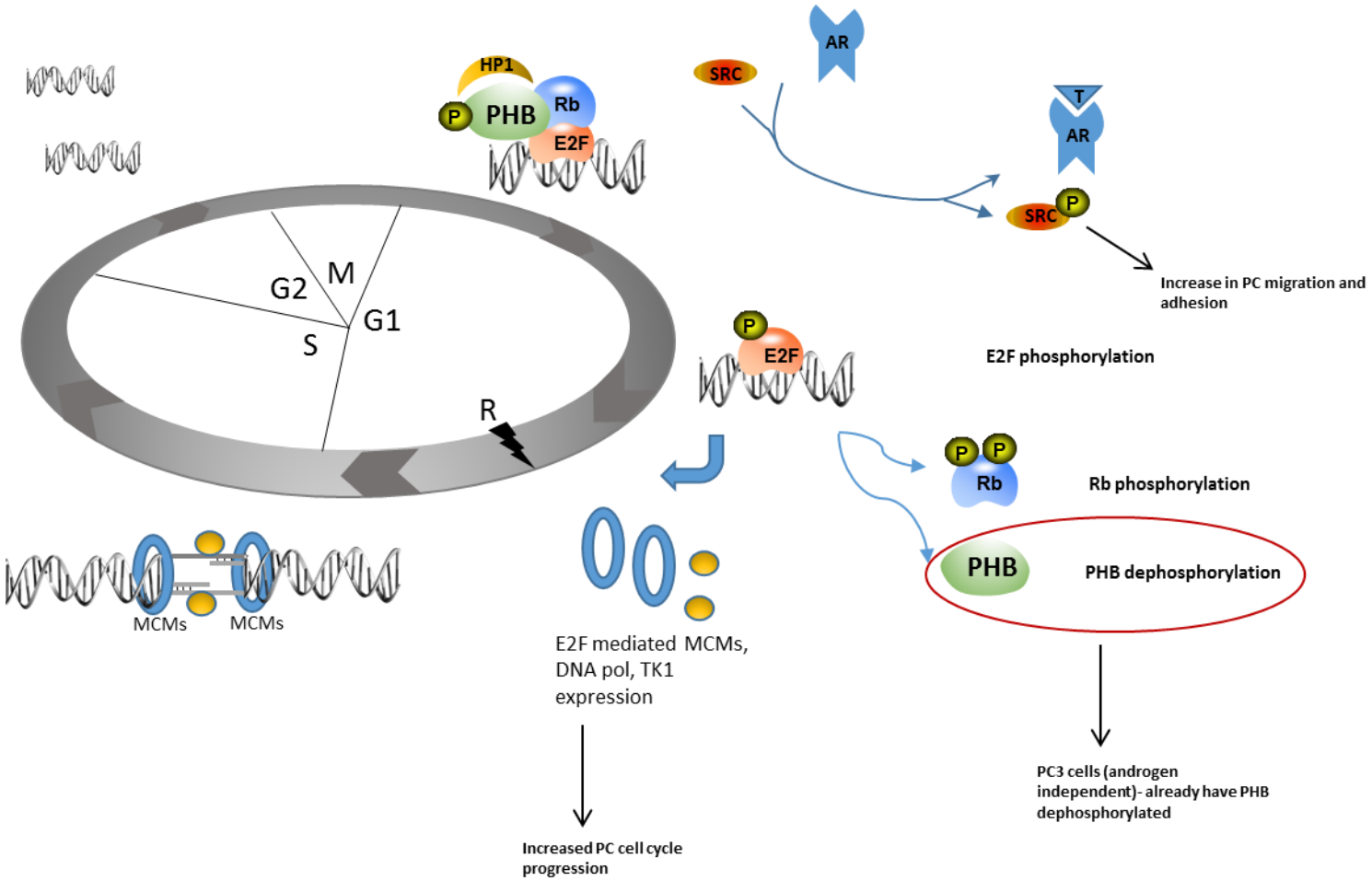

Figure 8.1. Final mechanism that could allude to how androgen independent PC occurs, involving AR activation leading to Src-phosphorylation, PHB dephosphorylation and how these events increase PC malignancy through increased cell cycle progression, cell migration and adhesion (137).

References

1. William K. Oh M, Mark Hurwitz, MD, Anthony V. D'Amico, MD, Jerome P. Richie, MD, and Philip W. Kantoff, MD. Biology of Prostate cancer. Cancer medicine 2003;6.

2. Schrecengost R, Knudsen KE. Molecular pathogenesis and progression of prostate cancer. Seminars in oncology. 2013;40(3):244-58.

3. Hudson DL, Guy AT, Fry P, O'Hare MJ, Watt FM, Masters JR. Epithelial cell differentiation pathways in the human prostate: identification of intermediate phenotypes by keratin expression. The journal of histochemistry and cytochemistry : official journal of the Histochemistry Society. 2001;49(2):271-8.

4. The McGraw-Hill Companies I. Junqueira's Basic Histology: Text and Atlas. 2010;12th

5. Kumar VL, Majumder PK. Prostate gland: structure, functions and regulation. International urology and nephrology. 1995;27(3):231-43.

6. Wilt TJ, Ahmed HU. Prostate cancer screening and the management of clinically localized disease. BMJ (Clinical research ed). 2013;346:f325.

7. Eeles R, Goh C, Castro E, Bancroft E, Guy M, Al Olama AA, et al. The genetic epidemiology of prostate cancer and its clinical implications. Nature reviews Urology. 2014;11(1):18-31.

8. Delongchamps NB, Singh A, Haas GP. Epidemiology of prostate cancer in Africa: another step in the understanding of the disease? Current problems in cancer. 2007;31(3):226-36.

9. Haas GP, Delongchamps N, Brawley OW, Wang CY, de la Roza G. The worldwide epidemiology of prostate cancer: perspectives from autopsy studies. The Canadian journal of urology. 2008;15(1):3866-71.

10. Gupta D, Lammersfeld CA, Trukova K, Lis CG. Vitamin D and prostate cancer risk: a review of the epidemiological literature. Prostate cancer and prostatic diseases. 2009;12(3):215-26.

11. Institute NC. Genetics of Prostate Cancer (PDQ®) 2014 [Available from: http://www.cancer.gov/cancertopics/pdq/genetics/prostate/HealthProfessional/page1.

12. Walker R, Louis A, Berlin A, Horsburgh S, Bristow RG, Trachtenberg J. Prostate cancer screening characteristics in men with BRCA1/2 mutations attending a high-risk prevention clinic. Canadian Urological Association Journal. 2014;8(11-12):E783-8.

13. Stangelberger A, Waldert M, Djavan B. Prostate cancer in elderly men. Reviews in urology. 2008;10(2):111-9.

14. Langeberg WJ, Kwon EM, Koopmeiners JS, Ostrander EA, Stanford JL. Population-based study of the association of variants in mismatch repair genes with prostate cancer risk and outcomes. Cancer epidemiology, biomarkers & prevention : a publication of the American Association for Cancer Research, cosponsored by the American Society of Preventive Oncology. 2010;19(1):258-64.

15. Rivlin N, Brosh R, Oren M, Rotter V. Mutations in the p53 Tumor Suppressor Gene: Important Milestones at the Various Steps of Tumorigenesis. Genes & Cancer. 2011;2(4):466-74.

16. Nesslinger NJ, Shi XB, deVere White RW. Androgen-independent growth of LNCaP prostate cancer cells is mediated by gain-of-function mutant p53. Cancer research. 2003;63(9):2228-33.

17. Narla G, Heath KE, Reeves HL, Li D, Giono LE, Kimmelman AC, et al. KLF6, a candidate tumor suppressor gene mutated in prostate cancer. Science. 2001;294(5551):2563-6.

18. Velonas VM, Woo HH, Remedios CG, Assinder SJ. Current status of biomarkers for prostate cancer. International journal of molecular sciences. 2013;14(6):11034-60.

19. Wang Y, Romigh T, He X, Tan MH, Orloff MS, Silverman RH, et al. Differential regulation of PTEN expression by androgen receptor in prostate and breast cancers. Oncogene. 2011;30(42):4327-38.

20. Dasgupta S, Srinidhi S, Vishwanatha JK. Oncogenic activation in prostate cancer progression and metastasis: Molecular insights and future challenges. Journal of Carcinogenesis. 2012;11.

21. Uysal-Onganer P, Kawano Y, Caro M, Walker MM, Diez S, Darrington RS, et al. Wnt-11 promotes neuroendocrine-like differentiation, survival and migration of prostate cancer cells. Molecular Cancer. 2010;9(1):1-11.

22. Hägglöf C, Hammarsten P, Strömvall K, Egevad L, Josefsson A, Stattin P, et al. TMPRSS2-ERG Expression Predicts Prostate Cancer Survival and Associates with Stromal Biomarkers. PLoS ONE. 2014;9(2):e86824.

23. Adamo P, Ladomery MR. The oncogene ERG: a key factor in prostate cancer. Oncogene. 2016;35(4):403-14.

24. Yang Z, Yu L, Wang Z. PCA3 and TMPRSS2-ERG gene fusions as diagnostic biomarkers for prostate cancer. Chinese Journal of Cancer Research. 2016;28(1):65-71.

25. Loeb S, Sanda MG, Broyles DL, Shin SS, Bangma CH, Wei JT, et al. The prostate health index selectively identifies clinically significant prostate cancer. The Journal of urology. 2015;193(4):1163-9.

26. Kriebel S, Schmidt D, Holdenrieder S, Goltz D, Kristiansen G, Moritz R, et al. Analysis of Tissue and Serum MicroRNA Expression in Patients with Upper Urinary Tract Urothelial Cancer. PLoS ONE. 2015;10(1).

27. Guenther MG, Barak O, Lazar MA. The SMRT and N-CoR corepressors are activating cofactors for histone deacetylase 3. Molecular and cellular biology. 2001;21(18):6091-101.

28. Scher HI, Fizazi K, Saad F, Taplin ME, Sternberg CN, Miller K, et al. Increased survival with enzalutamide in prostate cancer after chemotherapy. The New England journal of medicine. 2012;367(13):1187-97.

29. Tolkach Y, Joniau S, Van Poppel H. Luteinizing hormone-releasing hormone (LHRH) receptor agonists vs antagonists: a matter of the receptors? BJU international. 2013;111(7):1021-30.

30. Hodgson MC, Astapova I, Hollenberg AN, Balk SP. Activity of androgen receptor antagonist bicalutamide in prostate cancer cells is independent of NCoR and SMRT corepressors. Cancer research. 2007;67(17):8388-95.

31. .Abiraterone: a story of scientific innovation and commercial partnership. 2014. www.icr.ac.uk//news-features/latest-features/abiraterone-a-story-of-scientific-innovation-and-commercial-partnership. Accessed 2017.

32. Rehman Y, Rosenberg JE. Abiraterone acetate: oral androgen biosynthesis inhibitor for treatment of castration-resistant prostate cancer. Drug design, development and therapy. 2012;6:13-8.

33. Luu-The V, Belanger A, Labrie F. Androgen biosynthetic pathways in the human prostate. Best practice & research Clinical endocrinology & metabolism. 2008;22(2):207-21.

34. Gerritsen WR. The evolving role of immunotherapy in prostate cancer. Annals of oncology : official journal of the European Society for Medical Oncology / ESMO. 2012;23 Suppl 8:viii22-7.

35. Ren R, Koti M, Hamilton T, Graham CH, Nayak JG, Singh J, et al. A primer on tumour immunology and prostate cancer immunotherapy. Canadian Urological Association Journal. 2016;10(1-2):60-5.

36. Humphrey PA. Gleason grading and prognostic factors in carcinoma of the prostate. Mod Pathol. 2004;17(3):292-306.

37. Msaouel P, Pissimissis N, Halapas A, Koutsilieris M. Mechanisms of bone metastasis in prostate cancer: clinical implications. Best practice & research Clinical endocrinology & metabolism. 2008;22(2):341-55.

38. Logothetis CJ, Lin S-H. Osteoblasts in prostate cancer metastasis to bone. Nature reviews Cancer. 2005;5(1):21-8.

39. Tewari AK, Yardimci GG, Shibata Y, Sheffield NC, Song L, Taylor BS, et al. Chromatin accessibility reveals insights into androgen receptor activation and transcriptional specificity. Genome Biol. 2012;13(10):R88.

40. Shao J, Hou J, Li B, Li D, Zhang N, Wang X. Different types of androgen receptor mutations in patients with complete androgen insensitivity syndrome. Intractable & Rare Diseases Research. 2015;4(1):54-9.

41. Eisermann K, Wang D, Jing Y, Pascal LE, Wang Z. Androgen receptor gene mutation, rearrangement, polymorphism. Translational Andrology and Urology. 2013;2(3):137-47.

42. Bennett NC, Gardiner RA, Hooper JD, Johnson DW, Gobe GC. Molecular cell biology of androgen receptor signalling. The international journal of biochemistry & cell biology. 2010;42(6):813-27.

43. Dar JA, Masoodi KZ, Eisermann K, Isharwal S, Ai J, Pascal LE, et al. The N-terminal domain of the androgen receptor drives its nuclear localization in castration-resistant prostate cancer cells. The Journal of steroid biochemistry and molecular biology. 2014;143:473-80.

44. Lorente D, Mateo J, Zafeiriou Z, Smith AD, Sandhu S, Ferraldeschi R, et al. Switching and withdrawing hormonal agents for castration-resistant prostate cancer. Nature reviews Urology. 2015;12(1):37-47.

45. Hong CY, Gong EY, Kim K, Suh JH, Ko HM, Lee HJ, et al. Modulation of the expression and transactivation of androgen receptor by the basic helix-loop-helix transcription factor Pod-1 through recruitment of histone deacetylase 1. Mol Endocrinol. 2005;19(9):2245-57.

46. Jose D. Debes1 BC, Lucy J. Schmidt1, Scott M. Dehm1, Zoran Culig2, and Donald J. Tindall1. p300 Regulates Androgen Receptor–Independent Expression of Prostate-Specific Antigen in Prostate Cancer Cells Treated Chronically with Interleukin-6. Cancer research. 2005;65(5965).

47. Heemers HV, Debes JD, Tindall DJ. The role of the transcriptional coactivator p300 in prostate cancer progression. Advances in experimental medicine and biology. 2008;617:535-40.

48. Gong J, Zhu J, Goodman OB, Jr., Pestell RG, Schlegel PN, Nanus DM, et al. Activation of p300 histone acetyltransferase activity and acetylation of the androgen receptor by bombesin in prostate cancer cells. Oncogene. 2006;25(14):2011-21.

49. Gayther SA, Batley SJ, Linger L, Bannister A, Thorpe K, Chin S-F, et al. Mutations truncating the EP300 acetylase in human cancers. Nat Genet. 2000;24(3):300-3.

50. Gojis O, Rudraraju B, Gudi M, Hogben K, Sousha S, Coombes RC, et al. The role of SRC-3 in human breast cancer. Nature reviews Clinical oncology. 2010;7(2):83-9.

51. Burd CJ, Morey LM, Knudsen KE. Androgen receptor corepressors and prostate cancer. Endocrine-related cancer. 2006;13(4):979-94.

52. Waltering KK, Wallen MJ, Tammela TL, Vessella RL, Visakorpi T. Mutation screening of the androgen receptor promoter and untranslated regions in prostate cancer. The Prostate. 2006;66(15):1585-91.

53. Petre CE, Wetherill YB, Danielsen M, Knudsen KE. Cyclin D1: mechanism and consequence of androgen receptor co-repressor activity. J Biol Chem. 2002;277(3):2207-15.

54. Reutens AT, Fu M, Wang C, Albanese C, McPhaul MJ, Sun Z, et al. Cyclin D1 binds the androgen receptor and regulates hormone-dependent signaling in a p300/CBP-associated factor (P/CAF)-dependent manner. Mol Endocrinol. 2001;15(5):797-811.

55. Guoqing Liao L-YC, Aihua Zhang, Aparna Godavarthy, Fang Xia, Jagadish Chandra Ghosh, Hui Li and J. Don Chen‡. Regulation of Androgen Receptor Activity by the Nuclear Receptor Corepressor SMRT. Journal of Biological Chemistry. 2002;278:5052-61.

56. Jepsen K, Rosenfeld MG. Biological roles and mechanistic actions of co-repressor complexes. Journal of Cell Science. 2002;115(4):689-98.

57. Wong MM, Guo C, Zhang J. Nuclear receptor corepressor complexes in cancer: mechanism, function and regulation. American Journal of Clinical and Experimental Urology. 2014;2(3):169-87.

58. Gamble SC, Odontiadis M, Waxman J, Westbrook JA, Dunn MJ, Wait R, et al. Androgens target prohibitin to regulate proliferation of prostate cancer cells. Oncogene. 2004;23(17):2996-3004.

59. Wang S, Zhang B, Faller DV. Prohibitin requires Brg-1 and Brm for the repression of E2F and cell growth. Embo j. 2002;21(12):3019-28.

60. Wallace MB, Lim J, Cutler A, Bucci L. Effects of dehydroepiandrosterone vs androstenedione supplementation in men. Medicine and science in sports and exercise. 1999;31(12):1788-92.

61. Heinlein CA, Chang C. Androgen receptor in prostate cancer. Endocrine reviews. 2004;25(2):276-308.

62. Handelsman DJ. Testosterone: use, misuse and abuse. The Medical journal of Australia. 2006;185(8):436-9.

63. Manolagas SC, O'Brien CA, Almeida M. The role of estrogen and androgen receptors in bone health and disease. Nat Rev Endocrinol. 2013;9(12):699-712.

64. Rana K, Lee NKL, Zajac JD, MacLean HE. Expression of androgen receptor target genes in skeletal muscle. Asian Journal of Andrology. 2014;16(5):675-83.

65. Lai JJ, Lai KP, Zeng W, Chuang KH, Altuwaijri S, Chang C. Androgen Receptor Influences on Body Defense System via Modulation of Innate and Adaptive Immune Systems: Lessons from Conditional AR Knockout Mice. The American Journal of Pathology. 2012;181(5):1504-12.

66. Chang C, Lee SO, Wang R-S, Yeh S, Chang T-M. Androgen Receptor (AR) Physiological Roles in Male and Female Reproductive Systems: Lessons Learned from AR-Knockout Mice Lacking AR in Selective Cells. Biology of reproduction. 2013;89(1):21-.

67. Cochrane DR, Bernales S, Jacobsen BM, Cittelly DM, Howe EN, D'Amato NC, et al. Role of the androgen receptor in breast cancer and preclinical analysis of enzalutamide. Breast Cancer Research. 2014;16(1):R7.

68. Shiina H, Matsumoto T, Sato T, Igarashi K, Miyamoto J, Takemasa S, et al. Premature ovarian failure in androgen receptor-deficient mice. Proceedings of the National Academy of Sciences of the United States of America. 2006;103(1):224-9.

69. Saraon P, Jarvi K, Diamandis EP. Molecular alterations during progression of prostate cancer to androgen independence. Clinical chemistry. 2011;57(10):1366-75.

70. Guo Z, Yang X, Sun F, Jiang R, Linn DE, Chen H, et al. A novel androgen receptor splice variant is up-regulated during prostate cancer progression and promotes androgen depletion-resistant growth. Cancer research. 2009;69(6):2305-13.

71. Sun M, Yang L, Feldman RI, Sun XM, Bhalla KN, Jove R, et al. Activation of phosphatidylinositol 3-kinase/Akt pathway by androgen through interaction of p85alpha, androgen receptor, and Src. J Biol Chem. 2003;278(44):42992-3000.

72. Liu AY, Corey E, Bladou F, Lange PH, Vessella RL. Prostatic cell lineage markers: emergence of BCL2+ cells of human prostate cancer xenograft LuCaP 23 following castration. International journal of cancer Journal international du cancer. 1996;65(1):85-9.

73. Kinoshita H, Shi Y, Sandefur C, Meisner LF, Chang C, Choon A, et al. Methylation of the androgen receptor minimal promoter silences transcription in human prostate cancer. Cancer research. 2000;60(13):3623-30.

74. Lv Z, Zhang X, Liu L, Chen J, Nie Z, Sheng Q, et al. Characterization of a gene encoding prohibitin in silkworm, Bombyx mori. Gene. 2012;502(2):118-24.

75. Theiss AL, Sitaraman SV. The role and therapeutic potential of prohibitin in disease. Biochimica et biophysica acta. 2011;1813(6):1137-43.

76. Thuaud F, Ribeiro N, Nebigil CG, Desaubry L. Prohibitin ligands in cell death and survival: mode of action and therapeutic potential. Chemistry & biology. 2013;20(3):316-31.

77. Artal-Sanz M, Tavernarakis N. Prohibitin and mitochondrial biology. Trends in endocrinology and metabolism: TEM. 2009;20(8):394-401.

78. Chowdhury I, Thompson WE, Thomas K. Prohibitins role in cellular survival through Ras-Raf-MEK-ERK pathway. Journal of cellular physiology. 2014;229(8):998-1004.

79. Merkwirth C, Langer T. Prohibitin function within mitochondria: essential roles for cell proliferation and cristae morphogenesis. Biochimica et biophysica acta. 2009;1793(1):27-32.

80. Ross JA, Nagy ZS, Kirken RA. The PHB1/2 phosphocomplex is required for mitochondrial homeostasis and survival of human T cells. J Biol Chem. 2008;283(8):4699-713.

81. Emerson V, Holtkotte D, Pfeiffer T, Wang IH, Schnolzer M, Kempf T, et al. Identification of the cellular prohibitin 1/prohibitin 2 heterodimer as an interaction partner of the C-terminal cytoplasmic domain of the HIV-1 glycoprotein. Journal of virology. 2010;84(3):1355-65.

82. Christie DA, Lemke CD, Elias IM, Chau LA, Kirchhof MG, Li B, et al. Stomatin-like protein 2 binds cardiolipin and regulates mitochondrial biogenesis and function. Molecular and cellular biology. 2011;31(18):3845-56.

83. Mitsopoulos P, Chang YH, Wai T, Konig T, Dunn SD, Langer T, et al. Stomatin-like protein 2 is required for in vivo mitochondrial respiratory chain supercomplex formation and optimal cell function. Molecular and cellular biology. 2015;35(10):1838-47.

84. Takahashi A, Kawasaki T, Wong HL, Suharsono U, Hirano H, Shimamoto K. Hyperphosphorylation of a Mitochondrial Protein, Prohibitin, Is Induced. Plant Physiology. 2003;132(4):1861-9.

85. Theiss AL, Idell RD, Srinivasan S, Klapproth JM, Jones DP, Merlin D, et al. Prohibitin protects against oxidative stress in intestinal epithelial cells. FASEB journal : official publication of the Federation of American Societies for Experimental Biology. 2007;21(1):197-206.

86. Schleicher M, Shepherd BR, Suarez Y, Fernandez-Hernando C, Yu J, Pan Y, et al. Prohibitin-1 maintains the angiogenic capacity of endothelial cells by regulating mitochondrial function and senescence. The Journal of cell biology. 2008;180(1):101-12.

87. Rastogi S, Joshi B, Fusaro G, Chellappan S. Camptothecin induces nuclear export of prohibitin preferentially in transformed cells through a CRM-1-dependent mechanism. J Biol Chem. 2006;281(5):2951-9.

88. Fischer U, Huber J, Boelens WC, Mattaj IW, Luhrmann R. The HIV-1 Rev activation domain is a nuclear export signal that accesses an export pathway used by specific cellular RNAs. Cell. 1995;82(3):475-83.

89. Fusaro G, Dasgupta P, Rastogi S, Joshi B, Chellappan S. Prohibitin induces the transcriptional activity of p53 and is exported from the nucleus upon apoptotic signaling. J Biol Chem. 2003;278(48):47853-61.

90. Thompson WE, Asselin E, Branch A, Stiles JK, Sutovsky P, Lai L, et al. Regulation of prohibitin expression during follicular development and atresia in the mammalian ovary. Biology of reproduction. 2004;71(1):282-90.

91. Mishra S, Murphy LC, Nyomba BL, Murphy LJ. Prohibitin: a potential target for new therapeutics. Trends in molecular medicine. 2005;11(4):192-7.

92. Fletcher CE, Dart DA, Sita-Lumsden A, Cheng H, Rennie PS, Bevan CL. Androgen-regulated processing of the oncomir miR-27a, which targets Prohibitin in prostate cancer. Human molecular genetics. 2012;21(14):3112-27.

93. Ummanni R, Junker H, Zimmermann U, Venz S, Teller S, Giebel J, et al. Prohibitin identified by proteomic analysis of prostate biopsies distinguishes hyperplasia and cancer. Cancer letters. 2008;266(2):171-85.

94. Dart DA. Reducing prohibitin increases histone acetylation, and promotes androgen independence in prostate tumours by increasing androgen receptor activation by adrenal androgens. 2012;31(43):4588-98.

95. Key TJ, Verkasalo PK, Banks E. Epidemiology of breast cancer. The Lancet Oncology. 2001;2(3):133-40.

96. Lin Z, Reierstad S, Huang CC, Bulun SE. Novel estrogen receptor-alpha binding sites and estradiol target genes identified by chromatin immunoprecipitation cloning in breast cancer. Cancer research. 2007;67.

97. He B, Feng Q, Mukherjee A, Lonard DM, DeMayo FJ, Katzenellenbogen BS, et al. A repressive role for prohibitin in estrogen signaling. Mol Endocrinol. 2008;22(2):344-60.

98. Yoshimaru T, Komatsu M, Matsuo T, Chen YA, Murakami Y, Mizuguchi K, et al. Targeting BIG3-PHB2 interaction to overcome tamoxifen resistance in breast cancer cells. Nature communications. 2013;4:2443.

99. He B, Kim TH, Kommagani R, Feng Q, Lanz RB, Jeong JW, et al. Estrogen-regulated prohibitin is required for mouse uterine development and adult function. Endocrinology. 2011;152(3):1047-56.

100. Rakoff-Nahoum S. Why Cancer and Inflammation? The Yale Journal of Biology and Medicine. 2006;79(3-4):123-30.

101. Han J, Yu C, Souza RF, Theiss AL. Prohibitin 1 modulates mitochondrial function of Stat3. Cellular signalling. 2014;26(10):2086-95.

102. Sakaguchi M, Oka M, Iwasaki T, Fukami Y, Nishigori C. Role and regulation of STAT3 phosphorylation at Ser727 in melanocytes and melanoma cells. The Journal of investigative dermatology. 2012;132(7):1877-85.

103. Szczepanek K, Chen Q, Larner AC, Lesnefsky EJ. Cytoprotection by the modulation of mitochondrial electron transport chain: the emerging role of mitochondrial STAT3. Mitochondrion. 2012;12(2):180-9.

104. Boland ML, Chourasia AH, Macleod KF. Mitochondrial dysfunction in cancer. Frontiers in oncology. 2013;3:292.

105. Rizwani W, Alexandrow M, Chellappan S. Prohibitin physically interacts with MCM proteins and inhibits mammalian DNA replication. Cell Cycle. 2009;8(10):1621-9.

106. Meserve JH, Duronio RJ. Atypical E2Fs drive atypical cell cycles. Nat Cell Biol. 2012;14(11):1124-5.

107. Wang S, Nath N, Adlam M, Chellappan S. Prohibitin, a potential tumor suppressor, interacts with RB and regulates E2F function. Oncogene. 1999;18(23):3501-10.

108. Rukstalis DB. Treatment Options after Failure of Radiation Therapy—A Review. Reviews in urology. 2002;4(Suppl 2):S12-7.

109. Ebert MS, Sharp PA. MicroRNA sponges: Progress and possibilities. Rna. 2010;16(11):2043-50.

110. Wang N, Li Q, Feng N-H, Cheng G, Guan Z-L, Wang Y, et al. miR-205 is frequently downregulated in prostate cancer and acts as a tumor suppressor by inhibiting tumor growth. Asian Journal of Andrology. 2013;15(6):735-41.

111. Fraser M, Leung B, Jahani-Asl A, Yan X, Thompson WE, Tsang BK. Chemoresistance in human ovarian cancer: the role of apoptotic regulators. Reproductive biology and endocrinology : RB&E. 2003;1:66.

112. Jiang L, Dong P, Zhang Z, Li C, Li Y, Liao Y, et al. Akt phosphorylates Prohibitin 1 to mediate its mitochondrial localization and promote proliferation of bladder cancer cells. Cell death & disease. 2015;6:e1660.

113. Ande SR, Mishra S. Prohibitin interacts with phosphatidylinositol 3,4,5-triphosphate (PIP3) and modulates insulin signaling. Biochemical and biophysical research communications. 2009;390(3):1023-8.

114. Ande SR, Gu Y, Nyomba BL, Mishra S. Insulin induced phosphorylation of prohibitin at tyrosine 114 recruits Shp1. Biochimica et biophysica acta. 2009;1793(8):1372-8.

115. Thompson WE, Ramalho-Santos J, Sutovsky P. Ubiquitination of prohibitin in mammalian sperm mitochondria: possible roles in the regulation of mitochondrial inheritance and sperm quality control. Biology of reproduction. 2003;69(1):254-60.

116. Vermeulen K, Van Bockstaele DR, Berneman ZN. The cell cycle: a review of regulation, deregulation and therapeutic targets in cancer. Cell Proliferation. 2003;36(3):131-49.

117. Bieging KT, Mello SS, Attardi LD. Unravelling mechanisms of p53-mediated tumour suppression. Nature reviews Cancer. 2014;14(5):359-70.

118. Besson A, Dowdy SF, Roberts JM. CDK Inhibitors: Cell Cycle Regulators and Beyond. Developmental Cell. 2008;14(2):159-69.

119. Chen HZ. Emerging roles of E2Fs in cancer: an exit from cell cycle control. 2009;9(11):785-97.

120. Rowland BD, Bernards R. Re-Evaluating Cell-Cycle Regulation by E2Fs. Cell. 2006;127(5):871-4.

121. Du W, Searle JS. The Rb Pathway and Cancer Therapeutics. Current drug targets. 2009;10(7):581-9.

122. Bracken AP, Ciro M, Cocito A, Helin K. E2F target genes: unraveling the biology. Trends in biochemical sciences. 2004;29(8):409-17.

123. Forsburg SL. Eukaryotic MCM Proteins: Beyond Replication Initiation. Microbiology and Molecular Biology Reviews. 2004;68(1):109-31.

124. Gonzalez MA, Tachibana K-eK, Laskey RA, Coleman N. Control of DNA replication and its potential clinical exploitation. Nature reviews Cancer. 2005;5(2):135-41.

125. A.P. Tabancay SLF. Eukaryotic DNA Replication in a Chromatin Context. Current Topics in Developmental Biology. 2006

126. Mortazavi A, Williams BA, McCue K, Schaeffer L, Wold B. Mapping and quantifying mammalian transcriptomes by RNA-Seq. Nat Methods. 2008;5(7):621-8.

127. Cunningham D, You Z. In vitro and in vivo model systems used in prostate cancer research. 2015. 2015.

128. Dart DA, Spencer-Dene B, Gamble SC, Waxman J, Bevan CL. Manipulating prohibitin levels provides evidence for an in vivo role in androgen regulation of prostate tumours. Endocrine-related cancer. 2009;16(4):1157-69.

129. Gamble SC, Chotai D, Odontiadis M, Dart DA, Brooke GN, Powell SM, et al. Prohibitin, a protein downregulated by androgens, represses androgen receptor activity. Oncogene. 2007;26(12):1757-68.

130. Gamble SC, Chotai D, Odontiadis M, Dart DA, Brooke GN, Powell SM, et al. Prohibitin, a protein downregulated by androgens, represses androgen receptor activity. Oncogene. 2006;26(12):1757-68.

131. Wang C, Youle RJ. The Role of Mitochondria in Apoptosis(). Annual review of genetics. 2009;43:95-118.

132. Mason EF, Rathmell JC. Cell metabolism: an essential link between cell growth and apoptosis. Biochimica et biophysica acta. 2011;1813(4):645-54.

133. Giacinti C, Giordano A. RB and cell cycle progression. Oncogene. 0000;25(38):5220-7.

134. Leone G, DeGregori J, Yan Z, Jakoi L, Ishida S, Williams RS, et al. E2F3 activity is regulated during the cell cycle and is required for the induction of S phase. Genes & development. 1998;12(14):2120-30.

135. Müller H, Bracken AP, Vernel R, Moroni MC, Christians F, Grassilli E, et al. E2Fs regulate the expression of genes involved in differentiation, development, proliferation, and apoptosis. Genes & development. 2001;15(3):267–85.

136. Ohtani K, Iwanaga R, Nakamura M, Ikeda M, Yabuta N, Tsuruga H, et al. Cell growth-regulated expression of mammalian MCM5 and MCM6 genes mediated by the transcription factor E2F. Oncogene. 1999;18(14):2299-309.

137. Koushyar S, Economides G, Zaat S, Jiang W, Bevan CL, Dart DA. The prohibitin-repressive interaction with E2F1 is rapidly inhibited by androgen signalling in prostate cancer cells. Oncogenesis. 2017;6:e333.

138. Goel HL, Li J, Kogan S, Languino LR. Integrins in prostate cancer progression. Endocrine-related cancer. 2008;15(3):657-64.

139. Wang S, Nath N, Fusaro G, Chellappan S. Rb and Prohibitin Target Distinct Regions of E2F1 for Repression and Respond to Different Upstream Signals. Molecular and cellular biology. 1999;19(11):7447-60.

140. Abbas T, Dutta A. p21 in cancer: intricate networks and multiple activities. Nature reviews Cancer. 2009;9(6):400-14.

141. Hochegger H, Dejsuphong D, Sonoda E, Saberi A, Rajendra E, Kirk J, et al. An essential role for Cdk1 in S phase control is revealed via chemical genetics in vertebrate cells. The Journal of cell biology. 2007;178(2):257-68.

142. Tamura RE, de Vasconcellos JF, Sarkar D, Libermann TA, Fisher PB, Zerbini LF. GADD45 proteins: central players in tumorigenesis. Current molecular medicine. 2012;12(5):634-51.

143. McClung JK, Jupe ER, Liu XT, Dell'Orco RT. Prohibitin: potential role in senescence, development, and tumor suppression. Experimental gerontology. 1995;30(2):99-124.

144. Wang S, Fusaro G, Padmanabhan J, Chellappan SP. Prohibitin co-localizes with Rb in the nucleus and recruits N-CoR and HDAC1 for transcriptional repression. Oncogene. 2002;21(55):8388-96.

145. Ciechanover A. The unravelling of the ubiquitin system. Nat Rev Mol Cell Biol. 2015;16(5):322-4.

146. Galdieri L, Zhang T, Rogerson D, Lleshi R, Vancura A. Protein Acetylation and Acetyl Coenzyme A Metabolism in Budding Yeast. Eukaryotic Cell. 2014;13(12):1472-83.

147. Paik WK, Paik DC, Kim S. Historical review: the field of protein methylation. Trends in biochemical sciences. 2007;32(3):146-52.

148. Spiro RG. Protein glycosylation: nature, distribution, enzymatic formation, and disease implications of glycopeptide bonds. Glycobiology. 2002;12(4):43r-56r.

149. Saraon P, Musrap N, Cretu D, Karagiannis GS, Batruch I, Smith C, et al. Proteomic profiling of androgen-independent prostate cancer cell lines reveals a role for protein S during the development of high grade and castration-resistant prostate cancer. J Biol Chem. 2012;287(41):34019-31.

150. Leung JK, Sadar MD. Non-Genomic Actions of the Androgen Receptor in Prostate Cancer. Front Endocrinol (Lausanne). 2017;8.

151. Gelman IH. Androgen Receptor Activation in Castration-Recurrent Prostate Cancer: The Role of Src-Family and Ack1 Tyrosine Kinases. International Journal of Biological Sciences. 2014;10(6):620-6.

152. Guo Z, Dai B, Jiang T, Xu K, Xie Y, Kim O, et al. Regulation of androgen receptor activity by tyrosine phosphorylation. Cancer Cell. 2006;10(4):309-19.

153. Migliaccio A, Varricchio L, De Falco A, Castoria G, Arra C, Yamaguchi H, et al. Inhibition of the SH3 domain-mediated binding of Src to the androgen receptor and its effect on tumor growth. Oncogene. 2007;26(46):6619-29.

154. Perlmutter MA, Lepor H. Androgen Deprivation Therapy in the Treatment of Advanced Prostate Cancer. Reviews in urology. 2007;9(Suppl 1):S3-8.

155. Sanford M. Enzalutamide: A Review of Its Use in Metastatic, Castration-Resistant Prostate Cancer. Drugs. 2013;73(15):1723-32.

156. Hunter T. A tail of two src's: mutatis mutandis. Cell. 1987;49(1):1-4.

157. Varkaris A, Katsiampoura AD, Araujo JC, Gallick GE, Corn PG. Src signaling pathways in prostate cancer. Cancer metastasis reviews. 2014;33(2-3):595-606.

158. Fizazi K. The role of Src in prostate cancer. Annals of oncology : official journal of the European Society for Medical Oncology / ESMO. 2007;18(11):1765-73.

159. Goldenberg-Furmanov M, Stein I, Pikarsky E, Rubin H, Kasem S, Wygoda M, et al. Lyn is a target gene for prostate cancer: sequence-based inhibition induces regression of human tumor xenografts. Cancer research. 2004;64(3):1058-66.

160. Asim M, Hafeez BB, Siddiqui IA, Gerlach C, Patz M, Mukhtar H, et al. Ligand-dependent corepressor acts as a novel androgen receptor corepressor, inhibits prostate cancer growth, and is functionally inactivated by the Src protein kinase. J Biol Chem. 2011;286(43):37108-17.

161. ProstateCancerFoundation. Top 10 Things You Should Know About Prostate Cancer 2017 [updated 2017. Available from: https://www.pcf.org/c/top-10-things-you-should-know-about-prostate-cancer/.

162. Tewari A. Management of clinically localized prostate cancer: pathologic processing to robotic prostatectomy. Reviews in urology. 2003;5 Suppl 6:S33-9.

163. Chandran UR, Ma C, Dhir R, Bisceglia M, Lyons-Weiler M, Liang W, et al. Gene expression profiles of prostate cancer reveal involvement of multiple molecular pathways in the metastatic process. BMC cancer. 2007;7:64.

164. Yu YP, Landsittel D, Jing L, Nelson J, Ren B, Liu L, et al. Gene expression alterations in prostate cancer predicting tumor aggression and preceding development of malignancy. Journal of clinical oncology : official journal of the American Society of Clinical Oncology. 2004;22(14):2790-9.

165. Yang F, Li X, Sharma M, Sasaki CY, Longo DL, Lim B, et al. Linking β-Catenin to Androgen-signaling Pathway. Journal of Biological Chemistry. 2002;277(13):11336-44.

166. Ye L, Kynaston HG, Jiang WG. Bone metastasis in prostate cancer: molecular and cellular mechanisms (Review). International journal of molecular medicine. 2007;20(1):103-11.

167. Martin TA YL, Sanders AJ, Lane J. Jiang W. . Cancer Invasion and Metastasis: Molecular and Cellular Perspective. . Madame Curie Bioscience Database 2013.

168. Zheng D, Decker KF, Zhou T, Chen J, Qi Z, Jacobs K, et al. Role of WNT7B-induced Noncanonical Pathway in Advanced Prostate Cancer. Mol Cancer Res. 2013;11(5):482-93.

169. Saha B, Arase A, Imam SS, Tsao-Wei D, Naritoku WY, Groshen S, et al. Overexpression of E-cadherin and beta-catenin proteins in metastatic prostate cancer cells in bone. Prostate. 2008;68(1):78-84.

170. Verras M, Brown J, Li X, Nusse R, Sun Z. Wnt3a growth factor induces androgen receptor-mediated transcription and enhances cell growth in human prostate cancer cells. Cancer research. 2004;64(24):8860-6.

171. Wang G, Wang J, Sadar MD. Crosstalk between the androgen receptor and beta-catenin in castrate-resistant prostate cancer. Cancer research. 2008;68(23):9918-27.

172. Kumar A, White TA, MacKenzie AP, Clegg N, Lee C, Dumpit RF, et al. Exome sequencing identifies a spectrum of mutation frequencies in advanced and lethal prostate cancers. Proceedings of the National Academy of Sciences of the United States of America. 2011;108(41):17087-92.

173. Margolis RL. Divide and conquer: the surprising link between motility and the cell cycle (retrospective on DOI 10.1002/bies.201200119). BioEssays : news and reviews in molecular, cellular and developmental biology. 2014;36(12):1127.

174. Kagawa Y, Matsumoto S, Kamioka Y, Mimori K, Naito Y, Ishii T, et al. Cell cycle-dependent Rho GTPase activity dynamically regulates cancer cell motility and invasion in vivo. PLoS ONE. 2013;8(12):e83629.

175. Ganguly KK, Pal S, Moulik S, Chatterjee A. Integrins and metastasis. Cell Adhesion & Migration. 2013;7(3):251-61.

176. Trikha M, Raso E, Cai Y, Fazakas Z, Paku S, Porter AT, et al. Role of alphaII(b)beta3 integrin in prostate cancer metastasis. Prostate. 1998;35(3):185-92.

177. Feldman BJ, Feldman D. The development of androgen-independent prostate cancer. Nature reviews Cancer. 2001;1(1):34-45.

178. Sharifi N, Gulley JL, Dahut WL. Androgen deprivation therapy for prostate cancer. JAMA. 2005;294(2):238-44.

179. Koushyar S, Jiang WG, Dart DA. Unveiling the potential of prohibitin in cancer. Cancer letters.369(2):316-22.

180. Inoshita S, Terada Y, Nakashima O, Kuwahara M, Sasaki S, Marumo F. Regulation of the G1/S transition phase in mesangial cells by E2F1. Kidney international. 1999;56(4):1238-41.

181. Ande SR, Moulik S, Mishra S. Interaction between O-GlcNAc Modification and Tyrosine Phosphorylation of Prohibitin: Implication for a Novel Binary Switch. PLoS ONE. 2009;4(2):e4586.

182. Mishra S, Murphy LC, Murphy LJ. The Prohibitins: emerging roles in diverse functions. Journal of cellular and molecular medicine. 2006;10(2):353-63.

183. Ande SR, Gu Y, Nyomba BLG, Mishra S. Insulin induced phosphorylation of prohibitin at tyrosine114 recruits Shp1. Biochimica et Biophysica Acta (BBA) - Molecular Cell Research. 2009;1793(8):1372-8.

184. Westhoff MA, Serrels B, Fincham VJ, Frame MC, Carragher NO. Src-Mediated Phosphorylation of Focal Adhesion Kinase Couples Actin and Adhesion Dynamics to Survival Signaling. Molecular and cellular biology. 2004;24(18):8113-33.

185. Phillips R. Prostate cancer: Dasatinib fails to improve on docetaxel for metastatic CRPC. Nature reviews Urology. 2014;11(1):5-.

186. CancerResearchUK. Prostate cancer survival statistics. 2017.

187. Jang GB, Kim JY, Cho SD, Park KS, Jung JY, Lee HY, et al. Blockade of Wnt/beta-catenin signaling suppresses breast cancer metastasis by inhibiting CSC-like phenotype. Scientific reports. 2015;5:12465.

188. Zhan T, Rindtorff N, Boutros M. Wnt signaling in cancer. Oncogene. 2017;36(11):1461-73.

189. Kalluri R. EMT: When epithelial cells decide to become mesenchymal-like cells. The Journal of Clinical Investigation. 2009;119(6):1417-9.

190. Wu Z-Q, Li X-Y, Hu CY, Ford M, Kleer CG, Weiss SJ. Canonical Wnt signaling regulates Slug activity and links epithelial–mesenchymal transition with epigenetic Breast Cancer 1, Early Onset (BRCA1) repression. Proceedings of the National Academy of Sciences. 2012;109(41):16654-9.

191. Morgan-Fisher M, Wewer UM, Yoneda A. Regulation of ROCK Activity in Cancer. The journal of histochemistry and cytochemistry : official journal of the Histochemistry Society. 2013;61(3):185-98.

192. Lyons LS, Rao S, Balkan W, Faysal J, Maiorino CA, Burnstein KL. Ligand-independent activation of androgen receptors by Rho GTPase signaling in prostate cancer. Mol Endocrinol. 2008;22(3):597-608.

193. Esquela-Kerscher A, Slack FJ. Oncomirs [mdash] microRNAs with a role in cancer. Nature reviews Cancer. 2006;6(4):259-69.

194. Kang T, Lu W, Xu W, Anderson L, Bacanamwo M, Thompson W, et al. MicroRNA-27 (miR-27) targets prohibitin and impairs adipocyte differentiation and mitochondrial function in human adipose-derived stem cells. J Biol Chem. 2013;288(48):34394-402.

195. Liu T, Tang H, Lang Y, Liu M, Li X. MicroRNA-27a functions as an oncogene in gastric adenocarcinoma by targeting prohibitin. Cancer letters. 2009;273(2):233-42.

Supplemental data

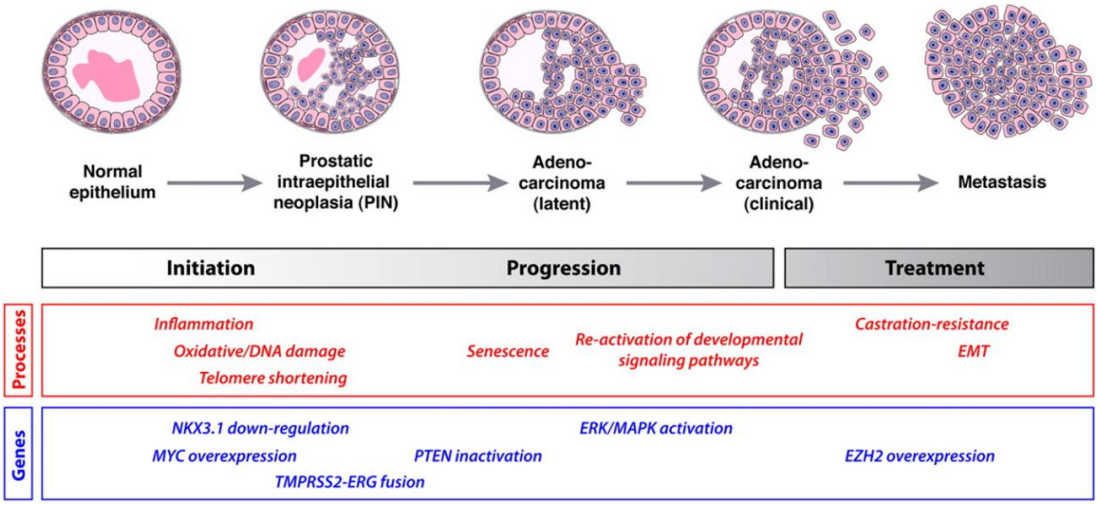

Supplemental figure 1. Stages of PC progression from normal epithelium to metastasis.

A wt MCM6 promoter

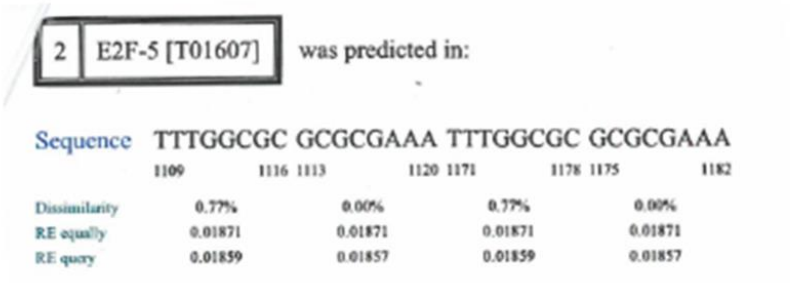

B mutated MCM6 promoter

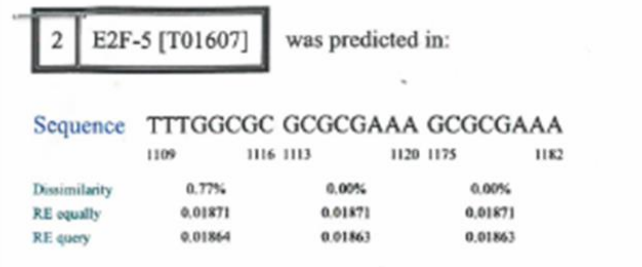

Supplemental figure 2. ALGGEN *in silico* analysis of the *MCM6* promoter. **A,** four predicted E2F binding sites are found in the wt MCM6 promoter. **B**, the mutated MCM6 promoter has an abolished predicted E2F binding site.

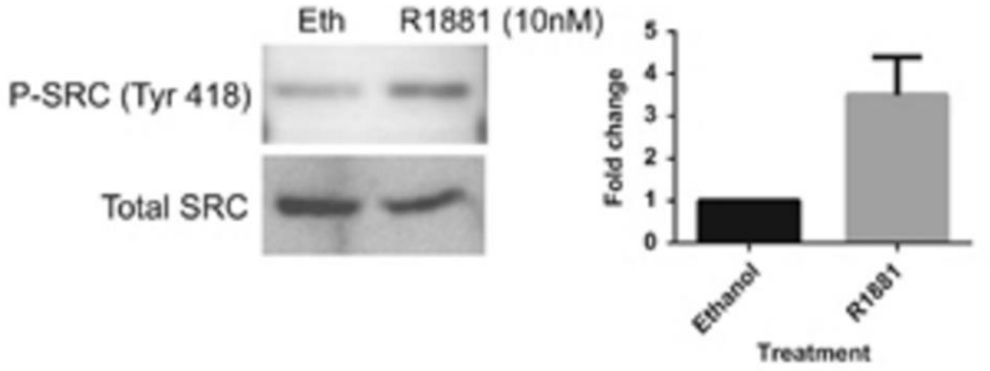

Supplemental figure 3. Western blot of total and Src-y418 phosphorylation from LNCaP cells. LNCaP cells were grown in charcoal stripped serum for 72 hr and then treated with ethanol or R1881. (10nM, 4 hr).

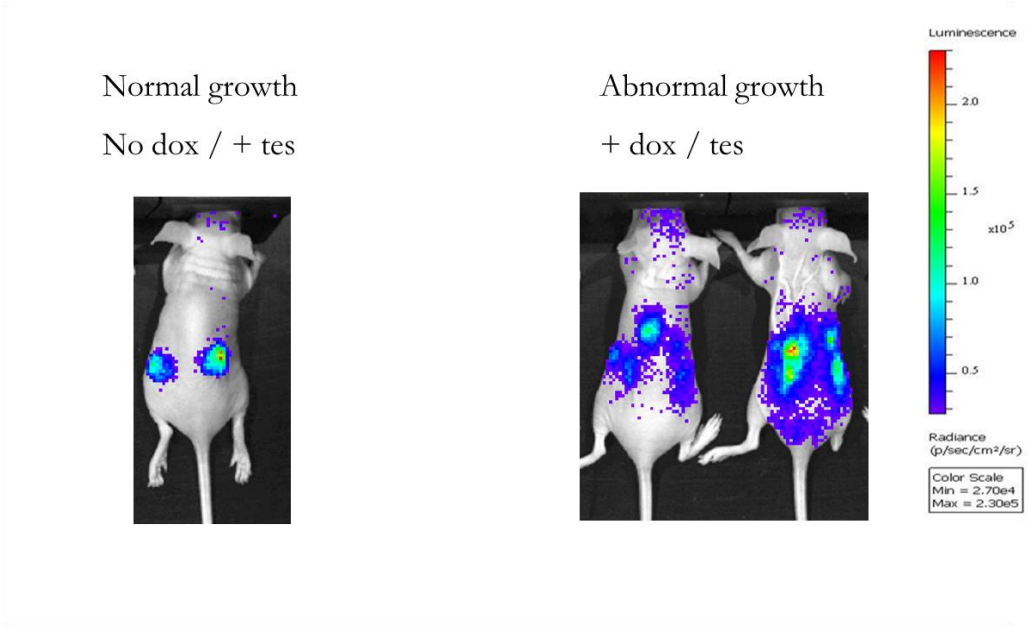

Supplemental figure 4. Bio-luminescence imaging of male mice carrying LNCaP/PHB siRNA xenografts treated with or without doxycycline.

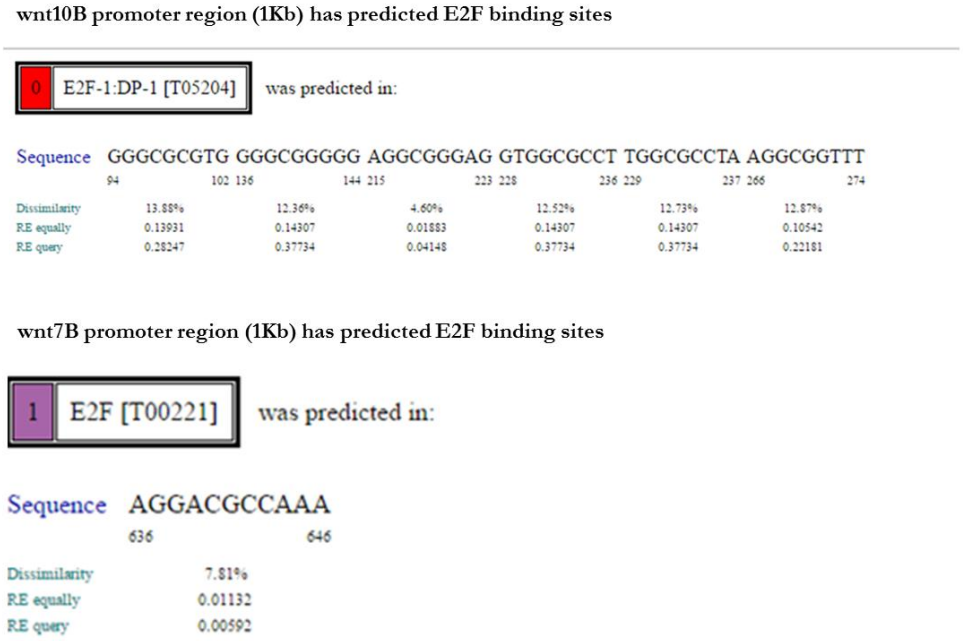

Supplemental figure 5. ALGGEN *in silico* analysis of the *wnt10B* and *wnt7B* promoter regions 1Kb up-stream of the stop codon. Both *wnt10B* and *wnt7B* have predicted E2F binding sites.

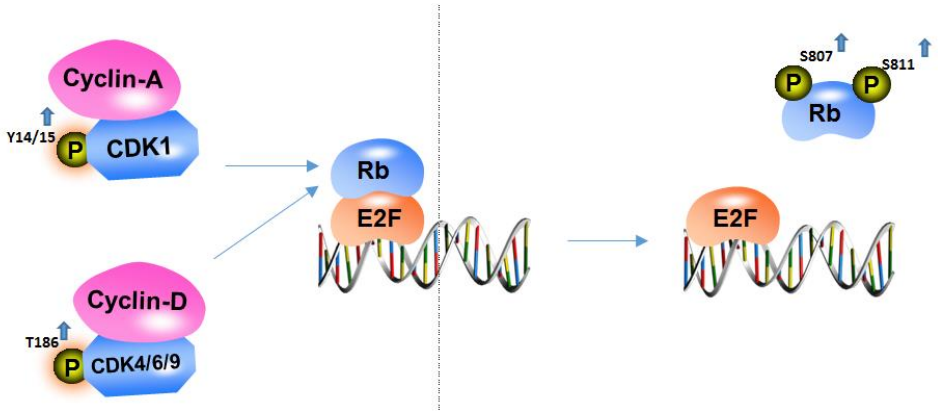

Supplemental figure 6. LNCaP cells treated with androgen incur a phosphorylation of cyclinA/D leading to Rb phosphorylation.